Beach Ridge Records of Late-Holocene Tropical Cyclone Behaviour

Thesis submitted by

Anthony John Forsyth

in July 2013

For the degree of Doctor of Philosophy

in the School of Earth and Environmental Sciences

James Cook University

Statement of Sources

Declaration

I declare that this thesis is my own work and has not been submitted in any form for another degree or diploma at any university or other institution of tertiary education. Information derived from the published or unpublished work of others has been acknowledged in the text and a list of references is given.

_____ _____

Signature Date

Statement of Access

I, the undersigned, author of this work, understand that James Cook University will make this thesis available for use within the University Library and, via the Australian Digital Thesis network, for use elsewhere.

I understand that, as an unpublished work, a thesis has significant protection under the Copyright Act and;

I do not wish to place any further restriction on access to this work.

_____ _____

Signature Date

Electronic Copy

I, the undersigned, the author of this work, declare that the electronic copy of this thesis provided to the James Cook University Library is an accurate copy of the print thesis submitted, within the limits of the technology available.

_____ _____

Signature Date

Acknowledgements

I would like to thank my supervisor Prof Jon Nott for his support, inspiration, and guidance through my candidature. To Prof David Hopley, Dr Raphael Wust and Prof Brian Roberts, I would like to thank you for your enthusiastic and well-timed advice on analytical approach and choice of field sites. It is doubtful that this project would have reached a successful conclusion without the assistance that these people were selflessly willing to provide.

Special thanks also go to my wonderful family, especially Erica Blythe who provided continual support and encouragement throughout my candidature. Thanks also for the generous moral support and sound practical advice provided on occasions by the cohort of post-graduate students at JCU between 2006 and 2013. I would like to express my gratitude for the administrative assistance provided by the staff of the School of Earth and Environmental Sciences of James Cook University. In particular, these thanks go to Janet Cateral, Meg Collis, Carly McKaskill, Teresa Carrette and Eva King.

This study was funded by under ARC Discovery Project DP0558346 titled Tropical Sand Beach Ridges – a new approach to palaeotempestology. Acknowledgement is also given to the Queensland Environmental Protection Agency for permission to carry out the sediment sampling program in Edward Kennedy National Park under permit # WITK04480707.

ABSTRACT

Currently, there is a lack of detailed knowledge about the frequency of extreme intensity tropical cyclones in Queensland, Australia. As a consequence, it is difficult to conduct a robust assessment of the accuracy of current tropical cyclone (TC) risk estimates for this region. The objective of this study was to determine whether the coastal barriers in this region might contain long-term TC records that will prove useful in overcoming this difficulty. Such long-term records have been identified in both coral shingle ridges in the past as they have in similar landforms composed of shell and sand. However, a more geographically abundant type of record is required in order to gain a realistic picture of regional TC behaviour.

Landform morphology, sedimentology and luminescence chronology were used in reconstruction of three beach ridge plains located along the northeast Queensland coast. These include a coarse-grained sand beach ridge plain at Rockingham Bay, a ‘complex barrier’ comprising fine- and coarse-grained sand ridges at Wonga Beach and a fine-grained sand beach ridge plain at Cungulla. Contrary to traditional interpretations about the origins of shore-parallel sand barriers, results suggest that aeolian processes are unlikely to have played a substantial role in the principal deposition of these ridges. Instead, it appears that marine inundations accompanying TCs are responsible for their deposition since the mid-Holocene. This is significant because these results suggest that sand beach ridges can be deposited by storm waves and surge and that the texture of these landforms need not necessarily be indicative of the processes responsible for ridge development.

Records contained in the coarse-grained sand beach ridges at Rockingham Bay and Wonga Beach suggest that there has been considerable variation in both the intensity and frequency of TCs at these locations over the past 6000 years. This variability is characterised by extended alternating periods (centuries to millennia) of relative quiescence and heightened intense TC activity. These results differ from most previous studies of long-term sedimentary records conducted using coral shingle or shell and sand beach ridges that display relatively uniform patterns of deposition. Therefore, pure sand ridges seem to provide a more sensitive record of variations in long-term TC climatology. Consequently, sand beach ridge records may contribute to a considerable improvement in our ability to understand the hazard posed by TCs.

There are chronological gaps in each of the ridge plains examined. The ridge plain at Cungulla offered an opportunity to determine whether these were caused by erosion or if they were due to quiescent phases in storm activity. Tropical cyclone records contained in the fine-grained sand beach ridge plain at Cungulla enabled characterisation of both erosional and non-erosional gaps. The erosional gaps are associated with changes in orientation between ridge sets and often a high ridge with hummocky topography that appears to have been disturbed by aeolian activity. River floods likely caused the partial erosion of ridge sets. Non-erosional gaps do not display these morphological characteristics and are likely associated with quiescence in severe tropical cyclone activity. These geomorphic and chronological signatures can be used to identify gaps of varying origin in other ridge plains and are an important tool in the reconstruction of long-term storm beach ridge records. Also, because

sand beach ridges are widespread in northeast Queensland, it appears likely that further studies of this kind may provide a means of testing current risk assessments for that region.

A comparison made between the northeast Queensland beach ridge records and long-term sedimentary TC records from elsewhere shows remarkable similarity in the behaviour of these hazards at the global scale. All of the records display extended alternating periods (centuries to millennia) of relative quiescence and heightened intense TC activity irrespective of both the resolution and type of record. Hence, patterns of TC behaviour in the beach ridge records are unlikely to be an artefact of the record type. And despite difficulty identifying the cause of punctuated activity, the identification of these patterns is vital for assessing the risk posed to coastal communities by TC hazards.

Table of Contents

List of Tables

List of Figures

Chapter 1: Introduction

There is currently a lack of detailed knowledge about the frequency of extreme intensity tropical cyclones in Australia. Tropical cyclone (TC) risk analyses in Queensland to date have chiefly utilized data collected since 1960 (e.g. Harper, 1999; McInnes et al., 2000; Hardy et al., 2004) due to concerns about the reliability of observations collected prior to satellite surveillance (Holland, 1981). As such, the frequency and magnitude of TCs in this region is currently estimated by simulating a large number of storm tides using the characteristics and frequency distributions of relatively few observed cyclones (e.g. Harper 1999; McInnes et al. 2000; Hardy et al. 2004). This type of time series analysis includes an assumption that the stationarity and lack of serial correlation usually apparent in a short time series will also be present in a time series of any length. Nott (2006) has suggested that this assumption may not be accurate and that longer time series often display non-stationarity and serial correlation. Also, Hardy et al. (2004) have assessed hazard risk using storm observations from the Coral Sea to compensate for the scarcity of TC landfalls at places of interest along the Queensland coast over the historical period. This assumes that the TC climatology of a particular coastal site can be estimated using observations collected elsewhere in the region. The overall reliability of this approach is currently unknown because there is insufficient knowledge of patterns in long-term tropical cyclone behaviour in this region against which to test the results. Periodicities in the past storm climate need to be identified at different temporal scales and at regionally representative sites in order to provide a scientific basis for these assessments. The provision of such a robust form of analysis is required to minimize community vulnerability and economic loss to TC hazards.

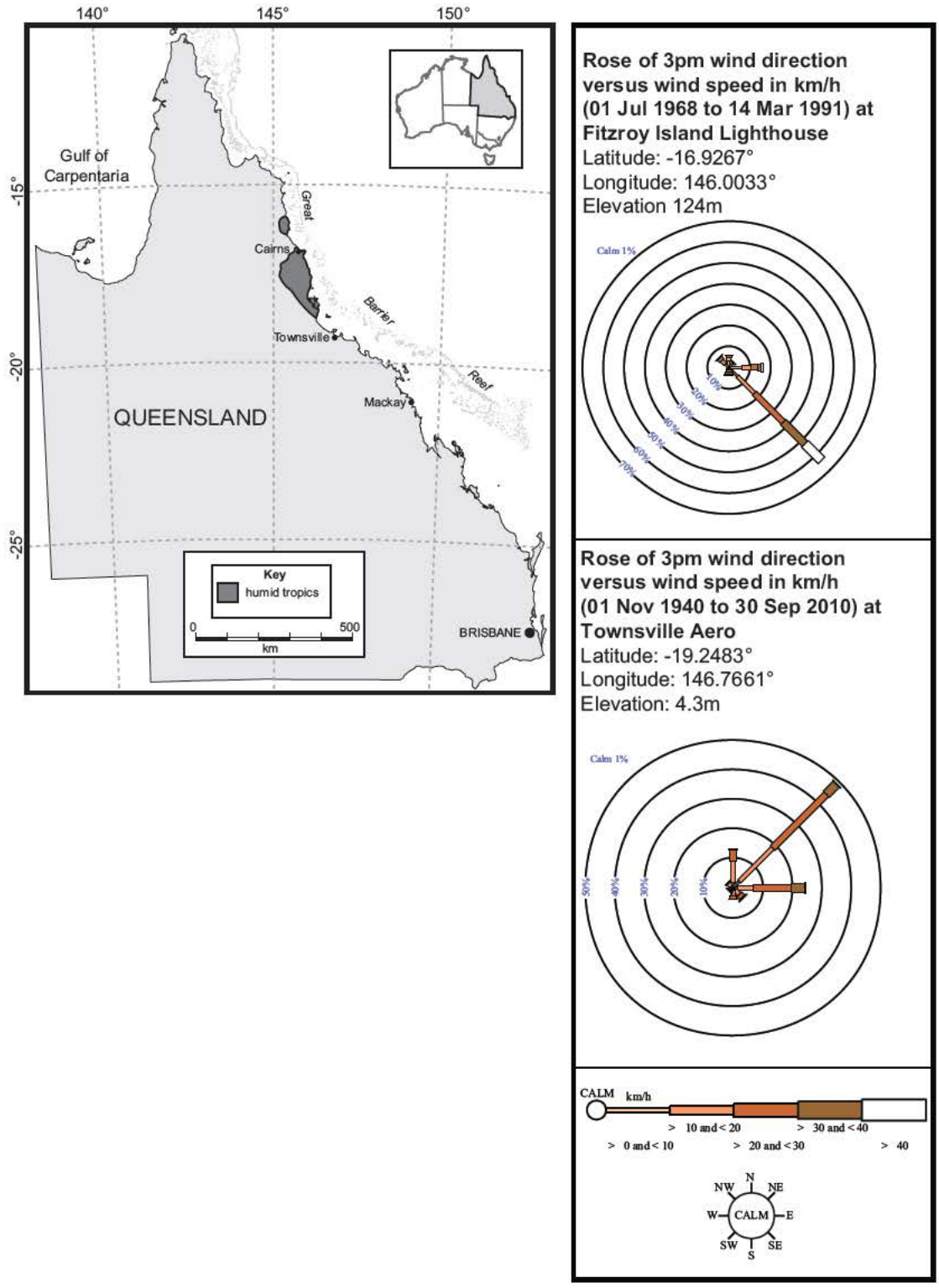

Figure 1-1 Location map of Queensland highlighting whereabouts of the humid tropical sector, including wind roses for Cairns and Townsville (Source, BOM, 2004)

One way of testing the accuracy of current TC risk assessments is through the development of a regional long-term TC record. A number of reports suggest that TCs are responsible for rhythmically depositing beach ridge plains composed of either coral fragments (coral rubble or shingle) or sand containing layers of marine shells along the Queensland coast since the mid-Holocene (Rhodes et al., 1980; Chappell et al., 1983; Chappell and Grindrod, 1984; Chivas et al., 1986; Hayne and Chappell, 2001). Nott and Hayne (2001) and Nott (2003) have also demonstrated a method for determining the intensity and frequency of prehistoric TCs using records contained in beach ridges. Essentially, the elevation of beach ridges deposited by TC events may suggest magnitude records of the most extreme TC events and chronological studies of these landforms might infer their frequency (Nott, 2003). A drawback of this approach is that the spatial distribution of beach ridges composed of detrital coral and shell is fairly limited in NE Australia. Therefore, a more widespread indicator is required if these types are records are to provide a truly regionally representative long-term TC record.

Shore parallel coastal barriers composed of sand are widespread along the coast of Queensland. Most beaches and barriers located along the humid tropical sector of the North Queensland coast are composed of poorly sorted, coarse-grained sand (Figure 1). Whereas, fine- to medium-grained sand dominate these environments along drier sections of this coastline. Unlike beach ridges composed of coarser material, many interpret that coastal barriers composed of sand are eroded by storm waves and not constructed by these events (e.g. Komar, 1976). Also, because these landforms can be morphologically similar it can be difficult to discriminate between beach ridge plains (wave emplaced) and foredune plains (aeolian emplaced) without conducting detailed studies (Hesp et al., 2005). Hence, shore-parallel ridges composed of sand in Queensland have occasionally been ascribed aeolian origins on the basis of their sedimentary texture (e.g. BPA, 1979; Brooke et al., 2006). However, a detailed study by Nott et al. (2009) suggested that inundations associated with TCs are responsible for depositing a coarse-grained sand beach ridge plain located centrally in the humid tropical sector of NE Queensland. The record of late-Holocene TC frequency and magnitude

contained in that ridge sequence also suggests that numerous similar landforms composed of coarse-grained sand located along the humid tropical sector coast may contain similar records. Furthermore, these findings raise questions about whether TC records may also be contained in beach ridge plains composed of fine-grained sand along the remainder of the Queensland coast. This possibility is clearly worth investigating because such a record would greatly enhance our understanding of past TC behaviour at both a local and regional level.

The main objective of this study is to ascertain whether sand beach ridge plains located along the eastern Queensland coast contain records of past TC behaviour. To achieve this objective the study focuses on four main aims.

1. To determine whether the palaeo-TC record contained in the coarse-grained sand beach ridge plain at Cowley Beach is an anomaly or whether similar landforms in the region also contain TC records;
2. To determine whether fine-grained sand beach ridges may also contain palaeo-TC records;
3. To determine the origin of chronological gaps in the depositional records of NE Queensland beach ridge plains; and
4. To assess patterns of TC behaviour in NE Queensland beach ridge records in a regional and global context.

Chapter 2 describes a chronological, sedimentological and morphological study of the coarse-grained sand beach ridge plain at Rockingham Bay, NE Queensland. Chapter 3 describes a similar study carried out at Wonga Beach, located approximately 200 km to the north of Rockingham Bay. Combined with data from Cowley Beach, these sedimentary records suggest that TC records are likely widespread within coarse-grained sand beach ridge plains that are prolific in this region. Chapter 4 presents a study of the beach ridge plain at Cungulla located in the seasonally wet tropical sector of NE Queensland. Ridges comprising this plain differ from those located in the humid tropics because they are composed of fine-grained sand. Hence, a traditional approach is likely to find that they are the product of aeolian processes. Nevertheless, Hopley (1970) suggested that waves were likely responsible for depositing the Cungulla ridge plain. This chapter presents a

method for determining the process origins of these ridges. In addition, this chapter presents a comparison of characteristic differences between chronological gaps of differing origin. These are likely to be useful in analysis of beach ridge plain development elsewhere in this region.

Chapter 5 presents an analysis of global long-term TC records through comparison of beach ridge records from northern Australia with overwash records from a number of northern hemisphere regions. The results suggest that extreme intensity TCs do not occur at random, addressing an important consideration for those assessing the risk posed by these hazards.

Chapter 6 summarizes major findings and discusses the implications of studies contained in Chapters 2 to 5. Results are discussed in the context of previous studies aimed at understanding the behaviour of TCs and rates of sand barrier development. By placing these studies within a local, regional and global context, this discussion provides practical recommendations for the role played by beach ridge records in future long-term TC research.

Chapter 2: Beach ridge plain evidence of a variable late-Holocene tropical cyclone climate

Forsyth, A. J., Nott, J., and Bateman, M. D., 2010, Beach ridge plain evidence of a variable late-Holocene tropical cyclone climate, North Queensland, Australia: Palaeogeography, Palaeoclimatology, Palaeoecology, v. 297, no. 3-4, p. 707-716.

Abstract

To date most studies of long-term tropical cyclone records from beach ridge plains (coral, shell and sand) have suggested that there has been little variation in the intensity of these events over the late Holocene. This study, of a sand beach ridge plain in northeast Queensland, Australia, using sedimentary analysis and luminescence chronology, suggests there has been considerable variation in both the intensity and frequency of tropical cyclones here since the mid-Holocene. Most of the previous beach ridge studies have been of relatively uniform elevation coral shingle, shell and sand beach ridges within the plain. Here, at Rockingham Bay the sediments are composed of coarse-grained sand and there is considerable variation in ridge height and the number of ridges emplaced over different time intervals. It may be that pure sand ridges provide a more sensitive record of variations in long-term tropical cyclone climatology, which in turn may contribute to a considerably improved understanding of the behaviour of this natural hazard.

2.1 Introduction

Beach ridges composed of coral, shell or sand and shell have been used to reconstruct millennial-scale records of tropical cyclones (TCs) in northeast Australia (Chappell et al., 1983; Chivas et al., 1986; Hayne and Chappell, 2001; Nott and Hayne, 2001). These studies suggested there had been a relatively uniform frequency of tropical cyclone induced beach ridge formation at a number of locations along the length of the Great Barrier Reef, since the mid Holocene. Nott and Hayne (2001) recognised that these ridges were a product of intense tropical cyclones (TCs) because smaller ridges deposited by less intense events were likely buried or removed and it was the highest ridges which have the greatest preservation potential. Hence the long-term tropical cyclone records were effectively censored and there appeared to be little variation in the frequency of the most intense events over time. The question remained however whether this apparent uniformity of TC occurrence was a true reflection of the long-term cyclone climatology or whether it was an artefact of the type of record. It may be that different types of beach ridge systems i.e. ones composed of other types of sediment, reveal different aspects of the long-term TC climatology because of the nature or sensitivity of that system to record the occurrence of these events. Sand beach ridge systems for example have different sediment supply issues compared with predominantly shell and coral rubble ridge plain systems. Nott et al. (Nott et al., 2009) examined a pure sand (coarse-grained sand) beach ridge sequence at Cowley Beach and the results there suggested this sand ridge system may register a more comprehensive record of long-term TC behaviour. However the results were inconclusive. The purpose of the present study was to further test this idea by examining a further pure coarse-grained beach ridge sequence at Rockingham bay, 40 km south of Cowley Beach. Here 19 shore-parallel beach ridges lie at elevations between 3 and 5.5 m above Australian Height Datum (AHD) or approximate mean sea level. We analysed these ridges using sedimentological, chronological (optically stimulated luminescence – OSL) and numerical wind and surge and shallow water wave modelling. Our analyses suggest that this type of record has registered considerable variation in the frequency of tropical cyclones in this region throughout the late Holocene.

2.2 Setting

Rockingham Bay is 32 km in length and is fronted by a medium to coarse-grained sand beach that stretches between Tam O'Shanter Point and Cardwell (Figure 2-1 (B)). Tidal range in the area is approximately 3.49 m, with the very highest tides reaching 1.82 m above Australian Height Datum (AHD) (NTF, 2007a). The barrier complex is composed of two parts – an inner and outer beach ridge plain. The outer barrier is up to 2km wide and is demonstrated below to be Holocene in age including 19 predominantly coarse-grained sand beach ridges (Figure 2-2) vegetated by tropical rainforest. The inner barrier is discontinuous and separated from the outer barrier by patchy sedge swamp and pockets of cultivated land. No chronological analysis has been undertaken on this barrier but we suggest that it may be Pleistocene in age.

The passive eastern Australian continental margin likely experienced relative tectonic stability throughout the Cainozoic (Nott et al., 2009), therefore it is unlikely that tectonics have contributed to development of this ridge sequence. The coastal plain in this region is approximately 37 km wide and covered by Quaternary fan and fluvial deposits (Fardon et al., 1963). The ranges and escarpment on the landward side of the coastal plain are composed predominantly of Carboniferous-Permian granites and acid volcanics (Fardon et al., 1963). Three streams (Hull, Tully and Murray Rivers) plus several other smaller coastal streams drain these ranges and foothills and intersect the coastal barrier system to enter the sea at Rockingham Bay. These streams are the most likely source of sediments in the nearshore coastal system.

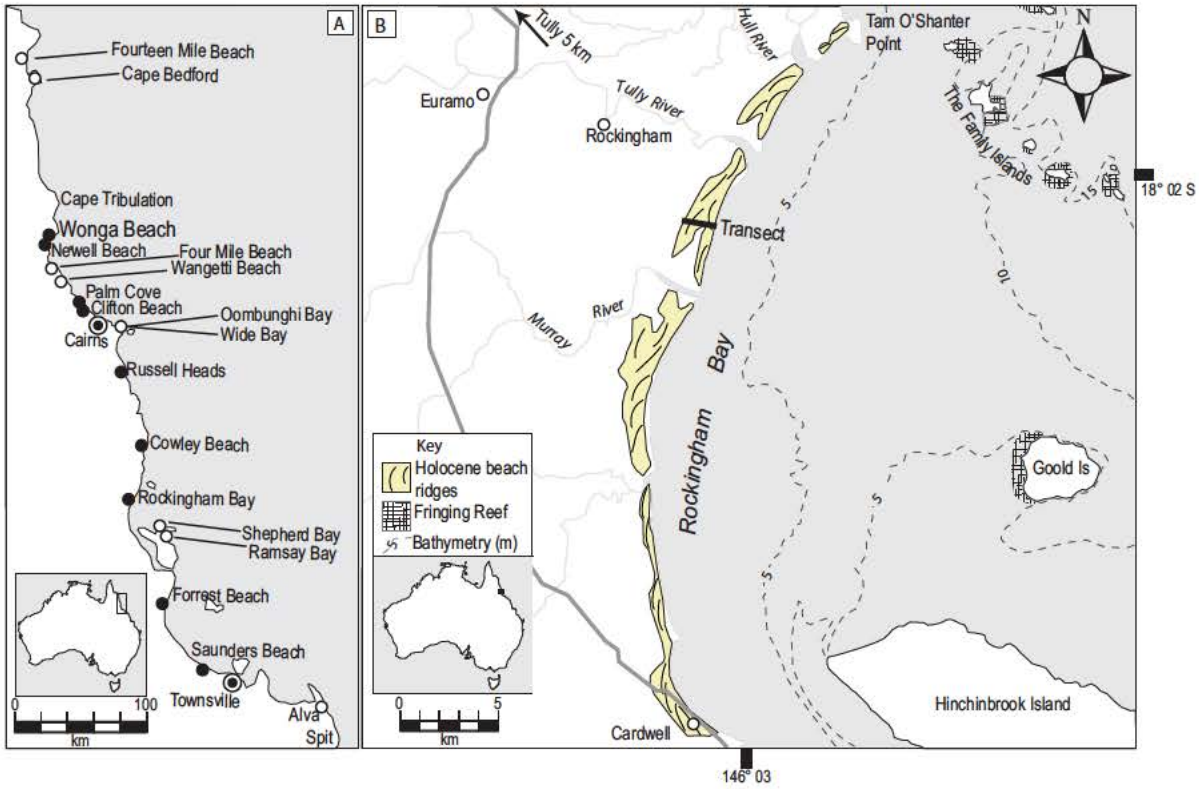

Figure 2-1 Location maps of: (A) coarse-grained sand beach ridge plains between Cape Tribulation and Townsville (denoted by black dots) and aeolian foredunes (white dots); and (B) Rockingham Bay, indicating the location of Holocene beach ridges extending between Tam O'Shanter Point and Cardwell, local bathymetry and the location of nearby islands relative to the study site.

Rockingham Bay, at latitude 18.1°S, has a tropical climate. The annual rainfall varies between 2600 and 4000 mm, over 70% of which falls between December and April (Johnson, 1998). A high proportion of this rainfall is generated by orographic uplift over the nearby east Australian highlands and convergence of the southeasterly trade winds into the monsoon trough. TCs also bring substantial amounts of rain.

This region experiences a relatively low wave energy climate. Figure 4-3 illustrates significant wave height (H_s) recorded in 20 m water depth near Cairns from 1975 until 2005 (QEPA, 2005). Maximum monthly average H_s was 0.79 m during October 1982. Otherwise, average H_s ranges between 0.4 m and 0.6 m. The type of waves recorded can be generally categorised as either:

- Sea waves generated inside the Great Barrier Reef (GBR) with a peak period (Tp) of 2.5–5.0 s; or
- Swell waves generated outside of the GBR with a Tp of 5.0–9.0 s.

Significant wave heights of 2–3 m occur less than 0.1% of the time, predominantly during summer months, coinciding with the passage of TCs. The predominant southeasterly trade winds rarely exceed velocities of 30 knots along the mainland coast and are the chief source of wave energy. The coast rarely experiences waves in excess of 0.5 m in height (at shore) with wave periods of 2–4 s even during strong trade wind conditions. The GBR limits the wave fetch in this region and the longest fetch is ~48 km to the east-southeast. TCs can generate significant wave heights of up to 10m and wave periods of 12 s between the GBR and the mainland. Such storms can also generate storm surges several metres above the normal tide.

2.3 Methodology

Beach ridge plains are common features along many of the world's sedimentary coasts and processes in their genesis differ between locations. Hence definitions vary as to what constitutes a beach ridge, beach ridge plain, relict foredune and plain, chenier and other shore-parallel/sub-parallel ridge features. A number of detailed reviews on the various origins of these landforms have recently been published (Tanner, 1995; Taylor and Stone, 1996; Otvos, 2000; Hesp, 2006) and some authors suggest that beach ridges consist only of wave built features (Johnson, 1919; Hesp, 2006) whereas others such as Otvos (2000) include both wave and aeolian constructed ridges or combinations of the two depositional processes. Here we refer to the ridges at Rockingham Bay as coarse-grained sand beach ridges *sensu* Johnson (1919) and Hesp (2006) corresponding with the definition and description provided by Nott et al., (2009) for the Cowley Beach sequence 40 km to the north.

A series of methodologies were employed to determine whether the Rockingham Bay coarse-grained sand beach ridges are a product of aeolian or storm wave processes. These methods included examination of the texture and sorting of sands within the ridges, surveying of ridge topography and analysis of the possible wave and storm surge conditions necessary to deposit sand onto a ridge of a given elevation above mean sea level.

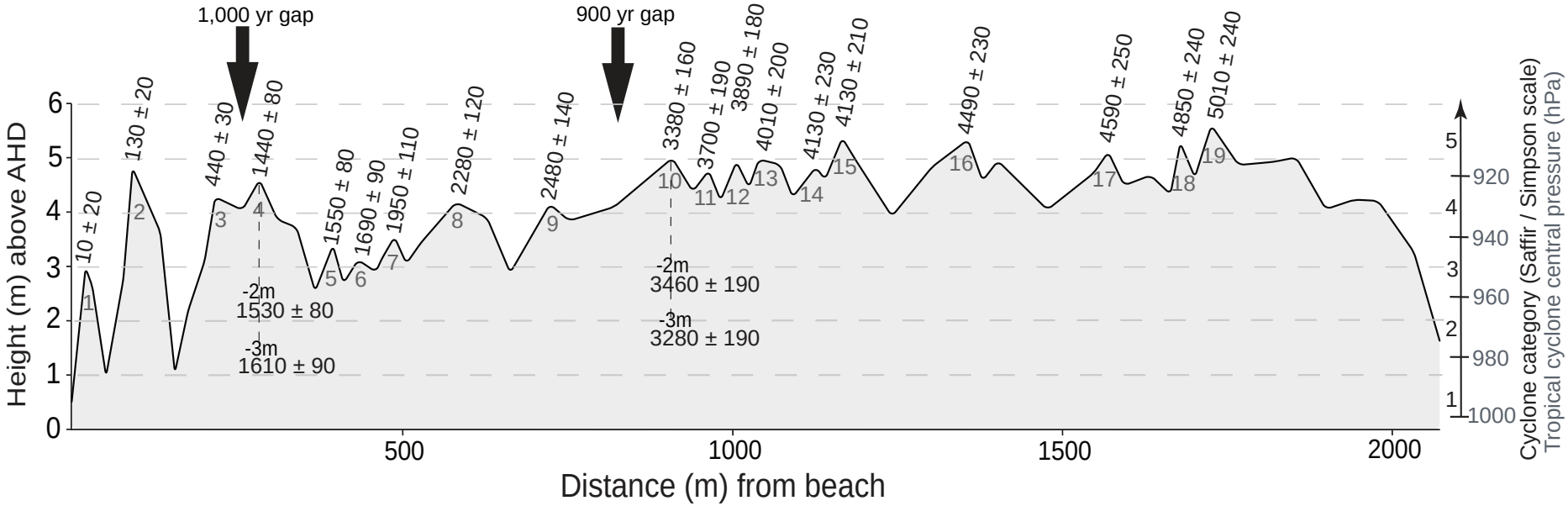

Figure 2-2 Cross-section of Rockingham Bay beach ridge plain, showing height of ridges above AHD, OSL dates with error margins and modelled TC intensity required to produce inundation level equal to ridge height based upon mean tide level. Origin denotes the location of shoreline at the time of survey.

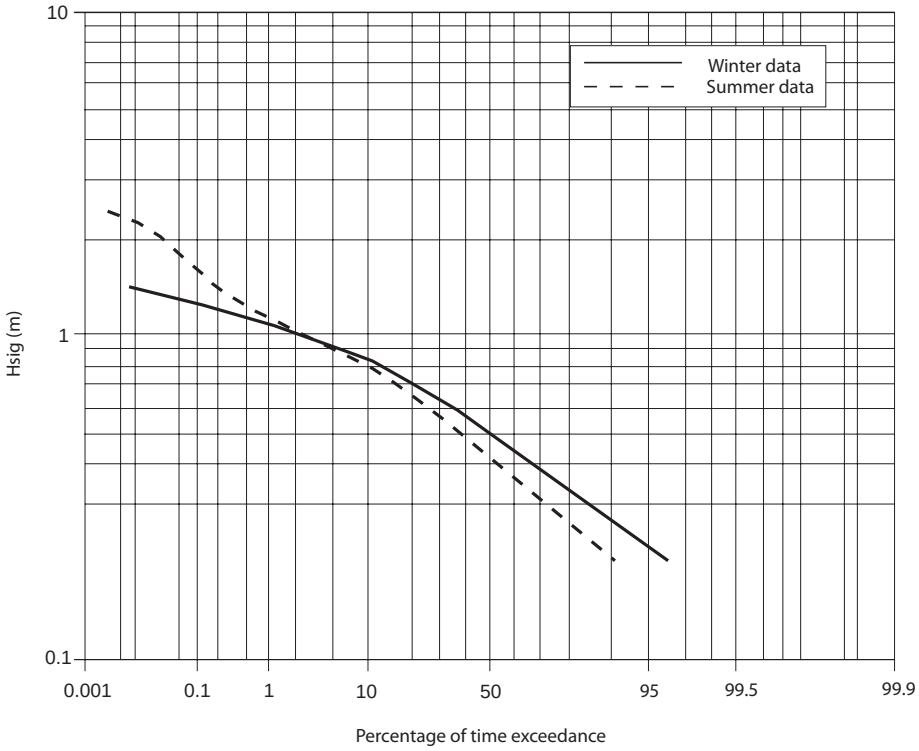

Figure 2-3 Average wave height (Hs) from wave rider buoy in 20 m depth water, Buchan Point, Cairns from 1975 to 2005 (QEPA, 2005).

2.3.1 Surveying

The 1.8 km wide ridge sequence at Rockingham Bay was surveyed by dumpy (spirit) level. Datum was calculated using surveyed tidal level compared to the tidal reading from nearby Mourilyan Harbour. We expect the error using this approach to be less than ±10 cm.

2.3.2 Sediment collection

Sediment samples were collected from all nineteen ridges that form the outer barrier complex at Rockingham Bay. These were collected along a shore-normal track across the sequence approximately 5 km southeast of the township of Rockingham (Figure 2-1). Thirty-eight samples, two from each ridge crest, were collected from 85-100 cm depth. The samples were collected by hammering lightproof PVC tubes into the side of 1.3 m deep pits and then sealing the tubes. One sample was used for an OSL age determination – this sample was carefully protected from solar radiation and precautions were made to ensure that the sample tubes were sufficiently well packed to eliminate mixing of sediments during transport. The second sample was used for sediment analysis, as described below. Sediment samples were also taken

from the modern beach to compare their textural characteristics with those taken from the ridges.

Dating of ridge sediments taken at different depths of a vertical profile may provide an indication of the rate of ridge emplacement within the error margin of individual OSL dates. For this reason, sediment samples from depths of 2 and 3 m were taken from ridges 4 and 10. For example, SEK-4 was collected from a depth of 1 m, SEK-4-2m was collected from a depth of 2 m and SEK-4-3m was collected from a depth of 3 m. To avoid exposure to light, samples from 2 and 3 m were taken by sand augur approximately 2 h after dusk then stored in lightproof PVC tubes.

2.3.3 OSL dating

Twenty-three samples representing all ridges forming the Rockingham Bay barrier complex were dated using OSL (Table 2-1). From each sample quartz grains in the size range 90-250 µm were extracted and cleaned under controlled red-light conditions (Bateman and Catt, 1996). The samples were initially assessed to determine quartz sample purity, signal sensitivity, approximate equivalent dose (D_e), and an indication of the degree of inter-aliquot variability. All OSL measurements were carried out using a DA-18 Risø luminescence reader, with blue LEDs for stimulation and OSL measured through a Hoya-340 filter. Infrared stimulated luminescence (IRSL) analysis indicated that extracted quartz included no feldspar contamination. Several of the samples had weak naturally acquired OSL signals, though all showed a marked increase in OSL signal with additional artificial laboratory dose.

To derive the palaeodose (De), each sample was measured using twenty-four 9.6 mm diameter aliquots using the single aliquot regenerative (SAR) approach (Murray and Wintle, 2003). Within this, an experimentally derived preheat of 200°C for 10 seconds prior to OSL measurement was used to remove unstable signal generated by laboratory irradiations. All samples responded well to SAR analysis resulting in well-defined growth curves and recycling ratios within 10% of unity. D_e replicates showed a low degree of scatter indicating good sunlight bleaching of sediment prior to burial. As a result, average D_e values for each sample were derived using the central age

model (Roberts et al., 2000) after the exclusion of statistical outliers (aliquots outside two-sigma of the mean).

Table 2-1 OSL age determinations and associated data from Rockingham Bay.

Field code	Lab. code	Ridge #	Depth (cm)	De (Gy)	Dose rate (Gy/ka)	Age (years before 2008)
SEK-1	Shfd08030	1	90	0.01 ± 0.03	1.875 ± 105	10 ± 20
SEK-2	Shfd08031	2	90	0.25 ± 0.03	1.907 ± 105	130 ± 20
SEK-3	Shfd08032	3	90	0.8 ± 0.03	1.810 ± 103	440 ± 30
SEK-4	Shfd08033	4	90	2.48 ± 0.04	1.722 ± 96	1440 ± 80
SEK-4-2m	Shfd08049	4	200	3.28 ± 0.04	2.138 ± 109	1530 ± 80
SEK-4-3m	Shfd08050	4	300	3.03 ± 0.05	1.878 ± 104	1610 ± 90
SEK-5	Shfd08034	5	90	4.86 ± 0.05	3.141 ± 164	1550 ± 80
SEK-6	Shfd08035	6	90	4.60 ± 0.05	2.719 ± 136	1690 ± 90
SEK-7	Shfd08036	7	90	4.04 ± 0.05	2.071 ± 118	1950 ± 110
SEK-8	Shfd08037	8	90	2.94 ±0.04	1.291 ± 64	2280 ± 120
SEK-9	Shfd08038	9	90	4.08 ± 0.04	1.644 ± 91	2480 ± 140
SEK-10	Shfd08039	10	90	4.51 ±0.05	1.333 ± 61	3380 ± 160
SEK-10-2m	Shfd08051	10	200	5.16 ± 0.07	1.490 ± 78	3460 ± 190
SEK-10-3m	Shfd08052	10	300	3.96 ± 0.09	1.207 ± 63	3280 ± 190
SEK-11	Shfd08040	11	90	3.76 ± 0.05	1.017 ± 49	3700 ± 190
SEK-12	Shfd08041	12	90	4.58 ± 0.04	1.176 ± 53	3890 ± 180
SEK-13	Shfd08042	13	90	4.36 ± 0.04	1.089 ± 54	4010 ± 200
SEK-14	Shfd08043	14	90	7.11 ± 0.06	1.721 ± 94	4130 ± 230
SEK-15	Shfd08044	15	90	6.27 ± 0.05	1.395 ± 71	4490 ± 230
SEK-16	Shfd08045	16	90	5.74 ± 0.06	1.388 ± 69	4130 ± 210
SEK-17	Shfd08046	17	90	6.95 ± 0.07	1.513 ± 82	4590 ± 250
SEK-18	Shfd08047	18	90	6.59 ± 0.05	1.359 ± 67	4850 ± 240
SEK-19	Shfd08048	19	90	8.03 ± 0.07	1.603 ± 77	5010 ± 240

Dose rates were based on inductively coupled plasma mass spectrometry (ICP-MS) elemental analysis carried out at SGS laboratories Ontario Canada and converted to annual dose rates using pre-determined data incorporating attenuation factors relating to density, sediment grain sizes and palaeomoisture (Ademiec and Aitken, 1998; Aitken, 1998; Marsh et al., 2002). The latter used the present-day moisture values as measured in the laboratory with a ± 5% error to incorporate seasonal and longer-term fluctuations in moisture, which the samples may have endured since burial.

The contribution to dose rates from cosmic sources was calculated using expression published in Prescott and Hutton (1994). OSL data are shown in Table 2-1 and ages are quoted in years from date of measurement (2008) with one-sigma confidence intervals.

2.3.4 Sediment size analysis

Samples for textural analysis were sieved at 4000, 2800, 2000 and 1400 µm intervals. These sieved fractions were measured as grain size frequency per unit weight. The remainder of each sample was then analysed in a Malvern Mastersizer 2000 providing measurement of grain size per unit volume. The raw data was statistically analysed using Gradistat Version 6.0 (Blott, 2008) and the data were then calibrated by recalculating the Malvern results as a fraction of the remainder of the sieved sample.

2.3.5 Numerical modelling

If waves are responsible for deposition of sediments to form a ridge then the height of a beach ridge can provide information about those waves or inundation conditions during ridge deposition (Nott, 2003; Nott et al., 2009). There are two possible wave or marine inundation processes that may be responsible for ridge deposition. The more conservative option was taken: wave run-up was assumed to play a substantial role in the formation of the beach ridges at Rockingham Bay. Furthermore, it has been assumed that the marine inundation including wave run-up was equal to the height of the ridges. A less conservative approach would have been to assume that flow depth (excluding wave run-up) was equal to or greater than the height of a ridge as this would require a more intense (lower central pressure) TC than the conservative approach we have used.

Numerical storm tide (GCOM2D TC storm tide model) and shallow water wave models (SWAN model) (Hubbert and McInnes, 1999) were used to determine the conditions necessary to generate a marine inundation (including wave run-up) equal to or greater than the height of the beach ridges. The GCOM2D model solves a set of mathematical equations over an equally spaced grid to determine water depth, currents, topography and bathymetry and incorporates wind stresses, atmospheric pressure gradients acting on the ocean surface and friction on the ocean floor. The model

incorporates a moveable coastal boundary and so simulates inundation of the coastal terrain. Further details of algorithms used within this model and its veracity in estimating surge heights against actual TC surge events can be found in Hubbert and McInnes (1999).

The SWAN shallow water wave model was tailored for local bathymetry and run in conjunction with the TC wind model incorporated within the GCOM2D storm tide model. The SWAN model used here was able to determine significant wave heights, wave periods, wave set-up and predominant wave travel directions at specified locations during a modelled cyclone event.

The marine inundation during a TC is composed of storm surge, tide, wave action, wave set-up and wave run-up. The GCOM2D model calculates the storm surge and can be run for any tidal scenario. Nott (2003) has previously estimated wave set-up at 10% of the significant wave height (H_s) in 15 – 20 m water depth and wave run-up at 30% of H_s. Subsequently, this estimate was tested against surveys of debris lines (3.5 m AHD) deposited by the marine inundation generated during TC Larry at Cowley Beach in March 2006. That surge did not reach the crest of the first major beach ridge. In that instance, set-up and run-up components combined were equal to 12% of the significant wave height at 20m water depth (Nott et al., 2009). Despite the proximity of Cowley Beach and similar offshore conditions, the more conservative estimate (wave set-up = 10% of H_s and wave run-up = 30% H_s) of Nott (2003) was used here.

A series of model runs were undertaken to determine the sensitivity of storm surge height to changes in cyclone translational velocity, radius of maximum winds (Rm), angle of cyclone approach and cyclone central pressure. Two other important variables that also influence storm surge are offshore bathymetry and coastal configuration. These factors remain fixed for the model runs and are incorporated within the model as a 250 m resolution DEM. A nested grid approach was used whereby a 100 m resolution fine grid was superimposed upon a 1000 m resolution coarse grid. Sensitivity tests indicated that storm surge increased substantially with increasing cyclone translational velocity, radius of maximum winds, decreasing central pressure and location of coastal crossing relative to the study site (Figure 2-4). The

parameters chosen for the final storm surge and shallow water wave model runs were Rm = 30 km, TC translational velocity = 30 km and a TC approach angle of 45^0 relative to the coast (from the north east). This track, as shown in the sensitivity tests, generates the largest possible surge for this site. The Rm and cyclone translational velocity of 30 km and 30km/hr respectively are the historical means for TCs in this region (McInnes et al., 2003).

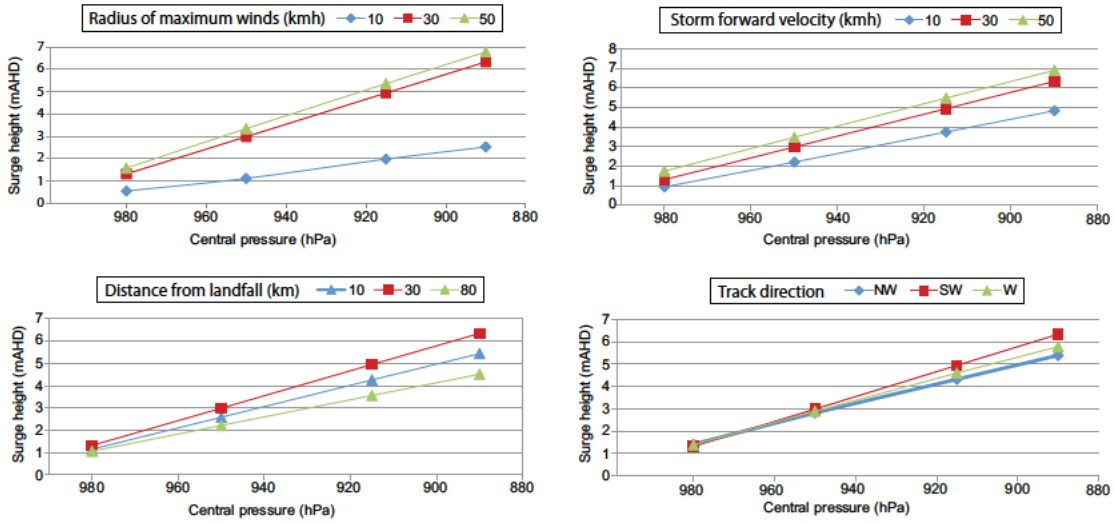

Figure 2-4 Results of sensitivity tests designed to calculate the TC parameters likely to produce the highest storm surge in the study area. Titles refer to the variable being compared in individual graphs.

2.4 Results

2.4.1 Surveying

The 19 sand beach ridges comprising the Rockingham Bay barrier complex have a mean elevation of 4.6 m above AHD (Table 2-2, Figure 2-2). The highest point in the sequence is ridge 19 at 5.59 m. Ten ridges are taller than 4.8 m above AHD. In contrast, ridges 5 – 7 are the lowest in the sequence ranging between 3.11 and 3.53 m above AHD.

2.4.2 Sedimentology

Although sedimentary structures may provide indications for differentiating between wind and wave formed ridges, no such sedimentary structures were identified in the Rockingham Bay beach ridge plain. Instead, sedimentary characteristics were used to help elucidate the depositional processes.

Beach sediment composition is pivotal in beach deflation and subsequent deposition of aeolian dunes. Bagnold (1941) established that the critical wind velocity for sand movement is minimised in uniform sand with an average grain size of approximately 100 μm and increases for both finer and coarser

grain sizes. Pye (1980) concluded that the generally low wind velocity in the humid tropical sector of northeast Queensland combined with coarse textured, poorly sorted sand beaches are partly responsible for the scarcity of foredune development in the region. Hence, the rare instances of dunes along this coast (Figure 2-1 (A)) are composed of very well sorted, fine to medium-grained sand and they are located behind beaches situated shore-normal to the predominant southeasterly trade winds (Bird, 1971; Pye, 1980). A Mann-Whitney U-test demonstrates that the mean grain size of beaches backed by dunes is significantly finer than the remainder of beaches in this region (significant at the 0.01% level) and those beaches backed by dunes are also significantly better sorted (at the 0.001% level) (Pye, 1980).

Table 2-2 Summary of survey data from Rockingham Bay.

Sample #	Ridge #	Height (m)
SEK-1	1	2.95*
SEK-2	2	4.81
SEK-3	3	4.28
SEK-4	4	4.60
TSEK-5	5	3.37
SEK-6	6	3.11
SEK-7	7	3.53
SEK-8	8	4.19
SEK-9	9	4.14
SEK-10	10	4.99
SEK-11	11	4.76
SEK-12	12	4.92
SEK-13	13	4.97
SEK-14	14	4.82
SEK-15	15	5.36
SEK-16	16	4.83
SEK-17	17	5.36
SEK-18	18	5.27
SEK-19	19	5.59

Table 2-3 Summary of sedimentary characteristics relating to ridge and beach samples from Rockingham Bay. Statistical summaries calculated according to the method described by Folk and Ward (1957).

Foredunes		**Mean (texture)**	**Sorting**	**Skewness**	**Kurtosis**	**Source**
Fourteen Mile Beach		medium sand	very well sorted	symmetrical	very platykurtic	Pye (1980)
Cape Bedford Beach		fine sand	very well sorted	symmetrical	very platykurtic	Pye (1980)
Ramsay Bay		medium sand	very well sorted	symmetrical	very platykurtic	Pye (1980)
Shepherd Bay		fine sand	very well sorted	symmetrical	very platykurtic	Pye (1980)
Alva Spit		medium sand	very well sorted	symmetrical	very platykurtic	Pye (1980)
Wangetti Beach		fine sand	very well sorted	symmetrical	very platykurtic	Pye (1980)
Four Mile Beach		fine sand	very well sorted	symmetrical	N/A	Bird (1971)
Rockingham Bay Beach (average)		coarse sand	poorly sorted	symmetrical	platykurtic	Author
Field code	Ridge #					
SEK-1	1	medium sand	moderately sorted	coarse skewed	mesokurtic	Author
SEK-2	2	very coarse sand	moderately sorted	symmetrical	platykurtic	Author
SEK-3	3	coarse sand	moderately sorted	coarse skewed	leptokurtic	Author
SEK-4	4	coarse sand	moderately sorted	symmetrical	mesokurtic	Author
SEK-4-2m		coarse sand	poorly sorted	symmetrical	mesokurtic	Author
SEK-4-3m		coarse sand	moderately sorted	coarse skewed	platykurtic	Author
SEK-5	5	medium sand	moderately sorted	symmetrical	mesokurtic	Author
SEK-6	6	medium sand	mod-well sorted	symmetrical	mesokurtic	Author
SEK-7	7	medium sand	moderately sorted	symmetrical	mesokurtic	Author
SEK-8	8	coarse sand	mod-well sorted	symmetrical	mesokurtic	Author
SEK-9	9	coarse sand	mod-well sorted	symmetrical	mesokurtic	Author
SEK-10	10	coarse sand	moderately sorted	symmetrical	mesokurtic	Author
SEK-10-2m		coarse sand	moderately sorted	coarse skewed	leptokurtic	Author
SEK-10-3m		coarse sand	mod-well sorted	symmetrical	mesokurtic	Author
SEK-11	11	coarse sand	mod-well sorted	symmetrical	mesokurtic	Author
SEK-12	12	coarse sand	mod-well sorted	symmetrical	mesokurtic	Author
SEK-13	13	coarse sand	mod-well sorted	symmetrical	mesokurtic	Author
SEK-14	14	coarse sand	moderately sorted	symmetrical	mesokurtic	Author
SEK-15	15	coarse sand	moderately sorted	symmetrical	mesokurtic	Author
SEK-16	16	coarse sand	mod-well sorted	symmetrical	mesokurtic	Author
SEK-17	17	coarse sand	mod-well sorted	symmetrical	mesokurtic	Author
SEK-18	18	coarse sand	mod-well sorted	symmetrical	mesokurtic	Author
SEK-19	19	medium sand	mod-well sorted	symmetrical	mesokurtic	Author

Summaries of the sediment characteristics are presented in Table 2-3. Sediment within Rockingham Bay ridges are moderately-well to poorly sorted, medium to very-coarse grained sand. Kurtosis values are predominantly mesokurtic, in contrast to the very platykurtic sand within foredunes of northeast Queensland (Pye, 1980). A plot of mean grain size versus sorting values (Figure 2-5) indicates that both beach and beach ridge sediment populations from Rockingham Bay are distinct from those derived from shore-parallel aeolian ridge sediments sampled in the region.

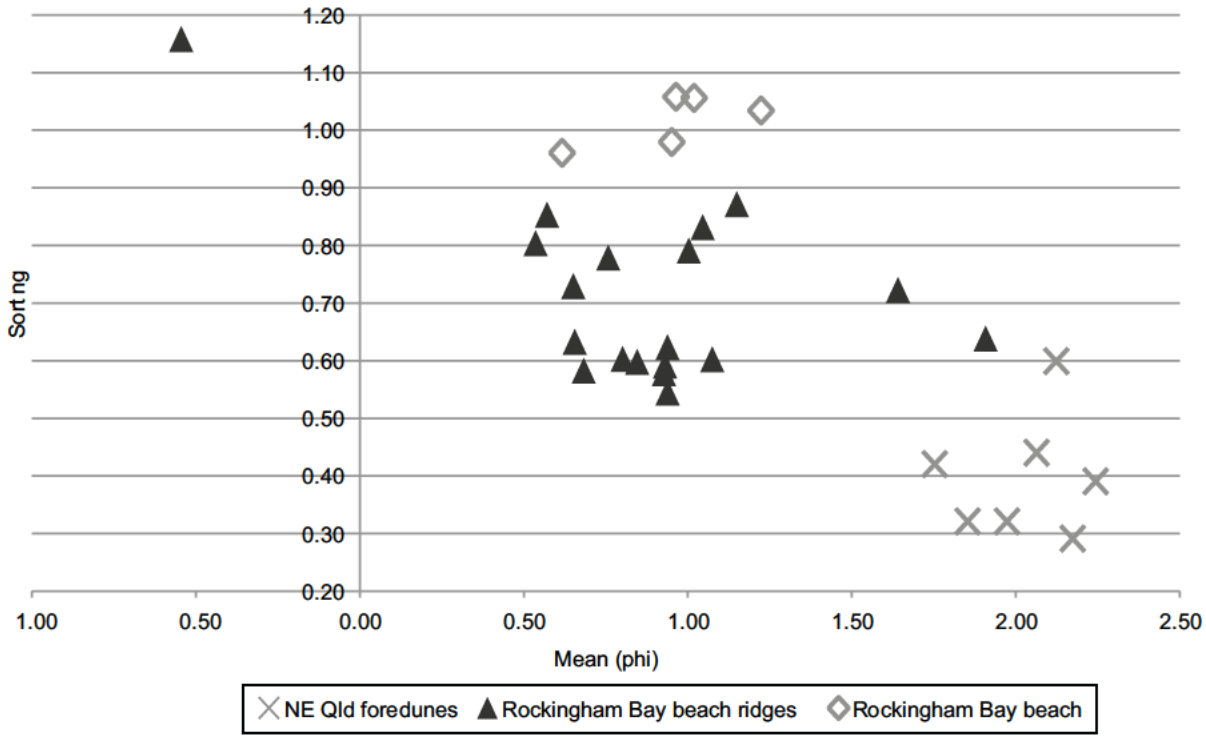

Figure 2-5 Mean grain size (phi) vs sorting (according to measures of Folk and Ward, 1957) for Rockingham Bay beach and beach ridge sediments and northeast Queensland foredune sediments

2.4.3 Chronology

The OSL age determinations show that the Rockingham Bay beach ridge plain increases in age progressively landward with the most landward ridge returning an age of 5.01 ± 0.24 kyr (Figure 2-2). There are two substantial age gaps of 1000 and 900 years between ridges 3 and 4 and ridges 9 and 10. These age gaps occur between 0.44 – 1.44 kyr and 2.48 – 3.38 kyr respectively (Figure 2-2). Ridges were deposited on average every 264 years. Though recurrence interval estimates could be recalculated to 164 years if a combined 1900 years of hiatus in ridge development (discussed below) were

assumed, the cause of age gaps remains unresolved and the more conservative (264-year) interpretation is preferred.

Ridge 4 returned ages of 1.44 ± 0.08 kyr at 1 m depth, 1.53 ± 0.08 kyr at 2m depth and 1.61 ± 0.09 kyr at 3 m depth. Ridge 10 returned ages of 3.38 ± 0.16 kyr at 1 m depth, 3.46 ± 0.19 kyr at 2 m depth and 3.28 ± 0.19 kyr at 3 m depth. The three age determinations from ridge 4 overlap within the uncertainty margins and the same is true of the three ages determined from ridge 10. It is likely that each of these ridges developed at timescales of 100 to 400 years.

2.4.4 Numerical Modelling

The results of the storm surge and shallow water wave modelling are presented in Figure 2-6. The majority of ridges (or deposition of the upper sedimentary units within these ridges) appear to have been deposited by inundations generated during Category 4 to 5 TCs. The modelling suggests that average ridge height (4.6 m AHD) may be reached by combined waves and surge during a TC with a central pressure of between 924 and 934 hPa within the 1σ tidal range and between 913 and 945 hPa within the 2σ tidal range. As a result, even if a TC crossed at close to the highest possible tide during a full nodal tidal cycle (= 95th tidal quintile) the TC would have a minimum intensity of 945 hPa. The highest ridge surveyed is 5.59 m AHD. In order for waves to deposit sediments at the crest of this ridge a total marine inundation, including wave run-up, would be generated by a TC with a central pressure of 912 hPa plus or minus 5 hPa at the 1σ and 16 hPa at the 2σ uncertainty margins.

An inundation of 4.81 m AHD (being the height of ridge 2) requires a TC with a central pressure of 925 hPa ± 5 hPa at the 1σ uncertainty level and ± 16 hPa at the 2σ uncertainty level. If the TC responsible for deposition of the final unit of sediment on ridge 2 occurred at the 95th centile highest tide then it would still need to be a severe Category 3 (942 hPa) event.

Uncertainty margins account for the uncertainty associated with not knowing the height of the tide during a prehistoric TC event. The 2σ probability tidal range of the frequency distribution of the nodal tide curve forms the 2σ

uncertainty margin and likewise for the 1σ uncertainty margin (Nott, 2003). The 1σ tidal range at Rockingham Bay is -0.30 – 0.27 m AHD and the 2σ tidal range is -0.935 – 0.970 m AHD.

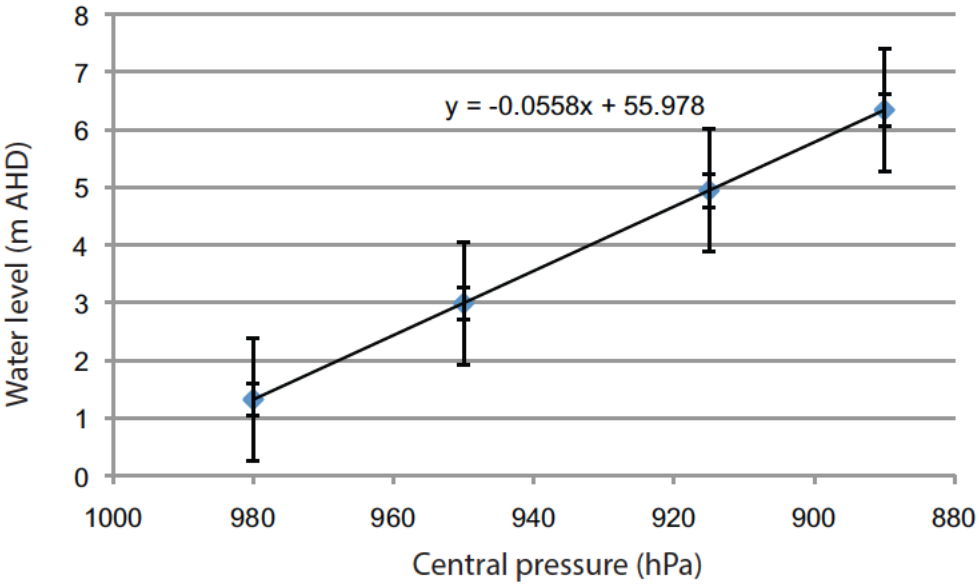

Figure 2-6 Projected inundation levels at Rockingham Bay as a function of system central pressure with 1σ and 2σ error margins indicating the probability of a given tidal level at the time of inundation.

2.5 Discussion

2.5.1 Beach ridge genesis

The sedimentary characteristics of the ridge sediments suggest that waves are responsible for deposition of the beach ridge plain at Rockingham Bay. The ridges here are composed of poorly to moderately sorted, medium to very coarse-grained sands. The beach is also composed of poorly to moderately sorted, medium to coarse-grained sands. Rockingham Bay sediment characteristics are clearly distinguishable from shore-parallel aeolian landforms in this region. In agreement with the findings of Pye (1980) we suggest that aeolian processes have not played a substantial role, if any, in the deposition of this ridge plain. In this region winds capable of transporting coarse-grained sand are largely confined to the passage of TCs. During TC events the marine inundation accompanying extreme winds is likely to submerge the beach. Hence, irrespective of wind strength there would be no sediment source available for aeolian transport of sand when the wind velocity is at its peak during a TC. Wave action, therefore, appears to be the most likely process responsible for deposition of this ridge plain.

The numerical modelling suggests that storm surge and wave action produced by intense TCs are required for water levels to reach the majority of ridge crests at Rockingham Bay. Nott et al. (2009) came to a similar conclusion for the Cowley Bay beach ridge plain approximately 40 km north of Rockingham Bay. At both locations marine inundations generated by Category 4 to 5 TCs are required to deposit the final units of sediment on a beach ridge above 3.5 m AHD (Figure 2-2). Marine inundations generated by lower intensity TCs are abundantly capable of depositing the sedimentary units now preserved at lower elevations within the beach ridges or, in other words, on the ridge crest when it was at a lower elevation. Indeed, initial formation of the beach ridge could have occurred as a result of inundations generated during non-TC events such as high spring tides coupled with strong trade winds generating small waves at shore. As the beach ridge has progressively increased in height the magnitude of the marine inundation, and correspondingly the intensity or severity of the weather system (TC in most cases) necessary to generate this, also needed to increase. Hence these beach ridges have increased their height to the point where lower magnitude TCs can no longer generate marine inundations capable of reaching the ridge crest. Only the most intense TCs generating relatively large marine inundations have been able to deposit sediments onto the ridge crest once that crest reaches a critical elevation – it is these marine inundations that have been responsible for the final form or elevation of the present ridge plain (excluding any later denudation of the ridges over time). The numerical modelling, in this sense, has elucidated the magnitude of the inundation and the intensity or central pressure of the TC responsible for the final sedimentary units forming the ridge crest. As a consequence, and as at Cowley Beach (Nott et al., 2009), we have been able to derive a late Holocene record of severe TC activity from the beach ridges at Rockingham Bay.

2.5.2 Variations in ridge heights

We suggest that the height of a beach ridge at Rockingham Bay is a reflection of the magnitude of the event responsible for deposition of the final sedimentary units on that ridge. Therefore, the ridge heights record the variation in magnitude or intensity of the TCs responsible for depositing these ridges. Ridges 2 to 4 and 10 to 19 were likely deposited (i.e. the final

sedimentary units) by category 4 to 5 TCs (Figure 2-2). Ridges 8 and 9 were likely deposited by category 3 to 4 TCs and ridges 5, 6 and 7 were deposited by category 1 to 3 TCs (Figure 2-2). There appears therefore to have been periods when higher magnitude TCs were responsible for ridge development and periods when lower magnitude TCs were responsible. The higher magnitude TC episodes occurred between 0.13 – 1.55 kyr (ridges 2 - 4) and 3.38 – 5.01 kyr (ridges 10 – 19) and the phase of lower magnitude events between 1.55 -3.38 kyr (ridges 5 – 9) (and particularly between 1.55 – 2.28 kyr). If the beach ridge evidence is considered as a record of TC magnitude and frequency then there appears to have been two phases of high intensity (category 4 – 5) TC activity separated by a phase of lower magnitude TC activity between 1.55 and 3.38 kyr.

Importantly, the absence of a high elevation ridge across a section of the beach ridge plain (or period of time) does not necessarily eliminate the possibility that an intense TC occurred during this interval of ridge deposition. It is possible that one of the lower elevation ridges was at least partly constructed by a high magnitude event. The presence of a low elevation ridge only suggests that high magnitude events did not continue to deposit sediments onto the ridge. It may have been the case that another ridge was developing to the seaward side and this ridge eventually increased in height to a level that precluded further deposition on the next landward ridge. In this situation it is possible that few, if any, further high magnitude events were responsible for deposition of the remainder of the low elevation ridges (i.e. those to the seaward side) or at the very least that the frequency of high magnitude events remained low until the start of the next constructional phase of high elevation ridges. In this sense sections or zones of low elevation ridges suggest a lower frequency of high magnitude TC events and sections of high elevation ridges represent periods of higher frequency high magnitude TC events.

2.5.3 Chronological gaps in the record

The beach ridge record at Rockingham Bay displays two substantial gaps in the chronology. A 1000-year gap occurs between ridges 3 and 4, and a 900-year gap between ridges 9 and 10 (Figure 2-2). There are two possibilities to

explain the origin of these gaps. The first is that ridges were deposited during these periods i.e. between 0.44 – 1.44 kyr (gap between ridges 3 and 4) and 2.48 to 3.38 kyr (gap between ridges 9 and 10) but these ridges were eroded. The second possibility is that ridge construction did not occur during these periods. Differentiating between these two possibilities is difficult. If erosion occurred then it is necessary to understand the processes responsible. An erosional episode is unlikely to be due to a period of higher frequency high magnitude events as TC marine inundations typically cause erosion of the beach and deposition of a sheet of sediments landward of the beach or onto ridge crests. This has been observed several times during the past decade following TC generated marine inundations between Cairns and Cowley Beach and also in Western Australia (Nott and Hubbert, 2005; Nott et al., 2009). Erosion of ridges may be more likely to result from a diminished sediment supply to the coast. This same process, however, could also cause a cessation in beach ridge plain progradation which does not necessitate the erosion of existing ridges and recession of the coast. Examination of the ridges either side of these chronological gaps showed no evidence of erosional episodes in their stratigraphy both at a single site or along the length of the ridge. At present therefore we have no evidence to support the erosion hypothesis to explain the chronological gaps. However, more weight to this hypothesis may be gained when further detailed studies of beach ridge plains are undertaken throughout this region. Chronology of the Cowley Beach sequence indicates a 970 year gap between deposition of the final sedimentary units on ridges 5 and 6 (Nott et al. 2009), which corresponds to a ~590 year overlap (between 0.85 and 1.55 kya) with the 1000 year gap at Rockingham Bay. If other beach ridge sequences also show gaps during the same time intervals then the most likely explanation might be a diminished supply of sediment to the coast resulting in a cessation of progradation. If, however, other gaps occur at differing time intervals then coastal recession might be a more likely hypothesis. Central to our reasoning here is that we would expect a diminished supply of sediment to the coast to be a regional phenomenon most likely caused by a short or longer term change in climatic conditions. This climatic change would likely relate to a decreased frequency of intense rain events that drive sediment delivery to the coast. In this region,

intense rain events are typically associated with TC activity or other tropical weather systems (Baddiley, 2003).

2.5.4 Rate of Coastal Progradation

The rate of coastal progradation at Rockingham Bay has been variable over the past 5,000 years. Ridge plain development here may be separated into three main phases (Figure 2-2). These are:

1. Present – 0.44 kyr (ridges 1 – 3), 215 m of progradation occurred at an average rate of 0.69 myr $^{-1}$;
2. 1.44 – 2.48 kyr (ridges 4 – 9), 435 m of progradation occurred at an average rate of 0.42 myr $^{-1}$; and
3. 3.38 – 5.01 kyr (ridges 10 – 19), 825 m of progradation occurred at an average rate of 0.51 myr $^{-1}$.

Period 2, between 1.44 and 2.48 kyr, experienced a 17.65% decrease in coastal progradation from the previous period (period 3 between 3.38 and 5.01 kyr). Conversely, period 1, between the present and 0.44 kyr experienced a 64.29% increase compared to period 2. These variations in progradation also correspond to the variations in ridge height across the ridge plain i.e. the highest rates of progradation occurred during periods 1 and 3 and the ridges deposited during these episodes are considerably higher than those deposited during period 2. Therefore, the periods that we suggest were associated with more frequent high magnitude TCs correspond to the most rapid phases of coastal progradation. The reasons behind this may be twofold. First, more frequent high intensity TCs were most probably associated with an increase in the frequency of the total number of TCs making landfall or passing close to the coast in this immediate region. Also a higher number of high intensity TCs, with or without a higher frequency of TCs, would likely result in more frequent high intensity rainfall events and therefore high discharge events in streams supplying sediment to the coast. Hence, periods 1 and 3 could have experienced a higher volume of sediment delivered to the coast compared to period 2 when coastal progradation was slower and our modelling suggests was also accompanied by a lower frequency of high intensity TCs. There appears therefore to be a relationship

between ridge height, the intensity of TCs and the rate of coastal progradation.

2.5.5 Sea level and beach ridge height

The development of beach ridge plains has been equated with changes in sea level, particularly a falling sea level, in some regions of the globe. It is likely that sea level has fallen by 1 – 1.5 m in northeast Queensland since 5.50 kyr. Chappell et al. (2003) suggested that sea level fell smoothly due to hydroisostastic flexure of the present coastal margin over this time. Chappell et al. (2003) suggested that sea level fell smoothly due to hydroisostastic flexure of the present coastal margin over this time. Larcombe et al. (1995) suggested sea level remained approximately 1.5 m above present between 6.50 and 3.00 kyr and then fell sharply. And Lewis et al. (2008) advocated two sea level oscillations with low stands around 4.50 kyr and again around 2.50 kyr before rising again to approximately 1m above present at 2.00 kyr and then falling to the present position. The extent to which any of these scenarios has affected the development of this beach ridge plain and particularly the present heights of the beach ridges above sea level today remains uncertain. If sea level has fallen then it could be expected that the elevation of the ridge crests here would progressively diminish with proximity to the coast or as the beach ridges decreased in age. Indeed the highest beach ridge is the most landward and oldest. However, there is little difference in elevation of the ridge crests between ridge 19 and ridge 15 deposited 5.01 and 4.13 kyr, respectively. And while the group of ridges between ridge 14 and 10 are lower than the older ones to their landward side, there is little difference in elevation amongst this group (4.13 to 3.38 kyr). The ridges do then fall progressively in elevation from ridge 10 (4.13 kyr) to ridge 5 (1.55 kyr) but ridges 4, 3 and 2 (1.44 to 0.13 kyr) increase in height to approximately that of the earliest and oldest group of ridges (ridges 19 to 15). This in itself suggests that falling sea level is unlikely to have been a principal driver controlling the elevation of ridge crests across this beach ridge plain over the past 5000 years.

We have already suggested that variations in TC frequency and intensity are the likely chief determinants, along with sediment supply to the coast, of ridge crest height. However, we also need to consider that a higher relative sea

level during the mid-Holocene would mean that the height of a marine inundation would have only needed to be 1 – 1.5 m lower than that required today to generate an equivalent ridge crest height. This means that the final units of sediment deposited onto a ridge crest of certain elevation 5000 years ago would have required a less intense TC (hence relatively lower marine inundation) compared to the present. Figure 2-6 shows that a marine inundation of approximately 5.2 m AHD (relative to current datum) requires a TC of approximately 920 hPa central pressure today compared to approximately 940 hPa central pressure 5000 years ago. It should be noted that a 940 hPa central pressure TC is still an intense storm (category 4).

The question can then be asked whether the beach ridge record at Rockingham Bay indicates that TCs have increased in intensity between 1.44 and 0.13 kyr (ridges 2-4) compared to any other time during the past 5000 years. This is because these ridges are much younger than the other set of higher elevation ridge crests (5.01 to 4.13 kyr) at the landward side of the ridge plain. When these younger ridges were deposited sea level had fallen considerably (1-1.5 m compared to 5.00 kyr) and construction of these ridges would have required more intense TCs to generate marine inundations capable of reaching their crests. To ascertain the answer to this question it is important to consider the relative roles of storm intensity versus sediment supply to the coast and the rate of coastal progradation. The period between 5.01 and 4.13 kyr had the most rapid rate of coastal progradation during the past approximately 5000 years (progradation of 550 m in 880 years = an average rate of 0.625 m yr^{-1}). Factors leading to this relatively rapid progradation include:

- A glut of nearshore sediment compared to today because there would have been a considerable volume of sediment reworked from the continental shelf during the post glacial marine transgression plus new fluvial inputs to the system. (Hopley, 1970).

- Sea level was probably between 1 and 1.5 m higher than present.

In contrast, coastal progradation during deposition of the most recent set of high elevation ridges (ridges 2 – 4) occurred at 160 m over 1110 years

equating to an average rate of 0.14 m yr^{-1}. The majority of the sediment supplied to the nearshore during this period was likely by fluvial sources alone as the volume of sediment available for reworking from the continental shelf would have been less than soon after the termination of the transgression.

The height a ridge can attain may be compromised during a phase of high sediment supply. This is because at these times the presumably faster rate at which an incipient ridge can develop to the seaward side of the main seaward ridge will limit the ability of successive marine inundations to deposit sediment onto the main seaward ridge as that incipient ridge increases in elevation. If the incipient ridge grows rapidly then it will accumulate relatively more sediment when a landward thinning unit of sediments is deposited during a high magnitude marine inundation. Hence the next landward ridge (main seaward ridge) progressively becomes starved of sediment as the next seaward ridge (incipient ridge) increases in height. And while this is true in any prograding beach ridge plain irrespective of the rate of sediment supply to the coast such a scenario will likely be exacerbated by high sediment supply to the coast. This suggests that the period between 5.01 and 4.13 kyr, which had a high rate of sediment supply to the coast, may not necessarily have experienced less intense TCs relative to the period (0.13 to 1.44 kyr) even though the ridge heights attained during both periods is similar. Instead, this more recent period of higher elevation ridge construction relative to sea level may be due to a much lower rate of sediment supply to the coast providing more prolonged (and thus increased) vertical sedimentation of individual beach ridges.

2.5.6 Beach Ridge Record and Tropical Cyclone Risk Assessment

The beach ridge long-term record of TCs from Rockingham Bay has implications for TC hazard risk assessments for this region. The standard approach to TC hazard risk assessment in northeast Queensland typically involves estimating the frequency of high magnitude events by extrapolating from a short historical time series. Such an approach assumes that the stationarity and lack of serial correlation usually apparent in short time series will also be present for time series of greater length. As Nott (2006) has demonstrated this is often not the case and longer time series often display

non-stationarity and serial correlation. The only way to test this assumption concerning short time series is to make comparisons with a much longer time series.

There is a substantial difference in the frequency of high magnitude TCs suggested by the Rockingham Bay beach ridge record compared to that extrapolated from the short historical time series. The latter suggests that high intensity TC events (Category 4-5 events) occur at millennial time scales (McInnes et al., 2003) whereas the geomorphic approach adopted here suggests they occur at centennial time-scales for this location. This implies that non-stationarity is likely to be a real artefact of the longer-term TC time series. Nott et al. (2009) arrived at a similar conclusion for the Cowley Beach beach ridge record. Such a conclusion is also confirmed by an 800 year long high resolution (annual) isotope TC record presented by Nott et al. (2007) suggesting centennial-scale variations in high magnitude TC frequency have occurred in this region over this period.

2.6 Conclusion

The sedimentary and morphological characteristics of the coarse-grained sand beach ridges at Rockingham Bay suggest these features were deposited by waves. Results of numerical storm surge and wave modelling further suggest that these waves were generated by TCs and it was the total marine inundation including waves, storm tide and wave run-up that likely deposited the final units of sediment onto the crests of the beach ridges. As such the beach ridges here record a 5000 year history of the magnitude and frequency of landfalling TCs in this immediate region. The Rockingham Bay beach ridge plain record suggests that there has been considerable variation in the frequency and magnitude of TCs at this location since the mid Holocene. High magnitude events occurred between 0.13 – 1.55 kyr (ridges 2 - 4) and 3.38 – 5.01 kyr (ridges 10 – 19) and a phase of lower magnitude events between 1.55 -3.38 kyr (ridges 5 – 9) and in this period there was a phase of very low magnitude events between 1.55 to 2.28 kyr. This long-term record of TCs further suggests that variations in the frequency of high intensity TC inundation events have occurred at centennial time-scales and the return intervals of these events is unlikely to have been consistent since the mid

Holocene. The results of this study suggest this pure sand beach ridge plain is a more sensitive record of long-term TC behaviour than the coral shingle and shell / sand beach ridge records found elsewhere throughout this broader region. As such these sand beach ridge records may help to elucidate a more realistic regional long-term climatology of these natural hazards.

Chapter 3: Juxtaposed beach ridges and foredunes within a ridge plain

Forsyth, A. J., Nott, J., Bateman, M. D., and Beaman, R., 2012, Juxtaposed beach ridges and foredunes within a ridge plain - Wonga Beach, northeast Australia: Marine Geology, v. 307-310, p. 111-116.

Abstract

Reports describing aeolian foredunes and wave-derived beach ridges juxtaposed within a single coastal barrier complex are rare, perhaps because morphological similarities make the two ridge types difficult to differentiate. This study of an approximately 4500 year-old sand ridge plain in northeast Queensland, Australia using landform morphology, sedimentology and luminescence chronology suggests that ridge plain development here has been interrupted along part of the sequence by localised alterations in coastal sedimentation. A switch from coarse to fine-grained sand supply along one part of the beach has caused the development of prograding foredunes in the northeastern sector of the sequence over the past 700 years. Contemporaneously, coarser textured beach ridges have continued to form behind the remainder of the beach. The result is a ‘complex barrier’ where a single ridge plain contains both foredunes developed through high frequency, low intensity events and beach ridges developed through high intensity, low frequency events associated with intense tropical cyclones.

3.1 Introduction

One process or another is generally considered responsible for depositing coastal ridge plains composed of sand. Hesp (1999) defined beach ridges as triangular to convex, swash aligned, swash and storm wave built ridges formed in the backshore at or above the normal spring high tide level. They are principally or purely marine deposits. Foredunes are convex shore-parallel features that form through aeolian sand deposition within backshore vegetation (Hesp, 1999). In some locations both wind and waves are thought to have played a role in developing a ridge over time (Davies, 1957; Taylor and Stone, 1996). In this instance each of these processes contributes to the development of individual ridges within the ridge plain at different times. Hence these processes vary temporally but occur within the same morphological unit. It is rare that geoscientists have observed or considered that ridges with similar shore-parallel morphology but having different origins can develop within a single coastal ridge plain. Hence wind may be entirely responsible for ridge growth at one location and elsewhere on the same ridge plain waves have deposited the sediment causing ridge growth.

A ridge plain containing at least fourteen shore parallel ridges at Wonga Beach in northeast Queensland, Australia appears to have developed through the action of both wind and waves operating at different times along the length of the embayment. We present a detailed analysis of this ridge plain including two surveyed transects across the ridge plain, textural and statistical analysis of the sands composing the ridges at numerous locations along the length of the embayment, the results of numerical wind and wave modelling to help determine the origin of the ridges and an Optically Stimulated Luminescence (OSL) chronology.

3.2 Regional setting

Wonga Beach (Figure 3-1) fronts a 10 km long barrier with an easterly to southeasterly aspect located toward the north of the humid tropical sector (as defined by Bird and Hopley, 1969) of northeast Queensland, Australia. Tidal range in the area is approximately 3.4 m, with the very highest tides reaching 1.81 m above Australian Height Datum (AHD) (NTF, 2007b). Wonga Beach, at latitude 16.3˚S, has a tropical climate. The average annual rainfall at nearby

Mossman is 2010 mm, over 70% of which falls between December and April (BOM, 2011a). Tropical cyclones (TCs) also bring substantial amounts of rain. The region around Wonga Beach experiences a relatively low wave energy climate in which significant wave heights of 2 to 3 m occur less than 0.1% of the time, predominantly during summer months, coinciding with the passage of TCs (QEPA, 2005).

3.3 Materials and Methods

Methodologies were devised to determine whether the sand ridges at Wonga Beach were deposited by aeolian or wave processes. Methods included examining the sedimentary characteristics of the ridges. Surveying of ridge topography and analysis of possible wave and storm surge conditions necessary to deposit sand onto a ridge of a given elevation above mean sea level was also conducted.

Patterns in ridge development were assessed using chronological and surveying studies performed on two separate (northern and southern) transects. Sediment sampling was also carried out on both transects and on six additional shorter transects (Figure 3-1). Northern transect samples are identified by the prefix NT; southern transect samples are prefixed ST; and the six shorter transects were named in order of their position ranging from north to south as T1, T2, T3, T4, T5 and T6. Sample nomenclature uses these prefixes followed by a number assigned according to the sequence of individual ridges identified along each transect.

3.3.1 Sediment Collection

Sediment samples were collected from thirteen ridges on the northern transect (Figure 3-1) and nine ridges along the southern transect. A total of forty-four samples, two from each ridge crest, were collected from 100 cm depth along these transects by hammering light-proof PVC tubes into the side of 1.3 m deep pits dug into the crests of the ridges and then sealing the tubes. One sample from each ridge crest was well packed and carefully protected from solar radiation for OSL age determination. The second sample was used for sediment analysis, as described below.

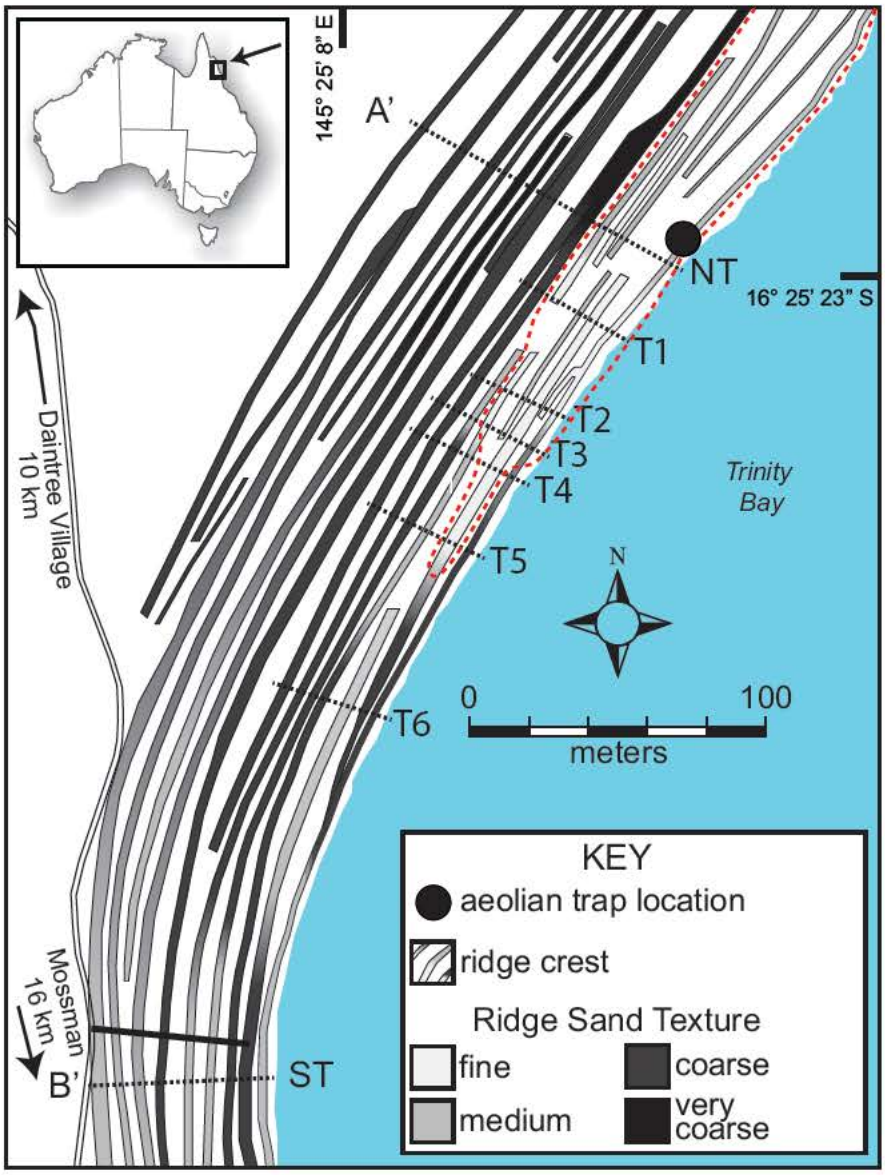

Figure 3-1 Map depicting sampling and survey transects, the aeolian sediment collection site and interpretations of ridge sediment textures at Wonga Beach. The dotted line indicates the inferred extent of foredune development.

Two further sediment sampling programs were undertaken. First, 36 samples from 100 cm depth were taken from below ridge crests located along transects T1 to T6. Second, 10 mid-beach samples were taken from 30 cm depth; 8 from where each transect intersected the shore plus two additional samples. These two sampling programs were designed to compare beach and ridge sedimentary characteristics.

Ridge sediments were taken for dating at 2 and 3 m depth (below ridge crests) from ridges NT-10 and NT-11 to assess the rate of ridge growth within the error margin of individual OSL dates. These sites are labelled so that 'NT-10' refers to the sample collected from a depth of 1 m, NT-10-2m was

collected from a depth of 2 m and NT-10-3m was collected from a depth of 3 m. To avoid exposure to light, these samples were taken by sand augur approximately two hours after dusk then stored in light-proof PVC tubes.

3.3.2 Aeolian Sediment Collection

A sediment trap constructed to specifications described by Leatherman (1978) was deployed adjacent to sample site NT-1 (Figure 3-1) during a relatively strong southeasterly trade wind event. The trap was oriented shore-normal, toward the onshore wind, for a 5-minute period at 1100 hrs on 7 August 2010. Average wind velocity over this period was 7.1 ms^{-1} measured adjacent to the sediment trap at 1 m elevation using a hand-held anemometer.

3.3.3 Sediment Size Analysis

Samples for textural analysis were split using a series of sieves graduated at 4000, 2800, 2000 and 1400 µm. These sieved fractions were measured as grain size frequency per unit weight. The remainder of each sample was then analysed in a Malvern Mastersizer 2000 providing measurement of grain size per unit volume. The raw data were statistically analysed using Gradistat Version 6.0 (Blott, 2008) and then calibrated by recalculating the Malvern results as a fraction of the remainder of the sieved sample.

3.3.4 OSL Dating

The cleaned and extracted quartz from twenty-six samples, representing all ridges along the two Wonga Beach transects, were dated using OSL (Table 2-1). Each sample was measured using 24 aliquots comprising of 9.6 mm in diameter upon which a monolayer of quartz grains in the size range of 180 to 250 µm were mounted. The samples were initially assessed using infrared stimulated luminescence (IRSL) to establish whether samples had feldspar contamination; none was found. Palaeodoses (De) were calculated based on luminescence measurements carried out using the single aliquot regenerative (SAR) approach (Murray and Wintle, 2003).

Table 3-1 Wonga Beach OSL age determinations and associated data.

Field code	Lab. code	Depth (cm)	De (Gy)	Dose rate (Gy/kya)	Age (years before 2008)
Northern Transect					
NT-1	Shfd08053	90	0.05 ± 0.001	1.289 ± 65	40 ± 10
NT-4	Shfd08054	90	0.48 ± 0.001	1.326 ± 65	360 ± 20
NT-5	Shfd08055	90	0.53 ± 0.001	1.512 ± 72	350 ± 20
NT-6	Shfd08056	90	0.60 ± 0.001	1.643 ± 84	370 ± 20
NT-7	Shfd08057	90	1.85 ± 0.03	2.731 ± 152	670 ± 40
NT-8	Shfd08058	90	2.47 ± 0.03	2.757 ± 166	890 ± 50
NT-9	Shfd08059	90	2.94 ± 0.03	2.499 ± 145	1180 ± 70
NT-10	Shfd08060	90	4.46 ± 0.05	3.294 ± 187	1360 ± 80
NT-11	Shfd08061	90	5.09 ± 0.1	2.504 ± 138	2020 ± 120
NT-12	Shfd08062	90	5.79 ± 0.08	2.986 ± 178	1940 ± 120
NT-12-2m	Shfd08068	200	6.18 ± 0.1	3.053 ± 153	2030 ± 110
NT-12-3m	Shfd08069	300	4.98 ± 0.07	2.818 ± 157	1770 ± 100
NT-13	Shfd08063	90	5.42 ± 0.08	2.562 ± 130	2120 ± 110
NT-13-2m	Shfd08066	200	5.87 ± 0.08	2.647 ± 134	2220 ± 120
NT-13-3m	Shfd08067	300	5.32 ± 0.09	2.878 ± 167	1850 ± 110
NT-14	Shfd08064	90	9.1 ± 0.1	2.384 ± 134	3820 ± 220
NT-15	Shfd08065	90	9.92 ± 0.1	2.180 ± 117	4550 ± 250
Southern Transect					
ST-1	Shfd08070	90	0.25 ± 0.006	2.907 ± 171	80 ± 10
ST-2	Shfd08071	90	0.30 ± 0.006	3.200 ± 161	90 ± 10
ST-3	Shfd08072	90	0.69 ± 0.02	2.838 ± 167	240 ± 20
ST-4	Shfd08073	90	0.85 ± 0.03	3.131 ± 166	270 ± 20
ST-5	Shfd09145	110	2.35± 0.07	3.320 ± 173	710 ± 40
ST-6	Shfd08075	90	6.34 ± 0.05	3.915 ± 208	1620 ± 90
ST-7	Shfd08076	90	4.48 ± 0.12	2.850 ± 155	1570 ± 100
ST-8	Shfd08077	90	7.06 ± 0.19	3.347 ± 173	2110 ± 120
ST-9	Shfd08078	90	7.28 ± 0.18	2.325 ± 121	3130 ± 180

As part of the SAR protocol a preheat of 220° C for 10 seconds prior to OSL measurement was used to remove unstable signal generated by laboratory irradiations. Several of the samples had weak naturally acquired OSL signals, though all showed a marked increase in OSL signal with additional artificial laboratory dose. As a result, all aliquots measured had recycling ratios within 10% of unity indicating adequate correction for sensitivity shifts within the SAR protocol. All samples had a low degree of replicate scatter reflected in over-dispersion values of <10% with unskewed De distributions. This is taken to indicate that sediment was well bleached prior to burial. In order to establish a De for age calculation purposes, the central age model (Roberts et al., 2000) was applied to the all the aliquots for each sample (excluding only outlier points outside two sigma of the mean).

To establish the dose rate for each sample, naturally occurring potassium (K), thorium (Th) and uranium (U) concentrations were determined by inductively

coupled plasma mass spectrometry and converted to annual dose rates using data from Adamiec and Aitken (1998), Aitken (1998) and Marsh et al. (2002) incorporating attenuation factors relating to sediment grain sizes used, density and palaeomoisture. In terms of the latter, present-day moisture values as measured in the laboratory with a ± 5% error were used to incorporate seasonal and longer-term fluctuations in moisture that the samples may have endured since burial. The contribution to dose rates from cosmic sources was calculated using the expression published in Prescott and Hutton (1994). Ages are shown in Table 2-1 and are shown in years from the time of measurement (2008) with one-sigma confidence intervals that incorporate systematic uncertainties with the dosimetry data, uncertainties with the palaeomoisture content and errors associated with the De determination.

3.3.5 Surveying

Two transects across the ridge sequence at Wonga Beach were surveyed by dumpy (spirit) level. Vertical datum (AHD) was calculated using tidal level at the time of survey compared to the tidal reading from nearby Port Douglas. We expect the error using this approach to be less than ±10 cm.

3.3.6 Numerical Modelling

Numerical storm tide (GCOM2D tropical cyclone storm tide model) and shallow water wave models (SWAN model) (Hubbert and McInnes, 1999) were used to determine the conditions necessary to generate a marine inundation (including wave run-up) equal to or greater than the height of the beach ridges. The procedure followed the described in detail by Nott et al. (2009). Hence, wave run-up was assumed to play a substantial role in the formation of the beach ridges at Wonga Beach and it was assumed that the marine inundation including wave run up was equal to the height of the ridges. The marine inundation (wave set-up = 12% of Hs and wave run-up = 30% Hs) of Nott et al. (2009) was used here.

A series of model runs were undertaken to determine the sensitivity of storm surge height to changes in cyclone translational velocity, radius of maximum winds (Rm), angle of cyclone approach and cyclone central pressure. Bathymetry and coastal configuration data were fixed for the model runs and incorporated within the model as a 250 m resolution digital elevation model

(DEM). A nested grid approach was used whereby a 100 m resolution fine grid was superimposed upon a 1000 m resolution coarse grid. Sensitivity tests carried out on this basis suggested that the storm surge and shallow water wave model runs generating the largest possible surge for this site which included storm parameters of Rm = 30 km, TC translational velocity = 30 km and a south-westerly TC track direction. The Rm and cyclone translational velocity of 30 km and 30 km/hr respectively are the historical means for TCs in this region (McInnes et al., 2003).

3.4 Results

3.4.1 Sedimentary Character

A scattergram (Figure 3-2 (a)) relating mean size to skewness of Wonga Beach ridge and beach sediment samples indicates that two distinct sedimentary units comprise this barrier. One unit confined to several ridges in the northeast of the study area is composed of fine- to medium-grained, unimodal sand that form a distinct population within relatively narrow skewness margins. A similarly distinct population representing the same ridge samples is apparent in a plot of mean grain size against sorting (Figure 3-2 (b)). There are several morphological and spatial contrasts between ridges populated by these relatively fine textured sediments and the remainder of the ridges. For example, ridges here are relatively low, discontinuous, narrow and of low amplitude. Scattergram plots representative of these ridge samples correspond with both aeolian sediment trap data collected here (Figure 3-2) and are in agreement with aeolian foredune data reported from elsewhere in the region (Bird, 1971; Pye, 1980). The parts of the ridge plain composed of these fine textured sediments are therefore likely foredunes and they are located exclusively in a zone of the barrier identified in Figure 3-1.

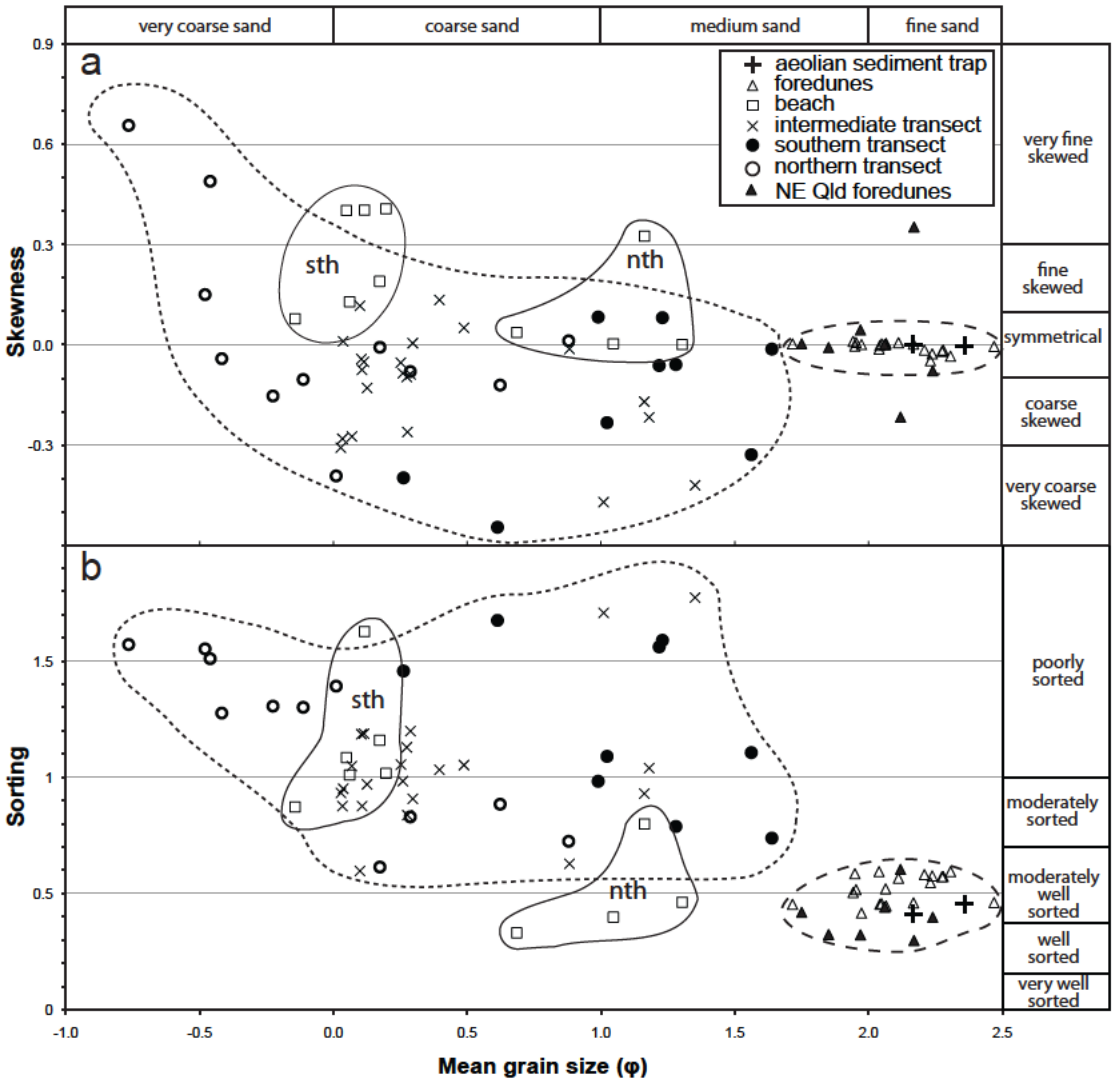

Figure 3-2 Scattergram plots of (a) mean versus graphic skewness values and (b) mean versus graphic sorting values of Wonga Beach ridge and beach samples in comparison with equivalent values from northeast Queensland foredunes as presented by Pye (1980).

The second unit composed of medium- to very-coarse grained beach sand forms the remainder of the sequence. Mean grain size analysis indicates that Wonga Beach ridge samples collected from outside the foredune zone range in sediment particle size between 321.1 and 1700.0 µm (1.639 and -0.766 ϕ). These samples plot across the skewness and sorting grades (Figure 3-2).

There is a contrast in beach sediment characteristics between the northern and southern section of the embayment. In the north the sediments are finer and better sorted. Analysis suggests that the spatial distribution of fine and coarse beach sediments is similar to the adjacent ridge.

3.4.2 Chronology

The chronology (Table 2-1) indicates that each ridge increases in age progressively landward when uncertainty margins are taken into account. The thirteen dated ridges of the northern transect range in age from 0.40 ± 0.001 to 4.55 ± 0.25 kya (Figure 2-3 (A)), indicating that the average period between ridge-building events is approximately 350 years. The nine dated ridges of the southern transect range in age from 0.08 ±0.01 to 3.13 ± 0.18 kya (Figure 2-3 (B)), indicating that the average period between ridge-building events is approximately 348 years.

Extra samples were collected on each of ridges NT-10 and NT-11 in order to ascertain rates of vertical ridge accretion. The three samples from NT-10 produced ages of 1.94 ± 0.12 kya at 1 m depth, 2.03 ± 0.11 kya at 2 m and 1.77 ± 0.10 kya at 3 m depth. The three samples from ridge NT-11 produced ages of 2.12 ± 0.11 kya at 1 m, 2.22 ± 0.12 kya at 2 m and 1.85 ± 0.11 kya at 3 m depth. The three age determinations from each of NT-10 and NT-11 overlap within the uncertainty margins suggesting that the ridge accretion rate of each is statistically indistinguishable.

3.4.3 Ridge Elevation

The thirteen sand beach ridge crests surveyed along the northern transect have an average height of 3.93 m above AHD. There is a trend of general increase in ridge height with distance from shore, with the highest point in the northern transect being 5.49 m above AHD at NT-12 and the lowest is 3.17 m at NT-1 (Figure 2-3). Ridge and swale patterns between ridges NT-4 and NT-13 are distinct and readily identifiable. However, low and relatively flat topography between NT-1 and NT-4 meant that swales and ridges here were difficult to distinguish in the field. Ridge height also generally increases with distance from shore along the southern transect. Only ridge ST-7, the tallest along this transect, deviates from that trend at 4.26 m.

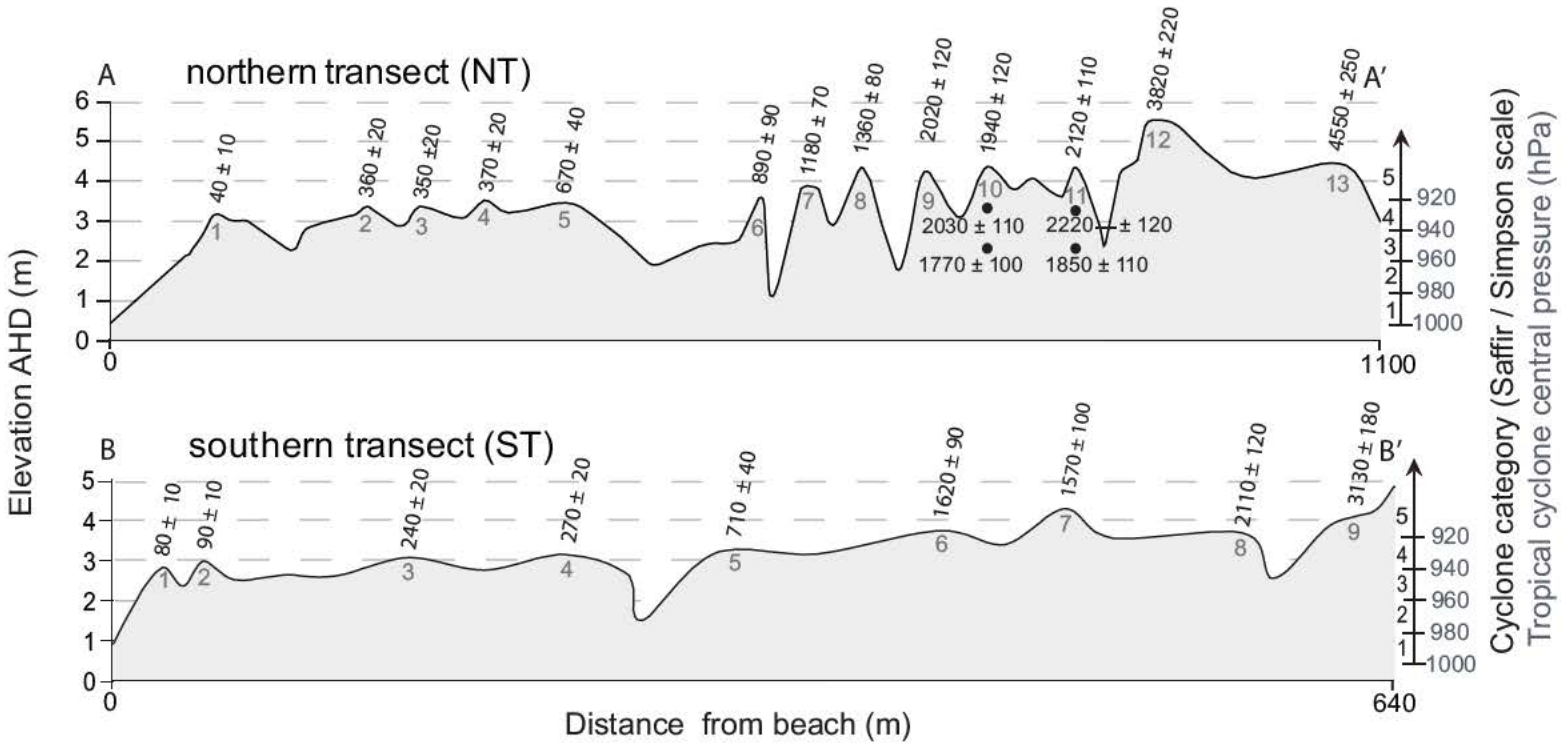

Figure 0-1 Cross-sections of two Wonga Beach ridge plain transects, showing height of ridges above AHD, OSL dates and modelled TC intensity required to produce inundation level equal to ridge height based upon mean tide level. Origin (0) denotes the location of shoreline at the time of survey.

3.4.4 Numerical Modelling

The results of the storm surge at mean tide and shallow water wave modelling are presented in Figure 2-3. Results suggest that the majority of ridges would require Category 4 to 5 TCs (Saffir-Simpson scale) to deposit the upper sedimentary units within beach ridges here. Uncertainty margins correlate with estimates of the tide during a prehistoric TC event based on the full nodal tide curve. Hence the 1σ probability tidal range of the frequency distribution of the nodal tide curve forms the 1σ uncertainty margin and likewise for the 2σ uncertainty margin. The 1σ tidal range at Wonga Beach is -0.27 to 0.280 m AHD and the 2σ tidal range is -0.90 to 1.84 m AHD.

3.5 Discussion

Ridges forming the ridge plain at Wonga Beach are composed of two distinct sedimentary units. Fine- to medium-grained sand dominates both the beach and ridges 1 to 4 in the northeastern sector of the plain. These finer-grained ridges were deposited over the past 0.67 kya. The ridges throughout the remainder of the barrier, however, are composed of sediments ranging between medium- to coarse-grained sand like the beach at the southern end of the ridge plain. This distinct zonation in clastic assemblages suggests that there has been a relatively recent change in the processes delivering sediment to the northern section of the coast.

3.5.1 Ridge development processes

Wind is likely responsible for depositing ridge sediments in the northeastern sector of the study area. The sedimentary characteristics of ridges in that sector are in agreement with descriptions of aeolian foredunes from this region (Pye, 1980) and elsewhere (Mason and Folk, 1958; Thom, 1983). The predominant southeasterly wind direction, southeasterly beach aspect and availability of fine-grained sand along this section of the shore combined with a vegetated back beach provide a likely setting for aeolian transportation and deposition. Ridge sands identified within the four ridges here are finer textured than the adjacent beach and are characteristically similar to those sediments collected from the aeolian sediment trap (Figure 3-2). We suggest therefore that aeolian processes are principally responsible for deposition of ridges 1 to 4 in the northeastern sector of the ridge plain.

The sedimentary characteristics suggest that the remainder of the ridges in this plain were not deposited by wind. Plots of mean against skewness and mean against sorting (Figure 3-2) offer little distinction between these ridge samples and those collected from along the southern part of the beach suggesting that waves have been responsible for their deposition. In this region winds able to transport the clasts of coarse-grained sand that comprise these ridges are principally limited to the passage of TCs and during such events the marine inundation accompanying extreme winds is likely to submerge the beach. Hence, there would be no sediment source available for aeolian transport of sand irrespective of wind strength when wind velocity is at its peak during a TC. The numerical modelling suggests that storm surge and wave action produced by intense (≥ Category 4) TCs are required for water levels to reach the crests of most beach ridges in this sequence (Figure 2-3). And differences in ridge heights within the sequence are likely due to variations in the intensity of TCs responsible for depositing the final sedimentary unit at each ridge crest. This conclusion is similar to those reached for beach ridge plains at Cowley Beach (Nott et al., 2009) and Rockingham Bay (Forsyth et al., 2010). Therefore, the Wonga Beach ridge plain is best described as a ‘complex barrier’ comprising foredunes (ridges 1 to 4 in the northeastern sector of the barrier) and beach ridges. Complex barriers are barriers comprising two types of landforms (cf. McKee, 1979).

The ridge chronology and morphology at the northern end of the Wonga Beach embayment show that ridges NT-2 to NT-4 reach an elevation of 3.38 to 3.54 m AHD (Figure 2-3) and were deposited between 0.67 and 0.37 kya. The first four ridges at the southern end were deposited between 0.08 and 0.27 kya and reach an elevation of 2.82 to 3.12 m AHD. The group of four northern ridges therefore appear to have been deposited before their four southern counterparts suggesting they are a separate group of ridges despite appearing to be continuous morphological features. It is possible that after 0.67 kya there was a change in transport and sedimentation processes in the near shore zone and on the beach at the northern end of the embayment. This was a change from a coarser grained beach to a finer grained beach for reasons that remain unclear at this stage. This resulted in the northern sector

of the beach containing sediment that could be entrained by wind and as a consequence four low aeolian ridges developed. The subsequent wave action responsible for deposition of the four later ridges at the southern end of the beach where coarse-grained sands still formed the beach was unable to contribute sediment to the crests of the northern four ridges. This is because these northern ridges had already attained an elevation higher than the wave action responsible for depositing the first four southern ridges (Figure 2-3). Hence no wave built ridges have developed since 0.67 kya in the northeastern sector of the ridge plain because the existing aeolian ridges there were too high for waves to achieve further accretion.

3.5.2 Sea level and beach ridge height

Parallels have been drawn between beach ridge plain development and changes in sea level, particularly a falling sea level, in some regions (Carter, 1988). Chappell et al. (1983) suggested that northeast Queensland sea levels fell smoothly through hydroisostastic flexure of the coastal margin since the mid-Holocene. Larcombe et al. (1995) suggested sea level remained approximately 1.5 m above present between 6.50 and 3.00 kya and then fell sharply. Lewis et al. (2008) proposed sea level oscillations with low stands around 4.50 kya and again around 2.50 kya before an approximately 1m rise above present at 2.00 kya before falling to the present level. The general trend of decreased ridge height with proximity to shore at Wonga Beach may suggest a smoothly decreasing late-Holocene sea level. However, regional trends in beach ridge plain elevations suggest that these landforms are not a reliable indicator of sea level. For example, the depositional record from Cowley Beach would suggest a relatively unchanged sea level between 4.91 to 0.85 kya if ridge heights were a key determinant. And the Rockingham Bay ridge plain would suggest that sea level fell almost 2 m between 3.30 to 1.55 kya then rose again to remain at almost prior levels until the present. It is highly unlikely that these three sites that occur within an approximately 100 km length of coast have experienced such varied sea levels. Therefore, the extent to which any reported sea level scenario has affected the development of the Wonga Beach beach ridge plain, and particularly the present heights of the beach ridges above sea level today, remains uncertain. Instead, as suggested above, it is likely that differences in beach ridge height are due to

variations in the frequency and intensity of TCs along with sediment supply to the coast. And a higher relative sea level during the mid-Holocene would mean that the height of a marine inundation would only have needed to be 1 – 1.5 m lower than that required today to deposit an equivalent ridge crest height.

3.6 Conclusion

The sedimentary and morphological characteristics of the prograding ridge sequence at Wonga Beach suggest that both beach ridges and foredunes have developed here within a single coastal barrier complex. Beach ridge development (i.e. developed from wave action) has been occurring here until approximately 0.70 kya when a change in nearshore transport and beach sedimentation processes resulted in the northern end of the beach changing from a medium- to coarse-grained sand environment to a fine-grained one. As a consequence four ridges or foredunes developed due to aeolian processes over an approximately 400-year period. Subsequent wave action during TCs resulted in beach ridges developing at the southern end of the embayment but this wave action was unable to contribute to the ridges or foredunes at the northern end because these features were already at an elevation above which wave action could reach. This resulted in development of a complex barrier where both aeolian and wave formed ridges exist adjacent to each other.

Chapter 4: The origin of centennial- to millennial-scale chronological gaps in storm emplaced beach ridge plains

Forsyth, A. J., Nott, J., Rhodes, E., O'Grady, D., In Review, The origin of – centennial- to millennial-scale chronological gaps in storm emplaced beach ridge plains Submitted to Earth-Science Reviews

Abstract

Recent studies of tropical cyclone surge and wave emplaced beach ridge plains have shown these sequences often contain centennial- to millennial-scale gaps in their chronologies. Two explanations for the gaps exist – they are due to erosion, or alternatively a cessation or substantial slowing of depositional processes suggestive of a quieter phase in intense storm activity. Differentiating between the two is important for uncovering reliable long-term storm histories from these sequences. We use landform morphology, sediment texture and luminescence chronology to determine the origin of substantial chronological gaps in a plain containing more than 100 shore-parallel ridges composed of fine-grained sand located in northeast Australia. We identify and describe the characteristics associated with both erosional and non-erosional gaps. The erosional gaps are associated with changes in orientation between ridge sets and often a high ridge with hummocky topography that appears to have been disturbed by aeolian activity. River floods likely caused the partial erosion of ridge sets. Non-erosional gaps do not display these morphological characteristics and are likely associated with quiescence in severe tropical cyclone activity. These geomorphic and chronological signatures can be used to identify different sorts of gaps in other ridge plains and are an important tool in the reconstruction of long-term storm histories from these coastal landforms. The data also suggests that fine-grained ridges can, like their coarse-grained counterparts, be deposited by storm waves and surge and their texture need not necessarily be indicative of the processes responsible for ridge development.

4.1 Introduction

One of the striking characteristics of long-term sedimentary records of tropical cyclones (TCs) globally is they display centennial- to millennial-scale chronological gaps (Nott and Forsyth, 2012). In the case of hurricane overwash deposits (Liu and Fearn, 2000; Donnelly and Woodruff, 2007; Woodruff et al., 2009) it is difficult to ascribe erosional processes to the gaps for the records are composed of sand layers within otherwise fine-grained sediment back barrier lagoon environments. Chronological gaps within beach ridge plains that record long-term TC histories (Nott, 2003; Nott et al., 2009; Forsyth et al., 2010) are possible via two causes; erosion and removal of ridges, and periods of slower or no ridge building likely associated with a quiescence in intense TC activity.

Beach ridge plains are extensive globally and this is especially so within many regions that are impacted by TCs (Scheffers et al., 2011), hence their potential for preserving long-term records of TCs is high. Differentiating between chronological gaps caused by erosion versus those due to periods of less intense TC activity is critical for uncovering accurate records of these storms.

An extensive sand beach ridge plain at Cungulla, approximately 30 km southeast of Townsville in NE Queensland, Australia, offers an opportunity to identify the key characteristics of erosional gaps versus those due to less intense TC activity. This is because the Cungulla sequence includes ridges arranged into distinctly unconformable sets with some ridges displaying smooth convex-up shaped profiles while others display hummocky profiles. Unlike other beach ridge plains studied in this region the plain here appears to contain evidence of gaps associated with erosion along with non-erosional chronological gaps. We present high-resolution LiDAR data to highlight the ridge morphologies, a statistical analysis of ridge sediments, a detailed Optically Stimulated Luminescence (OSL) chronology and results of numerical wind and wave modelling to help identify the characteristics useful for differentiating between erosional and non-erosional chronological gaps in these beach ridge plains.

4.2 Setting

The ridge plain at Cungulla is fronted by a 13 km long fine- to medium-grained sand beach stretching between the Haughton River and Cape Ferguson situated in the west of Bowling Green Bay (Figure 4-1). The barrier complex appears to have developed as an asymmetrical cuspate foreland tying Cape Cleveland and several isolated outcrops to the mainland. Ridges are generally oriented northwest, arranged sub-parallel to the modern shore and the majority have sharply recurved terminations. The ridge plain is approximately 5 km wide at its widest point and the ridges are, as shown later, Holocene in age. The weathered appearance of sediments comprising several ridges at the very rear of the sequence suggests that they are Pleistocene in age.

Ridge soils vary in degree and kind of profile development. Most are freely drained fine-textured sandy soils with uniform texture profiles, although some weakly developed podzols (spodosols) occur in the swales (Hopley, 1970). Sections of the sand ridges give way inland to salt pans and erosion cut-outs that are flooded with saline waters on the highest tides while seasonal runoff from Mt Elliott drains into extensive sedge swamps. These areas are comprised of Quaternary muds and silts that, further inland, are replaced by the soils and sediments of the coastal plain. Tidal range is approximately 3.84 metres at Cape Ferguson, with the very highest tides reaching 2.15 metres above Australian Height Datum (AHD) (DERM, 2010).

Mountainous outcrops comprising Cape Cleveland, The Cone and Feltham Cone are distinct in the predominantly low relief area around Cungulla. These outcrops are largely composed of adamellite and granite of Permian to Mesozoic age with small areas of older intermediate lavas and pyroclastics (Gregory, 1969). The area is drained seaward into Bowling Green Bay by the Haughton River, which runs for 5-6 months of the year, and a number of minor creeks. In addition, seasonal floodwaters from the Burdekin River overflow northward to discharge into Bowling Green Bay (Hopley, 1970).

Cungulla, at latitude 19.35°S, is situated centrally in the seasonally wet tropics (Dalla Pozza, 2005) and experiences pronounced wet and dry (<60 mm/month) seasons. The ridge plain is located in a rain shadow between substantially higher rainfall areas to both the north and the south. Annual

average precipitation is 1249 mm at Giru and 1165 mm at Cape Cleveland (BOM, 2011). The rainfall occurs predominantly in summer and 80% of that falls in the months December to April (BOM, 2011). A high proportion of this rainfall is generated by convergence of the southeasterly trade winds into the monsoon trough. Tropical cyclones also bring substantial amounts of rain.

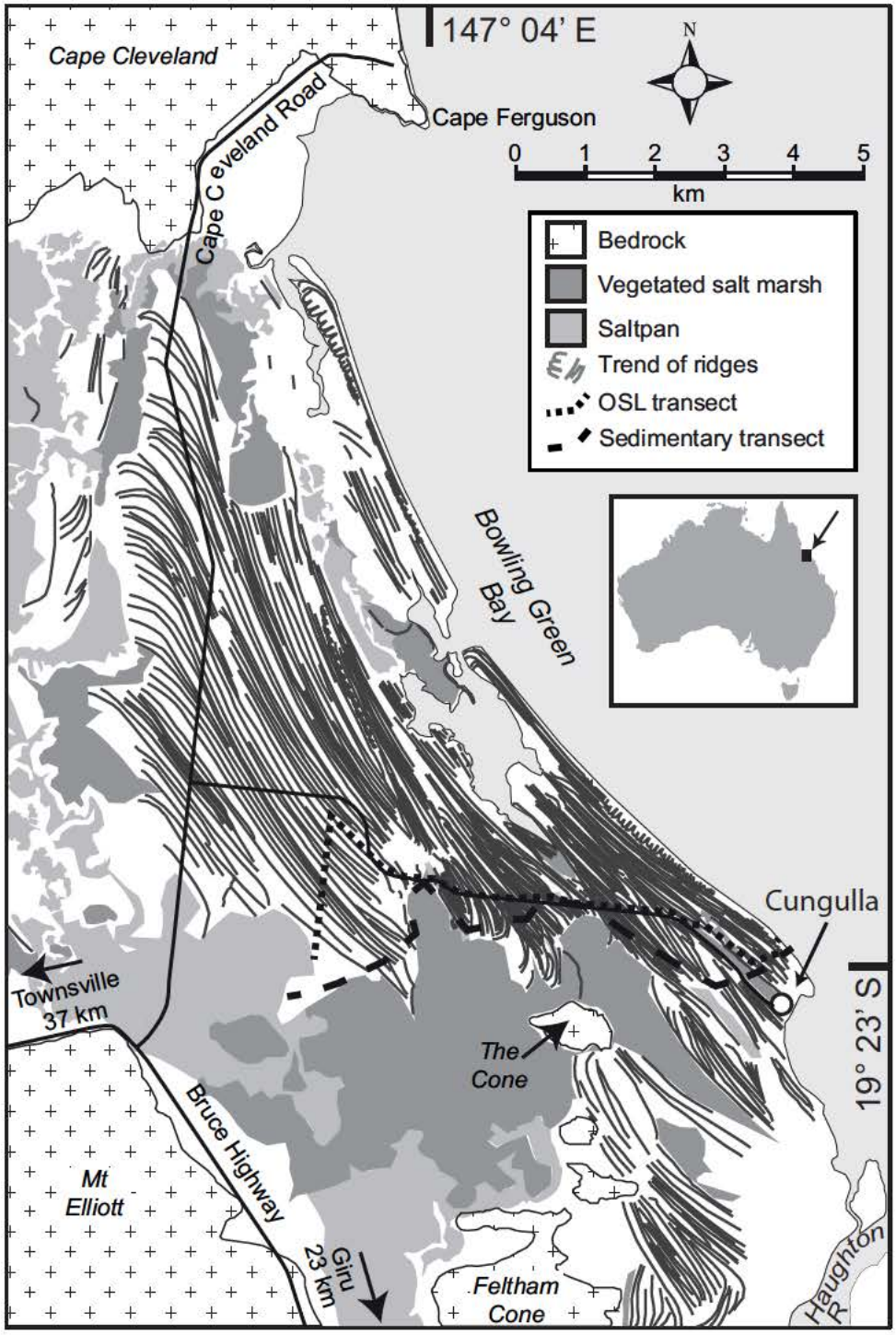

Figure 4-1 Location map of the Cungulla ridge plain including delineation of mapped ridge crests.

The region around Cungulla experiences a relatively low energy wave climate. Observations indicate that southeasterly trade winds averaging 5 – 16 knots (9 – 30 kmh^{-1}) predominate along the northeast Queensland coast and these winds are the chief source of wave energy at shore (Nott et al., 2009). The Great Barrier Reef (GBR) limits the wave fetch in this region and the longest fetch at Cungulla is approximately 75 km to the northeast. The coast rarely experiences waves in excess of 0.5 m in height with wave periods of 2 – 4 s even during strong trade wind conditions. Significant wave height (Hsig) records for 15 m water depth near Cape Cleveland indicate that Hsig ranges between 0.2 m to 0.6 m for 50 % of the time with a wave period of 3 to 5 s (Figure 4-2) (DERM, 2011). The type of waves recorded can be generally categorised as either sea waves generated inside the GBR with a peak period (Tp) of 2.5 to 5.0 s; or swell waves generated outside of the GBR with a Tp of 5.0 to 9.0 s. Maximum recorded average Hsig between 1975 and 2011 was 5.46 m on February 3, 2011 during the passage of TC Yasi (peak intensity 929 hPa) (DERM, 2011). Significant wave heights of 2 to 6 m occur less than 0.5% of the time, predominantly during summer months coinciding with the passage of tropical cyclones. Tropical cyclones can generate significant wave heights of up to 10m and wave periods of 12 s between the GBR and the mainland (Nott et al., 2009). Such storms can also generate storm surges several meters above the normal tidal range.

4.3 Methodology

Numerous sedimentary coasts include shore parallel / sub-parallel ridge features. The processes operating to develop these landforms differ between locations. Consequently there are several interpretations for the term ‘beach ridge’. Several recent reviews have sought to clarify their origins (e.g. Tanner, 1995; Taylor and Stone, 1996; Hesp, 1999, 2006; Otvos, 2000) and some authors have suggested that beach ridges consist exclusively of wave built features (Johnson, 1919) whereas others such as Tanner (1995) include both wave built and aeolian constructed ridges or combinations of the two depositional processes. Here we refer to beach ridges *sensu* Hesp (1999; 2006) who defined beach ridges as principally or purely marine deposits of triangular to convex form located in the backshore at or above the normal

spring high tide level. They are swash aligned and deposited by swash and storm wave processes (Hesp, 1999).

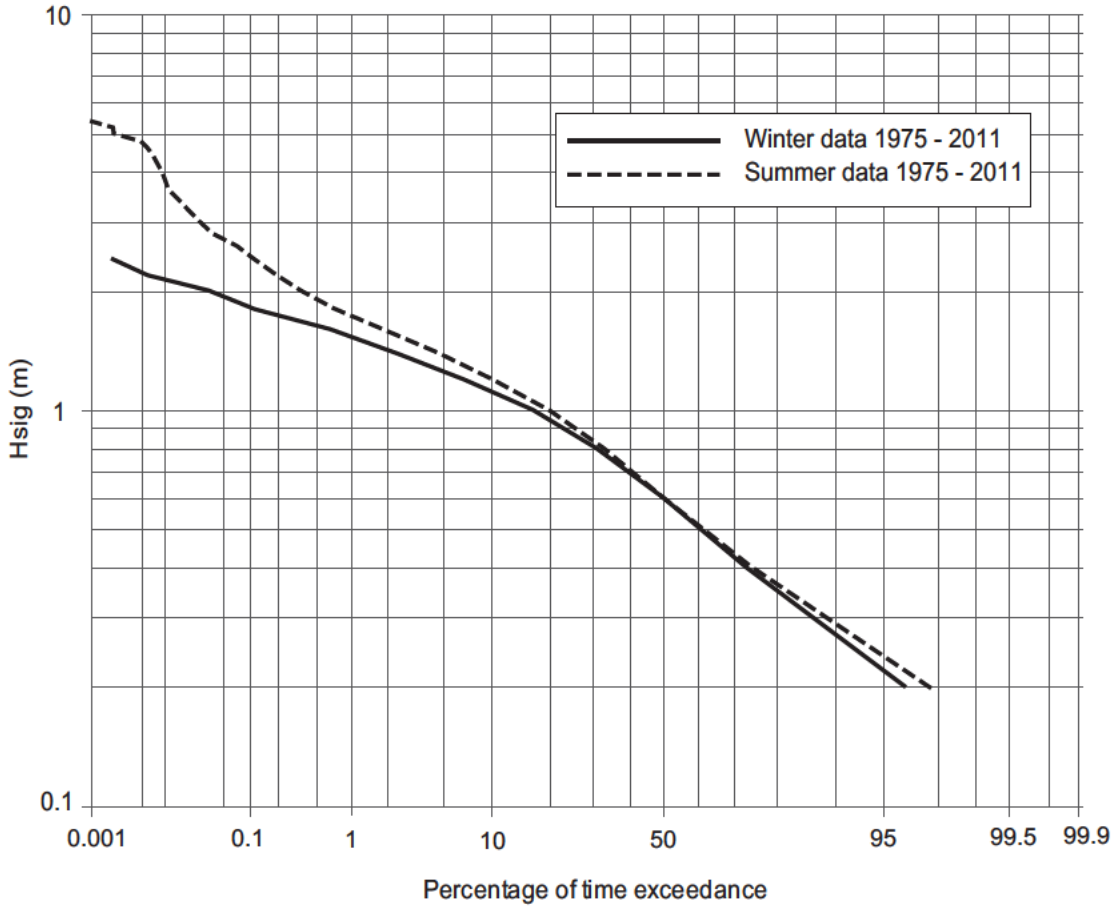

Figure 4-2 Average wave height (Hs) from wave rider buoy in 15 m depth water, Cape Cleveland, Townsville from 1975 to 2011

A series of methodologies were engaged to determine the origin of chronological gaps and whether the sand ridges at Cungulla were deposited by aeolian or wave processes. These methods included examining patterns in textural characteristic data of ridge sands and indications of depositional patterns in ridge development using OSL dating and LIDAR imagery. Analyses of ridge topography and of possible wave and storm surge conditions necessary to deposit sand onto a ridge of a given elevation above mean sea level was also conducted using numerical wave and surge models.

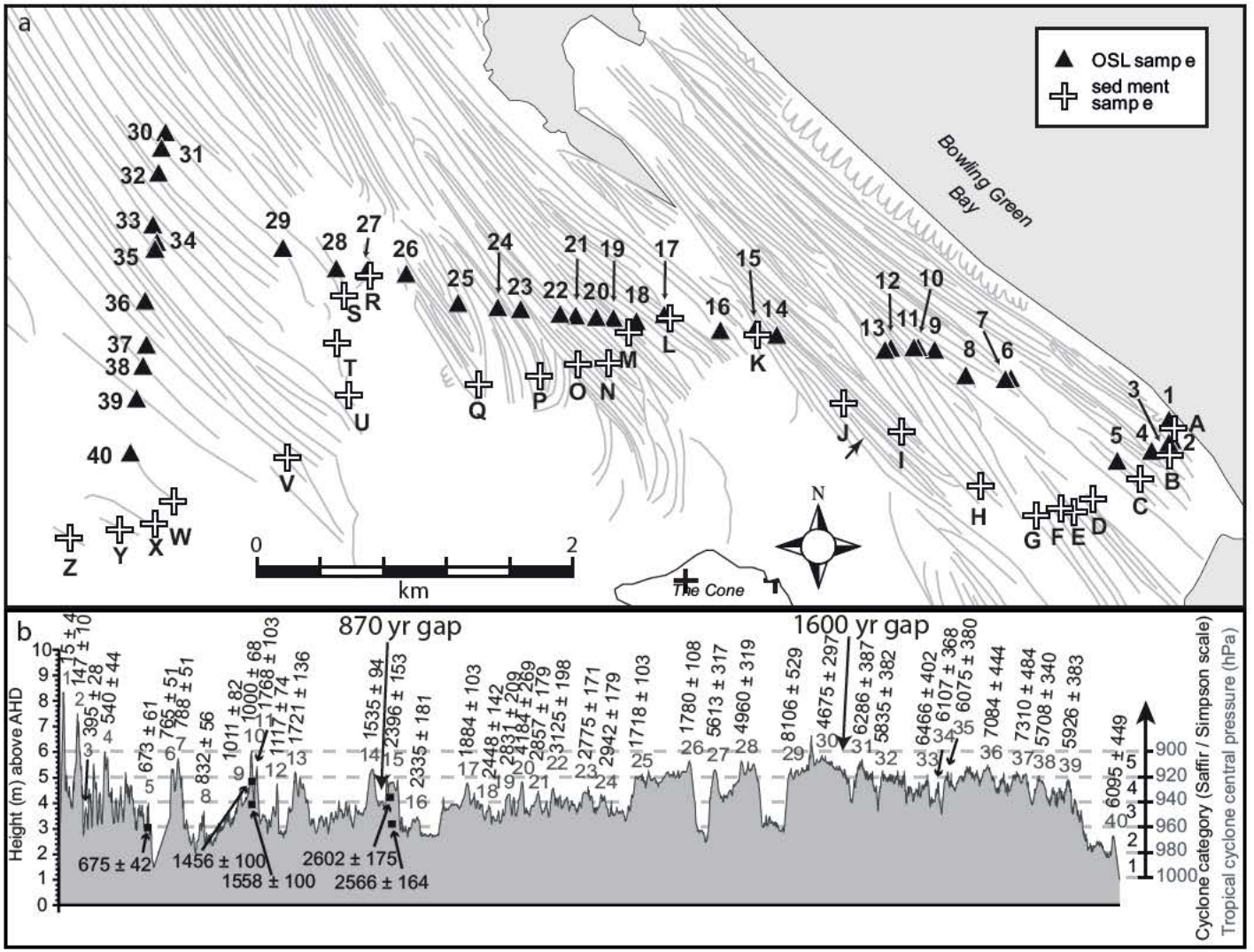

Figure 0-1 Graphic representation of Cungulla ridge plain elevation data overlain by: (a) OSL and sediment sampling sites; and (b) Cross-section of Cungulla ridge plain showing height of ridges above AHD, OSL dates with error margins and modelled TC intensity required to produce inundation level equal to ridge height based upon mean tide level.

4.3.1 Sediment Collection

A total of forty-five sediment samples were collected for the purpose of OSL age determination from forty ridges on a traverse across the Cungulla ridge sequence (Figure 4-3 (a)). Forty samples were collected from 85 to 100 cm below ridge crests by hammering lightproof PVC tubes into the side of 1.3 m deep pits and then sealing the tubes - samples were carefully protected from solar radiation and precautions were made to ensure that the sample tubes were well packed to eliminate subsequent mixing of sediments. Dating of ridge sediments taken at different depths of a vertical profile were collected to provide an indication of the rate of ridge emplacement. For this reason, three sediment samples from 2 m depth were taken from ridges 5, 10 and 15 and two further sediment samples from 3 m depth were taken from ridges 10 and 15.

4.3.2 OSL Analysis

Forty ridges from within the Holocene outer barrier complex at Cungulla were dated using the optically stimulated luminescence technique (Table 2-1). Each sample was measured for luminescence using twelve-multigrain single aliquots of 180–212 mm quartz grains, adopting a single aliquot regenerative-dose (SAR) protocol (Murray and Wintle, 2003). The samples were assessed initially using a preliminary procedure to determine infrared stimulated luminescence (IRSL) contamination, signal sensitivity, approximate equivalent dose (De), and an indication of the degree of inter-aliquot variability. Low IRSL values were observed for all samples, suggesting that good quartz separation had been achieved. Preheat conditions adopted for these samples were 220° C for 10 s for preheat 1 and 200° C for 10 s for preheat 2. The samples displayed high OSL signal sensitivities and also excellent recycling behaviour; the mean value for all samples was within 3% of unity. Generally low thermal transfer values were observed, though the younger samples showed some aliquots with values up to around 10% of the natural signal. Dose rates were calculated from determinations of U, Th and K concentration based on fusion–dissolution inductively coupled plasma mass spectrometry and optical emission spectrometry. These dose rate values were corrected for grain size attenuation and past water content, using 5% ± 5%. The cosmic dose rate estimation and a soft component were included for shallower samples.

4.3.3 Textural Analysis

Hopley (1970) carried out textural characteristic analyses of Cungulla ridge plain sands in an attempt to detail sea level changes and ridge plain sand provenance. Sands were collected during that study by using a post-hole auger along the transect shown in Figure 4-1. Data describing a total of 241 samples collected from 26 ridges and from along the beach are presented below. Samples were taken 0.3 m from the crest of every third or fourth ridge along the sequence down to a depth of 2.4 m. Sieve sizes used for analysis were related to the phi (ϕ) scale and sieves ranged in size between 4.5 ϕ and 0 ϕ (63 µm to 1000 µm) at half ϕ intervals. Analysis of sample statistics was calculated according to the method described by Friedman (1961).

4.3.4 LiDAR

LiDAR data were used to assist in mapping of the Cungulla ridge plain (Figure 2-3 and Figure 2-4). The LiDAR data were acquired by the Queensland Government Department of Environment and Resource Management as part of a larger North Queensland-wide LiDAR acquisition project and supplied under an agreement with the Townsville City Council as 1 m-resolution xyz (easting, northing, elevation) ASCII files. The source data horizontal datum used the Geocentric Datum of Australia 1994 (GDA94) with a UTM Zone 55 South projection. The vertical datum is AHD (or approximate MSL).

The data were imported into GRASS GIS. Horizontal resolution was maintained at 1m, avoiding the need for interpolation. The resultant individual tiles were then mosaicked into a single digital elevation model (DEM) covering the entire region of interest. Sample site coordinates were used as transects from which vertical profiles were generated at full 1m spatial resolution. The vertical profiles were then rendered in Scalable Vector Graphics (SVG) format (Figure 4-3 (b)). Expected error using this approach is ±0.15 m at the 1σ uncertainty margin according to metadata associated with the original LiDAR dataset.

Table 4-1 OSL age determinations and associated data from Cungulla.

Field Code	Ridge	Depth (m)	De (Gy)	Age (years before 2006)
CB-01	K1535	0.85	0.032	15±4
CB-02	K1536	0.85	0.305	147±10
CB-03	K1537	0.85	0.988	395±28
CB-04	K1538	0.85	1.204	540±44
CB-05	K1539	0.85	1.469	673±61
CB-06	K1540	0.85	1.719	765±51
CB-07	K1541	0.85	1.634	788±51
CB-08	K1542	0.85	1.598	832±56
CB-09	K1543	0.85	2.575	1011±82
CB-10	K1544	0.85	3.224	1000±68
CB-11	K1545	0.85	5.574	1768±103
CB-12	K1546	0.85	3.170	1117±74
CB-13	K1547	0.85	4.307	1721±136
CB-14	K1548	0.85	4.004	1535±153
CB-15	K1549	0.85	5.850	2396±153
CB-16	K1550	0.85	5.327	2335±181
CB-17	K1551	0.85	6.100	1884±103
CB-18	K1552	0.85	6.016	2448±142
CB-19	K1553	0.85	5.585	2831±142
CB-20	K1554	0.85	8.392	4184±269
CB-21	K1555	0.85	6.677	2857±179
CB-22	K1556	0.85	6.992	3125±198
CB-23	K1557	0.85	7.591	2775±171
CB-24	K1558	0.85	7.556	2942±179
CB-25	K1559	0.85	3.438	1718±103
CB-26	K1560	0.85	3.565	1780±108
CB-27	K1561	0.85	14.143	5613±317
CB-28	K1562	0.85	12.414	4960±319
CB-29	K1563	0.85	16.362	8106±529
CB-30	K1564	0.85	11.408	4675±297
CB-31	K1565	0.85	13.418	6286±387
CB-32	K1566	0.85	13.174	5835±382
CB-33	K1567	0.85	11.454	6466±402
CB-34	K1568	0.85	12.006	6107±368
CB-35	K1569	0.85	13.453	6075±380
CB-36	K1570	0.85	13.513	7084±444
CB-37	K1571	0.85	14.260	7310±484
CB-38	K1572	0.85	12.257	5708±340
CB-39	K1573	0.85	22.901	5926±383
CB-40	K1574	0.85	11.938	6095±449
CB-05	K1575	2.00	1.320	675±42
CB-10	K1576	2.00	2.884	1456±100
CB-10	K1577	3.00	2.627	1558±100
CB-15	K1578	2.00	5.246	2602±175
CB-15	K1579	3.00	4.934	2566±164

4.3.5 Numerical Modelling

Numerical storm tide (GCOM2D tropical cyclone storm tide model) and shallow water wave models (SWAN model) (Hubbert and McInnes, 1999) were used to determine the conditions necessary to generate a marine inundation (including wave run-up) equal to or greater than the height of the ridges. The procedure used in this study followed the methodology described in detail by Nott et al. (2009) and Forsyth et al. (2010). Hence, wave run-up was assumed to play a substantial role in the formation of the beach ridges at Cungulla and it was assumed that the marine inundation including wave run up was equal to the height of the ridges. The marine inundation (wave set-up = 12% of Hs and wave run-up = 30% Hs) of Nott et al. (2009) was used here.

A series of model runs were undertaken to determine the sensitivity of storm surge height to changes in cyclone translational velocity, radius of maximum winds (Rm), angle of cyclone approach and cyclone central pressure. Bathymetry and coastal configuration data were fixed for the model runs and incorporated within the model as a 250 m resolution DEM. A nested grid approach was used whereby a 100 m resolution fine grid was superimposed upon a 1000 m resolution coarse grid. Sensitivity tests carried out on this basis suggested that the storm surge and shallow water wave model runs generating the largest possible surge for this site included storm parameters of Rm = 30 km, TC translational velocity = 30 km and a south-westerly TC track direction. The Rm and cyclone translational velocity of 30 km and 30km/hr respectively are the historical means for TCs in this region (McInnes et al., 2003).

Uncertainty margins are associated with not knowing the height of the tide during a prehistoric TC event. The 2σ probability tidal range of the frequency distribution of the nodal tide curve forms the 2σ uncertainty margin and likewise for the 1σ uncertainty margin (Nott, 2003). The 1σ tidal range at Cungulla is -0.38 to 0.35 m AHD and the 2σ tidal range is -1.12 to 1.19 m AHD.

4.4 Results

The Cungulla plain contains over 100 shore-parallel ridges ranging in elevation between 2.8 and 8.4 m above height datum (AHD). Most ridges in

the sequence are curvilinear in planform and have sharply re-curved terminations (Figure 4-1).

4.4.1 Ridge Plain Morphology

LiDAR imagery suggests the occurrence of two distinct ridge types within the Cungulla ridge plain. Type 1 ridges have shore-parallel crests, are arranged in sets that are unconformable (Figure 4-4 (a)) and are fairly uniform in height, width and orientation. Type 2 ridges contain modern and relic blowouts and parabolic forms, they are relatively wide and tall and these ridges generally mark the most seaward ridge of each unconformable set of Type 1 ridges (Figure 4-4). The contrasting morphology of these different ridge types suggests that processes responsible for their development may also differ.

The 40 sampled ridges located along the OSL transect (Figure 4-3 (b)) are numbered with the ridge located adjacent to the beach designated as ridge 1 and the most landward ridge designated as ridge 40 (Figure 2-3). LiDAR imagery suggests that blowouts and parabolic forms are widespread along ridge 1 and in places spill over on to ridge 2 forming non-linear ridge crests (Figure 4-4). Ridges 1 and 2 therefore form Type 2 ridges and their morphology is reminiscent of coastal aeolian dunes. Also, a group of Type 1 ridges terminate along the landward flank of ridge 2. This unconformable relationship suggests that the shore-parallel ridges have been truncated by one or more erosion events and that ridges 1 and 2 have developed through re-working of eroded Type 1 ridge sediments. The imagery suggests that this pattern of truncated Type 1 ridges terminating on the landward side of Type 2 ridges is repeated in numerous instances along unconformities in the sequence. These truncations appear to be generally restricted to the southern part of sequence. Elsewhere, Hopley (1970) suggested that the saline flats composed of black clay soils and saltpan with sticky black muds shown in Figure 4-1 indicate the location of eroded areas around and within the ridge sequence.

4.4.2 Ridge Sediments

The 26 ridges sampled by Hopley (1970) (Figure 4-1) are named in alphabetical order. The ridge located adjacent to the beach is referred to as

ridge A and the most landward ridge along this transect as ridge Z (Figure 4-3 (a)).

4.4.3 Mean Grain Size

The overall mean size of all samples analysed was 2.5799 ϕ, which means that Cungulla beach ridge sediments lie within the fine-grained sand category according to the Udden-Wentworth scale. Mean grain sizes of Cungulla beach and ridge plain sediment samples ranged between 1.7660 ϕ and 3.2470 ϕ (105 µm and 294 µm), an overall range of 189 µm. The mean size of all samples was 2.6227 ϕ (162 µm). Mean grain size within individual ridges showed remarkable conformity with a maximum intra-ridge standard deviation of 38 µm from ridge G (Figure 4-3 (a)). Mean grain size along the beach was 2.4380 ϕ (185 µm), of ridge A was 2.8085 ϕ (143 µm) and of ridge B was 2.4643 ϕ (181 µm).

4.4.4 Sorting

The standard deviation of all ridge samples ranged between 0.3270 ϕ and 0.9241 ϕ, which suggests that the Cungulla sediments are moderately sorted according to the verbal Inclusive Graphic Standard Deviation scale (Folk and Ward, 1957). There was a remarkable conformity within individual ridges with a maximum intra-ridge standard deviation of 0.1295 ϕ from ridge T (Figure 4-3 (a)). The beach had a standard deviation of 0.6000 ϕ, ridge A of 0.3946 ϕ and ridge B of 0.4516 ϕ. No correlation was apparent between ridge sets and degree of sorting.

4.4.5 Skewness

Skewness has been used to successfully differentiate between dune and beach sands (e.g. Friedman, 1961; King, 1966; Sevon, 1966; Chappell, 1967; Pye, 1982). Skewness (phi) values for ridge samples ranged between -0.6758 (ridge H) and 0.4081 (ridge N) and a comparison of stratified sampling shows considerable intra-ridge variability (Figure 4-5). Values for the modern beach, ridge 1 and ridge 2 were -0.4133, -0.9427 and -0.8235 respectively. These results suggest that sorting values of the modern beach sands falls within the range of ridge sediment sorting values and that ridges 1 and 2 are generally better sorted than the remaining ridge samples.

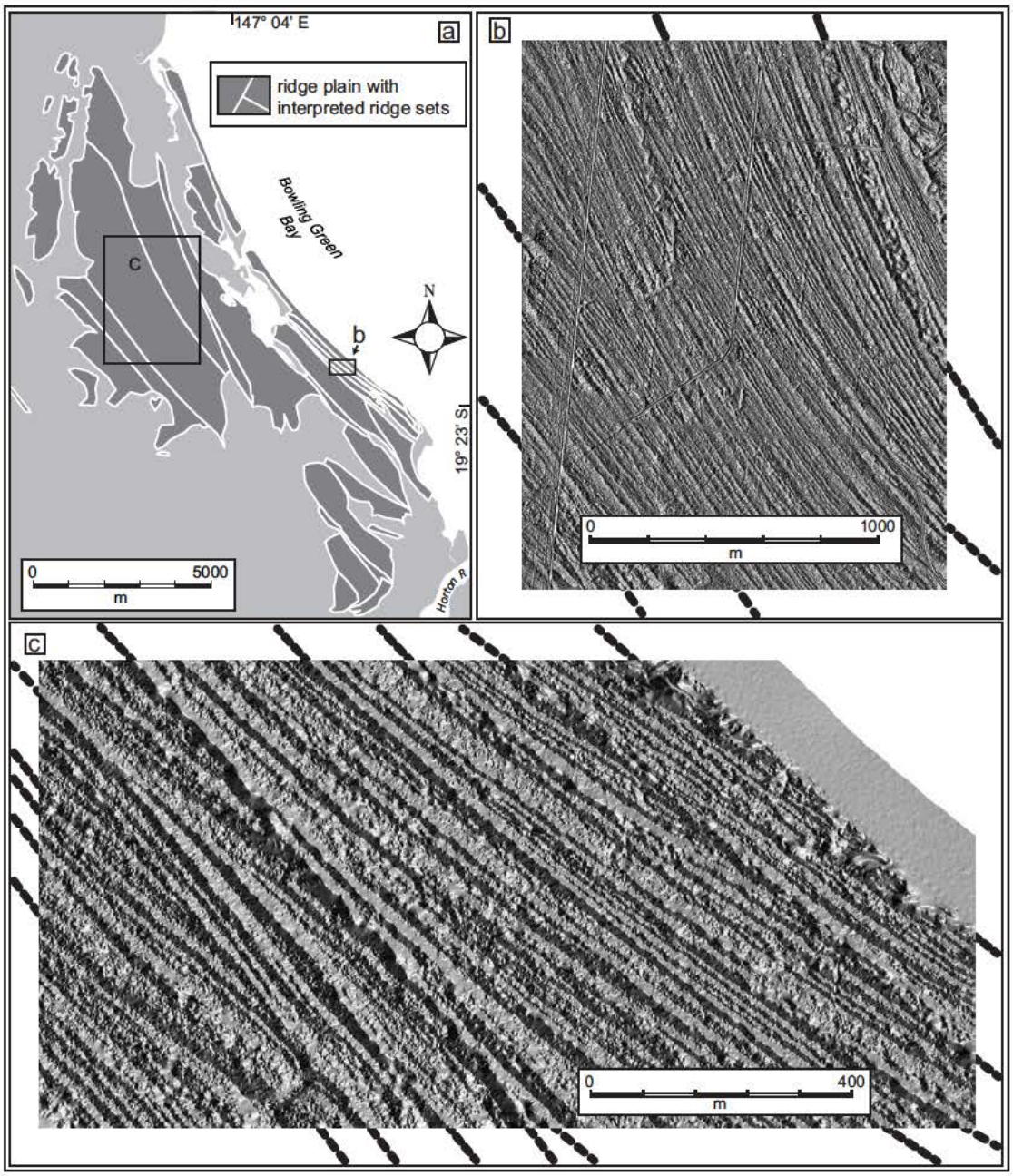

Figure 4-4 (a) Map showing the location of ASPECT analysis results and (b and c) sample images of ASPECT analysis data. Dotted lines indicate the orientation of Type 2 ridges and all other ridges in the sequence are likely Type 1 ridges. Solid lines indicate truncations in Type 1 ridges.

4.4.6 Kurtosis

Kurtosis values of ridge samples were generally high ranging between 2.3722 and 12.6189. Though values varied within each ridge, mean values for each ridge varied little (ranging between 3.6880 and 5.9271) with the exception of ridge H (7.0139). Mean kurtosis values for the beach, ridge 1 and ridge 2 were 2.6761, 6.4136 and 6.5814 respectively.

4.4.7 Local area sediment analysis

A number of studies have successfully discriminated between beach and dune sands using grain size distributions (e.g. Mason and Folk, 1958; Friedman, 1961; Chappell, 1967). However, it was recognised that the relatively small range of determined mean size values contained in Cungulla ridges required a different approach. Hopley (1970) designed a pilot study to determine the origin of Cungulla ridge sands using eighteen beach samples and ten dune samples from the Townsville area. The results of that study are presented here.

Mean sediment size values (phi) of dune and beach samples from the Townsville area fell within the range of Cungulla ridge samples (1.2965 ϕ to 3.2470 ϕ). The mean skewness value of beach sands was -1.0943 and dune sands was 0.0449. Some overlap occurred in the dataset suggesting that these values were not prescriptive of the depositional process. Therefore, the standard deviation for beach sands (0.7599) and for dune sands (0.5667) was calculated. These values were used to designate the probable deposition process of ridge samples. Interpretation was carried out as follows:

1. Skewness values beyond 2 standard deviations of the mean dune sand value (lower than -1.0885) were defined as ‘almost certainly beach sand’;
2. Skewness values between 1 standard deviation and 2 standard deviations of the mean dune sand value (from -1.0884 to -0.5218) were defined as ‘probably beach sand’;
3. Skewness values between 1 standard deviation and 2 standard deviations of the mean beach sand value (from -1.5217 to - 0.3344) were defined as of ‘indeterminate’ origin; and
4. Skewness values beyond 2 standard deviations of the mean beach sand value (greater than -0.3344) were defined as ‘almost certainly dune sand’

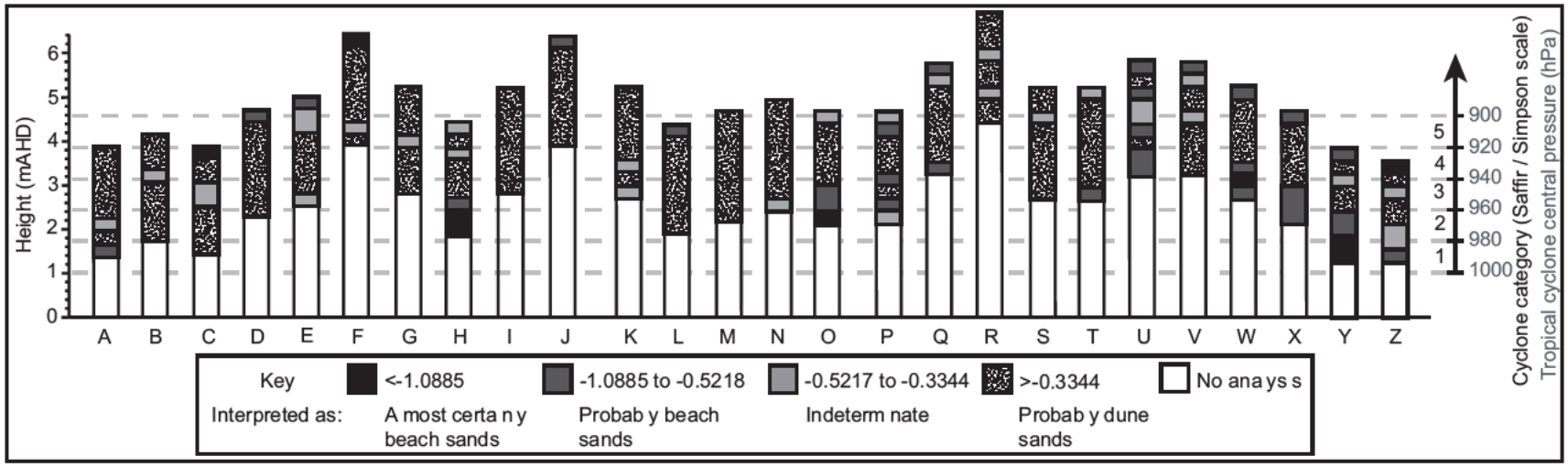

Figure 0-2 Cross-section of Cungulla ridge plain sediment data (after Hopley, 1970) showing height of ridges above AHD, skewness with interpretation and modelled TC intensity required to produce inundation level equal to ridge height based upon mean tide level.

Interpretations of Cungulla ridge sands are presented in Figure 4-5. These results suggest that marine processes are responsible, at least in part, for deposition of the 26 sampled ridges in this sequence. Most notable of these are a number of ridges that include well-elevated sedimentary units composed of 'likely beach sands'. These include ridges C, D, E, F, J, L, P, Q, U, V, W, X, Y and Z. Otherwise, the data suggest that sediments comprising the upper 2.4 m of two ridges (M and N) are composed entirely of aeolian sand and that aeolian processes have occasionally contributed to the elevation of all ridges in this sequence. Although these results suggest that ridge samples with skewness values greater than -0.3344 are aeolian in origin, Dalla Pozza (2005) showed that beach and nearshore sediments (i.e. sands forming the sediment source for ridge development) at Cungulla commonly display similar skewness values to those in the supposed aeolian units within the ridges. Dalla Pozza (2005) results suggest that the apparent aeolian units within the beach ridges at Cungulla may simply reflect the characteristics of the sediment source at the time. Hence a wave origin for these units cannot be ruled out.

4.4.8 Numerical Modelling

The results of the storm surge and shallow water wave modelling are presented in Figure 4-3 (a) and Figure 4-5. The data suggest that inundations generated by Category 4 or 5 tropical cyclones (TCs) are required to reach elevations equivalent to the upper sedimentary units within most of the Cungulla ridges. For example, the highest interpreted beach sand layer occurs at 6.4 m in ridge F. Modelling suggests that this level may be reached by combined waves and surge during a TC with a central pressure of between 883 and 897 hPa within the 1σ tidal range and between 870 and 912 hPa within the 2σ tidal range. As a result, even if a TC crossed at close to the highest possible tide during a full nodal tidal cycle (= 95th tidal quintile) the TC would have a minimum intensity of 912 hPa.

4.4.9 Chronology

The chronology (Table 2-1) indicates that the forty dated ridges range in age from 0.02 to 8.10 kya. The ridges generally increase in age with distance inland. However, a number of age reversals (from ridges 11, 17, 20, 25, 26, 27, 29, 36 and 37) are indicated where the uncertainty margins do not overlap

and they are likely a result of mechanical or biological disturbance. If these age reversals are disregarded, development of the Cungulla ridge plain commenced between approximately 6.00 and 6.50 kya and is in agreement with dated sequences elsewhere in this region (Rhodes et al., 1980; Rhodes, 1982; Chappell et al., 1983; Hayne and Chappell, 2001; Nott and Hayne, 2001; Nott et al., 2009; Forsyth et al., 2010; Forsyth et al., 2012). The overall progradation rate across the 5 km of ridge plain is calculated at between 0.83 and 0.77 m yr^{-1} when age reversals are disregarded.

4.5 Discussion

The ridges forming this plain at Cungulla are unlike ridges in other beach ridge plains studied so far in this region. The ridges here are composed of moderately sorted, fine-grained sands, whereas the beach ridges studied at the relatively nearby Cowley Beach (Nott et al., 2009), Rockingham Bay (Forsyth et al., 2010) and Wonga Beach (Forsyth et al., 2012) are all composed of coarse-grained sands. Furthermore, the Cungulla ridge plain displays numerous different sets of ridges with unconformable boundaries and saline flats and saltpans located around and within the ridge sequence. These characteristics are not present in the other ridge plains at Cowley Beach, Rockingham Bay and Wonga Beach.

4.5.1 Origins of Ridges at Cungulla

Type 1 Ridges – Beach Ridges

Most ridges in the Cungulla sequence display smooth, regular, curvilinear crest lines and incorporate recurved terminations (Figure 4-1). Similar curvilinear ridge morphologies elsewhere were suggested to have developed through swash processes (e.g. Curray et al., 1969; Tanner and Stapor, 1971; Missimer, 1973; Stapor et al., 1991; Donoghue et al., 1998; Bristow et al., 2000).

Unconformities in the Cungulla sequence likely reflect shoreline morphology following a past erosion event. The sub-parallel orientation of the subsequently deposited ridge set reflects the swash-alignment of ridge development along that shoreline. Although the data presented in Figure 4-5 suggests that these ridges may have received aeolian contributions over time, the morphology of Type 1 ridges suggests that they are beach ridges and

have been deposited by wave action. Furthermore, Dalla Pozza (2005) evidence suggests that the grain size, skewness and sorting characteristics may not necessarily be indicative of the depositional processes. Hence the apparent aeolian units could have been deposited by waves.

4.5.1.1 Palaeo-TC Record

The data suggests widespread distribution of beach sand within the upper sedimentary units of Cungulla ridges (Figure 4-5). The results of numerical modelling suggest that storm surge and wave action produced by intense (category 4 and above) TCs are required for water levels to reach an elevation of 4 m AHD at Cungulla (Figure 4-3 (b)). Nott et al. (2009) came to a similar conclusion for the Cowley Beach beach ridge plain, as did Forsyth et al. (2010) for Rockingham Bay. Marine inundations generated by lower intensity TCs may have deposited the sedimentary units composed of beach sand now preserved at lower elevations within the ridges and initial formation of the beach ridge could have occurred as a result of inundations generated during non-TC events. Subsequent beach ridge growth likely corresponded with higher magnitude marine inundations. These beach ridges have increased their elevation to a level where low magnitude events can no longer generate marine inundations capable of reaching the ridge crest. Only extreme intensity TCs generating relatively large marine inundations have been capable of depositing sediments onto the ridge crest once it reaches a critical height. We suggest that these marine inundations are responsible for deposition of beach sand layers in the upper sedimentary units of the Cungulla ridge plain.

4.5.1.2 Type 2 Ridges – Dunes

Type 2 ridges display a hummocky topography that has the appearance of a series of dune blowouts and parabolic forms. This topography suggests that aeolian processes have shaped these ridges. Hopley (1970) suggested that these features were originally beach ridges that had been subsequently disturbed by aeolian processes. Their common occurrence as the first ridge on the seaward side of a set or group of Type 1 ridges suggests that the unconformable nature of the Type 1 ridge sets and the origin of the Type 2 ridges may be linked. It is likely that the unconformable nature of the Type 1 ridge sets is due to occasional fluvial erosion.

Hopley (1970) suggested that the former distributaries of the Haughton River located between Mount Elliott and Feltham Cone and along the seaward side of The Cone (Figure 4-1) are responsible for occasionally diverting floodwaters to the north of its normal course. The expanse of saltpan and salt marsh in Figure 4-1 infers that such flows have removed large sections of ridges located once near the rear of the present sequence. Also, widespread ridge truncations located along the landward flank of ridge set boundaries appear to be confined to the southern part of the plain, close to the Haughton River, suggesting that here floodwaters may have occasionally pushed through the ridge sequence to the sea. The oblique orientation of ridge truncations infers the paths that fluvial incursions have followed through the ridge sequence. Hence flooding of the Haughton River has likely destroyed parts or all of some ridges resulting in gaps in the ridge chronology. The occurrence of parabolic forms on the Type 2 ridges suggests that these features may have developed after fluvial erosion has scarped the toe of this ridge exposing the sediments to aeolian activity. Such scarping leads to undermining of vegetation and ridge wall collapse (Hesp, 2002). Onshore wind velocities sufficient to entrain exposed ridge sediments may then initiate blowout development, subsequent blowout enlargement and downwind deposition of eroded sediments in parabolic-shaped depositional lobes (Carter et al., 1990). Over time a new beach ridge is deposited to seaward of the disturbed (Type 2) ridge and a new set of Type 1 ridges develops often with a different orientation to the previous Type 1 set. Type 2 ridges then are former beach ridges that have experienced aeolian reworking following fluvial erosion of part of a set of Type 1 ridges. The Type 2 ridges often mark the unconformable boundary between sets of Type 1 ridges. Re-working may also be responsible for the coincidence of dunes in this sequence with several reversals in the OSL chronology.

4.5.2 Chronological gaps in the record

The beach ridge record at Cungulla displays two substantial chronological gaps. An 870-year gap occurs between ridges 14 and 15 and a 1600-year gap occurs between ridges 30 and 31. The 870-year gap coincides with tall, hummocky Type 2 ridge morphology displayed by ridge 15. However, the 1600-year gap does not coincide with a Type 2 ridge. Nor does it coincide with

a Type 1 set unconformity. Hence, there are two types of chronological gaps here. The first is characterised by a coincidence with an unconformable ridge set boundary, blowouts and parabolic forms that suggest past erosion. The second type of gap is not characterised by these morphological features and appears to be the result of a cessation or slowing down in beach ridge development.

4.5.2.1 Gap due to erosion

Floodwaters exploiting the former distributary along the seaward side of The Cone are likely responsible for the unconformity that occurs between ridges 14 and 15 (Figure 4-3). Figure 4-1 shows the extent of salt marsh and saltpan that form erosion surfaces likely remnant from one or possibly several flood events stretching along the front of ridge 15 to the northern end of the sequence. The chronology suggests that this erosion occurred between approximately 1.53 to 2.40 kya. The widespread nature of other similarly oriented unconformities here also suggests that the depositional record contained in the Cungulla beach ridge plain includes evidence of numerous past fluvial erosion events.

4.5.2.2 Gap due to cessation of severe TC activity

Erosion is unlikely to be responsible for the approximately 1600-year gap between ridges 30 and 31. A detailed examination of ridges either side of this gap suggests that these two ridges are conformable and that no ridge truncations, parabolic forms or other evidence of past erosion occur either at a single site or along the length of these ridges. The lack of any sign of an unconformity associated with this gap suggests a decrease or cessation in the incidence of beach ridge-building processes occurring during the period approximately 6.29 to 4.67 kya. The modelling, as shown in Figure 4-5, suggests that inundations associated with TCs are responsible for depositing the upper sedimentary units of beach ridges in this sequence. Low elevation ridges and chronological gaps in the sequence are therefore likely to be periods when a decrease or cessation in the incidence of extreme intensity TCs occurred.

The Cungulla ridge plain is not the only ridge plain in the region to display these non-erosional gaps. Indeed, every ridge plain examined so far throughout this region displays one or more of these types of gaps. Nott and Forysth (2012) compared TC deposited beach ridge plains from around Australia (northeast Queensland, Gulf of Carpentaria and Western Australia) with hurricane overwash sequences in the Gulf of Mexico, US Atlantic and Japan and found that all of these long-term TC sedimentary sequences display chronological gaps between one and many centuries to a millennium in length. Nott and Forsyth (2012) conclusion was that these gaps appear to be an inherent characteristic of the long-term TC sedimentary records globally and that they are most likely caused by periods of relative quiescence in intense TC or hurricane activity. The chronological gap between 6.29 and 4.67 kya at Cungulla appears to be another of these types of gaps associated with a period of less intense TC activity.

4.5.3 TC-records

Shore-parallel ridges composed of fine-grained sand in this region have been routinely ascribed aeolian origins (e.g. BPA, 1979). The recurved ends of ridges and different orientations of Type 1 ridge sets suggests that waves are responsible for their deposition. The numerical modelling further suggests that only TCs of severe intensity are able to generate inundations capable of depositing sediments on the crests of most of these ridges. Observations of ridge stratigraphy elsewhere have suggested that each ridge in a plain develops through inundation processes exploiting an abundant sediment source, probably at the beach or nearshore, and re-depositing those sediments at the rear of the beach (Nott et al., 2009). Ridges then increase in elevation over time with successive TC generated marine inundation events. Tropical cyclones are thought responsible for depositing numerous beach ridge plains in this way, including those composed of coral shingle (Hayne and Chappell, 2001; Nott and Hayne, 2001), sand and shell (Rhodes et al., 1980) and coarse-grained sand (Nott et al, 2009; Forsyth et al, 2010; Forsyth et al., 2012). There is nothing to indicate that extremely energetic sediment transport processes associated with TC inundations will discriminate between fine-grained sand and coarser-grained sediments. To the contrary, data presented by Dalla Pozza (2005) suggests that 79% of beach and nearshore (collected

within 1 km of shore) sediments at Cungulla display skewness values that would be classified as ‘almost certainly dune’ or ‘indeterminate’ under the scheme illustrated in Figure 4-5. These data infer that the sedimentary characteristics of ridges forming this plain are not necessarily the result of sorting processes incurred during transport from the beach or nearshore to their present position. Instead, beach ridge sediment characteristics may simply reflect the characteristics of the sediment source. Accordingly, it is likely that inundations associated with TCs are the principal process responsible for depositing beach ridges within the Cungulla ridge plain. It further suggests that other beach ridge plains composed of fine-grained sand elsewhere along the coast of this broader region may contain palaeo-TC records.

4.5 Conclusion

Numerical modelling and sedimentary analysis suggests that marine inundations associated with TCs are principally responsible for depositing beach ridges composed of fine-grained sand at Cungulla. Comparative studies of local barrier and nearshore sediments suggest that marine processes, not wind, are responsible for depositing beach ridges within this sequence. The numerical modelling suggests that the upper sedimentary units of most beach ridges in this sequence were deposited by inundations associated with the nearby passage of extreme intensity TCs. These findings suggest that detailed studies are required to determine the origin of shore-parallel fine-grained sand coastal barriers and that the texture of these landforms may not necessarily be diagnostic of their origin.

The beach ridge plain at Cungulla also contains two types of chronological gaps. Angular unconformities in ridge orientation and variations in ridge morphology between smooth and convex to hummocky probably signals past erosion. Other chronological gaps where these morphological characteristics are absent are likely due to periods of quiescence in terms of ridge development due to less intense TC activity. These morphological characteristics may be used as diagnostic indicators of the origin of chronological gaps in other beach ridge plains constructed by TC inundations globally.

Chapter 5: Punctuated global tropical cyclone activity over the past 5,000 years

Nott, J., and Forsyth, A. J., 2012, Punctuated global tropical cyclone activity over the past 5,000 years: Geophysical Research Letters, v. 39, L14703.

Abstract

There are now a substantial number of millennial scale records of tropical cyclones from a variety of locations globally. Some of these, such as those in the Atlantic and Gulf of Mexico, show patterns of long-term, generally intense, tropical cyclone (TC) behaviour that have been suggested to be due to either variations in ENSO or shifts in the position of the Atlantic High pressure system and the jet stream. Comparisons are made here of the sedimentary overwash records from the Gulf of Mexico and Atlantic Ocean Basin with the overwash records from the north-west Pacific and beach ridge records from the south-west Pacific and south east Indian Ocean basins. There is a substantial degree of synchroneity in global intense TC behaviour over the past 3,000 to 5,000 years. One of the most striking aspects of these records is they all display extended alternating periods (centuries to millennia) of relative quiescence and heightened intense TC activity irrespective of both the resolution and type of long-term TC record. The cause(s) of this punctuated activity are at present difficult to identify but are likely exogenic in origin rather than due to an intrinsic aspect of the records or the methods used to derive them. The identification of punctuated global long-term TC behaviour is important for understanding future TC activity and for assessing risk to coastal communities.

5.1 Introduction

Understanding the long-term natural variability of tropical cyclones (TC) is important for forecasting their future behaviour and for the detection and attribution of changes in their activity as a consequence of anthropogenically induced climate change. Critical to these endeavours is determining whether, over the long-term, TCs occur randomly or display identifiable patterns influenced by one or several factors. Such patterns are beginning to emerge from the overwash sedimentary records from the Gulf of Mexico and Atlantic and northwest Pacific Ocean basins. Respectively, they have been attributed to changes in the latitudinal position of the Atlantic High / Jet Stream or variations in ENSO (Liu and Fearn, 1993, 2000; Donnelly and Woodruff, 2007; Mann et al., 2009b). To date, however, no attempt has been made to ascertain whether there is a global signature to long-term TC activity and if so whether these same factors, as suggested for the Atlantic, are responsible. This is principally because there have been, until now, a limited number of such records from the southern hemisphere. Here, we help to correct this imbalance by presenting new sedimentary data from the southwest (SW) Pacific and southeast (SE) Indian Ocean regions which allow us to make comparisons with existing sediment records from the Atlantic Ocean (Donnelly and Woodruff, 2007; Mann et al., 2009b), northwest (NW) Pacific (Woodruff et al., 2009), Gulf of Mexico (Liu and Fearn, 1993, 2000; Lane et al., 2011) and the Gulf of Carpentaria, Australia (Rhodes et al., 1980) (Figure 5-1). Unlike the northern hemisphere this southern hemisphere data is in the form of late Holocene TC records derived from quartz rich, coarse-grained sand beach ridges (northeastern Australia) and almost pure shell beach ridges (Western Australia). These records favour the register of intense TC activity as opposed to all TC activity and they also reflect landfalling TCs and not necessarily TC activity in the entire adjacent ocean basin.

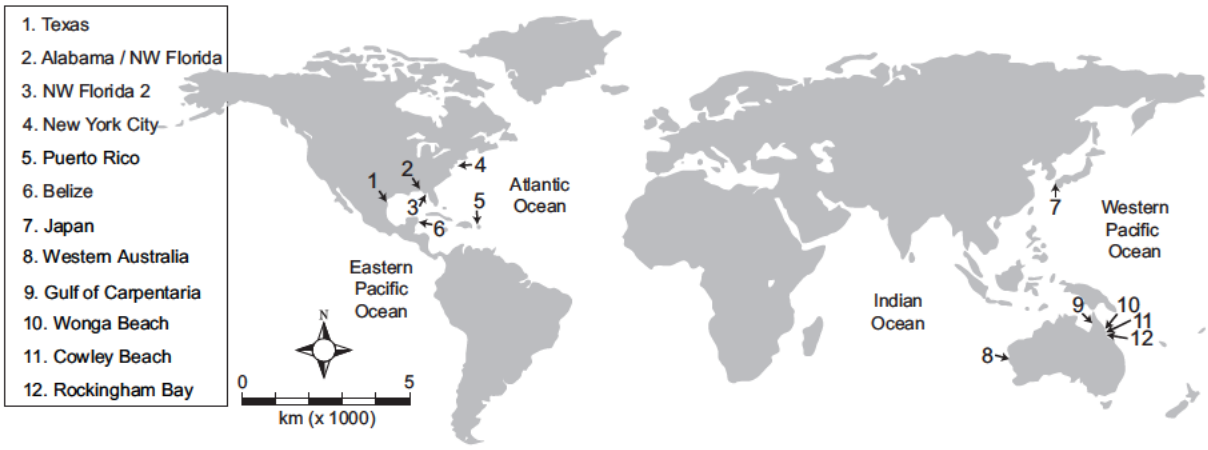

Figure 5-1 Map of global late Holocene tropical cyclone sedimentary records. 1 = Texas (Wallace and Anderson, 2010), 2 = Alabama/NW Florida (Liu and Fearn, 1993, 2000), 3 = NW Florida 2 (Lane et al., 2011), 4 = New York City (Scileppi and Donnelly, 2007), 5 = Puerto Rico (Woodruff et al., 2008b), 6 = Belize (McCloskey and Keller, 2009), 7 = Japan (Woodruff et al., 2009), 8 = Western Australia (Nott, 2011a), 9 = Gulf of Carpentaria (Rhodes et al., 1980), 10 = Wonga (Forsyth et al., 2012), 11 = Cowley Beach (Nott et al., 2009), 12 = Rockingham Bay (Forsyth et al., 2010).

5.2 Southern Hemisphere Long-Term TC Records

5.2.1 Beach Ridge Plain Development

The coarse-grained beach ridges in northeastern, northern (Gulf of Carpentaria) and Western Australia have been deposited by wave action usually associated with intense TC generated marine inundations (Rhodes et al., 1980; Nott et al., 2009; Forsyth et al., 2010; Nott, 2011). Each ridge in the plain is initially deposited at the rear of the beach. Over time (past ~6,000 years) a sequence of ridges develops to form a plain of between 10 and 30 shore parallel ridges. The addition of each new ridge causes the plain to prograde seaward. The developing ridge at the rear of the beach increases in elevation over time with successive TC generated marine inundation events. These inundations consist of storm surge, tide, wave action, wave run-up and wave set-up. Each event deposits a sedimentary unit that varies between several centimetres and approximately one meter thick. Progressively higher marine inundations are required to continue depositing sediment onto the sand ridge as it increases in height. The ridges generally attain a maximum elevation of 4–6 m above mean sea level. Only the largest marine inundations can reach and deposit sediment onto the crests of ridges at this height hence the final sedimentary unit on each ridge crest registers the largest marine inundation responsible for depositing the ridge. It is possible for large inundations to deposit sediment onto the ridge when the ridge is still at low

elevation. However, low elevation ridges identify a period of time when the frequency of large inundations and hence high intensity TCs are less frequent.

Ridge plains usually develop at locations where abundant sediment is supplied to the coastal system by streams. It is common for a lower elevation ridge to be developing seaward of a larger ridge. As the most seaward ridge increases in elevation it will progressively limit the amount of sediment the more landward ridge receives. Hence ridge height is a function of TC intensity and frequency as well as sediment supply to the coast. Ridge height can be equated to the intensity of the TC responsible as has been demonstrated with coral shingle and shell ridges elsewhere (Nott and Hayne, 2001; Nott, 2003). The chronology of the ridges provides the frequency of events. Gaps in the chronology of these ridge plains represent periods of low frequency or no high intensity TC activity (Nott et al., 2009; Forsyth et al., 2010; Nott, 2011a). These gaps are unlikely due to erosion as the ridges do not display any erosional breaks in their stratigraphies. Also they do not display any evidence of erosion in the plan form of the ridges composing these ridge plains, which is to be expected when parts of the ridge plain are eroded from a coastal embayment.

5.2.2 Beach Ridge Plain Characteristics

In NE Australia three separate sand beach ridge plains over a 400 km distance were analysed. Rockingham Bay, the most southerly of these sites contains 19 shore parallel, coarse-grained sand beach ridges, ranging in height from approximately 4 to 5.5 m above Australian Height Datum (AHD) or approximately mean sea level. Cowley Beach 50 km north of Rockingham Bay contains 29 coarse-grained sand beach ridges ranging in elevation from 4 to 6 m AHD. Wonga Beach, approximately 400 km north of Rockingham Bay, contains 10 coarse-grained sand beach ridges varying in elevation from 3 to 5 m AHD. Numerical modelling of storm surge and tide along with shallow water waves using a well documented technique (Nott and Hayne, 2001; Nott, 2003; Nott et al., 2009) showed that the TCs responsible for deposition of the final units of sediments onto these ridges needed to be category 3 to 5 events (Saffir-Simpson scale) for all three sites (Figure 5-2). The ages of the ridges, using optically stimulated luminescence (OSL) (Table 2-1, Table 2-2 and

Table 5-1), shows that the ridges increase in age with distance inland (Figure 5-2). Occasionally there are age reversals such that a more inland ridge returns an age that is apparently younger than the next adjacent seaward ridge. Most of these are apparent reversals as the ages overlap at the 2 sigma uncertainty margin level. Others can be attributed to deposition of more recent sediment due to an exceptionally large overwash event or possible bioturbation. Which ever is the cause these reversals are not common and do not detract from the general chronological interpretations of these ridge plain sequences.

The shell beach ridges in Western Australia are composed entirely of one species of marine cockleshell (Fragum eragatum) and stand between 3 and 6 m AHD (Figure 5-2). These shell beach ridges are not cheniers as the swales are composed of the same material as the ridge. Radiocarbon analyses shows that the ridges were deposited between 500 and 7,000 cal yrs BP (Nott, 2011a) (Table 5-2).

5.3 Punctuated Long-Term TC Behaviour

5.3.1 Southern Hemisphere Data

The most notable characteristic of all of the ridge plain chronologies (including the sand beach ridges in the Gulf of Carpentaria) is the presence of substantial gaps in ridge plain formation over the late Holocene (Figure 2-2 and Figure 2-3). The sand beach ridge plains of northeastern and northern Australia show 2 prominent chronological gaps. Rockingham Bay has a 900-year gap between 3,380 to 2,480 yrs BP and a 1,000-year gap between 1,440 to 440 yrs BP. Cowley Beach has a 650-year gap between 3,230 and 2,580 yrs BP and a 970-year gap between 1,820 and 850 yrs BP. Two major gaps of 1,700 years and 900 years occur at Wonga Beach between 3,820 and 2,110 yrs BP, and 1,620 and 710 yrs BP, respectively. These gaps could be the result of either erosion of existing ridges or a lack of ridge development because of limited sediment supply via stream channels to the coast and / or a decrease in the frequency of TC generated inundations capable of causing ridge accretion. Erosion is unlikely to be responsible because the gaps are broadly coeval across all three ridge plains. Also there is no evidence either in the plan form and morphology of these ridges or in their stratigraphy to

suggest that the chronological gaps are due to erosion. These gaps are most likely due to periods when fewer high intensity TCs made landfall. These periods of fewer high intensity TCs resulted in fewer or no sufficiently large inundations capable of depositing enough sediment to promote the development of the highest ridges in the plain.

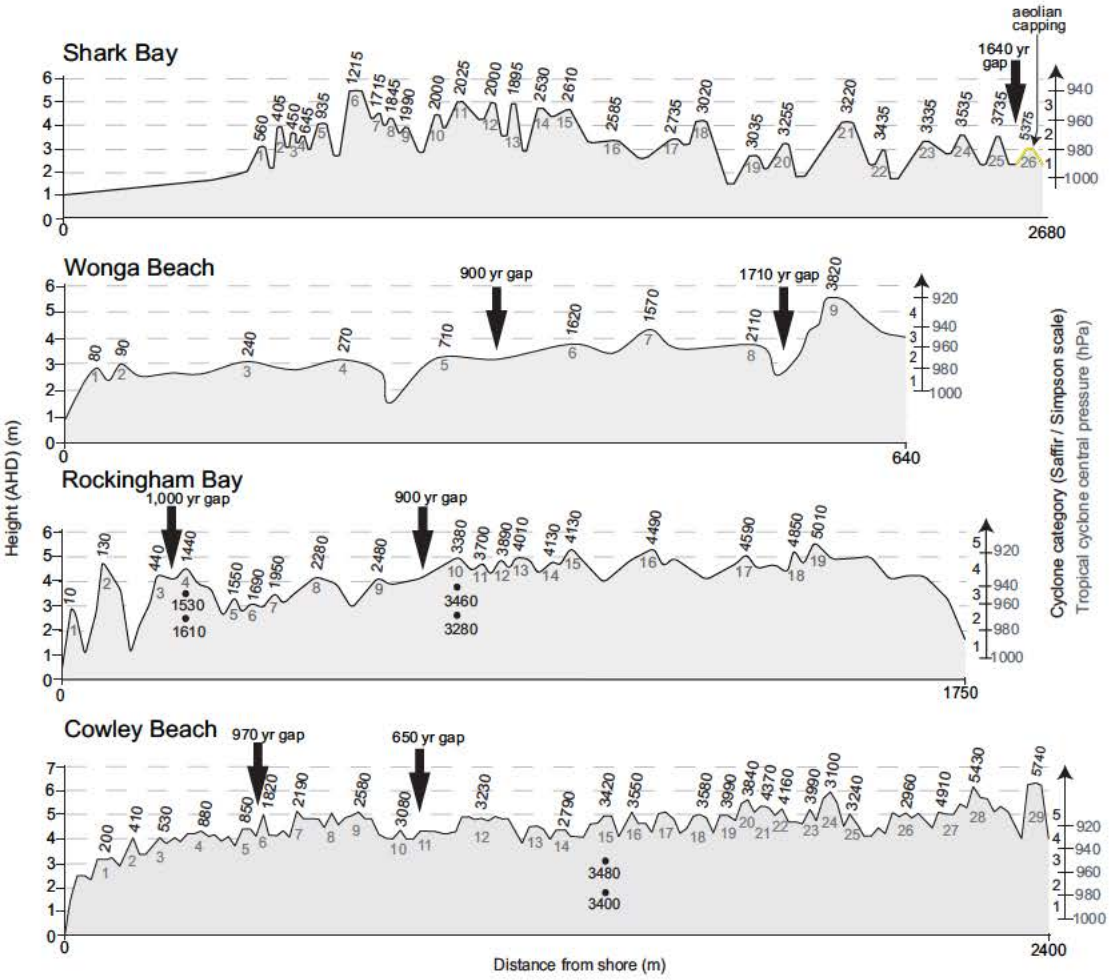

Figure 5-2 Beach ridge cross-sections and chronologies (Shark Bay is dated using radiocarbon and remainder using OSL). Note that chronological gaps identified in manuscript refer to those periods with no or less activity in high intensity TC activity - i.e. gaps in major ridge building. Minor (low elevation) ridges can still be deposited during these periods of less activity. Hence the 650 yr gap at Cowley Beach is still a gap despite the age of 3080 yrs BP at ridge 10 as this ridge is of low elevation and represents a period of less TC activity.

Table 5-1 OSL chronology for the Cowley Beach sand beach ridge plain (Nott et al., 2009).

Field code	Lab. code	Ridge #	Depth (cm)	De (Gy)	Dose rate (Gy/ka)	Age (years before 2008)
Ridge 1	K0451	1	70	0.35±0.01	1.73±0.11	200±10
Ridge 2	K0442	2	60	0.65±0.02	1.58±0.10	410±30
Ridge 3	K0443	3	65	0.79±0.02	1.48±0.09	530±40
Ridge 4	K0444	4	60	1.37±0.04	1.56±0.10	880±60
Ridge 5	K0390	5	70	1.26±0.04	1.52±0.12	850±50
Ridge 7	K0445	7	70	2.57±0.08	1.41±0.09	1820±130
Ridge 8	K0446	8	60	3.91±0.10	1.78±0.11	2190±150
Ridge 9	K0447	9	60	4.23±0.10	1.64±0.10	2580±170
Ridge 10	K0448	10	70	4.86±0.13	1.58±0.10	3080±210
Ridge 12	K0449	12	40	3.88±0.11	1.20±0.08	3230±240
Ridge 14	K0450	14	50	3.23±0.08	1.16±0.07	2790±180
Ridge 15	K0391	15	75	3.98±0.09	1.23±0.06	3420±120
Ridge 15	K0392	15	170	4.23±0.08	1.21±0.08	3480±120
Ridge 15	K0393	15	340	4.43±0.08	1.34±0.11	3400±120
Ridge 16	K0452	16	40	4.81±0.15	1.36±0.09	3550±260
Ridge 17	K0453	17	40	4.67±0.14	1.42±0.10	3300±240
Ridge 18	K0454	18	100	5.22±0.14	1.46±0.08	3580±220
Ridge 19	K0455	19	40	4.59±0.14	1.15±0.09	3990±320
Ridge 20	K0456	20	40	5.10±0.14	1.33±0.10	3840±290
Ridge 21	K0457	21	70	7.34±0.28	1.68±0.11	4370±340
Ridge 22	K0458	22	50	5.05±0.12	1.22±0.08	4160±280
Ridge 23	K0459	23	70	6.26±0.18	1.57±0.09	3990±250
Ridge 24	K0460	24	50	5.36±0.15	1.73±0.11	3100±210
Ridge 25	K0461	25	30	5.02±0.16	1.55±0.12	3240±280
Ridge 26	K0462	26	30	4.61±0.15	1.56±0.13	2960±260
Ridge 27	K0463	27	80	3.91±0.10	0.80±0.05	4910±320
Ridge 28	K0464	28	100	3.54±0.11	0.65±0.04	5430±350
Ridge 29	K0465	29	70	4.21±0.13	0.73±0.05	5740±400

Table 5-2 Radiocarbon chronology for Shark Bay (Nott, 2011a) and Gulf of Carpentaria (Rhodes, 1980)

lab Code	14C age (yr BP)	cal. age range (1σ)	med. prob. (cal. yr BP)	minus 615 yr
Shark Bay				
WK14764	1702±44	1120-1270	1175	560
WK 14765	1520±36	920-1060	1020	405
WK 14766	1582±35	980-1140	1065	450
WK 14767	1783±38	1200-1330	1260	645
WK 14768	2068±37	1480-1650	1550	935
WK 14769	2299±35	1750-1910	1830	1215

WK 14770	2492±43	1970-2150	2330	1715
WK 14771	2762±36	2310-2480	2460	1845
WK 14772	2947±37	2550-2730	2605	1990
WK 14773	2959±35	2570-2740	2615	2000
WK 14774	2977±35	2600-2760	2640	2025
WK 14775	2954±37	2560-2740	2615	2000
WK 14776	2945±39	2550-2730	2600	1985
WK 14777	3375±35	3060-3240	3145	2530
WK 14778	3450±39	3170-3340	3225	2610
WK 14779	3424±39	3140-3320	3200	2585
WK 14780	3539±39	3270-3430	3350	2735
WK 14781	3780±41	3540-3720	3635	3020
WK 14782	3810±41	3570-3760	3650	3035
WK 14783	3967±36	3790-3970	3870	3255
WK 14784	3927±35	3720-3900	3835	3220
WK 14785	4097±36	3950-4140	4050	3435
WK 14786	4021±38	3850-4040	3950	3335
WK 14787	4162±39	4040-4240	4150	3535
WK 14788	4329±37	4260-4450	4350	3735
WK 14789	5639±45	5880-6050	5990	5375
Gulf of Carpentaria				
ANU1690	6400±90	6610-6870	6730	n/a
ANU 1728	1920±120	1230-1510	1350	n/a
ANU 1729	6160±180	6270-6680	6470	n/a
ANU 1730	5590±250	6140-6150	5850	n/a
ANU 1732	5370±60	5520-5710	5610	n/a
ANU 1733	5570±120	5650-5950	5820	n/a
ANU 1735	3110±65	2680-2870	2770	n/a
ANU 2093	1670±90	1400-1610	1510	n/a
ANU 2100	6000±100	6170-6420	6300	n/a
ANU 2101	5760±110	5910-6180	6040	n/a
ANU 2102	3430±100	3000-3300	3140	n/a
ANU 2103	1880±90	1180-1410	1340	n/a
ANU 1736	3130±65	2700-2890	2790	n/a
ANU 1737	3220±70	2760-2980	2890	n/a
ANU 1738	6450±100	7250-7430	7320	n/a
ANU 1739A	6060±90	6250-6480	6360	n/a
ANU 1739B	5530±90	5660-5890	5780	n/a
ANU 1898	610±70	160-190	130	n/a
ANU 1899	690±80	70-290	190	n/a

The minus 615 years column for Shark Bay is due to the approximately 615 year residence time of shells on the beach and nearshore environment before deposition onto a ridge (see Nott [2011a] for detailed explanation).

The coarse-grained sand beach ridge plain in the Gulf of Carpentaria was dated using radiocarbon analyses of marine shells incorporated within the ridge (Rhodes et al., 1980). These radiocarbon analyses have been recalibrated using the INTCAL09 and MARINE09 radiocarbon age calibration curves (Reimer et al., 2009) (Calib 6.0) and are presented in Table 5-2. The calibrated age of these ridges extends to almost 7,500 cal yrs BP and here three major gaps in the chronology occur between approximately 5,500 and 3,500 cal yrs BP, 2,700 and 1,800 cal yrs BP, and 1,000 to 500 cal yrs BP (Figure 5-3). There is only one major gap in the radiocarbon chronology (also marine corrected and calibrated) for the shell beach ridges in Western Australia and this occurs between approximately 5,400 and 3,600 cal yrs BP which mirrors the earliest major gap in the Gulf of Carpentaria sand beach ridge record (Figure 5-2 and Figure 5-3). A second possible gap occurs in the Western Australian sequence between 500 cal yrs BP and the present although it is not certain whether this is genuine cessation in TC activity or an erosional gap in the record. The first major gap in the Western Australian sequence is definitely not due to erosion but rather is climatic in origin as the ridges deposited prior to this gap have been buried by a 0.5–0.75 m thick layer of well-sorted, very fine-grained sediment which is aeolian in origin (Figure 5-2). This wind blown unit does not occur on the ridges after the gap suggesting that here this gap was caused by a markedly drier period of climate during which few if any TCs made landfall at this location - but this does not necessarily suggest there were fewer intense TCs in the eastern Indian Ocean during this period just that there was a substantial reduction in landfalling TCs (Nott, 2011a). This same period (5,400 to 3,600 cal yrs BP), known as the Neoglacial, was also marked by aridity in eastern and central Australia (McGowan et al., 2008). The gaps in TC activity in the Gulf of Carpentaria and in Western Australia are out of phase with those in NE Australia hence the periods of heightened TC activity in NE Australia occurred during periods of relative quiescence in Western Australia and the Gulf of Carpentaria (Figure 5-3).

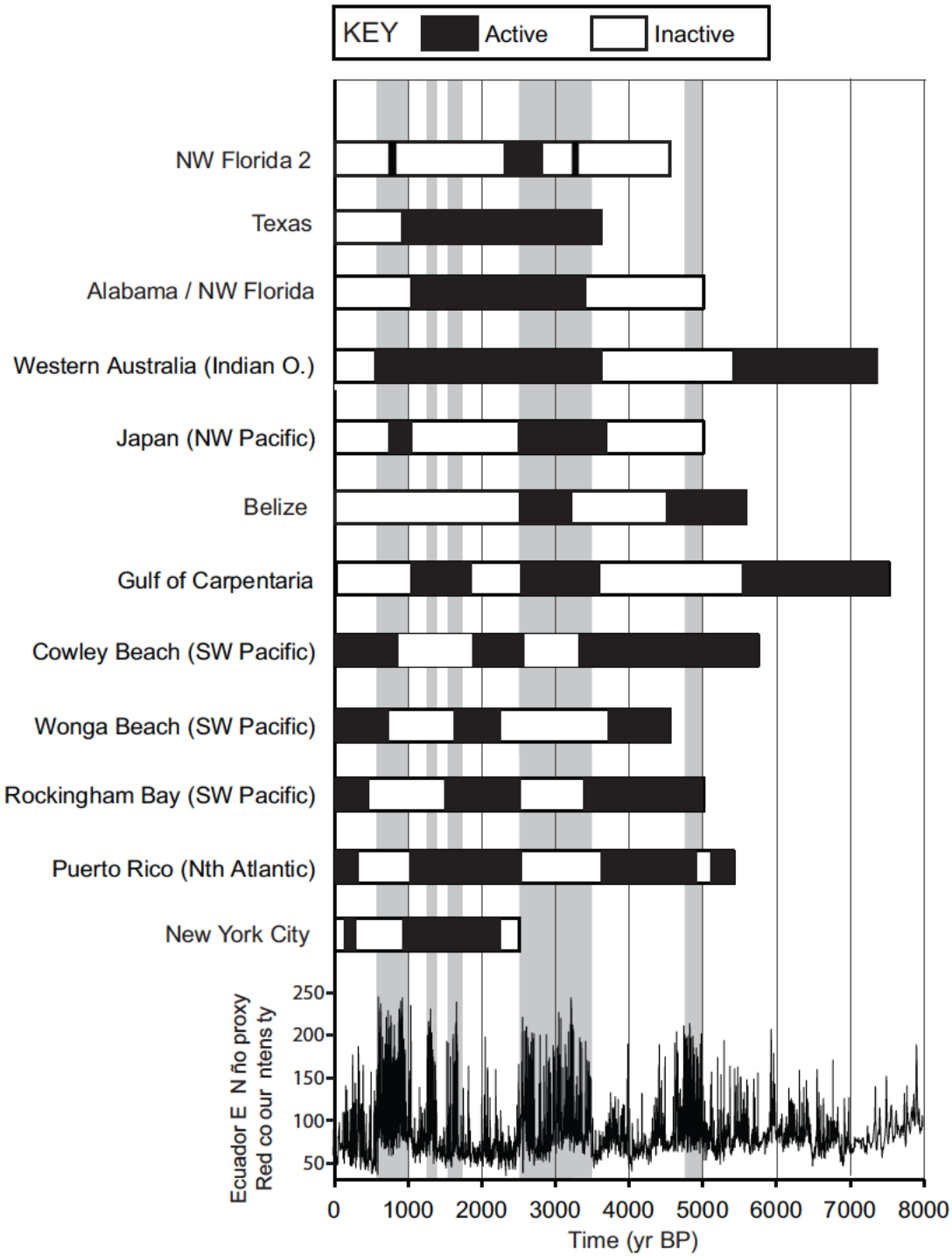

Figure 5-3 Global phases of tropical cyclone activity and inactivity over past 5,000 to 7,000 years (see caption of Figure 5-2 for references).

5.3.2 Comparisons With Northern Hemisphere Records

The overwash sedimentary records from the North Atlantic (Puerto Rico) and the Gulf of Mexico also have major gaps suggestive of periods of quieter hurricane activity (Liu and Fearn, 1993, 2000; Donnelly and Woodruff, 2007; Wallace and Anderson, 2010). These two regions also display an out-of-phase relationship with each other in terms of hurricane activity during the late Holocene (Figure 5-3). The Atlantic deposits suggest hurricanes were inactive between approximately 3,500 and 2,500 cal yrs BP and again between approximately 1,000 to 500 cal yrs BP (Scileppi and Donnelly, 2007; Woodruff et al., 2008b) whereas the Gulf of Mexico deposits show hurricane inactivity from approximately 5,000 to 3,400 cal yrs BP and again from approximately 1,000 cal yrs BP to the present (Liu and Fearn, 1993; Donnelly and Woodruff, 2007). The NW Florida deposits (Lane et al., 2011) display broadly similar gaps except for a brief period of activity at approximately 800 cal yrs BP. (Figure 5-3). Comparisons between the NE Australian and Puerto Rico deposits show that both the SW Pacific and North Atlantic oceans experienced 2 major periods of TC quiescence at approximately the same times since 5,000 yrs BP. Coevally there was heightened TC activity in the NW Pacific (Japan), East Indian Ocean and the Gulfs of Carpentaria and Mexico (Figure 5-3). When the NW Pacific, Indian Ocean and Gulfs experienced a major phase of TC quiescence centred on 4,500 to 4,000 yrs BP the North Atlantic and SW Pacific experienced heightened TC activity and the same was true of the phase of TC quiescence centred on approximately 2,000 yrs BP in the NW Pacific and Gulf of Carpentaria, although the Indian Ocean and Gulf of Mexico continued to have high TC activity during this time (Figure 5-3).

5.4 Possible Causes of the Punctuated Long-Term TC Activity

The periods of inactivity over the past 5,000 years in the Atlantic basin have been suggested to be associated with periods dominated by El Niños (Donnelly and Woodruff, 2007). Comparisons with a long-term record of ENSO from Ecuador (Moy et al., 2002) suggests the same may be true of the SW Pacific (Figure 5-3) between approximately 3,500 and 2,500 cal yrs BP but the later phase of less TC activity in the SW Pacific (~1,800 to ~900 yrs B.P.) appears to begin between 500 to 800 yrs earlier than the Atlantic record

(~1,000 to ~500 cal yrs B.P.) suggesting it may not be due to more frequent El Niños. If El Niños are the cause of this punctuated activity globally then it could be expected there would be an anti-phase relationship between the Atlantic / SW Pacific and the East Indian Ocean, NW Pacific (southern Japan) and the Gulf of Carpentaria. Apart from the Gulf of Mexico, where the North Atlantic Oscillation (NAO) has possibly played an important role (Liu and Fearn, 1993, 2000), El Niños today can cause an increase in TC activity in the Gulf of Carpentaria and Western Australia and the southern Japan region (Chan and Xu, 2009). A much higher percentage of TCs develop off the Western Australian coast during El Niños (61%) compared to La Niñas (38%) (Broadbridge and Hanstrum, 1998). The same is true of the Gulf of Carpentaria where TC activity appears to be depressed during La Niñas because the monsoon trough, within which most TCs form in this region, tends to move southward of the Gulf of Carpentaria over the Australian landmass during La Niñas and sits over the Gulf during El Niños. TC activity in the Gulf of Carpentaria today is out-of-phase with TC activity in the nearby SW Pacific which experiences fewer TCs during El Niños (Basher and Zheng, 1995). The long-term TC records do show an anti-phase relationship between these locations and the Atlantic / SW Pacific between 3,500–2,500 yrs BP but this relationship is not as obvious during the late Holocene. Hence there is not a clear coincidence between the major periods of El Niños suggested by the Ecuadorian record and all of the periods of less TC activity in the Atlantic and SW Pacific or the periods of heightened TC activity in the NW Pacific and east Indian Oceans and the Gulf of Carpentaria. This apparent lack of coincidence between ENSO and long-term global punctuated TC activity may in part be due to the Ecuadorian ENSO record itself for it differs from other, albeit much shorter, proxy records of ENSO (Lander and Guard, 1998; Cobb et al., 2003; Conroy et al., 2009; Mann et al., 2009a).

Hence there is still a substantial degree of uncertainty in the accuracy of the long-term ENSO records recovered so far making comparisons with the long-term TC records difficult. The same is true of other, generally much shorter, records of other potential climatic causes such as the NAO, Atlantic Multidecadal Oscillation (AMO) and Interdecadal Pacific Oscillation (IPO)

(Mann et al., 2009a). Attributing causes to these punctuated phases of global long-term TC activity requires robust, but so far unavailable, longer-term records of these various climatic factors.

The lags in the precise onset and cessation of TC activity between the ocean basins and Gulfs globally may also be due to differences in depositional processes between overwash and beach ridge sedimentary environments. Furthermore, these lags may be in part due to the different chronological techniques used between sites – the North Atlantic, NW Pacific and Indian Oceans, and Gulfs of Mexico and Carpentaria have been dated using radiocarbon whereas OSL has been used on the sand beach ridge records of the SW Pacific. It is also possible that regional climatic factors have influenced TC activity in each basin such as the NAO in the North Atlantic and possibly the IPO in the Pacific and Indian Ocean Dipole in the Indian Ocean. Despite these factors, and our inability thus far to attribute definitive climatic causes, it is clear that all of the long-term TC records recovered to date globally display alternating phases of high activity and less activity which appears to be a genuine characteristic of the long-term climatology of intense TCs.

5.5 Conclusion

On a seasonal basis it is increasingly apparent that TCs are influenced by various climate states (Landsea, 2000; Sabbatelli and Mann, 2007; Knutson et al., 2010). Now it also appears that long-term global TC activity is not random. Understanding this phenomenon is dependent upon identifying whether a predominant global factor or regional ones are more important in causing this punctuated activity. At this stage we are still hindered by the lack of reliable and sufficiently detailed longer-term climate proxies with which to compare our TC records. However, despite these present shortcomings the observation that long-term TC climatologies display centennial- to millennial-scale punctuated activity is an important step towards better hazard risk assessments and the identification of the influence of humans on TC behaviour.

Chapter 6: Discussion

6.1 Background

As referred to in the introduction, there is a lack of detailed knowledge about the frequency of extreme intensity TCs in Queensland, Australia. That is because TC frequency / magnitude relationships in this region are currently estimated through extrapolation of relatively few observed cyclones. Such records provide little information about the behaviour of the rare but most destructive events. Furthermore, the current methodology includes the assumption that return intervals for TCs at any particular site in the region can be represented by observations collected elsewhere, which is otherwise known as space for time substitution. The overall reliability of these methods is unknown because we lack knowledge of patterns in long-term tropical cyclone behaviour against which to test the results of current risk assessments. Therefore, it is important to develop regional long-term TC records. Such records will provide better understanding of patterns in extreme intensity TC behaviour that can be used to minimize community vulnerability and economic loss to TC hazards.

Detrital coral and shell beach ridges are considered too limited in their spatial distribution to facilitate development of a regionally representative record for NE Queensland. However, similar landforms composed of sand are widespread in this region. Discussed here are the results and implications of a study into the origin of sand beach ridge plains along the coast of Queensland, Australia, conducted specifically to determine whether beach ridge plains in this region contain records of past TC behaviour. These landforms can be divided into two distinct categories: those located within the humid tropical sector (Figure 6-1) composed predominantly of poorly sorted, coarse-grained sand (Pye, 1983) and those located along the remaining eastern coast that are predominantly composed of fine- to medium-grained sand (Short, 2000).

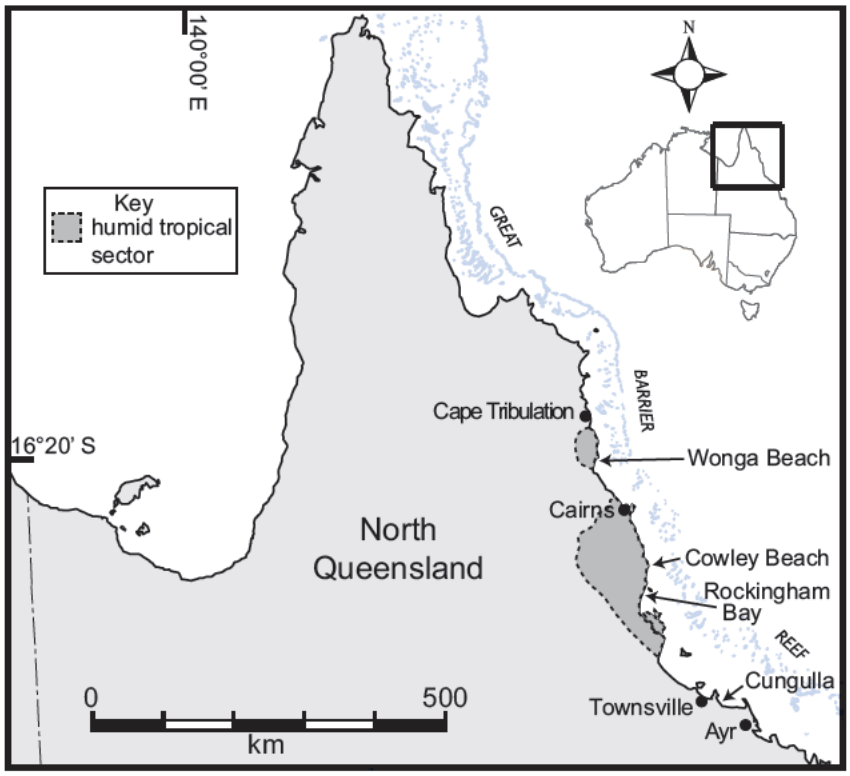

Figure 6-1 Map showing the location of the humid tropical sector of NE Queensland in relation to the relatively dryer areas that surround it and locations of sand beach ridge plain studies from this region.

6.2 Discussion of Beach Ridge Studies

6.2.1 Implications of Study at Rockingham Bay

This study was conducted to determine whether the palaeo-TC record contained in the coarse-grained sand beach ridge plain at Cowley Beach is an anomaly or whether similar landforms in the region also contain TC records. The Rockingham Bay deposition record was reconstructed using a number of data sources, including sediment size analysis, ridge morphology and ridge chronology. Sedimentary analysis was used to determine the processes responsible for depositing ridge sediments. Results suggest that aeolian processes have probably not played a substantial role, if any, in the deposition of the Rockingham Bay ridge plain. That is because the similarity between beach and ridge sands indicates comparable deposition processes. Also, the incidence of wind sufficient to transport coarse-grained sand is extremely rare in this region and largely confined to the passage of nearby TCs. Marine inundation is likely to submerge the beach during such events. Therefore, irrespective of wind strength there would be no sediment source available for aeolian transport of sand when the wind velocity is at its peak during a TC. Hence, marine (wave) processes are likely responsible for

depositing all 19 coarse-grained sand beach ridges in this sequence. Numerical modelling infers that wave processes associated with extreme intensity (Category 4 – 5) TCs are required to deposit sediments at elevations equivalent to the crests of most of these ridges. Optically Stimulated Luminescence analysis further implies that the plain has prograded to its present form over the past approximately 5000 years and that extreme intensity TCs have occurred at centennial-scale intervals at Rockingham Bay over much of the late Holocene. These results are similar to conclusions of the Cowley Beach study. Also, observations of markedly differing ridge crest elevations within the Rockingham Bay sequence (ranging between 3.11 m and 5.59 m) suggest periodic variation in the TC intensities responsible for ridge crest deposition at this site. On this basis, the data strongly suggest considerable variability at centennial time-scales in the late-Holocene TC climate at Rockingham Bay and that return intervals of these events are unlikely to have been consistent since the mid Holocene.

Two relatively large gaps were noted in the ridge chronology at Rockingham Bay. One gap of approximately 1000 years occurs between 0.44 and 1.44 kyr and the other gap of approximately 900 years occurs between 2.48 and 3.38 kyr. There are two possibilities to explain these gaps – either there was a variable climate where the gaps correspond to periods of fewer high intensity TCs or sediment supply variability has lead to the development of gaps due to erosion of parts of the beach ridge plain sequence. Either way, identification of these gaps prompted re-evaluation of the Cowley Beach data and identification of a 970-year gap in major ridge building events was evident there between 0.85 and 1.82 kya and another gap of 650 years between 2.58 and 3.23 kya. Although these gaps are not exactly synchronous with the gaps at Rockingham Bay, they are broadly coeval.

6.2.2 Implications of Study at Wonga Beach

This study was conducted to determine whether substantial gaps occurred during deposition of the Wonga Beach ridge plain. Some ridges composed of coarse-grained sand within the plain at Wonga Beach display similar morphological and sedimentary characteristics to those at Cowley Beach and Rockingham Bay. Additionally, other ridges located within the same plain are

composed of fine- to medium-grained sand. Aeolian processes have probably not played a substantial role in the deposition of the coarse-grained sand ridges that form much of the Wonga Beach ridge plain. Instead, it appears likely that marine processes are responsible for their deposition. According to numerical modelling, the crests of these ridges were likely deposited by extreme intensity TCs and the record of these events contained therein infers a similar pattern of late Holocene TC intensity and frequency to depositional records from Cowley Beach and Rockingham Bay. This pattern includes a gap in beach ridge construction of 970 years between 0.71 kya and 1.62 kya and another gap of 1710 years between 2.11 and 3.82 kya. The relative proximity (approximately 200 km) between three sites displaying broadly coeval timing of gaps in ridge construction suggests a regional pattern in TC behaviour. However, the results of the Wonga Beach study provide little evidence that might be useful in clarifying the cause of the gaps.

Examining the sedimentary and morphological character of ridges assisted in identifying contrasting origins for different parts of the plain at Wonga Beach. Four ridges located immediately adjacent to the northern part of the beach are composed of fine- to medium-grained sand that display improved sediment sorting relative to sands comprising the adjacent beach. These four ridges are therefore likely to be foredunes belonging to a separate group of ridges to the four coarse-grained sand beach ridges located behind the southern part of the beach despite appearing to be continuous morphological features. As a consequence, the Wonga Beach plain is considered a complex barrier comprised of both beach ridges and foredunes. This result suggests the need for further studies to determine whether fine- to medium-grained sand ridge plains elsewhere may contain TC records.

6.2.3 Implications of Study at Cungulla

This study was conducted to test results of an unpublished study indicating wave genesis of fine- to medium-grained sand beach ridges at Cungulla, NE Queensland. Wave origins could not be ruled out for any of the ridges on the basis of sedimentary analysis because ridge, beach and nearshore sands (i.e. sands forming the sediment source for ridge development) at Cungulla are characteristically alike. LiDAR imagery appeared to be more effectively

diagnostic suggesting that there are two main types of ridges comprising the Cungulla barrier – intact beach ridges and beach ridges that have been disturbed by aeolian processes. The majority of the ridges display recurved morphology, suggesting origins associated with marine processes. Whereas, the oblique orientation of ridge truncations infers that the paths of fluvial incursions have flowed through the ridge sequence at different times during ridge plain development. This appears to have caused localised alterations in coastal alignment and destruction of parts or all of some ridges resulting in gaps in the ridge chronology. Overall, continuous deposition records are confined to individual sets of intact beach ridges and development of the truncations and crosscutting relationships between sets has contributed to a complex and discontinuous record that is of limited use in the estimation of TC intensity / frequency calculations.

The deposition record contained in the Cungulla beach ridge plain is of great value despite its discontinuous nature. This is because it infers that TCs can deposit beach ridges composed of fine- to medium-grained sand. Hence, it appears possible that similar landforms located elsewhere may contain similar records. For example, numerous barriers displaying shore-parallel ridge morphology and fine-grained sand sediment textures occur along the Queensland coast (Short, 2000). Detailed morphological studies of these plains could be relatively inexpensively conducted with use of LiDAR imagery. It is currently uncertain whether the abundance of sand ridge plains along the Queensland coast may provide a basis for understanding TC behaviour throughout the broader region. However, the results of the Cungulla study and the abundance of shore-parallel sand ridge plains along the Queensland coast suggest such potential.

Studies of the Cungulla beach ridge record highlight the characteristics of different types of chronological gaps. The distinction between different gap types has important implications for the origin of chronological gaps in other sand beach ridge sequences. For instance, gaps in deposition located adjacent to unconformities in the ridge sequence are likely associated with ridge plain erosion. Whereas, decreases or cessations in extremely intense TC activity are likely responsible for gaps that occur in continuous and

conformable beach ridge sequences such as those described at Cowley Beach, Rockingham Bay and Wonga Beach.

6.3 Evaluation of Sedimentary Palaeo-TC Record Types

Chapter 5 (Nott and Forsyth, 2012) presents analysis of and commentary on trends apparent in a comparison between long-term sedimentary TC records published to date. Comparison is made between overwash records that infer TC behaviour in the northern Atlantic, Gulf of Mexico and the NW Pacific with sand, shell and sand/shell beach ridge records that preserve aspects of TC activity from the SW Pacific, SE Indian Ocean and Gulf of Carpentaria respectively. It does not include a number of TC records contained in beach ridge plains composed of detrital coral along the eastern Queensland coast (Chappell et al., 1983; Chappell and Grindrod, 1984; Chivas et al., 1986; Hayne and Chappell, 2001). That is because these coarse-textured ridge plains display relatively uniform elevation throughout the sequence and are, therefore, thought insufficiently sensitive to record variation in long-term TC climatology (Forsyth et al., 2010).

The most striking aspect of the long-term sedimentary records considered in this study is the clustering in extreme intensity TC events punctuated by periods of relative quiescence that are centuries to millennia in length. This signal is particularly significant because it is present in all long-term sedimentary TC records thought to be sensitive enough to record variation in the long-term TC climatology. Hence, fluctuations in the TC climate may be a global phenomenon. Additionally, some unidentified factor or factors appear responsible for organization in the timing of fluctuations in the global TC climate. For example, beach ridge records suggest that three periods of heightened extremely intense TC activity have occurred in NE Queensland over the past 5,000 years (Figure 5-3) and a similar, broadly coeval pattern of TC behaviour is apparent in overwash records from the North Atlantic. The sedimentary records also suggest that timing of quiescence in these two regions roughly coincides with hyperactive periods of extreme intensity TC activity in the NW Pacific, East Indian Ocean, Gulf of Mexico and the Gulf of Carpentaria. These results are the first of their kind and appear to be a true reflection of patterns in global cyclone climatology because similar patterns in

the frequency of extreme intensity TCs are inferred despite variations in resolution and different record types.

6.4 The Challenges of Determining Causality

One method used to determine the causes of variability in TC behaviour involves comparing patterns in the frequency and magnitude of past events with indices of climatic state variables observed over the same period. As detailed in Chapter 5, numerous such studies have found links between historical TC behaviour and modulations in various climatic indices. However, these records are generally too short to fully elucidate millennial-scale patterns of fluctuation such as those suggested by long-term sedimentary TC records.

Only a few studies that have identified long-term TC records contained in sedimentary deposits have also made suggestions about the causes of punctuated TC behaviour (e.g. Liu and Fern, 2000; Donnelly and Woodruff, 2007; Woordruff et al., 2009). These records suggest correlations between variable climatic states and TC behaviour at the local or basin-wide scale, which is insufficient to relate directly to global climate fluctuations. They also refer to variable climatic states over only a relatively short time period (to 1500 years maximum), which is insufficient to be useful in comparison with the centennial- to millennial-scale variability apparent in sedimentary TC records. The present study concludes that the task of identifying drivers of punctuated TC behaviour is going to require more comprehensive knowledge of the long-term global climate than currently available.

6.5 Description of Other Long-term TC Records

There are a number of record types used to estimate TC behaviour during the past. Of those, only records contained in beach ridges and overwash deposits have been shown to preserve the intensity of events extending back several thousands of years (Nott, 2011b). Such long-term records are useful for revealing the spatial and temporal variability of TCs and examining relationships with climatic changes.

Overwash deposits are recognizable as a swathe of sediment (often sand) eroded from the nearshore, beach and barrier that is deposited as a layer up

to tens of centimetres thick in relatively quiescent backbarrier environments (Liu and Fearn, 2000; Donnelly and Webb, 2004). They often appear in core samples as discrete, relatively coarse sand layers within finer, organic-rich sediments and the sand layers are theoretically thickest nearer to the ocean and thinner with distance to landward. They have also been recognized using opal phytoliths (Lu and Liu, 2005), marine microfossils (Collins et al., 1999; Hippensteel and Martin, 1999; Scott et al., 2003) and stratigraphic variations in grain size, mineralogy, and geochemistry (Donnelly, 2005). The age of overwash deposition events has been estimated using radiocarbon, lead-210 or caesium-137 dating of terrestrial sediments located directly above and below the storm deposits. And the frequency of palaeo-TCs responsible for deposition is generally estimated by dividing the period of deposition in years by the number of storm layers preserved in the stratigraphy. Published accounts of TC deposits contained in overwash deposits emanate from various coastal lagoons (Donnelly, 2005; Donnelly and Woodruff, 2007; Woodruff et al., 2008a; Woodruff et al., 2008b; Wallace and Anderson, 2010), lakes (Liu and Fearn, 1993, 2000, 2002; Lambert et al., 2003; Lambert et al., 2008), marshes (Donnelly et al., 2001a; Donnelly et al., 2001b; Donnelly and Woodruff, 2007; Scileppi and Donnelly, 2007; Boldt et al., 2010) and sinkholes (Lane et al., 2011). Most notably, several studies have described TC records extending back periods of between 3000 to 7000 years contained in overwash from the Gulf of Mexico (e.g. Liu and Fearn, 1993, 2000; Wallace and Anderson, 2010; Lane et al., 2011), the NE Atlantic Ocean (Donnelly and Woodruff, 2007) and the NW Pacific (Woodruff et al., 2009) preserving aspects of TC behaviour solely from the northern hemisphere. Long-term overwash records consistently suggest that the behaviour of extreme intensity TCs is characterized by anomalous centennial- to millennial-scale hiatuses preserved as chronological gaps in overwash sedimentation.

6.6 The Importance of Understanding Regional Patterns in Long-term TC Behaviour

As described in Chapter 5, the most remarkable aspect of long-term beach ridge and overwash records is that they all display centennial- to millennial-scale fluctuations between relative quiescence and heightened intense TC activity. And this pattern is reflected in late-Holocene records arising from the NE Atlantic, Gulf of Mexico, Caribbean, NE Pacific, SW Pacific, Gulf of

Carpentaria and SE Indian Ocean. This result is important because it suggests that the most destructive TCs do not occur at random. Also, the pattern apparent in the sedimentary records suggests that these events are linked at the global-scale. For example, late-Holocene fluctuations in extremely intense TC activity in the North Atlantic appear to be out-of-phase with similar fluctuations apparent in records from the Gulf of Mexico and broadly coeval with fluctuations in the SW Pacific. This result is important because it suggests a previously unrecognised level of organization within past global TC behaviour. This apparent organization further suggests that some external factor or factors are likely to exert their influence on the occurrence of future extreme intensity TCs. Because the records providing these indications (i.e. beach ridge and overwash records) arise from different methodologies and from such varied settings, the signals of punctuated global TC activity suggested are unlikely to be artefacts of respective methodologies. The arrival at these conclusions represents a significant advance in our understanding of TC behaviour despite difficulties in identifying the cause(s) of punctuated global TC activity.

6.7 Implications for the Understanding of Barrier Development

6.7.1 The merits of using sediment texture to infer barrier origin

Geomorphologists have long considered that storms perform quite different roles in the development of shore-parallel barriers composed of sand compared to barriers displaying similar morphology composed of relatively coarser sediments. Redman (1852) first suggested that storm waves are responsible for depositing numerous sub-aerial barriers composed of gravel-sized sediments located along the coast of southern Britain. Numerous subsequent reports have designated storm wave origins to lithic gravel barriers located on high- to mid-latitude, paraglacial coasts (Gilbert, 1885; Johnson, 1919; Armon, 1974; Carter and Orford, 1984; McKay and Terich, 1992), coral rubble barriers on tropical island shorelines in the Pacific (Blumenstock, 1958; Maragos et al., 1973; Scoffin, 1993) and coral rubble and sand / shell shorelines in tropical NE Australia (Rhodes et al., 1980; Chappell et al., 1983; Chappell and Grindrod, 1984; Chivas et al., 1986; Hayne and Chappell, 2001; Nott and Hayne, 2001; Nott, 2003). Conversely, lower-energy processes are suggested responsible for development of swash-deposited

sand barriers in Europe (van Straaten, 1965), eastern USA (Fisk, 1959; Bernard and le Blanc, 1965), the Gulf of Mexico (Curray et al., 1969; Tanner and Stapor, 1971) and SE Australia (Davies, 1957; Davies, 1958; Bird, 1961; Thom et al., 1981; Roy et al., 1994). Hence, gravel barriers are generally considered morphodynamically distinct from sand barriers because the former are thought the product of high intensity / low frequency processes and the latter are thought the product of low intensity / high frequency events (Komar, 1976; Carter and Orford, 1984; Otvos, 2000; Tanner, 1995; Taylor and Stone, 1996; Woodroffe, 2003; Scheffers et al., 2011; Tamura, 2012).

Results of recent studies (Nott et al., 2009) including those presented in Chapters 2 to 4 suggest that inundations associated with extreme intensity TCs are responsible for development of four pure sand beach ridge plains located in NE Queensland. There is little doubt that these plains are barriers. However, they do not appear to conform with the model of barrier distinction based on sediment texture described above because they are composed of sand and likely deposited by high intensity / low frequency (TC) marine processes. Unlike reports of sand beach ridge genesis elsewhere, the predominantly quiescent wave climate in this region is unlikely to have contributed significantly to the elevations of these NE Queensland beach ridges. These results are important because they cast doubt upon conclusions of low-energy origins previously ascribed to numerous eastern Queensland coastal barriers based on their sand composition and shore-parallel morphology alone (BPA, 1979; Hopley, 1970; Pye, 1980, 1983; Brooke et al., 2006;).

Some recent commentaries (e.g. Otvos, 2011; Scheffers et al., 2011, Tamura, 2012) prefer that aeolian processes are responsible for depositing the crests of coarse-grained sand beach ridge plains along the coast of NE Australia on the basis of textural composition alone. However, these conclusions were never tested against the coarse-grained sand barriers located along the humid tropical coast of NE Queensland. As such, these commentaries provide no account for the local predominance of coarse-grained sand at ridge crests elevated several meters above normal tidal influence. The threshold of wind velocity for transporting coarse-grained sand is approximately 30 m/s (i.e. 110

km/h) (Bagnold, 1941; Mountney, 2006). Onshore winds of that strength are mostly confined to the passage of nearby TCs along the humid tropics coast and the beach is likely covered by tidal inundation during periods of peak wind velocity during such an event. Therefore, aeolian processes are likely to have played little or no part in deposition of coarse-grained sand at ridge crest elevation in this region. Also, where detailed studies of these specific landforms have occurred (i.e. Nott el al., 2009; Forsyth et al, 2010, 2012), it has been concluded that marine processes associated with extreme intensity TCs likely deposited beach ridges composed of pure sand. These results suggest that future enquiry into the development processes of sand barriers should include careful comparisons between the sedimentary characteristics of barrier, beach and nearshore environments. That is because the evidence from the humid tropical coast of NE Queensland suggests that the texture of a barrier alone is not the key to its origin.

The results of studies described in Chapters 2 to 4 infer that distinction of barrier process origins cannot be made on the basis of gravel or sand composition for sites located along the GBR coast. This is not to say that *a priori* assumptions of a distinction between gravel and sand barriers are generally incorrect because the sedimentary response to extreme events varies at different locations. However, it does suggest that future assessments of barrier origin both in Queensland and elsewhere should not be made on the basis of shore-parallel morphology and sediment composition alone.

6.7.2 Limits to the probable spatial distribution of sand beach ridge plains deposited by storm waves

It is important to compare observations of sedimentary response to storm waves at the coast reported in this thesis with observations from elsewhere. This might help elucidate whether the sedimentary response to storm waves observed in NE Queensland is unique or whether storm-deposited sand beach ridges may be more widespread than is currently acknowledged. Furthermore, it may help identify why storm waves deposit beach ridge sediments in this region when the opposite is true of many regions outside of NE Queensland.

The recent literature suggests that sand beach ridges are constructed when waves transport sand to the subaerial environment during periods of moderate sea conditions (e.g. Tanner, 1995; Taylor and Stone, 1996; Otvos, 2000; Hesp et al., 2005; Scheffers et al., 2011; Tamura, 2012). On this basis, two recent reviews (Scheffers et al., 2011; Tamura, 2012) have refuted claims of TC origins for NE Queensland beach ridges. However, a number of reports describe sand beach ridge construction during high intensity events. For example, McIntire and Harley (1964), Thom (1964) and Psuty (1965) suggest that storm waves are responsible for depositing layers of sand at the crests of beach ridges in Mauritius, Campeche (Mexico) and Tobasco (Mexico) respectively. In each case, the sediments were thought eroded from the beach then directly deposited at the crest of the beach ridge fronting a plain composed of multiple ridges of similar origin. In this sense, the sediment source, mode of sediment transport and description of the eventual sediment storage are in agreement with recent descriptions of sand beach ridge construction in NE Queensland (Nott et al., 2013). Additionally, Donnelly (2007) successfully simulated deposition of sand at the barrier crest caused by wave run-up associated with storm surge. According to results, crest accumulation occurs when entrained sediment falls from suspension as overtopping wave run-up decelerates up to and on to the ridge crest, especially where ridge crests are relatively wide (Donnelly, 2007). It is apparent, therefore, that sand beach ridges deposited by storm waves may be more widespread than currently acknowledged in recent reviews.

Aside from questions surrounding sedimentary response to wave energy, reviews describe a number of conflicting ideas regarding sand beach ridge construction. Importantly, aeolian processes are widely considered responsible for depositing ridge sands at elevations greater than the extent of uprush during fair weather wave conditions (e.g. Davies, 1958; McKenzie, 1958; Tanner, 1995; Otvos, 2000; Hesp et al., 2006). Hence, aeolian origins are occasionally ascribed to NE Queensland beach ridges (e.g. BPA, 1979; Short, 2000; Brookes et al., 2006) despite prior reports suggesting the contrary (e.g. Hopley, 1970; Pye, 1982, 1983). Elsewhere, varying inferences have been made about the role of wind, waves and plants in the initiation of

ridge construction and stabilisation. For example, McKenzie (1958) infers that vegetation located to seaward of the first beach ridge is responsible for accumulating the nucleus of an incipient beach ridge. Whereas, numerous others (e.g. Davies, 1958; Thom, 1964; Hesp et al., 2006) conclude that berms form the nucleus upon which subsequent beach ridge construction occurs.

Unlike sand beach ridges, gravel barriers are particularly common where reworked glacigenic sediments are deposited on mid- to high-latitude, wave-dominated coasts (Armon, 1974; Randall, 1977; Carter and Orford, 1980; Wang and Piper, 1982). Additionally, reports of beach ridges composed of gravel-sized particles of coral reef debris emanate from the tropical Pacific (Maragos et al., 1973; Scoffin, 1993; Nott et al., 2001).

High-energy sedimentary processes are required to transport gravels. Processes underlying gravel barrier construction revolve around the incidence of waves with sufficient energy to transport gravel-sized (between 2 and 2000 mm) clasts up the beach face (Orford et al., 1991). The net result of these processes is deposition of a ridge around the high water swash limit, which is often accentuated by meteorological surge and storm wave set-up (Orford et al., 1991). Gravel beach ridges at Chesil Beach, England extend to 14 m AHD and exposed gravel beaches in northwest Ireland have crests at 10 to 15 m AHD (Orford et al., 1991). Hence, the sediment texture and elevation of gravel beach ridges are clear indicators of their storm wave origins.

Sediment texture is also thought central to beach ridge construction. The size and shape of gravel clasts causes high porosity in deposited sediments, which allows percolation of waves and attenuation of erosion during downwash (Carter, 1988). Hence, the sediment porosity is considered an important factor in gravel beach ridge construction.

Processes responsible for barrier erosion counter the processes responsible for ridge construction. The literature suggests that there are two main types of storm wave conditions that result in erosion of sand barriers. These include:

Type A - Where the total storm-induced water levels (including a combination of surge, tides, and wave runup) reach but do not exceed crest elevation of

the most seaward ridge resulting in seaward transport of eroded beach and barrier sands and scarping leading to complete collapse of the ridge if the storm persists (Long et al., 2014); and

Type B - Where the total storm-induced water levels do exceed crest elevation of the most seaward ridge resulting in overwash of the barrier and landward transport of eroded beach and barrier sands (Long et al., 2014).

Examples of Type A erosion are found in reports of marine inundation associated with the landfall of Hurricane Hugo on the eastern USA coast (e.g. Katuna, 1991; Sexton and Hayes, 1991) and elsewhere in the aftermath of storm inundations in SE Australia (e.g. Thom and Hall, 1991) and western USA (Shih and Komar, 1994). In each case, beach and ridge sediments were transported and deposited offshore as sand bars. This process of erosion has been linked with the high rates of water retention in sand (compared to gravel) providing for relatively high effectiveness of storm wave downwash (Komar, 1998). Contrastingly, Type B erosion during overtopping by storm waves can result in erosion and rapid lowering of the sand ridge crest leading to an increase in wave overtopping and eventual destruction of the entire ridge if storm conditions persist (Donnelly, 2007; Long et al., 2014). Nott (2006) describes complete destruction of three rows of unconsolidated sand ridges during a single TC event by overtopping storm inundation in Western Australia. In this case, sands eroded from the ridges were redistributed as a sub aerial splay to landward (Nott, 2006). It also stands to reason that some storms erode only part of a ridge. For example, inundation associated with Hurricane Ivan breached lower sections of the sand barrier while more elevated sections experienced crest lowering due to overwash at Dauphin Island (USA) (Long et al., 2014). In summary, the literature suggests that storm waves can result in destruction of part or the entirety of a shore-parallel sand ridge.

Patterns of unconformity at Cungulla suggest that storm waves are unlikely to be responsible for much of the pattern of erosion evident in the landscape there. The LiDAR data (Figure 4.4) suggests that the northern part of many eroded Cungulla ridges remain in the landscape located at or adjacent to the seaward boundary of ridge sets. Therefore, it appears that the southern part

of these ridges was eroded. Patterns of wave erosion discussed above infer that relationships between ridge sets are likely to be conformable to sub-conformable if storm waves were responsible for that erosion. They may also be difficult to distinguish in the imagery as a result. However, the ridges at Cungulla have been diagonally or orthogonally truncated in most cases. Furthermore, the ridge plain is generally oriented toward the northeast, which is the direction of greatest fetch. Yet, orientation of ridge truncations suggests that the likely energetic source of erosion comes from the southeast of the plain and not from the northeast. Because the southeast of the area is girthed by land, waves are unlikely to have caused ridge plain erosion that resulted in the unconformable relationships between numerous ridge sets across the Cungulla sequence.

Instead of wave attack, conclusions of fluvial erosion are supported by geomorphic expressions in the landscape at Cungulla. Storm surge and heavy rains accompanying nearby TCs are likely to cause flooding of the Horton River (Figure 4.1). Also, raised water levels associated with storm surge are likely to inhibit drainage of the river resulting in flooding of low-lying areas surrounding the ridge plain. Erosion along the southern part of the plain would be especially likely under this scenario if sufficiently high flow velocities were to eventuate within floodwaters. Therefore, flooding of the Horton River appears very likely to have caused erosion that has led to the current pattern of unconformable ridge sets at Cungulla.

In general, gravel beach ridges remain relatively stable in the face of wave attack over the short term because only extreme energy inundations are likely to entrain constituent sediments (Carter and Orford, 1993). However, that is not always the case. For example, Bradbury and Powell (1992) describe the sudden failure of shingle ridges when the crest is initially overtopped and subsequently eroded down. This may result from a period in which storm waves transported sediments sourced at the ridge flank and deposited them at the ridge crest. Although this may reduce the likelihood of overwash in the short term, it would render the ridge more vulnerable to collapse because of its steepening profile in the long term (Orford et al., 2003). Otherwise, inertia is the chief counterforce to gravel barrier breakdown because the resistance

of coarse clasts to sediment transport slows overall barrier response. Therefore, extreme storms are commonly past their peaks before their full potential impacts on a gravel beach ridge are imparted (Orford et al., 2003). However, unlike widespread belief about sand barriers, slow moving storms or a series of intense events are thought required to overcome the forces that provide relative stability to gravel barriers.

Keys to assessing why beach ridges are constructed by storm waves in NE Queensland must explain why sand is transported to the ridge crest rather than offshore. Nott et al. (2009; 2013) and studies described in Chapters 2 and 3 suggest that crest sediments are deposited by TC inundations that overtop the seaward side of a coastal barrier. Hence, the level of inundation is greater than the elevation of the most seaward ridge. In agreement with Donnelly (2007), sand eroded from the beach is subsequently deposited at the crest of the overtopped ridge. According to this model, beach sediments may have been transported to seaward and deposited as a nearshore bar if inundation had been lower than the ridge located adjacent to the beach. Overtopping of this ridge is likely possible because aeolian contributions to beach ridge elevation is generally minimal or absent along the NE Queensland coast (Pye, 1982). Therefore, inundations associated with TCs appear to be responsible for depositing the entirety of sand beach ridges in NE Queensland largely because aeolian processes are not important along much of the NE Queensland coast.

Knowledge of the reasons behind a lack of aeolian contributions to beach ridge construction in NE Queensland is likely to suggest why sand beach ridges with storm wave origins are rare elsewhere. Pye (1983) suggested several reasons for the scarcity of aeolian contributions to beach ridge elevation in this region, including:

a. Generally low energy wind regime in this region;

b. Local coastal orientation and shelter from headlands results in decreased wind energy at the shoreline;

c. High evaporation rates of sea spray or residual beach moisture result in formation of a salt crust on beach surfaces diminishing aeolian deflation; and

d. Beach sands are consistently wet due to rain and humidity in the humid tropical sector, raising the threshold of wind velocity required for aeolian entrainment.

Beach morphology may provide another reason. Sherman and Lyons (1994) showed that all aeolian sand transport models require a flat, horizontal and unobstructed surface for aeolian deflation. In SE Queensland and elsewhere, this occurs in the form of a broad back beach area over which sand can be entrained (Short, 2000). However, the subaerial beaches along much of the NE Queensland coast can be characterised as narrow and steep (Short, 2000). Therefore, aeolian deflation is unlikely. Additionally, winds capable of transporting coarse-grained sands comprising many beaches in this region are largely confined to the passage of TCs. The marine inundation accompanying extreme winds during these events is likely to submerge the beach. Hence, there would be no sediment source available for aeolian transport of sand when the wind velocity is at its peak during a TC irrespective of wind strength. These factors combine within a climatic environment where either tropical cyclones or trade wind strength governs wind velocity (Short, 2000). Similar combinations of geomorphic and climatic conditions are unlikely to be found in temperate or polar climates. Particularly because the sub-cyclonic winds often reach greater velocities than the trade winds prevalent along the NE Queensland coast. However, similar combinations of geomorphic and climatic conditions may have lead to the development of sand beach ridges with TC-origins elsewhere in the tropics.

6.8 The Significance of Improved Hazard Assessments

Hazard assessments are likely to improve through the use of beach ridge records. That is because, according to the results of studies described in Chapter 4, storm deposited beach ridges appear to be widespread in northern Australia. And many of these plains likely contain long-term TC records suitable for testing TC hazard estimates assessed through other methods. The following discussion focuses upon some of the issues surrounding TC hazard estimates in Australia and how beach ridge records may contribute to future improvements in this field.

In Australia, TC hazard assessments are derived through extrapolation of the short historical record (McInnes et al., 2000; Harper et al., 2001; McInnes et al., 2003;) and the same is true of general trends in TC behaviour in this region (e.g. Kuleshov et al., 2010; Callaghan and Power, 2011). However, the validity of assuming that a short time series can be accurately representative of TC behaviour in general has been vigorously debated in the literature (e.g. Landsea, 2005; Pielke and Landsea, 1998; Landsea et al., 2006; Chan, 2006; Kossin et al., 2007; Nott, 2005, 2006). Although the short-term TC record preserves events over the instrumental period at high resolution, it is unlikely to provide signals of non-stationarity and serial correlation normally present in longer time-series data (Nott et al., 2005, 2006).

Beach ridge records are capable of providing tools to substantially improve precision in the assessment of risk posed by TC-induced marine inundation in Queensland, Australia. The apparent tendency for beach ridge records to display relatively low resolution and preferably preserve the most intense events results in the filtering out of low-intensity / high frequency storms from the record. This results in the ability to focus upon return intervals for the most destructive events. Also, because the crests of many NE Queensland beach ridges are composed of sediments deposited by past inundation events, their elevations serve as direct observations of known total inundation levels including wave setup and wave run-up. Therefore, unlike current methods of TC risk estimate beach ridge records do not rely on data that substitute for direct measurements to estimate total inundation associated with extreme intensity events. Wave setup and run-up deliver much of the energy responsible for backshore impacts associated with marine inundations at the coast (Sallenger, 2000; Ruggiero et al., 2001). As such, the resolution of TC records contained in beach ridge deposits plus the tendency to preserve actual events instead of proxy-data provide a level of precision that is an improvement on current practice in TC risk assessment. Therefore, it is important to incorporate beach ridge studies into future hazard estimates.

Nott and Jagger (2013) have demonstrated a statistical method for estimating the frequency / magnitude curve for TC-induced inundations using an example beach ridge record (i.e. Forsyth et al., 2010) in comparison to

records from a known extreme intensity event. This study has established TC-risk estimates that are a valuable resource for those assessing risk at Rockingham Bay, on the NE Queensland coast. However, this information is of limited use to those assessing risk at other locations. Therefore, it is important that future studies of beach ridge records apply their results to similar statistical analyses as those described by Nott and Jagger (2013). This will provide a robust means of testing TC-risk assessments that use alternative methods of enquiry.

6.9 Significance and Use of Quaternary TC Records

The relatively recent emergence of sedimentary Quaternary TC records is likely to be key to detection of past changes in extreme TC behaviour and attribution of the causes of such changes. This is because evidence of long-term patterns in the TC climate contained in these records appears to suggest the occurrence of prehistoric and therefore otherwise unobservable phenomena. Records of past TC incidence are contained in numerous proxies, including lake sediment archives (Besonen et al., 2008), oxygen isotope anomalies in speleothems, tree rings and corals (Malmquist, 1997; Miller et al., 2006; Nott et al., 2007; Frappier et al., 2007; Hetzinger et al., 2008), preserved offshore sedimentary structures (Duke, 1985; Ito et al., 2001; Keen et al., 2004; Keen et al., 2006) and more (see review in Nott, 2011b). These records vary according to their length, chronological resolution and nature. To date, only beach ridge and overwash records extend back periods of 3000 to 5000 years producing the longest palaeo-TC records resolved to date. Hence, the studies resulting in long-term TC records described in Chapters 2 to 4 form an important part of current understandings about Quaternary TC behaviour.

It is important here to discuss the role for sedimentary records in future studies of Quaternary TC behaviour. The first sand beach ridge TC-records came to light relatively recently (Nott et al., 2009). Since then, sufficient evidence has arisen to suggest that beach ridge plains composed of sand are suitably abundant in northern Australia to form the basis of regional-scale long-term TC records (Forsyth et al., in review; Chapter 4). As such, signals of cyclone climatology contained in beach ridge records extracted from along the

coast of northern Australia in the future are likely to significantly advance our knowledge of TC behaviour in the SW Pacific, Gulf of Carpentaria and SE Indian Ocean. Moreover, the readily available imagery suggests that there are widespread examples of ridge plains composed of sand that display shore-parallel morphology scattered along the coasts of regions such as East Asia, SE Asia, Western Mexico and islands of the SW Indian Ocean. And because these locations are occasionally subject to the impacts of TCs, it is also possible that some of these landforms are beach ridge plains that contain palaeo-TC records. This possibility ought to be considered by those assessing long-term TC behaviour in these regions in the future. Furthermore, the high elevation of ridge plains displaying similar morphology along the coast of the Caribbean, Gulf of Mexico and eastern United States have long been ascribed to aeolian processes in a fashion similar to examples from NE Queensland (BPA, 1979; Brooke et al., 2006). These findings remain untested by the model of analysis described in Chapters 2 to 4 and the possibility of TC genesis should not be discounted until they are. As such, there are numerous ways in which future beach ridge studies using the methodologies developed as part of this project may advance our understandings of Quaternary cyclone climatology.

6.10 Treatment of late-Holocene Sea Level Fluctuations

There appears to be some disagreement about the role that changes in sea level have played in beach ridge construction. For instance, Tanner (1995) found that processes associated with sea level oscillations over several years to decades are responsible for the elevation of beach ridge crests in locations around the Caribbean, the USA and Central America. Whereas, Davies (1958) and Orford et al. (2002) detailed description of supply control and forcing control as the most important aspects of ridge building. These authors warned against the use of variations in the beach ridge crest elevations as a basis for defining sea-level changes without knowledge of past storm frequency. Tamura (2012) also contests the notion that sea levels are preserved in ridge elevations when suggesting that aeolian components of ridge development are likely to bias any estimates of sea level change. The disagreement found on these points of sand barrier construction suggest

considerable uncertainty surrounding the role of late-Holocene sea levels on beach ridge elevations.

Although Chapter 2 and 3 provide discussion about the possible effects of sea-level change on the TC record, questions remain about whether such fluctuations might have influenced the TC records presented in this thesis. Analysis presented in Chapters 2 and 3 suggest that beach ridges deposited between 4.5 kyr to 5.5 kyr display greater elevation than most ridges deposited since that time. Additionally, sea level is thought to have fallen by 1 – 1.5 m in northeast Queensland since 5.50 kyr. One might surmise, therefore, that descending beach ridge elevations may be correlated with drops in sea level. Figure 6.2 indicates that TCs have been getting more intense with time if sea level is accounted for in this way, or at least, that recent TCs are more intense than they were at 5 kyr. However, there has been no evidence provided to date suggesting that is the case. Therefore, the addition of sea level data is likely to add considerable levels of uncertainty to the results of analysis.

Uncertainty margins associated with central pressure estimates are presented in Chapters 2 and 3. These reflect the range of possible tide states within the full nodal tidal cycle that could have occurred during deposition of sediments onto the beach ridges during previous TCs. For example the tide range in Cairns is greater than 3.4 m and sea level has only fallen by 1 to 1.5 m since the mid-Holocene. The range of tide levels and hence sea-level at the time of deposition of a unit of sediment is at least double that of the sea-level fall. The uncertainty margins or the variation in tide levels are likely to mask any influence of previous sea levels in this region. Figure 6.2 illustrates these uncertainty margins and highlights the possibility that any sea-level signal could be swamped by central pressure uncertainty margins, especially when combined with the possibility of ridge settling. Furthermore, the fact that there is a progressive decrease in height in ridge crests towards the coast may support the idea that beach ridges are poor indicators of late-Holocene sea levels in this region.

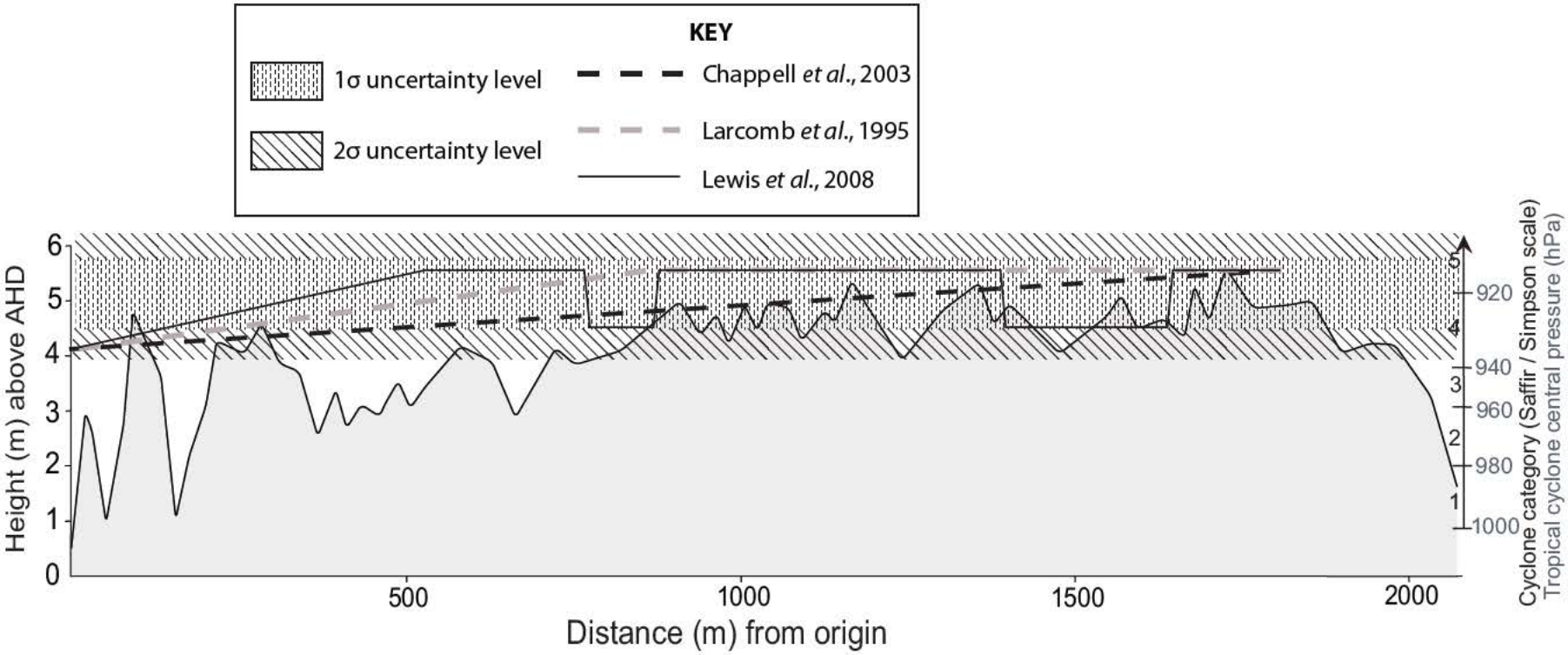

Figure 6 - 2 Cross-section of Rockingham Bay beach ridge plain, showing height of ridges above AHD and modelled TC intensity required to produce inundation level equal to ridge height based upon mean tide level. Also, the various sea level curves for NE Queensland are denoted and shaded areas show 1σ and 2σ uncertainty margins associated with central pressure estimates. Origin denotes the location of shoreline at the time of survey.

6.11 Limitations to the Present Methodologies

The difficulties explaining drivers of punctuated TC behaviour discussed above are not the sole limitation associated with the use of beach ridge TC records. Other limitations with these records include those associated with the calibration of event magnitude estimation and methods in developing deposit chronologies.

The first limitation concerns TC event magnitude estimation using beach ridge records. Such records published to date account for the approximate storm inundation elevations (including error margins associated with tidal probabilities) using the modern ridge crest height. This method does not account for the possibility that multiple events have contributed to the overall elevation of the ridge. Hence, there is no way of knowing whether low- or high-intensity events are responsible for depositing any lower elevation depositional units of that ridge. Palaeo-TC magnitude estimates based on these records may not, therefore, account for all of the extreme intensity TCs responsible for depositing any particular beach ridge plain. In this way, methodologies described in Chapters 2 to 4 are likely to underestimate the magnitude of the most intense TC events at a location and are extremely unlikely to overestimate them. Future work may improve on this situation through higher resolution stratigraphic and chronological analysis of beach ridges. This type of work may clarify whether each ridge is the product of multiple wave events and whether high-resolution stratigraphic sampling may enable more detailed magnitude estimates. However, this type of analysis would still only suggest a minimum inundation level. Also, resultant records are still unlikely to elucidate every extreme intensity event because each ridge represents such a long and complex past.

The second limitation concerns methods used to develop palaeo-TC chronologies. Beach ridge records published to date have relied mainly upon the approximate deposition dates of ridge crest sediments to assess TC frequency. As described above, this method is limited by our current inability to account for the number of storms required to deposit any single ridge. More detailed stratigraphic studies in the future are likely to improve the resolution

of beach ridge chronologies and further clarify long-term TC intensity / frequency relationships.

Chapter 7: Conclusions of the Dissertation

Wind is routinely assumed responsible for genesis of shore-parallel coastal barriers composed of sand and waves are used to account for landforms of similar morphology when comprised of coarser materials. However, this concept was challenged by results of a study suggesting that inundation associated with extreme intensity tropical cyclones are responsible for depositing a sequence of beach ridges composed of coarse-grained sand at Cowley Beach, NE Queensland, Australia (Nott et al., 2009).

Beach ridge development studies at Rockingham Bay, Wonga Beach and Cungulla were conducted with four main aims:

1. To determine whether the palaeo-TC record contained in the coarse-grained sand beach ridge plain at Cowley Beach is an anomaly or whether similar landforms in the region also contain TC records;
2. To determine whether fine-grained sand beach ridges may also contain palaeo-TC records;
3. To determine the origin of chronological gaps in the depositional records of NE Queensland beach ridge plains; and
4. To assess patterns of TC behaviour in NE Queensland beach ridge records in a regional and global context.

Sedimentary analysis results suggest that the crests of all ridges in the Rockingham Bay beach ridge plain and most ridges in the plain at Wonga Beach are composed of coarse-grained sand that is too coarse in texture to have been deposited by the predominantly low-energy local wind regime. Also, a clear distinction is apparent between the sediments populating the crests of these ridges and (aeolian) foredune sediments elsewhere in this region. Therefore, marine processes are likely responsible for their deposition. Furthermore, numerical modelling results suggest that most ridge crest sediments at Rockingham Bay and Wonga Beach are elevated well above the reach of all but the most extreme events. Therefore, ridges comprising both plains likely have similar origins to those comprising the Cowley Beach beach ridge plain – i.e. inundations associated with extreme intensity TCs are likely

the principal agent of their deposition. Because a number of other ridge plains in the humid tropical sector of NE Queensland display similar morphological and sedimentary characteristics, it appears likely that TCs play an important depositional role in coastal development in this region.

Analysis suggests that marine inundations associated with TCs are principally responsible for depositing beach ridges composed of fine-grained sand at Cungulla. Comparative studies of local barrier and nearshore sediments suggest that marine processes and not wind are responsible for depositing these ridges. The numerical modelling suggests that the upper sedimentary units of most beach ridges in this sequence were deposited by inundations associated with the nearby passage of extreme intensity TCs. As such, they appear to have similar origins to beach ridge plains in the adjacent humid tropical sector. These findings suggest that detailed studies are required to determine the origin of sand barriers and that the genesis of shore-parallel fine-grained sand coastal barriers cannot reliably be determined using sediment texture alone.

Morphological and chronological analysis suggests that the beach ridge plain at Cungulla contains two types of chronological gaps. Unconformities in ridge orientation and variations in ridge morphology between smooth and convex to hummocky ridge crests characterize the ridges located adjacent to some chronological gaps. These are likely morphological signatures of occasional erosion and reworking of parts of the ridge sequence. However, such morphological characteristics were not found in association with certain other chronological gaps in this ridge plain. And it was suggested that the origins of chronological gaps in TC-deposited beach ridge sequences that do not coincide with morphological signals of past erosion are likely to be linked to decreased ridge development during periods of less intense TC activity. These morphological characteristics were used as diagnostic indicators of the origin of chronological gaps in beach ridge plain construction in the humid tropical sector and they may also be useful in a similar role elsewhere around the globe.

Comparing the TC intensity data with chronological studies suggested that the cyclone climate in the humid tropical sector of NE Queensland fluctuates over

time. Essentially, the storm climate in this region appears to be characterized by centennial- to millennial-scale periods of relative quiescence when relatively few extreme intensity events occur. It is also apparent that these periods are punctuated by millennial-scale periods during which extreme intensity TCs are relatively common. The same is true of long-term sedimentary TC records from Australia and around the globe. Hence, it appears likely that the global frequency of extreme intensity TCs is not random. Instead, long-term sedimentary records from the SW Pacific, NW Pacific, Caribbean, North Atlantic and the SE Indian ocean basins suggest that the global cyclone climate is characterized by centennial- to millennial-scale periods of relative quiescence punctuated by millennial-scale periods during which extreme intensity TCs are relatively common. Understanding the cause of this variability is currently hindered by a lack of comparable proxies. However, the observation that long-term TC climatologies display centennial- to millennial-scale punctuated activity is an important step towards identifying the influence, if any, of humans on TC behaviour and improving the basis upon which the risk of TC-hazards are assessed.

The results of studies from NE Queensland suggest that many beach ridge plains composed of sand located in that region may contain palaeo-TC records. According to these results, similar studies of sand beach ridge records in that region are likely to contribute to a more realistic indication of the return period of TC-generated inundations than provided by current methods of risk assessment. They are also likely to provide a robust means of testing the contemporary understandings of TC climatology. This is because beach ridge plains appear to preserve a record of actual events rather than the synthetic time series used in the probabilistic modelling that underpins current methods in risk assessment. Consideration of the beach ridge record is important for reducing community vulnerability and mitigating the impacts of TC hazard in Queensland, especially within the context of projected increased sea levels associated with global climate change.

Bibliography

Ademiec, G., and Aitken, M., 1998, Dose-rate conversion factors update: Ancient TL, v. 16, p. 37-50.

Aitken, M. J., 1998, An Introduction to Optical Dating: The dating of Quaternary sediments by the use of Photo-Stimulated Luminescence, Oxford, Oxford Science.

Armon, J. W., 1974, Late-Quaternary shore lines near Lake Ellesmere Canterbury, New Zealand: New Zealand Journal of Geology and Geophysics, v. 17, p. 63-73.

Atwater, B. F., 1987, Evidence for Great Holocene Earthquakes along the Outer Coast of Washington State: Science, v. 236, no. 4804, p. 942-944.

Baddiley, P., 2003, The Flood Risk in Cairns: Natural Hazards, v. 30, p. 155-164.

Bagnold, R. A., 1941, The Physics of Blown Sand and Desert Dunes, London, Methuen, 265 p.:

Basher, R. E., and Zheng, X., 1995, Tropical cyclones in the southwest Pacific: Spatial patterns and relationships to the Southern Oscillation and sea surface temperature: Journal Of Climate, v. 8, p. 1249-1260.

Bateman, M. D., and Catt, J. A., 1996, An absolute chronology for the raised beach deposits at Sewerby, E. Yorkshire,UK: Journal of Quaternary Science, v. 11, p. 389-395.

Bernard, H. A., and le Blanc, R. J., 1965, Resume of the Quaternary geology of the northwestern Gulf of Mexico, in Wright, H. E., Jr., and Frey, D. G., eds., The Quaternary of the United States: Princeton, New Jersy, Princeton University Press, p. 137-185.

Besonen, M., Bradley, R., Mudelsee, M., Abbott, M., and Francus, P., 2008, A 1,000-year, annually-resolved record of hurricane activity from Boston, Massachusetts: Geophysical Research Letters, v. 35, no. 14, p. L14705.

Bird, E. C. F., 1961, The coastal barriers of East Gippsland, Australia: The Geographical Journal, v. 127, no. 4, p. 460-468.

-, 1971, The origin of beach sediments on the North Queensland coast: Earth Science Journal, v. 5, no. 2, p. 95-104.

Bird, E. C. F., and Hopley, D., 1969, Geomorphological features on a humid tripical sector of the Australian coast: Australian Geographical Studies, v. 7, no. 2, p. 89-108.

Blott, S., 2008, Gradistat Version 6.0, A Grain Size Distribution and Statistics Package of Unconsolidated Sediments by Seiving or Laser Granulometer: Egham.

Blumenstock, D. I., 1958, Typhoon Effects at Jaluit Atoll in the Marshall Islands: Nature, v. 182, no. 4645, p. 1267-1269.

Boldt, K. V., Lane, P., Woodruff , J. D., and Donnelly, J., 2010, Calibrating a sedimentary record of overwash from Southeastern New England using modeled historic hurricane surges: Marine Geology, v. 275, p. 127-139.

BOM, 2011a, Mossman monthly climate statistics: Australian Government Bureau of Meteorology.

BOM, 2011b, Cape Cleveland monthly climate statistics: Australian Government Bureau of Meteorology.

BPA, 1979, Capricorn Coast beaches: Beach Protection Authority, Queensland Government.

Bristow, C. S., Chroston, P. N., and Bailey, S. D., 2000, The structure and development of foredunes on a locally prograding coast: insights from ground-penetrating radar surveys, Norfolk, UK: Sedimentology, v. 47, no. 5, p. 923-944.

Bradbury, A. P., and Powell, K. A., 1992, The short term profile response of shingle spits to storm wave action: Proceedings of the 23rd Coastal Engineering Conference, v. 3, p. 2694-2707.

Broadbridge, N. W., and Hanstrum, B. N., 1998, The relationship between tropical cyclones near Western Australia and the Southern Oscillation Index: Australian Meteorological Magazine, v. 47, p. 183-189.

Brooke, B., Ryan, D., Radke, L., Pietsch, T., Olley, J., Douglas, G., Flood, P., and Packett, B., 2006, A 1500 year record of coastal sediment accumulation preserved in beach deposits at Keppel Bay, Queensland, Australia: Cooperative Research Centre for Coastal Zone, Estuary and Waterway Management.

Callaghan, J., and Power, S. B., 2011, Variability and decline in the number of severe tropical cyclones making land-fall over eastern Australia since the late nineteenth century: Climate Dynamics, v. 27, p. 647-662.

Carter, R. W. G., 1988, Coastal environments: an introduction to the physical, ecological and cultural systems of coastlines, London, Academic Press, 617 p.:

Carter, R. W. G., Hesp, P. A., and Nordstrom, K. F., 1990, Erosional landforms in coastal dunes, London, Wiley, Coastal Dunes: Form and Process.

Carter, R. W. G., and Orford, J. D., Gravel barrier genesis and management: a contrast, in Proceedings Coastal Zone `80, Proceedings of the 2nd Symposium on Coastal and Ocean Management, Hollywood, Florida, 1980, American Society of Civil Engineers, p. 1304-1320.

Carter, R. W. G., and Orford, J. D., 1984, Coarse clastic barrier beaches: A discussion of the distinctive dynamic and morphosedimentary characteristics: Marine Geology, v. 60, no. 1-4, p. 377-389.

Carter, R. W. G., and Orford, J. D., 1993, The Morphodynamics of Coarse Clastic Beaches and Barriers: A Short- and Long-term Perspective: Journal of Coastal Research, v. Beach and Surf Zone Morphodynamics, no. SI 15, p. 158-179.

Chan, J., 2006, Comment on ‘changes in tropical cyclone number, duration, and intensity in a warming environment: Science, v. 311, p. 1713.

Chan, J. C. L., and Xu, M., 2009, Inter-annual and inter-decadal variations of landfalling tropical cyclones in East Asia. Part I: time series analysis: International Journal of Climatology, v. 29, no. 9, p. 1285-1293.

Chappell, J., 1967, Recognizing fossil strand lines from grain-size analysis: Journal of Sedimentary Research, v. 37, no. 1, p. 157-165.

Chappell, J., Chivas, A. R., Wallensky, E., Polach, H., and Aharon, P., 1983, Holocene palaeo-environmental changes, central to north Great Barrier Reef inner zone: BMR Journal of Australian Geology and Geophysics, v. 8, p. 223-235.

Chappell, J., and Grindrod, J., 1984, Chenier Plain formation in northern Australia, in Thom, B. G., ed., Coastal Geomorphology in Australia: Sydney, Academic Press, p. 197-232.

Chivas, A., Chappell, J., Polach, H., Pillans, B., and Flood, P., 1986, Radiocarbon evidence for the timing and rate of Island development, beach-rock formation and phosphatization at Lady Elliot Island, Queensland, Australia: Marine Geology, v. 69, no. 3-4, p. 273-287.

Cobb, K. M., Charles, C. D., Cheng, H., and Edwards, R. L., 2003, El Niño/Southern Oscillation and tropical Pacific climate during the last millennium: Nature, v. 424, p. 271-276.

Collins, E. S., Scott, D. B., and Gayes, P. T., 1999, Hurricane records on the South Carolina coast: can they be detected in the sediment record?: Quaternary International, v. 56, p. 15-26.

Conroy, J. L., Restrepo, A., Overpeck, J. T., Steinitz-Kannan, M., Cole, J. E., Bush, M. B., and Colinvaux, P. A., 2009, Unprecedented recent warming of surface temperatures in the eastern tropical Pacific Ocean: Nature Geosci, v. 2, no. 1, p. 46-50.

Curray, J. R., Emmel, F. J., and Crampton, P. J. S., 1969, Holocene history of a strandplain, lagoonal coast, Nayarit, Mexico, in Castanares, A. A., and Phleger, F. B., eds., Coastal Lagoons, A Symposium: Mexico, UNAM-UNESCO.

Dalla Pozza, R. I., 2005, A Holocene Sand Budget for the Seasonally Wet Tropics of North Queensland (Unpublished Thesis) [PhD: James Cook University, 215 p.

Davies, J. L., 1957, The importance of cut and fill in the development of sand beach ridges: The Australian Journal of Science, v. 20, p. 105-111.

Davies, J. L., 1958, Analysis of height variation in sand beach ridges: Australian Journal of Science, v. 21, p. 51-52.

DERM, 2010, Storm tide gauge site: Cape Ferguson, Queensland Government, Department of Environment and Resource Management.

-, 2011, Coastal Services Data Report: Queensland Department of Resource Management.

Donnelly, J. P., Bryant, S. S., Butler, J., Dowling, J., Fan, L., Hausmann, N., Newby, P., Shuman, B., Stern, J., Westover, K., and Webb, T., 2001a, 700 yr sedimentary record of intense hurricane landfalls in southern New England: Geological Society of America Bulletin, v. 113, no. 6, p. 714-727.

Donnelly, J. P., Roll, S., Wengren, M., Butler, J., Lederer, R., and Webb, T., 2001b, Sedimentary evidence of intense hurricane strikes from New Jersey: Geology, v. 29, no. 7, p. 615-618.

Donnelly, J., 2005, Evidence of Past Intense Tropical Cyclones from Backbarrier Salt Pond Sediments: A Case Study from Isla de Culebrita, Puerto Rico, USA: Journal of Coastal Research, Special Issue, v. 42, p. 201-210.

Donnelly, J., 2007, Morphologic Change by Overwash: Establishing and Evaluating Predictors: Journal of Coastal Research, v. SI 50, p. 520-526.

Donnelly, J., and Webb, T., 2004, Back-barrier Sedimentary Records of Intense Hurricane Landfalls in the Northeastern United States, in Murnane, R. a. L., K., ed., Hurricanes and Typhoons: Past Present and Potential: New York, Columbia Press, p. 58-96.

Donnelly, J., and Woodruff, J., 2007, Intense hurricane activity over the past 5,000 years controlled by El Nino and the West African monsoon: Nature, v. 447, p. 465-468.

Donnelly, J. P., Bryant, S. S., Butler, J., Dowling, J., Fan, L., Hausmann, N., Newby, P., Shuman, B., Stern, J., Westover, K., and Webb, T., 2001a, 700 yr

sedimentary record of intense hurricane landfalls in southern New England: Geological Society of America Bulletin, v. 113, no. 6, p. 714-727.

Donnelly, J. P., Roll, S., Wengren, M., Butler, J., Lederer, R., and Webb, T., 2001b, Sedimentary evidence of intense hurricane strikes from New Jersey: Geology, v. 29, no. 7, p. 615-618.

Donoghue, J. F., Stapor, F. W., and Tanner, W. F., 1998, Discussion of: Otvos, E.G., 1995. Multiple Pliocene-Quaternary Marine Highstands, Northeast Gulf Coastal Plain-Fallacies and Fact: Journal of Coastal Research, v. 14, no. 2, p. 669.

Duke, W., 1985, Hummocky cross-stratification, tropical hurricanes, and intense winter storms: Sedimentology, v. 32, p. 167-194.

Fardon, R., de Ferranti, R., and Peninguel JR, F., 1963, Ingham, Queensland 1:250,000 Geological Sheet SE 55-10: Bureau of Mineral Resources, Geology and Geophysics.

Fisk, H. N., Padre Island and the Laguna Madre flats, coastal south Texas, in Proceedings 2nd Coastal Geography Conference, Baton Rouge, Louisiana, 1959.

Folk, R. L., and Ward, W. C., 1957, Brazos River Bar: A study in the significance of grain size parameters: Journal of Sedimentary Petrology, v. 27, no. 1, p. 3-26.

Forsyth, A. J., Nott, J., and Bateman, M. D., 2010, Beach ridge plain evidence of a variable late-Holocene tropical cyclone climate, North Queensland, Australia: Palaeogeography, Palaeoclimatology, Palaeoecology, v. 297, no. 3-4, p. 707-716.

Forsyth, A. J., Nott, J., Bateman, M. D., and Beaman, R., 2012, Juxtaposed beach ridges and foredunes within a ridge plain - Wonga Beach, northeast Australia: Marine Geology, v. 307-310, p. 111-116.

Frappier, A. B., Sahagian, D., Carpenter, S. J., Gonzalez, L. A., and Frappier, B. R., 2007, Stalagmite stable isotope record of recent tropical cyclone events: Geology, v. 35, no. 2, p. 111-114.

Friedman, G. M., 1961, Distinction between dune, beach, and river sands from their textural characteristics: Journal of Sedimentary Petrology, v. 31, no. 4, p. 514-529.

Gilbert, G. K., 1885, The topographic features of lake shores: United States Geological Survey Annual Report, v. 5, p. 75-123.

Gregory, C. M., 1969, 1;250,000 Geological Series - Explanatory Notes - Ayr, Queensland, Canberra, Bureau of Mineral Resources, 14 p.:

Hardy, T., Mason, L., and Astorquia, A., 2004, Ocean Hazards Assessment - Stage 3: Department of Natural Resources and Mines.

Harper, B., 1999, Storm tide threat in Queensland: History, prediction and relative risks. Conservation Technical Report No. 10: Department of Environment and Heritage.

Harper, B., Hardy, T., Mason, L., Bode, L., Young, I., and Nielson, P., 2001, Ocean Hazards Assessment - Stage 1: Department of Natural Resources and Mines.

Hayne, M., and Chappell, J., 2001, Cyclone frequency during the last 5000 years at Curacoa Island, north Queensland, Australia: Palaeogeography, Palaeoclimatology, Palaeoecology, v. 168, p. 207-219.

Hesp, P. A., 1999, The beach, backshore and beyond, in Short, A. D., ed., Handbook of Beach and Shoreface Morphodynamics: Chichester, John Wiley & Sons.

-, 2002, Foredunes and blowouts: initiation, geomorphology and dynamics: Geomorphology, v. 48, p. 245-268.

-, 2006, Sand Beach Ridges: Definitions and Re-Definition: Journal of Coastal Research, v. Special Issue 39, p. 72 - 75.

Hesp, P. A., Dillenberg. S. R, Barboza, E. G., Tomazelli, L. J., Ayup-Zouain, R. N., Esteves, L. S., Gruber, N. L. S., Toldo, E. E. J., Tabajara, L. L. C. D. A., and Clerot, L. C. P., 2005, Beach ridges, foredunes or transgressive dunefields? Definitions and an examination of the Torres to Tramandaí barrier system, Southern Brazil: Anais da Academia Brasileira de Ciências, v. 77, no. 3, p. 493-508.

Hetzinger, S., Pfeiffer, M., Dullo, W.-C., Keenlyside, N., Latif, M., and Zinke, J., 2008, Caribbean coral tracks Atlantic multidecadal oscillation and past hurricane activity: Geology, v. 36, p. 11-14.

Hippensteel, S. P., and Martin, R. E., 1999, Foraminifera as an Indicator of Overwash Deposits, Barrier Island Sediment Supply, and Barrier Island Evolution, Folly Island, South Carolina: Palaeogeography, Palaeoclimatology, Palaeoecology, v. 149, p. 115-125.

Holland, G., 1981, On the quality of the Australian tropical cyclone database: Australian Meteorological Magazine, v. 29, p. 161-181.

Hopley, D., 1970, Coastal Geomorphology in the Townsville Region, [Unpublished PhD Thesis]: James Cook University of North Queensland, 352 p.

Hubbert, G. D., and McInnes, K. L., 1999, A Storm Surge Inundation Model for Coastal Planning and Impact Studies: Journal of Coastal Research, v. 15, no. 1, p. 168-185.

Ito, M., Ishigaki, A., Nishikawa, T., and Saito, T., 2001, Temporal variation in the wavelength of hummocky cross-stratification: implications for storm intensity through Mesozoic and Cenozoic: Geology, v. 29, p. 87-89.

Johnson, D. W., 1919, Shore Processes and Shoreline Development, New York, Prentice Hall.

Johnson, D. P., 1998, Tully and Murray Rivers and major tributaries : an ecological and physical assessment of the condition of streams in the drainage basins of the Tully and Murray Rivers Indoorapilly, Department of Natural Resources.

Katuna, M. P., 1991, The Effects of Hurricane Hugo on the Isle of Palms, South Carolina: From Destruction to Recovery: Journal of Coastal Research, v. SI 8, p. 263-273.

Keen, T. R., Bentley, S. J., Vaughan, W. C., and Blain, C. A., 2004, The generation and preservation of multiple hurricane beds in the northern Gulf of Mexico: Marine Geology, v. 210, p. 79-105.

Keen, T. R., Furukawa, Y., Bentley, S. J., Slingerland, R. L., Teague, W. J., Dykes, J. D., and Rowley, C. D., 2006, Geological and oceanographic perspectives on event bed formation during Hurricane Katrina: Geophysical Research Letters, v. 33, p. L23614.

King, C. A. M., 1966, Techniques in geomorphology, London, Edward Arnold, 342 p.:

Knutson, T. R., McBride, J. L., Chan, J., Emanuel, K., Holland, G., Landsea, C., Held, I., Kossin, J. P., Srivastava, A. K., and Sugi, M., 2010, Tropical cyclones and climate change: Nature Geosci, v. 3, no. 3, p. 157-163.

Komar, P. D., 1976, Beach Processes and Sedimentation, Upper Saddle River, Prentice Hall.

Komar, P. D., 1998, Beach Processes and Sedimentation, Upper Saddle River, NJ, Prentice Hall, 544 p.:

Kossin, J. P., Knapp, K., Vimont, D., Murnane, R., and Harper, B., 2007, A globally consistent reanalysis of hurricane variability and trends: Geophysical Research Letters, v. 34, p. L04815.

Kuleshov, Y., Fawcett, R., Qi, L., Trewin, B., Jones, D., McBride, J., and Ramsay, H., 2010, Trends in tropical cyclones in the South Indian Ocean and the South Pacific Ocean: Journal of Geophysical Research, v. 115, D01101.

Lambert, W. J., Aharon, P., and Rodriguez, A. B., 2003, An Assessment of the Late Holocene Record of Severe Storm Impacts from Lake Shelby, Alabama: Gulf Coast Association of Geological Societies, Transactions, v. 53, p. 443-452.

Lambert, W. J., Aharon, P., and Rodriguez, A. B., 2008, Catastrophic hurricane history revealed by organic geochemical proxies in coastal lake sediments: a case study of Lake Shelby, Alabama (USA): Paleolimnology, v. 39, p. 117-131.

Lander, M. A., and Guard, P. A., 1998, Contrasting high Atlantic activity with low activity in other basins: Monthly Weather Review, v. 126, p. 1163-1173.

Landsea, C., 2000, Climate variability of tropical cyclones: Past, Present and Future., in Pielke, R. A. J., and Pielke, R. S., eds., Storms: New York, Routledge, p. 220-241.

-, 2005, Hurricanes and Global Warming: Nature, v. 438, p. E11-13.

Landsea, C. W., Harper, B. A., Hoarau, K., and Knaff, J. A., 2006, Can we detect trends in extreme tropical cyclones: Science, v. 313, p. 452-454.

Lane, P., Donnelly, J., and Hawkes, A., 2011, A decadally-resolved paleohurricane record archived in the late Holocene sediments of a Florida sinkhole: Marine Geology, v. 287, p. 14-30.

Larcombe, P., Carter, R. M., Dye, J., Gagan, M. K., and Johnson, D. P., 1995, New evidence for episodic post-glacial sea-level rise, central Great Barrier Reef, Australia: Marine Geology, v. 127, no. 1-4, p. 1-44.

Leatherman, S. P., 1978, A new aeolian sand trap design: Sedimentology, v. 25, p. 303-306.

Lewis, S. E., Wust, R. A. J., Webster, J. M., and Shields, G. A., 2008, Mid–late Holocene sealevel variability in eastern Australia: Terra Nova, v. 20, p. 74-81.

Liu, K., and Fearn, M. L., 1993, Lake-sediment record of late Holocene hurricane activities from coastal Alabama: Geology, v. 21, no. 9, p. 793-796.

-, 2000, Reconstruction of Prehistoric Landfall Frequencies of Catastrophic Hurricanes in Northwestern Florida from Lake Sediment Records: Quaternary Research, v. 54, no. 2, p. 238-245.

-, 2002, Lake Sediment Evidence of Coastal Geologic Evolution and Hurricane History from Western Lake, Florida: Reply to Otvos: Quaternary Research, v. 57, no. 3, p. 429-431.

Long, J. W., deBakker, A. T. M., and Plant, N. G., 2014, Scaling coastal dune elevation changes across storm-impact regimes: Geophysical Research Letters, v. 41, no. 8, p. 2899-2906.

Lu, H.-Y., and Liu, K.-b., 2005, Phytolith assemblages as indicators of coastal environmental changes and hurricane overwash deposition: The Holocene, v. 15, no. 7, p. 965-972.

Malmquist, D., 1997, Oxygen isotopes in cave stalagmites as a proxy record of past tropical cyclone activity, 22nd Conference on Hurricanes and Tropical Meteorology: Fort Collins, American Meterological Society, p. 393-394.

Mann, M. E., Zhang, Z., Rutherford, S., Bradley, R. S., Hughes, M. K., Shindell, D., Ammann, C., Faluvegi, G., and Ni, F., 2009a, Global Signatures and Dynamical Origins of the Little Ice Age and Medieval Climate Anomaly: Science, v. 326, no. 5957, p. 1256-1260.

Mann, M. E., Woodruff, J. D., Donnelly, J. P., and Zhang, Z., 2009b, Atlantic hurricanes and climate over the past 1,500 years: Nature, v. 460, p. 880-883.

Maragos, J., Baines, G., and Beveridge, P., 1973, Tropical cyclone Bebe creates a new land formation on Funafuti Atoll: Science, v. 181, p. 1161-1164.

Marsh, R. E., Prestwich, W. V., Rink, W. J., and Brennan, B. J., 2002, Monte Carlo determinations of the beta dose rate to tooth enamel: Radiation Measurements, v. 35, p. 609-616.

Mason, C. C., and Folk, R. L., 1958, Differentiation of beach, dune, and aeolian flat environments by size analysis, Mustang Island, Texas: Journal of Sedimentary Research, v. 28, no. 2, p. 211-226.

McCloskey, T., and Keller, G., 2009, 5000 year sedimentary record of hurricane strikes on the central coast of Belize: Quaternary International, v. 195, p. 53-68.

McGowan, H., Petherick, L., and Kamber, B., 2008, Aeolian sedimentation and climate variability during the late Quaternary in southeast Queensland, Australia: Palaeogeography, Palaeoclimatology, Palaeoecology, v. 265, p. 171-181.

McInnes, K., Walsh, K. J. E., and Pittock, A. B., 2000, Impact of Sea-level Rise and Storm Surges on Coastal Resorts. A report for CSIRO Tourism Research: CSIRO Atmospheric Research.

McInnes, K., Walsh, K., Hubbert, G., and Beer, T., 2003, Impact of sea-level rise and storm surges on a coastal community: Natural Hazards, v. 30, p. 187-207.

McIntire, W., and Walker, H., 1964, Tropical Cyclones and Coastal Morphology in Mauritius: Annals of the Association of American Geographers, v. 54, no. 4, p. 582-596.

McKay, P. J., and Terich, T. A., 1992, Gravel Barrier Morphology: Olympic National Park,Washington State, U.S.A: Journal of Coastal Research, v. 8, no. 4, p. 813-829.

McKee, E. D., 1979, A Study of Global Sand Seas, Washington D.C., U.S. Government Printing Office, Geological Survey Professional Paper.

McKenzie, P., 1958, The development of sand beach ridges: Australian Journal of Science, v. 20, p. 213-214.

Miller, D. L., Mora, C. I., Grissino-Mayer, H. D., Mock, C. J., Uhle, M. E., and Sharp, Z., 2006, Tree-Ring Isotope Records of Tropical Cyclone Activity: Proceedings of the National Academy of Sciences of the United States of America, v. 103, no. 39, p. 14294-14297.

Missimer, T., 1973, Growth rates of beach ridges on Sanibel Island, Florida: Transactions, Gulf Coast Association of Geological Societies, v. 23, p. 383-388.

Morton, R. A., Gelfenbaum, G., and Jaffe, B. E., 2007, Physical criteria for distinguishing sandy tsunami and storm deposits using modern examples: Sedimentary Geology, v. 200, no. 3–4, p. 184-207.

Mountney, N. P., 2006, Eolian facies models, in Posamentier, H. W., and Walker, R. G., eds., Facies Models Revisited, Volume 84, SEPM, p. 19-83.

Moy, C. M., Seltzer, G. O., Rodbell, D. T., and Anderson, D. M., 2002, Variability of El Nino/Southern Oscillation activity at millennial timescales during the Holocene epoch: Nature, v. 420, no. 6912, p. 162-165.

Murray, A., and Wintle, A., 2003, The single aliquot regenerative dose protocol: potential for improvements in reliability: Radiation Measurements, v. 37, p. 377-381.

Nott, J., 2003, Intensity of prehistoric tropical cyclones: Journal of Geophysical Research, v. 108, no. D7, p. 4212.

-, 2006, Tropical cyclones and the evolution of the sedimentary coast of Northern Australia: Journal of Coastal Research, v. 22, no. 1, p. 49-62.

-, 2011a, A 6000 year tropical cyclone record from Western Australia: Quaternary Science Reviews, v. 30, p. 713-722.

-, 2011b, Tropical cyclones, global climate change and the role of Quaternary studies: Journal of Quaternary Science, v. 26, no. 5, p. 468-473.

Nott, J., and Forsyth, A. J., 2012, Punctuated global tropical cyclone activity over the past 5,000 years: Geophysical Research Letters, v. 39.

Nott, J., Haig, J., and Gillieson, D., 2007, Greater frequency variability of landfalling tropical cyclones at centennial compared to seasonal and decadal scales: Earth and Planetary Science Letters, v. 255, p. 367-372.

Nott, J., and Hayne, M., 2001, High frequency of `super-cyclones' along the Great Barrier Reef over the past 5,000 years: Nature, v. 413, no. 6855, p. 508-512.

Nott, J., and Hubbert, G., 2005, Comparisons between topographically surveyed debris lines and modelled inundation levels from severe tropical cyclones Vance and Chris, and their geomorphic impact on the sand coast: Australian Meteorological Magazine, v. 54, p. 187-196.

Nott, J., 2005, Letter to the Editor: Comment on the Paper ‘Quantifying Storm Tide Risk in Cairns’ by Ken Granger: Natural Hazards, v. 34, p. 375-379.

Nott, J., 2006, Tropical cyclones and the evolution of the sedimentary coast of Northern Australia: Journal of Coastal Research, v. 22, no. 1, p. 49-62.

Nott, J., Chague-Goff, C., Goff, J., Sloss, C., and Riggs, N., 2013, Anatomy of sand beach ridges: evidence from severe Tropical Cyclone Yasi and its predecessors, northeast Queensland, Australia: Journal of Geophysical Research, v. 118, no. 3, p. 1710-1719.

Nott, J., and Jagger, T. H., 2013, Deriving robust return periods for tropical cyclone inundations from sediments: Geophysical Research Letters, v. 40, no. 2, p. 370-373.

Nott, J., Smithers, S., Walsh, K., and Rhodes, E., 2009, Sand beach ridges record 6000 year history of extreme tropical cyclone activity in northeastern Australia: Quaternary Science Reviews, v. 28, no. 15-16, p. 1511-1520.

NTF (National Tidal Facility), 2007a, Mourilyan - hourly sea level observations - 1984 to 2005.

-, 2007b, Port Douglas Tide Data - 26 - 27 July 2007: National Tidal Facility.

Orford, J. D., Carter, R. W. G., and Jennings, S. C., 1991, Coarse clastic barrier environments: Evolution and implications for quaternary sea level interpretation: Quaternary International, v. 9, no. 0, p. 87-104.

Orford, J. D., Murdy, M. M., and Wintle, A. G., 2003, Prograded Holocene beach ridges with superimposed dunes in north-east Ireland: mechanisms and timescales of fine and coarse beach sediment decoupling and deposition: Marine Geology, v. 194, p. 47-64.

Orford, J. D., Forbes, D. L., and Jennings, S. C., 2002, Organisational controls, typologies and time scales of paraglacial gravel-dominated coastal systems: Geomorphology, v. 48, p. 51-85.

Otvos, E. G., 2000, Beach ridges - definitions and significance: Geomorphology, v. 32, p. 83-108.

-, 2011, Hurricane signatures and landforms—toward improved interpretations and global storm climate chronology: Sedimentary Geology, v. 239, no. 1–2, p. 10-22.

Pielke, R. A., and Landsea, C., 1998, Nominalised Hurricane Damage in the United States: Weather and Forecasting, v. 13, p. 621-631.

Popper, K. R., 1959, The logic of scientific discovery, London, Routledge, 479 p.

Prescott, J. R. Hutton, J.T., 1994, Cosmic ray contributions to dose rates for luminescence and ESR dating: large depths and long-term time variations: Radiation Measurements, v. 2/3, p. 497-500.

Psuty, N. P., 1965, Beach-Ridge Development in Tabasco, Mexico: Annals of the Association of American Geographers, v. 55, no. 1, p. 112-124.

Pye, K., 1980, Geomorphic Development of Coastal Dunes in a Humid Tropical Environment, North Queensland, [Unpublished PhD Thesis]: Cambridge University.

Pye, K., 1982, Negatively skewed aeolian sands from a humid tropical coastal Dunefield, Northern Australia: Sedimentary Geology, v. 31, no. 3-4, p. 249-266.

Pye, K., 1983, Dune formation on the humid tropical sector of the North Queensland coast, Australia: Earth Surface Processes and Landforms, v. 8, p. 371-381.

QEPA, 2005, Coastal Services Data Report: Queensland Environmental Protection Agency.

Redman, J. B., 1852, On the alluvial formations and local changes, of the south coast of England: Proceedings of the Institute of Civil Engineers, v. 11, p. 191-193.

Randall, R. E., 1977, Shingle Foreshores, in Barnes, R. S. K., ed., The Coast: London, Wiley, p. 49-61.

Reimer, P. J., Baillie, M. G. L., Bard, E., Bayliss, A., Beck, J. W., Blackwell, P. G., Ramsey, C. B., Buck, C. E., Burr, G. S., Edwards, R. L., Friedrich, M., Grootes, P. M., Guilderson, T. P., Hajdas, I., Heaton, T. J., Hogg, A. G., Hughen, K. A., Kaiser, K. F., Kromer, B., McCormac, F. G., Manning, S. W., Reimer, R. W., Richards, D. A., Southon, J. R., Talamo, S., Turney, C. S. M., van der Plicht, J., and Weyhenmeyer, C. E., 2009, IntCal09 and Marine09 Radiocarbon Age Calibration Curves, 0-50,000 Years cal BP, v. 51, p. 1111-1150.

Rhodes, E. G., Polach, H. A., Thom, B. G., and Wilson, S. R., 1980, Age structure of Holocene coastal sediments, Gulf of Carpentaria, Australia: Radiocarbon, v. 22, p. 718-727.

Rhodes, E. G., 1982, Depositional model for chenier plain, Gulf of Carpentaria, Australia: Sedmentology, v. 29, p. 201-229.

Richmond, B. M., Watt, S., Buckley, M., Jaffe, B. E., Gelfenbaum, G., and Morton, R. A., 2011, Recent storm and tsunami coarse-clast deposit characteristics, southeast Hawai'i: Marine Geology, v. 283, no. 1–4, p. 79-89.

Roberts, R. G., Galbraith, R. F., Yoshida, H., Laslett, G. M., and Olley, J. M., 2000, Distinguishing dose populations in sediment mixtures: a test of optical dating procedures using mixtures of laboratory-dosed quartz: Radiation Measurements, v. 32, p. 459-465.

Roy, P. S., Cowell, M. A., Ferland, M. A., and Thom, B. G., 1994, Wave-dominated Coasts, in Carter, R. W. G., and Woodroffe, C. D., eds., Coastal Evolution - Late Quaternary shoreline morphodynamics: Cambridge, Cambridge University Press.

Ruggiero, P., Komar, P. D., McDougal, W. G., Marra, J. J., and Beach, R. A., 2001, Wave runup, extreme water levels and the erosion of properties backing beaches: Journal of Coastal Research, v. 17, p. 407-419.

Sabbatelli, T. E., and Mann, M. E., 2007, The influence of climate state variables on Atlantic tropical cyclone occurrence rates: Journal of Geophysical Research, v. 112, p. D17114.

Sallenger, A. H., 2000, Storm impact scale for barrier islands: Journal of Coastal Research, v. 16, p. 890-895.

Scheffers, A., Engel, M., Scheffers, S., Squire, P., and Kelletat, D., 2011, Beach ridge systems - archives for Holocene coastal events?: Progress in Physical Geography, v. 36, no. 1, p. 5-37.

Shih, S. M., and Komar, P. D., 1994, Sediments, Beach Morphology and Sea Cliff Erosion within an Oregon Coast Littoral Cell: Journal of Coastal Research, v. 10, no. 1, p. 144-157.

Scileppi, E., and Donnelly, J. P., 2007, Sedimentary evidence of hurricane strikes in western Long Island, New York: Geochem. Geophys. Geosyst., v. 8, no. 6, p. Q06011.

Scoffin, T. P., 1993, The geological effects of hurricanes on coral reefs and the interpretation of storm deposits: Coral Reefs, v. 12, no. 3-4, p. 203-221.

Scott, D. B., Collins, E. S., Gayes, P. T., and Wright, E., 2003, Records of prehistoric hurricanes on the South Carolina coast based on micropaleontological and sedimentological evidence, with comparison to other Atlantic Coast records: Geological Society of America Bulletin, v. 115, no. 9, p. 1027-1039.

Sevon, D. W., 1966, Distinction of New Zealand beach, dune and river sands by their grain size distribution characteristics: New Zealand Journal of Geology and Geophysics, v. 9, p. 212-223.

Sexton, W. J., and Hayes, M. O., 1991, The Geologic Impact of Hurricane Hugo and Post-Storm Shoreline Recovery Along the Undeveloped Coastline of South Carolina, Dewees Island to the Santee Delta: Journal of Coastal Research, p. 275-290.

Sherman, D., and Lyons, W., 1994, Beach state controls on aeolian sand delivery to coastal dunes: Physical Geography, v. 15, p. 381-395.

Short, A. D., 2000, Beaches of the Queensland Coast, Cooktown to Coolangatta : a guide to their nature, characteristics, surf and safety Sydney, Sydney University Press, 360 p.:

Stapor, F. W., Jr., Mathews, T. D., and Lindfors-Kearns, F. E., 1991, Barrier-Island Progradation and Holocene Sea-Level History in Southwest Florida: Journal of Coastal Research, v. 7, no. 3, p. 815-838.

Tamura, T., 2012, Beach ridges and prograded beach deposits as palaeoenvironment records: Earth-Science Journal, v. 114, p. 279-297.

Tanner, W. F., 1995, Origin of beach ridges and swales: Marine Geology, v. 129, p. 149-161.

Tanner, W. F., and Stapor, F. W., 1971, Tabasco Beach-ridge Plain: an Eroding Coast: Transactions: Gulf Coast Association of Geological Societies, v. 21, p. 231-232.

Taylor, M. J., and Stone, G. W., 1996, Beach ridges: a review: Journal of Coastal Research, v. 12, no. 3, p. 612-621.

Thom, B. G., 1983, Transgressive and Regressive Stratigraphies of Coastal Sand Barriers in Southeast Australia: Marine Geology, v. 56, p. 137-158.

Thom, B. G., 1964, Origin of sand beach-ridges: Australian Journal of Science, v. 26, p. 351-352.

Thom, B. G., Bowman, G. M., and Roy, P. S., 1981, Late Quaternary evolution of coastal sand Barriers, Port Stephens-Myall Lakes Area, central New South Wales, Australia: Quaternary Research, v. 15, no. 3, p. 345-364.

Thom, B. G., and Hall, W., 1991, Behaviour of beach profiles during accretion and erosion dominated periods: Earth Surface Processes and Landforms, v. 16, p. 113-127.

van Straaten, L. M. J. U., 1965, Coastal barrier deposits in South- and North-Holland, in particular in the areas around Scheveningen and Ijmuiden: Mededelingen van de Geologische Stichting, v. 17, p. 41-76.

Wallace, D. J., and Anderson, J. B., 2010, Evidence of similar probability of intense hurricane strikes for the Gulf of Mexico over the late Holocene: Geology, v. 38, no. 6, p. 511-514.

Woodroffe, C. D., 2003, Coasts: form, process and evolution, Cambridge, Cambridge University Press.

Woodruff, J. D., Donnelly, J. P., Emanuel, K., and Lane, P., 2008a, Assessing sedimentary records of paleohurricane activity using modeled hurricane climatology: Geochem. Geophys. Geosyst., v. 9, no. 9, p. Q09V10.

Woodruff, J. D., Donnelly, J. P., Mohrig, D., and Geyer, W. R., 2008b, Reconstructing relative flooding intensities responsible for hurricane-induced deposits from Laguna Playa Grande, Vieques, Puerto Rico: Geology, v. 36, no. 5, p. 391-394.

Woodruff , J. D., Donnelly, J. P., and Okusu, A., 2009, Exploring typhoon variability over the mid-to-late Holocene: evidence of extreme coastal flooding from Kamikoshiki, Japan: Quaternary Science Reviews, v. 28, p. 1774-1785.

Appendices

Appendix 1 Plots and data associated with modelling sensitivity results

Appendix 1. 1 Data (a) and plot (b) of tropical cyclone surge height versus central pressure as a function of storm forward velocity (kmh) for the Rockingham Bay beach ridge plain

(a)

Central pressure	Storm forward velocity (kmh)		
(hPa)	10	30	50
980	0.815	1.405	1.575
950	1.817	2.983	2.861
915	2.86	4.768	4.291
890	3.855	6.022	5.308

(b)

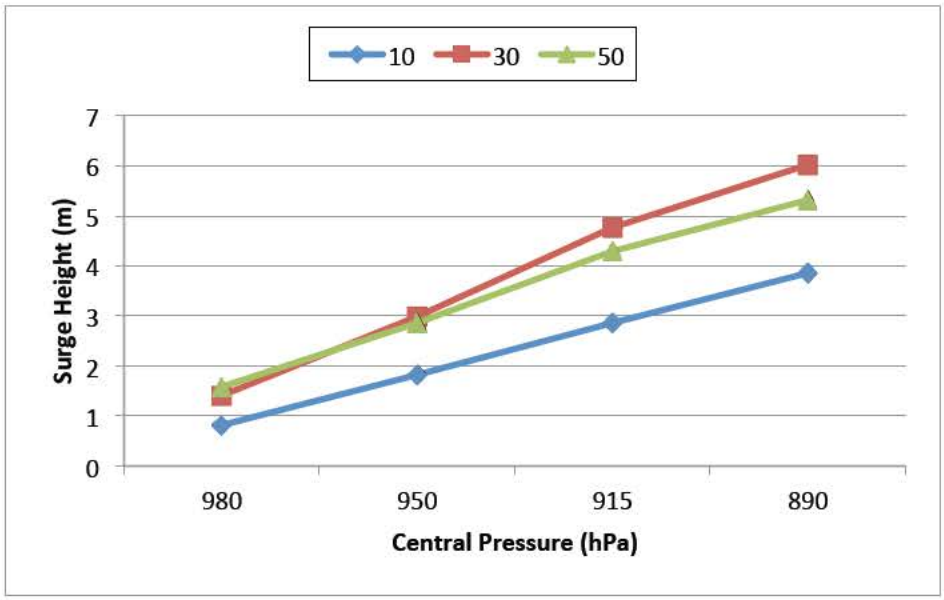

Appendix 1. 2 Data (a) and plot (b) of tropical cyclone surge height versus central pressure as a function of radius (km) of maximum winds (Rm) for the Rockingham Bay beach ridge plain.

(a)

Central pressure	Radius of maximum winds (km)		
(hPa)	10	30	60
980	0.508	1.405	1.408
950	1.091	2.983	2.896
915	1.764	4.768	4.631
890	2.244	6.022	5.871

(b)

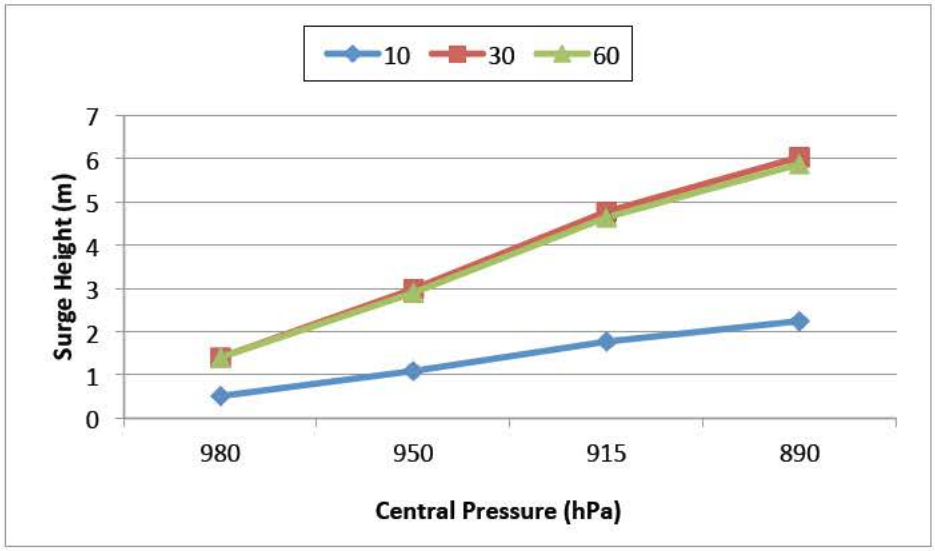

Appendix 1. 3 Data (a) and plot (b) of surge height versus distance of tropical cyclone land crossing location from site (km) for the Rockingham Bay beach ridge plain.

(a)

Central pressure	Distance of tropical cyclone land crossing location from site (km)		
(hPa)	10	30	60
980	0.508	1.405	1.408
950	1.091	2.983	2.896
915	1.764	4.768	4.631
890	2.244	6.022	5.871

(b)

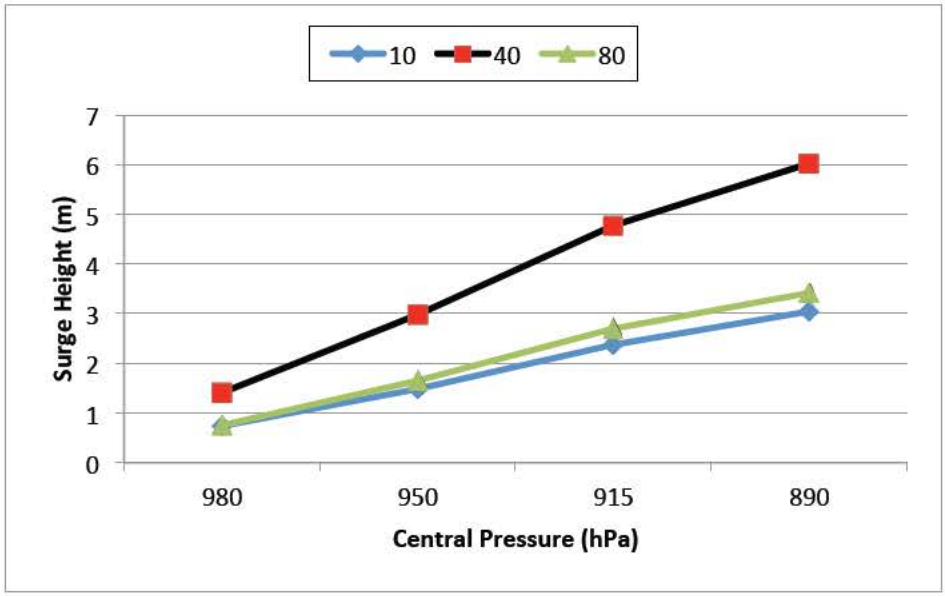

Appendix 1. 4 Data (a) and plot (b) of tropical cyclone surge height versus central pressure as a function of track direction for the Rockingham Bay beach ridge plain.

(a)

Central pressure	Track direction				
(hPa)	NW	WNW	W	WSW	SW
980	1.33	1.33	1.336	1.405	1.163
950	2.67	2.67	2.826	2.983	2.603
915	4.188	4.188	4.516	4.768	4.271
890	5.271	5.271	5.706	6.022	5.456

(b)

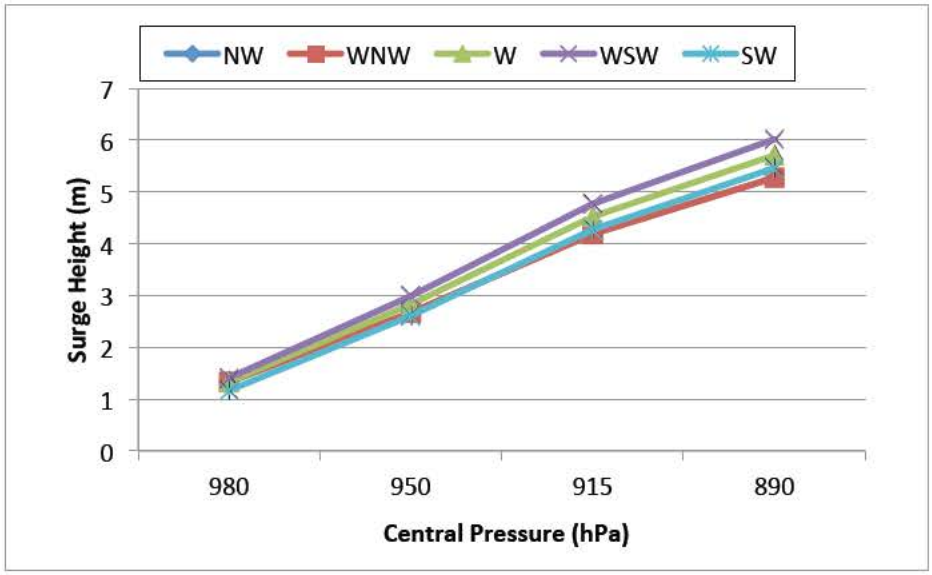

Appendix 1. 5 Data (a) and plot (b) of tropical cyclone surge height versus central pressure as a function of storm forward velocity (kmh) for the Wonga Beach beach ridge plain

(a)

Central pressure (hPa)	Storm forward velocity (kmh) 10	30	50
980	0.568	0.93	0.846
950	1.391	1.954	1.675
915	2.399	3.237	2.711
890	3.161	4.133	3.497

(b)

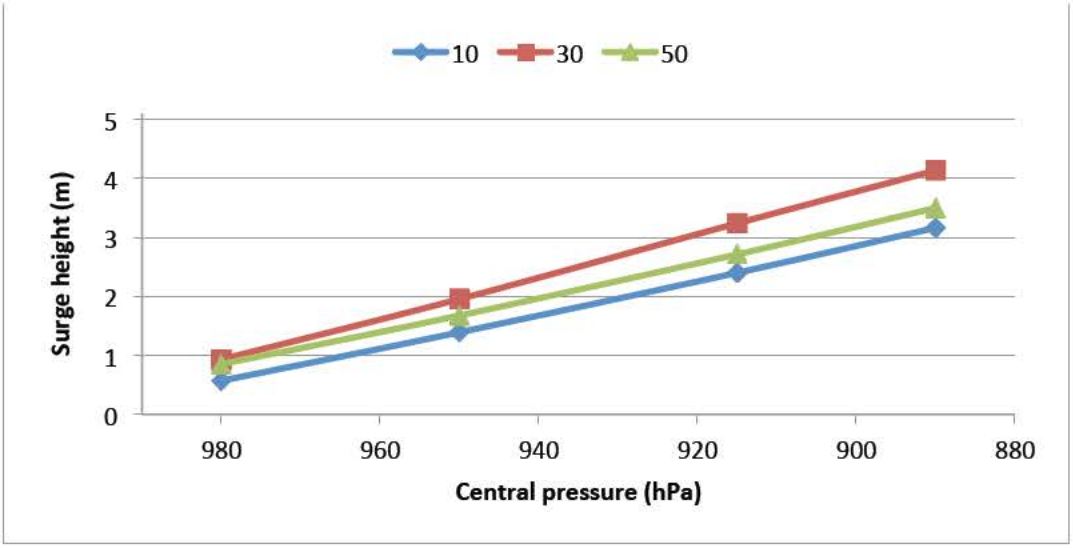

Appendix 1. 6 Data (a) and plot (b) of tropical cyclone surge height versus central pressure as a function of radius (km) of maximum winds (Rm) for the Wonga Beach beach ridge plain.

(a)

Central pressure	Radius of maximum winds (km)		
(hPa)	10	30	50
980	0.642	0.93	1.486
950	1.124	1.954	2.81
915	1.632	3.237	4.266
890	1.975	4.133	5.28

(b)

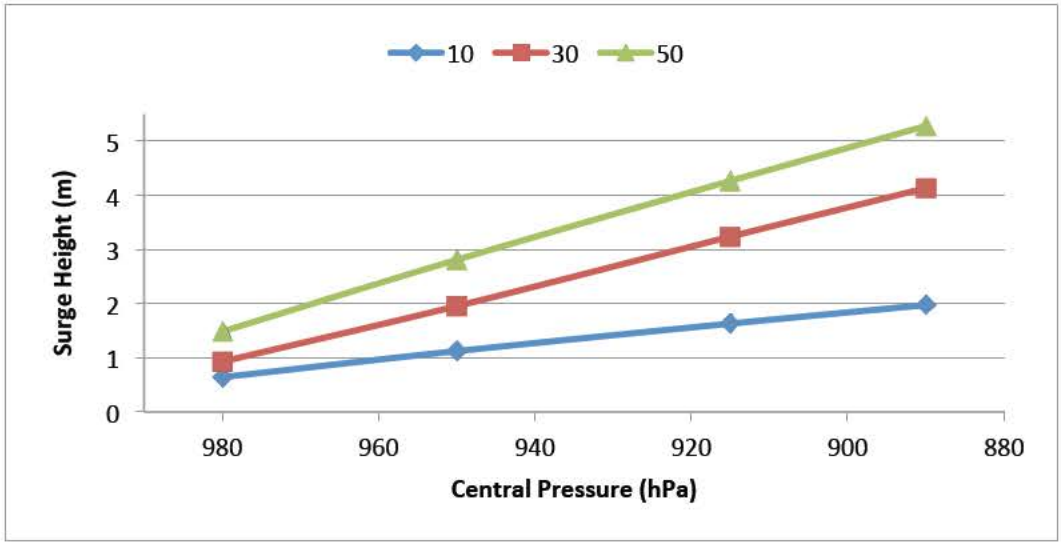

Appendix 1. 7 Data (a) and plot (b) of surge height versus distance of tropical cyclone land crossing location from site (km) for the Wonga Beach beach ridge plain.

(a)

Central pressure	Distance of tropical cyclone land crossing location from site (km)		
(hPa)	10	40	80
980	1.29	0.93	0.543
950	2.34	1.954	1.208
915	3.537	3.237	1.973
890	4.354	4.133	2.555

(b)

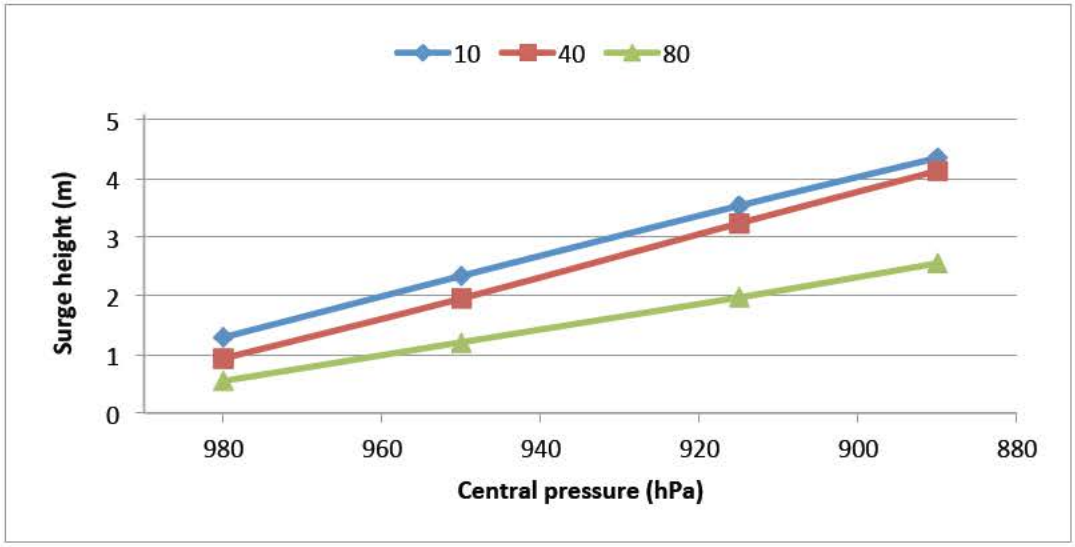

Appendix 1. 8 Data (a) and plot (b) of tropical cyclone surge height versus central pressure as a function of track direction for the Wonga Beach beach ridge plain.

(a)

Central pressure (hPa)	Track direction NW	W	SW
980	0.869	0.931	0.93
950	1.856	1.932	1.954
915	3.074	3.143	3.237
890	3.963	4.015	4.133

(b)

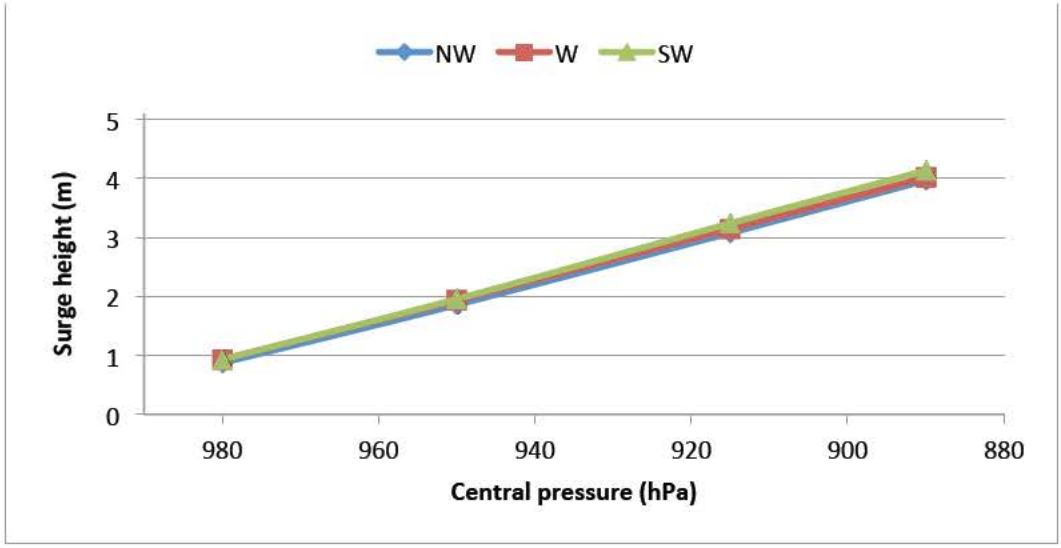

Appendix 1. 9 Data (a) and plot (b) of tropical cyclone surge height versus central pressure as a function of storm forward velocity (kmh) for the Cungulla beach ridge plain.

(a)

Central pressure (hPa)	Storm forward velocity (kmh) 10	30	50
980	0.977	1.245	1.851
950	2.192	2.675	3.583
915	3.628	4.478	5.464
890	4.64	5.68	6.715

(b)

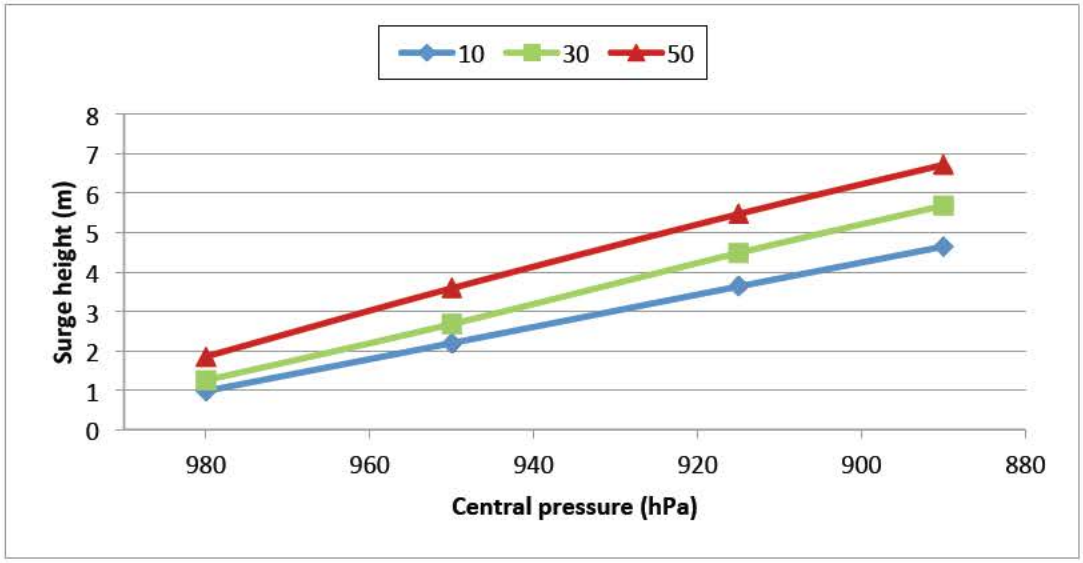

Appendix 1. 10 Data (a) and plot (b) of tropical cyclone surge height versus central pressure as a function of radius (km) of maximum winds (Rm) for the Cungulla beach ridge plain.

(a)

Central pressure	Radius of maximum winds (km)		
(hPa)	10	30	50
980	0.528	1.245	1.487
950	1.094	2.675	3.112
915	1.738	4.478	4.993
890	2.225	5.68	6.322

(b)

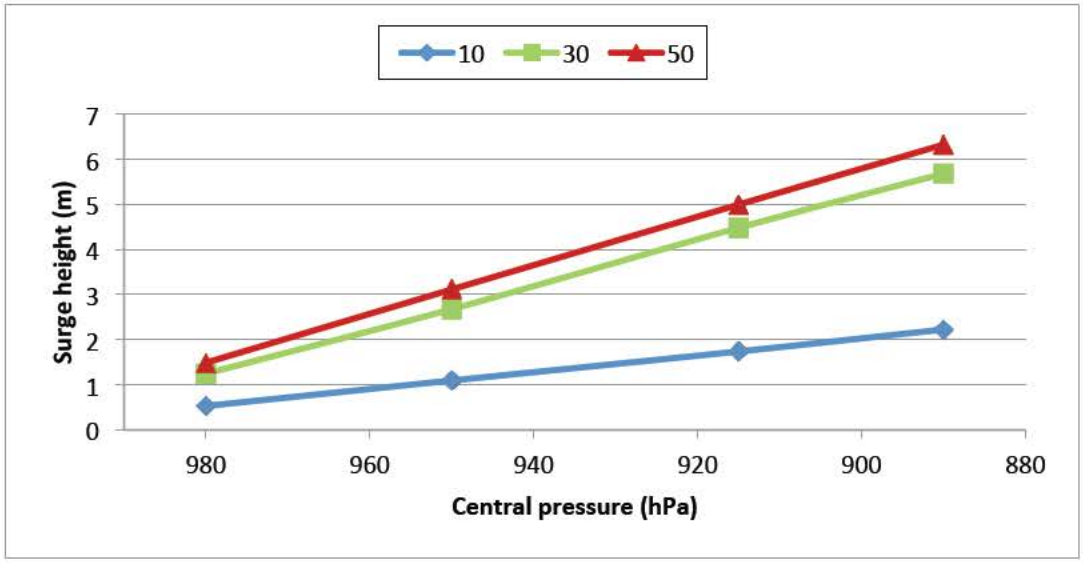

Appendix 1. 11 Data (a) and plot (b) of surge height versus distance of tropical cyclone land crossing location from site (km) for the Cungulla beach ridge plain.

(a)

Central pressure (hPa)	Distance of tropical cyclone land crossing location from site (km)		
	10	40	80
980	0.947	1.245	0.953
950	1.927	2.675	2.051
915	3.072	4.478	3.343
890	3.902	5.68	4.25

(b)

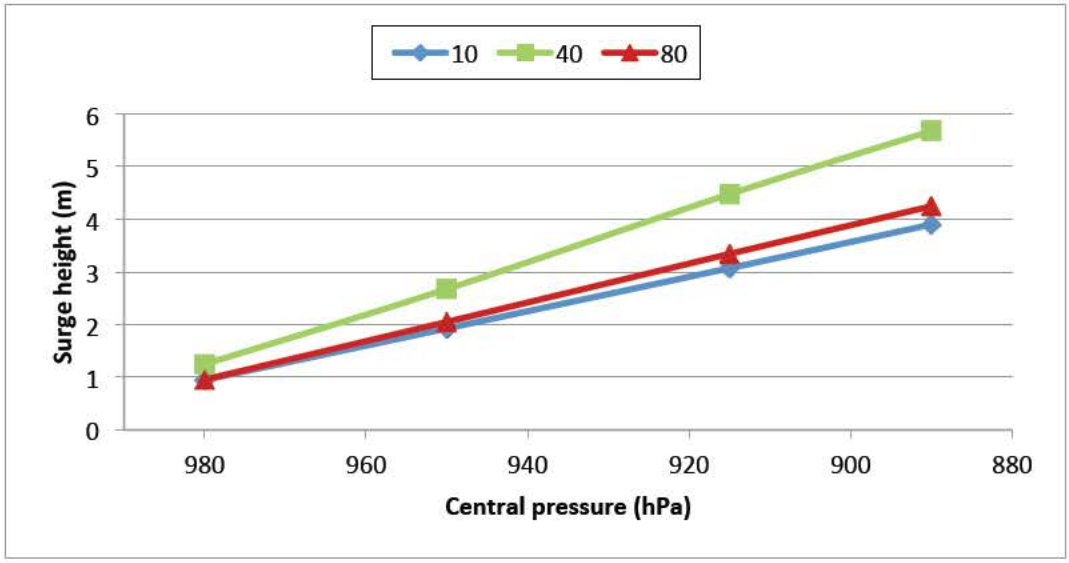

Appendix 1. 12 Data (a) and plot (b) of tropical cyclone surge height versus central pressure as a function of track direction for the Cungulla beach ridge plain.

(a)

Central pressure (hPa)	Track direction NW	W	SW
980	1.245	1.285	1.42
950	2.675	2.738	3.027
915	4.478	4.555	4.89
890	5.68	5.858	6.178

(b)

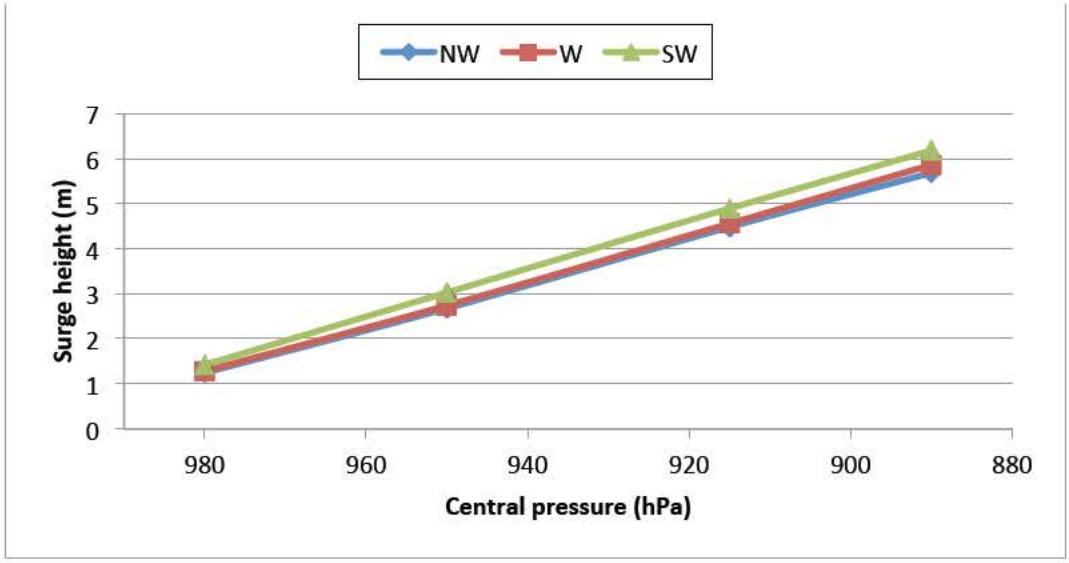

Appendix 2 Sedimentary statistical analysis results from the Rockingham Bay, Wonga Beach and Cungulla beach ridge plain studies.

Appendix 2. 1 Table of sedimentary statistical analysis results for beach ridge samples from Rockingham Bay (sample locations are indicated in Figure 2-2).

		SEK-1	SEK-2	SEK-3	SEK-4	SEK-4-2m	SEK-4-3m
	ANALYST AND DATE:	Tony, 11/13/2007	Tony, 11/13/2007	Tony, 11/13/2007	Tony, 11/13/2007	Tony, 11/13/2007	Tony, 11/13/2007
	SIEVING ERROR:	0.0%	1.1%	0.0%	0.1%	0.3%	0.1%
	SAMPLE TYPE:	Unimodal, Moderately Sorted	Bimodal, Poorly Sorted	Bimodal, Moderately Sorted	Unimodal, Moderately Sorted	Unimodal, Moderately Sorted	Bimodal, Poorly Sorted
	TEXTURAL GROUP:	Slightly Gravelly Sand	Sandy Gravel	Gravelly Sand	Slightly Gravelly Sand	Slightly Gravelly Sand	Gravelly Sand
	SEDIMENT NAME:	lightly Very Fine Gravelly Medium San	Sandy Very Fine Gravel	Very Fine Gravelly Coarse Sand	lightly Very Fine Gravelly Coarse San	lightly Very Fine Gravelly Coarse San	Very Fine Gravelly Coarse Sand
METHOD OF MOMENTS Arithmetic (μm)	MEAN ($\overline{x}_a$):	598.0	1901.2	860.4	827.4	772.1	1311.5
	SORTING (σ_a)	573.9	1407.8	689.8	579.1	512.0	1275.5
	SKEWNESS (Sk_a):	3.713	0.851	2.733	2.912	2.633	1.467
	KURTOSIS (K_a):	20.52	2.627	11.73	16.45	15.42	4.272
METHOD OF MOMENTS Geometric (μm)	MEAN ($\overline{x}_g$):	466.2	1322.8	699.2	684.9	649.0	777.9
	SORTING (σ_g):	1.894	2.925	1.813	1.857	1.782	3.472
	SKEWNESS (Sk_g):	0.805	-2.979	0.671	-0.390	0.120	-2.054
	KURTOSIS (K_g):	3.906	20.62	3.571	4.989	2.929	12.08
METHOD OF MOMENTS Logarithmic (ϕ)	MEAN ($\overline{x}_\phi$):	1.101	-0.502	0.516	0.546	0.624	0.234
	SORTING (σ_ϕ):	0.922	1.153	0.858	0.893	0.834	1.421
	SKEWNESS Sk_ϕ):	-0.805	0.301	-0.671	0.390	-0.120	0.434
	KURTOSIS (K_ϕ):	3.906	2.626	3.571	4.989	2.929	4.002
FOLK AND WARD METHOD (μm)	MEAN (M_G):	451.5	1458.6	673.9	690.4	646.2	932.4
	SORTING (σ_G):	1.833	2.239	1.810	1.748	1.778	2.678
	SKEWNESS (Sk_G):	0.137	0.084	0.134	-0.016	-0.013	0.160
	KURTOSIS (K_G):	1.008	0.791	1.199	1.006	0.943	0.872
FOLK AND WARD METHOD (ϕ)	MEAN (M_ϕ):	1.147	-0.545	0.569	0.534	0.630	0.101
	SORTING (σ_I):	0.874	1.163	0.856	0.806	0.830	1.421
	SKEWNESS (Sk_I):	-0.137	-0.084	-0.134	0.016	0.013	-0.160
	KURTOSIS (K_G):	1.008	0.791	1.199	1.006	0.943	0.872
FOLK AND WARD METHOD (Description)	MEAN:	Medium Sand	Very Coarse Sand	Coarse Sand	Coarse Sand	Coarse Sand	Coarse Sand
	SORTING:	Moderately Sorted	Poorly Sorted	Moderately Sorted	Moderately Sorted	Moderately Sorted	Poorly Sorted
	SKEWNESS:	Coarse Skewed	Symmetrical	Coarse Skewed	Symmetrical	Symmetrical	Coarse Skewed
	KURTOSIS:	Mesokurtic	Platykurtic	Leptokurtic	Mesokurtic	Mesokurtic	Platykurtic
	MODE 1 (μm):	377.4	947.9	671.0	671.0	671.0	671.0
	MODE 2 (μm):		3400.0	2400.0			3400.0
	MODE 3 (μm):						
	MODE 1 (ϕ):	1.408	0.080	0.578	0.578	0.578	0.578
	MODE 2 (ϕ):		-1.743	-1.243			-1.743
	MODE 3 (ϕ):						
	D_{10} (μm):	220.2	531.7	343.9	334.6	304.6	283.2
	D_{50} (μm):	433.1	1354.6	664.7	693.1	649.2	799.1
	D_{90} (μm):	1043.0	3990.6	1409.8	1398.5	1352.5	3481.3
	(D_{90} / D_{10}) (μm):	4.736	7.505	4.100	4.179	4.440	12.29
	(D_{90} - D_{10}) (μm):	822.7	3458.9	1066.0	1063.9	1047.8	3198.0
	(D_{75} / D_{25}) (μm):	2.265	3.682	2.075	2.128	2.245	4.316
	(D_{75} - D_{25}) (μm):	374.5	2152.8	499.5	534.0	537.4	1539.9
	D_{10} (ϕ):	-0.061	-1.997	-0.496	-0.484	-0.436	-1.800
	D_{50} (ϕ):	1.207	-0.438	0.589	0.529	0.623	0.324
	D_{90} (ϕ):	2.183	0.911	1.540	1.579	1.715	1.820
	(D_{90} / D_{10}) (ϕ):	-35.956	-0.456	-3.108	-3.264	-3.937	-1.011
	(D_{90} - D_{10}) (ϕ):	2.244	2.908	2.036	2.063	2.150	3.620
	(D_{75} / D_{25}) (ϕ):	3.046	-0.203	21.03	-103.105	26.58	-1.103
	(D_{75} - D_{25}) (ϕ):	1.179	1.880	1.053	1.090	1.167	2.110
	% GRAVEL:	3.9%	39.3%	7.4%	3.5%	2.2%	25.1%
	% SAND:	96.1%	60.7%	92.6%	96.0%	97.8%	73.5%
	% MUD:	0.0%	0.0%	0.0%	0.4%	0.0%	1.4%
	% V COARSE GRAVEL:	0.0%	0.0%	0.0%	0.0%	0.0%	0.0%
	% COARSE GRAVEL:	0.0%	0.0%	0.0%	0.0%	0.0%	0.0%
	% MEDIUM GRAVEL:	0.0%	0.0%	0.0%	0.0%	0.0%	0.0%
	% FINE GRAVEL:	0.3%	9.9%	0.4%	0.4%	0.2%	6.1%
	% V FINE GRAVEL:	3.6%	29.4%	7.1%	3.1%	2.0%	19.0%
	% V COARSE SAND:	7.0%	24.8%	15.5%	21.9%	21.0%	15.2%
	% COARSE SAND:	29.8%	27.4%	47.5%	46.5%	43.4%	31.7%
	% MEDIUM SAND:	43.7%	6.5%	27.5%	24.2%	28.5%	20.2%
	% FINE SAND:	15.6%	1.6%	2.1%	2.5%	4.8%	5.1%
	% V FINE SAND:	0.0%	0.4%	0.0%	1.0%	0.0%	1.3%
	% V COARSE SILT:	0.0%	0.0%	0.0%	0.4%	0.0%	0.8%
	% COARSE SILT:	0.0%	0.0%	0.0%	0.0%	0.0%	0.4%
	% MEDIUM SILT:	0.0%	0.0%	0.0%	0.0%	0.0%	0.2%
	% FINE SILT:	0.0%	0.0%	0.0%	0.0%	0.0%	0.0%
	% V FINE SILT:	0.0%	0.0%	0.0%	0.0%	0.0%	0.0%
	% CLAY:	0.0%	0.0%	0.0%	0.0%	0.0%	0.0%

		SEK-5	SEK-6	SEK-7	SEK-8	SEK-9	SEK-10
	ANALYST AND DATE:	Tony, 11/13/2007	Tony, 11/13/2007	Tony, 11/13/2007	Tony, 11/13/2007	Tony, 11/13/2007	Tony, 11/13/2007
	SIEVING ERROR:	0.0%	0.0%	0.0%	0.0%	0.0%	0.0%
	SAMPLE TYPE:	Unimodal, Moderately Sorted	Unimodal, Moderately Well Sorted	Unimodal, Moderately Sorted	Unimodal, Moderately Well Sorted	Unimodal, Moderately Well Sorted	Unimodal, Moderately Sorted
	TEXTURAL GROUP:	Slightly Gravelly Sand	Slightly Gravelly Sand	Slightly Gravelly Sand	Slightly Gravelly Sand	Slightly Gravelly Sand	Slightly Gravelly Sand
	SEDIMENT NAME:	Slightly Very Fine Gravelly Medium Sand	Slightly Fine Gravelly Medium Sand	Slightly Very Fine Gravelly Medium Sand	Slightly Fine Gravelly Coarse Sand	Slightly Very Fine Gravelly Coarse Sand	Slightly Very Fine Gravelly Coarse Sand
METHOD OF MOMENTS Arithmetic (µm)	MEAN ($\overline{x}_a$):	366.1	294.5	576.8	625.2	740.9	731.9
	SORTING σ_a	219.6	182.7	380.5	277.5	512.6	421.5
	SKEWNESS	5.417	11.96	3.100	2.527	4.221	2.582
	KURTOSIS	78.56	276.8	24.14	27.65	27.93	16.84
METHOD OF MOMENTS Geometric (µm)	MEAN ($\overline{x}_g$):	320.8	260.9	486.7	568.8	639.2	639.2
	SORTING σ	1.677	1.745	1.772	1.613	1.758	1.675
	SKEWNESS	-0.832	-3.711	0.130	-3.462	-2.805	-0.333
	KURTOSIS	14.05	40.54	2.847	48.59	40.85	8.973
METHOD OF MOMENTS Logarithmic (ϕ)	MEAN ($\overline{x}_\phi$):	1.633	1.899	1.039	0.799	0.623	0.643
	SORTING σ_ϕ	0.712	0.637	0.826	0.591	0.685	0.730
	SKEWNESS α_ϕ	-0.205	-0.319	-0.130	-0.064	-0.817	-0.165
	KURTOSIS β	3.101	4.033	2.847	2.853	4.842	2.967
FOLK AND WARD METHOD (µm)	MEAN (M_G):	321.3	267.1	485.2	574.6	635.7	637.8
	SORTING σ_G	1.652	1.558	1.783	1.520	1.552	1.660
	SKEWNESS	0.026	0.012	0.005	-0.003	0.047	0.002
	KURTOSIS	0.946	0.945	0.931	0.940	0.985	0.944
FOLK AND WARD METHOD (ϕ)	MEAN (M_ϕ):	1.638	1.905	1.043	0.799	0.654	0.649
	SORTING σ_ϕ	0.724	0.639	0.834	0.604	0.634	0.731
	SKEWNESS	-0.026	-0.012	-0.005	0.003	-0.047	-0.002
	KURTOSIS	0.946	0.945	0.931	0.940	0.985	0.944
FOLK AND WARD METHOD (Description)	MEAN:	Medium Sand	Medium Sand	Medium Sand	Coarse Sand	Coarse Sand	Coarse Sand
	SORTING:	Moderately Sorted	Moderately Well Sorted	Moderately Sorted	Moderately We l Sorted	Moderately Well Sorted	Moderately Sorted
	SKEWNESS:	Symmetrical	Symmetrical	Symmetrical	Symmetrical	Symmetrical	Symmetrical
	KURTOSIS:	Mesokurtic	Mesokurtic	Mesokurtic	Mesokurtic	Mesokurtic	Mesokurtic
	MODE 1 (µm):	299.7	267.1	475.1	598.1	598.1	671.0
	MODE 2 (µm):						
	MODE 3 (µm):						
	MODE 1 (ϕ):	1.741	1.907	1.076	0.744	0.744	0.578
	MODE 2 (ϕ):						
	MODE 3 (ϕ):						
	D_{16} (µm):	169.2	151.0	230.1	333.8	368.7	330.8
	D_{50} (µm):	319.1	266.2	483.8	574.7	630.7	637.3
	D_{84} (µm):	620.6	476.2	1028.4	988.1	1133.1	1229.7
	(D_{84} / D_{16}) (µm):	3.667	3.153	4.469	2.961	3.090	3.719
	(D_{84} - D_{16}) (µm):	451.4	325.1	798.3	654.4	766.4	899.1
	(D_{75} / D_{25}) (µm):	2.018	1.859	2.267	1.801	1.826	2.033
	(D_{75} - D_{25}) (µm):	229.9	168.1	408.4	343.1	387.6	462.0
	D_{16} (ϕ):	0.888	1.070	-0.040	0.017	-0.180	-0.298
	D_{50} (ϕ):	1.648	1.910	1.047	0.799	0.685	0.650
	D_{84} (ϕ):	2.563	2.727	2.120	1.583	1.447	1.597
	(D_{84} / D_{16}) (ϕ):	3.724	2.548	-52.477	91.72	-8.029	-5.353
	(D_{84} - D_{16}) (ϕ):	1.875	1.657	2.160	1.566	1.628	1.895
	(D_{75} / D_{25}) (ϕ):	1.893	1.613	3.610	3.267	4.899	8.469
	(D_{75} - D_{25}) (ϕ):	1.013	0.895	1.181	0.849	0.869	1.023
	% GRAVEL:	0.3%	0.5%	0.8%	0.3%	2.9%	1.3%
	% SAND:	99.7%	99.5%	99.2%	99.7%	97.1%	98.7%
	% MUD:	0.0%	0.0%	0.0%	0.0%	0.0%	0.0%
	% V COARSE GRAVEL:	0.0%	0.0%	0.0%	0.0%	0.0%	0.0%
	% COARSE GRAVEL:	0.0%	0.0%	0.0%	0.0%	0.0%	0.0%
	% MEDIUM GRAVEL:	0.0%	0.0%	0.0%	0.0%	0.0%	0.0%
	% FINE GRAVEL:	0.1%	0.4%	0.1%	0.2%	0.6%	0.1%
	% V FINE GRAVEL:	0.2%	0.1%	0.8%	0.2%	2.3%	1.2%
	% V COARSE SAND:	0.2%	0.0%	10.1%	9.0%	12.5%	18.1%
	% COARSE SAND:	19.2%	7.4%	37.0%	53.1%	54.7%	48.3%
	% MEDIUM SAND:	48.5%	47.4%	39.2%	35.8%	29.2%	29.7%
	% FINE SAND:	30.0%	41.0%	12.7%	1.7%	0.6%	2.6%
	% V FINE SAND:	1.9%	3.6%	0.3%	0.0%	0.0%	0.0%
	% V COARSE SILT:	0.0%	0.0%	0.0%	0.0%	0.0%	0.0%
	% COARSE SILT:	0.0%	0.0%	0.0%	0.0%	0.0%	0.0%
	% MEDIUM SILT:	0.0%	0.0%	0.0%	0.0%	0.0%	0.0%
	% FINE SILT:	0.0%	0.0%	0.0%	0.0%	0.0%	0.0%
	% V FINE SILT:	0.0%	0.0%	0.0%	0.0%	0.0%	0.0%
	% CLAY:	0.0%	0.0%	0.0%	0.0%	0.0%	0.0%

		SEK-10-2m	SEK-10-3m	SEK-11	SEK-12	SEK-13	SEK-14
	ANALYST AND DATE:	Tony, 11/13/2007	Tony, 11/13/2007	Tony, 11/13/2007	Tony, 11/13/2007	Tony, 11/13/2007	Tony, 11/13/2007
	SIEVING ERROR:	0.0%	0.0%	0.0%	0.0%	0.0%	0.0%
	SAMPLE TYPE:	Bimodal, Moderately Sorted	Unimodal, Moderately Well Sorted	Unimodal, Moderately Well Sorted	Unimodal, Moderately Well Sorted	Unimodal, Moderately Well Sorted	Unimodal, Moderately Sorted
	TEXTURAL GROUP:	Gravelly Sand	Slightly Gravelly Sand	Slightly Gravelly Sand	Slightly Gravelly Sand	Slightly Gravelly Sand	Slightly Gravelly Sand
	SEDIMENT NAME:	Very Fine Gravelly Coarse Sand	Slightly Very Fine Gravelly Coarse Sand	Slightly Very Fine Gravelly Coarse Sand	Slightly Very Fine Gravely Coarse Sand	Slightly Very Fine Gravelly Coarse Sand	Slightly Very Fine Gravelly Medium Sand
METHOD OF MOMENTS Arithmetic (μm)	MEAN ($\overline{x}_a$):	1021.1	759.3	612.7	704.8	571.1	618.9
	SORTING s	881.4	522.0	311.5	431.8	260.8	511.6
	SKEWNESS	2.246	4.279	4.696	4.951	4.405	4.064
	KURTOSIS	8.133	28.67	52.46	40.26	57.98	26.19
METHOD OF MOMENTS Geometric (μm)	MEAN ($\overline{x}_g$):	786.1	659.8	557.2	632.2	523.8	506.9
	SORTING σ	2.002	1.681	1.541	1.536	1.544	1.836
	SKEWNESS	-0.252	-1.435	-0.851	0.743	-2.394	-0.451
	KURTOSIS	10.77	29.20	19.33	5.114	38.68	13.53
METHOD OF MOMENTS Logarithmic (ϕ)	MEAN ($\overline{x}_\phi$):	0.338	0.589	0.840	0.662	0.924	0.971
	SORTING s_ϕ	0.956	0.685	0.600	0.620	0.570	0.833
	SKEWNESS	-0.664	-0.778	-0.267	-0.743	-0.136	-0.617
	KURTOSIS	3.047	4.828	3.712	5.114	3.330	3.905
FOLK AND WARD METHOD (μm)	MEAN (M_G):	761.3	651.0	557.2	623.7	526.6	499.7
	SORTING s_ϕ	1.942	1.548	1.514	1.498	1.494	1.733
	SKEWNESS	0.197	0.014	-0.011	0.018	-0.018	0.053
	KURTOSIS	1.169	0.967	0.927	0.958	0.928	0.953
FOLK AND WARD METHOD (ϕ)	MEAN (M_ϕ):	0.394	0.619	0.844	0.681	0.925	1.001
	SORTING s	0.958	0.630	0.599	0.583	0.579	0.793
	SKEWNESS	-0.197	-0.014	0.011	-0.018	0.018	-0.053
	KURTOSIS	1.169	0.967	0.927	0.958	0.928	0.953
FOLK AND WARD METHOD (Description)	MEAN:	Coarse Sand	Coarse Sand	Coarse Sand	Coarse Sand	Coarse Sand	Medium Sand
	SORTING:	Moderately Sorted	Moderately Well Sorted	Moderately Well Sorted	Moderately Wel l Sorted	Moderately Wel l Sorted	Moderately Sorted
	SKEWNESS:	Coarse Skewed	Symmetrical	Symmetrical	Symmetrical	Symmetrical	Symmetrical
	KURTOSIS:	Leptokurtic	Mesokurtic	Mesokurtic	Mesokurtic	Mesokurtic	Mesokurtic
	MODE 1 (μm):	671.0	671.0	533.0	598.1	533.0	475.1
	MODE 2 (μm):	3400.0					
	MODE 3 (μm):						
	MODE 1 (ϕ):	0.578	0.578	0.910	0.744	0.910	1.076
	MODE 2 (ϕ):	-1.743					
	MODE 3 (ϕ):						
	D_{16} (μm):	364.6	372.4	324.0	371.8	311.6	251.5
	D_{50} (μm):	723.4	650.6	558.4	621.7	528.6	492.3
	D_{84} (μm):	2281.2	1147.4	951.0	1057.3	881.6	1037.8
	(D_{84} / D_{16}) (μm):	6.257	3.082	2.935	2.843	2.829	4.126
	(D_{84} - D_{16}) (μm):	1916.6	775.1	627.0	685.5	570.0	786.3
	(D_{75} / D_{25}) (μm):	2.259	1.831	1.801	1.754	1.767	2.156
	(D_{75} - D_{25}) (μm):	622.7	399.4	332.9	354.7	304.3	391.8
	D_{16} (ϕ):	-1.190	-0.198	0.073	-0.080	0.182	-0.053
	D_{50} (ϕ):	0.467	0.620	0.841	0.686	0.920	1.022
	D_{84} (ϕ):	1.456	1.425	1.626	1.427	1.682	1.991
	(D_{84} / D_{16}) (ϕ):	-1.224	-7.183	22.42	-17.751	9.250	-37.229
	(D_{84} - D_{16}) (ϕ):	2.646	1.624	1.553	1.508	1.500	2.045
	(D_{75} / D_{25}) (ϕ):	-6.349	5.738	3.029	3.921	2.803	3.448
	(D_{75} - D_{25}) (ϕ):	1.176	0.872	0.849	0.811	0.821	1.108
	% GRAVEL:	11.9%	3.0%	0.6%	1.6%	0.3%	2.8%
	% SAND:	88.1%	97.0%	99.4%	98.4%	99.7%	97.2%
	% MUD:	0.0%	0.0%	0.0%	0.0%	0.0%	0.0%
	% V COARSE GRAVEL:	0.0%	0.0%	0.0%	0.0%	0.0%	0.0%
	% COARSE GRAVEL:	0.0%	0.0%	0.0%	0.0%	0.0%	0.0%
	% MEDIUM GRAVEL:	0.0%	0.0%	0.0%	0.0%	0.0%	0.0%
	% FINE GRAVEL:	1.2%	0.6%	0.1%	0.3%	0.1%	0.4%
	% V FINE GRAVEL:	10.7%	2.4%	0.5%	1.3%	0.2%	2.4%
	% V COARSE SAND:	18.4%	13.7%	7.0%	10.9%	4.4%	8.3%
	% COARSE SAND:	44.1%	55.6%	52.4%	57.7%	50.5%	37.8%
	% MEDIUM SAND:	24.4%	27.3%	38.1%	29.6%	42.3%	41.3%
	% FINE SAND:	1.3%	0.5%	2.0%	0.3%	2.6%	9.8%
	% V FINE SAND:	0.0%	0.0%	0.0%	0.0%	0.0%	0.0%
	% V COARSE SILT:	0.0%	0.0%	0.0%	0.0%	0.0%	0.0%
	% COARSE SILT:	0.0%	0.0%	0.0%	0.0%	0.0%	0.0%
	% MEDIUM SILT:	0.0%	0.0%	0.0%	0.0%	0.0%	0.0%
	% FINE SILT:	0.0%	0.0%	0.0%	0.0%	0.0%	0.0%
	% V FINE SILT:	0.0%	0.0%	0.0%	0.0%	0.0%	0.0%
	% CLAY:	0.0%	0.0%	0.0%	0.0%	0.0%	0.0%

		SEK-15	SEK-16	SEK-17	SEK-18	SEK-19
	ANALYST AND DATE:	Tony, 11/13/2007	Tony, 11/13/2007	Tony, 11/13/2007	Tony, 11/13/2007	Tony, 11/13/2007
	SIEVING ERROR:	0.0%	0.0%	0.0%	0.0%	0.0%
	SAMPLE TYPE:	Unimodal, Moderately Sorted	Unimodal, Moderately Well Sorted	Unimodal, Moderately Well Sorted	Unimodal, Moderately Well Sorted	Unimodal, Moderately Well Sorted
	TEXTURAL GROUP:	Slightly Gravelly Sand	Slightly Gravelly Sand	Slightly Gravelly Sand	Slightly Gravelly Sand	Slightly Gravelly Sand
	SEDIMENT NAME:	Slightly Very Fine Gravelly Coarse Sand	Slightly Very Fine Gravelly Coarse Sand	Slightly Very Fine Gravelly Coarse Sand	Slightly Very Fine Gravelly Coarse Sand	Slightly Very Fine Gravelly Medium Sand
METHOD OF MOMENTS Arithmetic (μm)	MEAN ($\bar{x}_a$):	716.4	578.6	564.7	558.5	520.7
	SORTING σ	549.1	295.1	235.2	209.5	250.5
	SKEWNESS	3.623	3.970	1.309	1.261	4.485
	KURTOSIS	22.10	40.92	11.63	10.32	58.83
METHOD OF MOMENTS Geometric (μm)	MEAN ($\bar{x}_g$):	580.8	524.0	509.7	521.4	476.1
	SORTING σ	1.973	1.540	1.673	1.444	1.510
	SKEWNESS	-1.278	0.207	-2.564	-0.025	0.170
	KURTOSIS	11.09	3.411	18.50	2.572	3.316
METHOD OF MOMENTS Logarithmic (ϕ)	MEAN ($\bar{x}_\phi$):	0.780	0.932	0.972	0.940	1.071
	SORTING σ_ϕ	0.964	0.623	0.742	0.530	0.595
	SKEWNESS	1.018	-0.207	2.564	0.025	-0.170
	KURTOSIS	8.666	3.411	18.50	2.572	3.316
FOLK AND WARD METHOD (μm)	MEAN (M_G):	592.3	522.6	525.3	522.6	475.5
	SORTING I_I	1.718	1.541	1.508	1.459	1.519
	SKEWNESS	-0.038	-0.015	-0.048	-0.009	-0.009
	KURTOSIS	1.012	0.930	0.954	0.936	0.930
FOLK AND WARD METHOD (ϕ)	MEAN (M_ϕ):	0.756	0.936	0.929	0.936	1.072
	SORTING σ	0.781	0.624	0.592	0.545	0.603
	SKEWNESS	0.038	0.015	0.048	0.009	0.009
	KURTOSIS	1.012	0.930	0.954	0.936	0.930
FOLK AND WARD METHOD (Description)	MEAN:	Coarse Sand	Coarse Sand	Coarse Sand	Coarse Sand	Medium Sand
	SORTING:	Moderately Sorted	Moderately Well Sorted	Moderately Well Sorted	Moderately Well Sorted	Moderately Well Sorted
	SKEWNESS:	Symmetrical	Symmetrical	Symmetrical	Symmetrical	Symmetrical
	KURTOSIS:	Mesokurtic	Mesokurtic	Mesokurtic	Mesokurtic	Mesokurtic
	MODE 1 (μm):	598.1	533.0	533.0	533.0	475.1
	MODE 2 (μm):					
	MODE 3 (μm):					
	MODE 1 (ϕ):	0.744	0.910	0.910	0.910	1.076
	MODE 2 (ϕ):					
	MODE 3 (ϕ):					
	D_{16} (μm):	292.2	296.8	304.7	319.2	275.9
	D_{50} (μm):	598.0	524.3	529.9	523.3	476.2
	D_{84} (μm):	1168.9	911.1	880.9	850.8	814.7
	(D_{84} / D_{16}) (μm):	4.000	3.070	2.891	2.666	2.953
	(D_{84} - D_{16}) (μm):	876.6	614.3	576.2	531.6	538.8
	(D_{84} / D_{50}) (μm):	2.076	1.844	1.773	1.704	1.805
	(D_{84} - D_{50}) (μm):	440.7	325.1	306.1	282.1	285.3
	D_{16} (ϕ):	-0.225	0.134	0.183	0.233	0.296
	D_{50} (ϕ):	0.742	0.932	0.916	0.934	1.070
	D_{84} (ϕ):	1.775	1.752	1.714	1.648	1.858
	(D_{84} / D_{16}) (ϕ):	-7.884	13.05	9.374	7.066	6.283
	(D_{84} - D_{16}) (ϕ):	2.000	1.618	1.532	1.414	1.562
	(D_{84} / D_{50}) (ϕ):	5.708	2.788	2.620	2.397	2.321
	(D_{84} - D_{50}) (ϕ):	1.053	0.883	0.826	0.769	0.852
	% GRAVEL:	3.2%	0.6%	0.1%	0.0%	0.3%
	% SAND:	95.6%	99.4%	98.9%	100.0%	99.7%
	% MUD:	1.2%	0.0%	1.0%	0.0%	0.0%
	% V COARSE GRAVEL:	0.0%	0.0%	0.0%	0.0%	0.0%
	% COARSE GRAVEL:	0.0%	0.0%	0.0%	0.0%	0.0%
	% MEDIUM GRAVEL:	0.0%	0.0%	0.0%	0.0%	0.0%
	% FINE GRAVEL:	0.4%	0.0%	0.0%	0.0%	0.0%
	% V FINE GRAVEL:	2.8%	0.5%	0.1%	0.0%	0.2%
	% V COARSE SAND:	13.2%	5.5%	4.4%	3.3%	2.3%
	% COARSE SAND:	46.5%	48.0%	50.9%	51.2%	43.0%
	% MEDIUM SAND:	31.0%	41.9%	40.6%	43.5%	48.4%
	% FINE SAND:	4.1%	4.0%	2.6%	2.0%	6.0%
	% V FINE SAND:	0.8%	0.0%	0.4%	0.0%	0.0%
	% V COARSE SILT:	0.6%	0.0%	0.4%	0.0%	0.0%
	% COARSE SILT:	0.3%	0.0%	0.2%	0.0%	0.0%
	% MEDIUM SILT:	0.3%	0.0%	0.3%	0.0%	0.0%
	% FINE SILT:	0.0%	0.0%	0.1%	0.0%	0.0%
	% V FINE SILT:	0.0%	0.0%	0.0%	0.0%	0.0%
	% CLAY:	0.0%	0.0%	0.0%	0.0%	0.0%

Appendix 2. 2 Table of sedimentary statistical analysis results for beach ridge samples from Wonga Beach (samples were collected at the intersection of beach ridge crests and transects indicated in Figure 3-1).

		W-01	W-02	W-03	W-04	W-05	W-06	W-07
	ANALYST AND DATE:	Tony, 11/13/2007	Tony, 11/13/2007	Tony, 11/13/2007	Tony, 11/13/2007	Tony, 11/13/2007	Tony, 11/13/2007	Tony, 11/13/2007
	SIEVING ERROR:	0.0%	0.0%	0.0%	0.0%	0.0%	1.1%	0.0%
	SAMPLE TYPE:	Unimodal, Well Sorted	Unimodal, Well Sorted	Unimodal, Well Sorted	Unimodal, Well Sorted	Bimodal, Poorly Sorted	nimodal, Moderately Well Sorte	Unimodal, Moderately Sorted
	TEXTURAL GROUP:	Sand	Sand	Sand	Sand	Sandy Gravel	Slightly Gravelly Sand	Gravelly Sand
	SEDIMENT NAME:	Wel Sorted Medium Sand	Well Sorted Medium Sand	Well Sorted Fine Sand	Well Sorted Fine Sand	Sandy Very Fine Gravel	tly Very Fine Gravelly Coarse S	ery Fine Gravelly Coarse Sand
METHOD OF MOMENTS Arithmetic (µm)	MEAN($\bar{x}_a$):	319.0	265.4	233.4	254.5	2240.9	983.3	831.2
	SORTING(σ_a):	98.41	75.69	72.80	78.90	1787.6	473.9	678.3
	SKEWNESS:	0.679	0.693	0.684	0.711	0.231	2.149	2.803
	KURTOSIS:	3.147	3.331	3.155	3.248	1.651	12.27	12.53
METHOD OF MOMENTS Geometric (µm)	MEAN($\bar{x}_g$):	303.9	254.6	222.2	242.4	864.3	891.5	669.3
	SORTING(σ_g):	1.359	1.326	1.363	1.360	9.173	1.536	1.845
	SKEWNESS:	-0.028	-0.009	-0.032	-0.012	-1.986	0.221	0.592
	KURTOSIS:	2.542	2.635	2.544	2.563	6.430	3.072	3.422
METHOD OF MOMENTS Logarithmic (ϕ)	MEAN($\bar{x}_\phi$):	1.718	1.974	2.170	2.044	-0.489	0.166	0.579
	SORTING(σ_ϕ):	0.442	0.407	0.447	0.443	1.748	0.620	0.884
	SKEWNESS:	0.028	0.009	0.032	0.012	1.215	-0.221	-0.592
	KURTOSIS:	2.542	2.635	2.544	2.563	4.833	3.072	3.422
FOLK AND WARD METHOD (µm)	MEAN(M_g):	304.4	254.6	222.5	242.7	1700.0	886.6	649.3
	SORTING(σ_g):	1.399	1.334	1.376	1.370	2.971	1.531	1.846
	SKEWNESS:	-0.003	-0.001	-0.002	0.002	-0.856	0.008	0.121
	KURTOSIS:	0.947	0.958	0.965	0.953	0.829	0.944	1.121
FOLK AND WARD METHOD (ϕ)	MEAN(M_ϕ):	1.716	1.974	2.168	2.043	-0.766	0.174	0.623
	SORTING(σ_ϕ):	0.453	0.416	0.480	0.454	1.571	0.614	0.884
	SKEWNESS:	0.003	0.001	0.002	-0.002	0.856	-0.008	-0.121
	KURTOSIS:	0.947	0.958	0.965	0.953	0.829	0.944	1.121
FOLK AND WARD METHOD (Description)	MEAN:	Medium Sand	Medium Sand	Fine Sand	Fine Sand	Very Coarse Sand	Coarse Sand	Coarse Sand
	SORTING:	Well Sorted	Well Sorted	Well Sorted	Wel Sorted	Poorly Sorted	Moderately Well Sorted	Moderately Sorted
	SKEWNESS:	Symmetrical	Symmetrical	Symmetrical	Symmetrical	Very Fine Skewed	Symmetrical	Coarse Skewed
	KURTOSIS:	Mesokurtic	Mesokurtic	Mesokurtic	Mesokurtic	Very Platykurtic	Mesokurtic	Leptokurtic
	MODE 1 (µm):	299.7	267.1	212.2	238.1	3400.0	844.8	598.1
	MODE 2 (µm):					423.4		
	MODE 3 (µm):							
	MODE 1 (ϕ):	1.741	1.907	2.239	2.073	-1.743	0.246	0.744
	MODE 2 (ϕ):					1.242		
	MODE 3 (ϕ):							
	D_{10} (µm):	202.6	175.6	147.0	161.6	273.5	511.8	319.2
	D_{50} (µm):	304.2	254.7	222.4	242.4	2649.3	885.2	637.4
	D_{90} (µm):	456.4	370.1	336.0	364.4	5620.4	1542.8	1415.0
	(D_{90} / D_{10}) (µm):	2.252	2.107	2.286	2.255	20.55	3.015	4.433
	(D_{90} - D_{10}) (µm):	253.7	194.4	189.0	202.8	5346.9	1031.1	1095.8
	(D_{75} / D_{25}) (µm):	1.553	1.491	1.554	1.552	6.801	1.817	2.188
	(D_{75} - D_{25}) (µm):	135.0	102.4	98.94	107.5	3449.5	537.2	517.9
	D_{10} (ϕ):	1.132	1.434	1.573	1.456	-2.491	-0.626	-0.501
	D_{50} (ϕ):	1.717	1.973	2.169	2.045	-1.406	0.176	0.650
	D_{90} (ϕ):	2.303	2.509	2.766	2.630	1.870	0.966	1.647
	(D_{90} / D_{10}) (ϕ):	2.035	1.750	1.758	1.806	-0.751	-1.545	-3.289
	(D_{90} - D_{10}) (ϕ):	1.171	1.075	1.193	1.173	4.361	1.592	2.148
	(D_{75} / D_{25}) (ϕ):	1.454	1.342	1.344	1.367	-0.372	-2.359	17.59
	(D_{75} - D_{25}) (ϕ):	0.635	0.577	0.636	0.634	2.766	0.862	1.129
	% GRAVEL:	0.0%	0.0%	0.0%	0.0%	63.6%	2.6%	6.0%
	% SAND:	100.0%	100.0%	100.0%	100.0%	34.3%	97.4%	94.0%
	% MUD:	0.0%	0.0%	0.0%	0.0%	2.0%	0.0%	0.0%
	% V COARSE GRAVEL:	0.0%	0.0%	0.0%	0.0%	0.0%	0.0%	0.0%
	% COARSE GRAVEL:	0.0%	0.0%	0.0%	0.0%	0.0%	0.0%	0.0%
	% MEDIUM GRAVEL:	0.0%	0.0%	0.0%	0.0%	0.0%	0.0%	0.0%
	% FINE GRAVEL:	0.0%	0.0%	0.0%	0.0%	25.5%	0.1%	0.4%
	% V FINE GRAVEL:	0.0%	0.0%	0.0%	0.0%	38.1%	2.5%	5.7%
	% V COARSE SAND:	0.0%	0.0%	0.0%	0.0%	3.6%	36.6%	16.5%
	% COARSE SAND:	5.3%	0.5%	0.0%	0.4%	11.1%	51.9%	44.0%
	% MEDIUM SAND:	67.5%	52.0%	36.1%	45.8%	13.2%	8.9%	30.1%
	% FINE SAND:	27.2%	47.2%	60.8%	52.6%	5.9%	0.0%	3.4%
	% V FINE SAND:	0.0%	0.3%	3.1%	1.2%	0.6%	0.0%	0.0%
	% V COARSE SILT:	0.0%	0.0%	0.0%	0.0%	0.8%	0.0%	0.0%
	% COARSE SILT:	0.0%	0.0%	0.0%	0.0%	0.5%	0.0%	0.0%
	% MEDIUM SILT:	0.0%	0.0%	0.0%	0.0%	0.3%	0.0%	0.0%
	% FINE SILT:	0.0%	0.0%	0.0%	0.0%	0.3%	0.0%	0.0%
	% V FINE SILT:	0.0%	0.0%	0.0%	0.0%	0.1%	0.0%	0.0%
	% CLAY:	0.0%	0.0%	0.0%	0.0%	0.0%	0.0%	0.0%

		W-08	W-09	W-10	W-10-2m	W-10-3m	W-11	W-12	W-13
	ANALYST AND DATE:	Tony, 11/13/2007	Tony, 11/13/2007	Tony, 11/13/2007	Tony, 11/13/2007	Tony, 11/13/2007	Tony, 11/13/2007	Tony, 11/13/2007	Tony, 11/13/2007
	SIEVING ERROR:	0.7%	1.1%	1.1%	0.3%	0.7%	0.0%	0.9%	0.0%
	SAMPLE TYPE:	Bimodal, Poorly Sorted	Bimodal, Poorly Sorted	Bimodal, Poorly Sorted	Bimodal, Poorly Sorted	Bimodal, Poorly Sorted	Unimodal, Moderately Sorted	Unimodal, Moderately Sorted	Bimodal, Poorly Sorted
	TEXTURAL GROUP:	Sandy Gravel	Sandy Gravel	Gravelly Sand	Sandy Gravel	Sandy Gravel	Slightly Gravelly Sand	Gravelly Sand	Gravelly Sand
	SEDIMENT NAME:	Sandy Very Fine Gravel	Sandy Very Fine Gravel	Very Fine Gravelly Coarse Sand	Sandy Very Fine Gravel	Sandy Very Fine Gravel	Slightly Very Fine Gravelly Coarse Sand	Very Fine Gravelly Coarse Sand	Very Fine Gravelly Coarse Sand
METHOD OF MOMENTS Arithmetic (μm)	MEAN ($\bar{x}_a$):	1630.1	1801.5	1475.2	1931.0	1886.7	628.2	1001.2	1300.8
	SORTING (σ_a):	1379.7	1422.3	1274.7	1487.5	1721.7	415.8	693.5	1404.8
	SKEWNESS (β_1):	1.018	0.915	1.262	0.382	0.703	3.931	2.316	1.677
	KURTOSIS (β_2):	2.898	2.752	3.708	1.919	2.047	30.32	10.04	4.519
METHOD OF MOMENTS Geometric (μm)	MEAN ($\bar{x}_g$):	1052.2	1184.5	973.4	1149.5	765.9	532.8	836.1	718.9
	SORTING (σ_g):	3.156	3.230	2.941	3.610	7.861	1.835	1.772	4.173
	SKEWNESS (β_1):	-2.517	-2.797	-2.223	-1.831	-2.043	-1.740	0.381	-2.640
	KURTOSIS (β_2):	16.79	17.69	15.66	9.632	7.094	18.66	3.049	13.93
METHOD OF MOMENTS Logarithmic (ϕ)	MEAN ($\bar{x}_l$):	-0.193	-0.372	-0.049	-0.290	-0.235	0.896	0.258	0.177
	SORTING (σ_g):	1.234	1.229	1.243	1.582	1.663	0.816	0.826	1.208
	SKEWNESS (β_1):	-0.082	0.259	0.089	0.744	0.969	0.479	-0.381	-0.700
	KURTOSIS (β_2):	1.906	2.491	2.631	3.052	4.697	5.755	3.049	2.559
FOLK AND WARD METHOD (μm)	MEAN (M_G):	1169.7	1335.6	1081.5	1376.4	1394.7	543.6	819.5	993.0
	SORTING (σ_G):	2.473	2.422	2.464	2.848	2.933	1.653	1.777	2.625
	SKEWNESS (Sk_G):	0.153	0.042	0.104	-0.489	-0.150	-0.012	0.080	0.392
	KURTOSIS (K_G):	0.717	0.806	0.819	0.692	0.697	0.970	1.068	1.097
FOLK AND WARD METHOD (ϕ)	MEAN (M_z):	-0.226	-0.417	-0.113	-0.461	-0.480	0.879	0.287	0.010
	SORTING (σ_I):	1.306	1.276	1.301	1.510	1.552	0.725	0.830	1.392
	SKEWNESS (Sk_I):	-0.153	-0.042	-0.104	0.489	0.150	0.012	-0.080	-0.392
	KURTOSIS (K_G):	0.717	0.806	0.819	0.692	0.697	0.970	1.068	1.097
FOLK AND WARD METHOD (Description)	MEAN:	Very Coarse Sand	Very Coarse Sand	Very Coarse Sand	Very Coarse Sand	Very Coarse Sand	Coarse Sand	Coarse Sand	Coarse Sand
	SORTING:	Poorly Sorted	Poorly Sorted	Poorly Sorted	Poorly Sorted	Poorly Sorted	Moderately Sorted	Moderately Sorted	Poorly Sorted
	SKEWNESS:	Coarse Skewed	Symmetrical	Coarse Skewed	Very Fine Skewed	Fine Skewed	Symmetrical	Symmetrical	Very Coarse Skewed
	KURTOSIS:	Platykurtic	Platykurtic	Platykurtic	Platykurtic	Platykurtic	Mesokurtic	Mesokurtic	Mesokurtic
	MODE 1 (μm):	3400.0	3400.0	844.8	3400.0	3400.0	533.0	752.9	598.1
	MODE 2 (μm):	752.9	947.9	3400.0	475.1	844.8			3400.0
	MODE 3 (μm):								
	MODE 1 (ϕ):	-1.743	-1.743	0.246	-1.743	-1.743	0.910	0.412	0.744
	MODE 2 (ϕ):	0.412	0.080	-1.743	1.076	0.246			-1.743
	MODE 3 (ϕ):								
	D_{16} (μm):	384.3	426.8	348.3	278.9	302.2	284.3	409.4	348.4
	D_{50} (μm):	1030.4	1269.0	985.7	2030.7	1401.6	544.3	810.0	741.4
	D_{84} (μm):	3788.8	3994.5	3545.0	3865.0	5433.5	1035.5	1738.5	4268.9
	(D_{84} / D_{16}) (μm):	9.858	9.359	10.18	13.86	17.98	3.642	4.246	12.25
	(D_{84} - D_{16}) (μm):	3404.4	3567.7	3196.7	3586.1	5131.4	751.1	1329.1	3920.5
	(D_{84} / D_{50}) (μm):	4.723	4.062	3.954	6.348	6.287	2.002	2.123	2.978
	(D_{84} - D_{50}) (μm):	2171.7	2143.3	1628.4	2668.7	3125.4	385.5	629.2	955.0
	D_{16} (ϕ):	-1.922	-1.998	-1.826	-1.950	-2.442	-0.050	-0.798	-2.094
	D_{50} (ϕ):	-0.043	-0.344	0.021	-1.022	-0.487	0.878	0.304	0.432
	D_{84} (ϕ):	1.380	1.228	1.522	1.842	1.727	1.814	1.288	1.521
	(D_{84} / D_{16}) (ϕ):	-0.718	-0.615	-0.833	-0.944	-0.707	-36.100	-1.615	-0.726
	(D_{84} - D_{16}) (ϕ):	3.301	3.226	3.347	3.793	4.169	1.865	2.086	3.615
	(D_{84} / D_{50}) (ϕ):	-0.532	-0.341	-0.764	-0.803	-0.400	3.658	-3.342	-2.006
	(D_{84} - D_{50}) (ϕ):	2.240	2.022	1.983	2.866	2.652	1.002	1.086	1.575
	% GRAVEL:	33.4%	37.6%	27.3%	50.7%	44.5%	1.8%	7.5%	23.2%
	% SAND:	66.6%	62.3%	72.3%	48.1%	53.3%	97.7%	92.5%	76.8%
	% MUD:	0.0%	0.1%	0.4%	1.1%	2.2%	0.7%	0.0%	0.0%
	% V COARSE GRAVEL:	0.0%	0.0%	0.0%	0.0%	0.0%	0.0%	0.0%	0.0%
	% COARSE GRAVEL:	0.0%	0.0%	0.0%	0.0%	0.0%	0.0%	0.0%	0.0%
	% MEDIUM GRAVEL:	0.0%	0.0%	0.0%	0.0%	0.0%	0.0%	0.0%	0.0%
	% FINE GRAVEL:	7.4%	9.9%	5.7%	7.4%	21.7%	0.3%	0.4%	11.3%
	% V FINE GRAVEL:	26.0%	27.6%	21.6%	43.3%	22.8%	1.3%	7.0%	11.8%
	% V COARSE SAND:	17.8%	22.4%	22.1%	7.7%	14.4%	9.7%	27.9%	12.0%
	% COARSE SAND:	30.1%	26.2%	29.4%	16.5%	20.7%	45.3%	46.0%	37.9%
	% MEDIUM SAND:	16.7%	11.4%	17.6%	17.2%	12.9%	37.3%	18.0%	24.9%
	% FINE SAND:	2.0%	2.1%	3.2%	6.0%	4.1%	4.6%	0.7%	2.0%
	% V FINE SAND:	0.0%	0.2%	0.1%	0.8%	1.2%	0.9%	0.0%	0.0%
	% V COARSE SILT:	0.0%	0.1%	0.4%	0.7%	1.0%	0.7%	0.0%	0.0%
	% COARSE SILT:	0.0%	0.0%	0.0%	0.2%	0.6%	0.0%	0.0%	0.0%
	% MEDIUM SILT:	0.0%	0.0%	0.0%	0.2%	0.4%	0.0%	0.0%	0.0%
	% FINE SILT:	0.0%	0.0%	0.0%	0.0%	0.2%	0.0%	0.0%	0.0%
	% V FINE SILT:	0.0%	0.0%	0.0%	0.0%	0.0%	0.0%	0.0%	0.0%
	% CLAY:	0.0%	0.0%	0.0%	0.0%	0.0%	0.0%	0.0%	0.0%

		WS-01	WS-2	WS-3	WS-4	WS-5	WS-6
	ANALYST AND DATE:	Tony, 11/13/2007	Tony, 11/13/2007	Tony, 11/13/2007	Tony, 11/13/2007	Tony, 11/13/2007	Tony, 11/13/2007
	SIEVING ERROR:	0.0%	0.0%	0.0%	0.0%	0.0%	0.0%
	SAMPLE TYPE:	Unimodal, Moderately Sorted	Bimodal, Poorly Sorted	Unimodal, Moderately Sorted	Bimodal, Poorly Sorted	Bimodal, Poorly Sorted	Bimodal, Poorly Sorted
	TEXTURAL GROUP:	Slightly Gravelly Sand	Gravelly Sand	Slightly Gravelly Sand	Gravelly Sand	Gravelly Sand	Gravelly Sand
	SEDIMENT NAME:	Slightly Very Fine Gravelly Coarse Sand	Very Fine Gravelly Coarse Sand	Slightly Very Fine Gravelly Medium Sand	Very Fine Gravelly Medium Sand	Very Fine Gravelly Medium Sand	Very Fine Gravelly Medium Sand
METHOD OF MOMENTS Arithmetic (μm)	MEAN ($\bar{x}_g$):	627.3	1074.5	513.4	697.4	757.1	918.5
	SORTING (σ_g):	448.4	1245.3	477.0	897.9	1021.5	1312.3
	SKEWNESS:	2.184	1.983	4.880	2.945	2.561	2.063
	KURTOSIS:	11.83	6.000	34.49	12.17	9.155	5.969
METHOD OF MOMENTS Geometric (μm)	MEAN ($\bar{x}_g$):	498.3	547.4	406.8	368.4	396.0	392.8
	SORTING (σ_g):	2.014	4.827	2.061	3.788	3.414	4.913
	SKEWNESS:	-0.389	-2.469	-2.495	-1.468	-0.931	-1.820
	KURTOSIS:	3.621	11.36	26.70	7.380	6.480	9.072
METHOD OF MOMENTS Logarithmic (ϕ)	MEAN ($\bar{x}_g$):	1.005	0.444	1.246	1.329	1.291	0.928
	SORTING (σ_g):	1.010	1.215	0.840	1.700	1.674	1.429
	SKEWNESS:	0.389	-0.715	-0.760	0.901	0.555	-0.822
	KURTOSIS:	3.621	2.782	4.536	5.194	4.948	3.283
FOLK AND WARD METHOD (μm)	MEAN (M_g):	503.7	834.0	411.8	426.4	430.0	653.8
	SORTING (σ_g):	1.976	2.745	1.727	3.009	2.950	3.193
	SKEWNESS:	-0.083	0.398	0.059	-0.081	0.062	0.546
	KURTOSIS:	0.960	1.192	0.977	1.657	1.715	1.479
FOLK AND WARD METHOD (ϕ)	MEAN (M_g):	0.989	0.262	1.280	1.230	1.217	0.613
	SORTING (σ_g):	0.983	1.457	0.789	1.589	1.561	1.675
	SKEWNESS:	0.083	-0.398	-0.059	0.081	-0.062	-0.546
	KURTOSIS:	0.960	1.192	0.977	1.657	1.715	1.479
FOLK AND WARD METHOD (Description)	MEAN:	Coarse Sand	Coarse Sand	Medium Sand	Medium Sand	Medium Sand	Coarse Sand
	SORTING:	Moderately Sorted	Poorly Sorted	Moderately Sorted	Poorly Sorted	Poorly Sorted	Poorly Sorted
	SKEWNESS:	Symmetrical	Very Coarse Skewed	Symmetrical	Symmetrical	Symmetrical	Very Coarse Skewed
	KURTOSIS:	Mesokurtic	Leptokurtic	Mesokurtic	Very Leptokurtic	Very Leptokurtic	Leptokurtic
	MODE 1 (μm):	598.1	533.0	377.4	475.1	377.4	336.3
	MODE 2 (μm):		2400.0		3400.0	3400.0	3400.0
	MODE 3 (μm):						
	MODE 1 (ϕ):	0.744	0.910	1.408	1.076	1.408	1.574
	MODE 2 (ϕ):		-1.243		-1.743	-1.743	-1.743
	MODE 3 (ϕ):						
	D_{16} (μm):	200.9	286.0	208.4	98.28	142.4	205.1
	D_{50} (μm):	520.1	625.7	406.1	441.6	398.0	402.3
	D_{84} (μm):	1169.0	3868.7	853.8	1451.8	2346.2	3894.5
	(D_{84} / D_{16}) (μm):	5.820	13.53	4.098	14.77	16.47	18.99
	(D_{84} - D_{16}) (μm):	968.2	3582.8	645.4	1353.5	2203.8	3689.5
	(D_{75} / D_{25}) (μm):	2.575	2.976	2.119	2.983	2.829	2.626
	(D_{75} - D_{25}) (μm):	498.4	796.8	315.6	499.2	450.2	448.8
	D_{16} (ϕ):	-0.225	-1.952	0.228	-0.538	-1.230	-1.961
	D_{50} (ϕ):	0.943	0.677	1.300	1.179	1.329	1.314
	D_{84} (ϕ):	2.316	1.806	2.263	3.347	2.812	2.286
	(D_{84} / D_{16}) (ϕ):	-10.277	-0.925	9.924	-6.223	-2.285	-1.165
	(D_{84} - D_{16}) (ϕ):	2.541	3.758	2.035	3.885	4.042	4.247
	(D_{75} / D_{25}) (ϕ):	5.821	-4.982	2.459	4.817	3.874	3.999
	(D_{75} - D_{25}) (ϕ):	1.365	1.574	1.084	1.577	1.500	1.393
	% GRAVEL:	1.6%	22.0%	2.8%	9.5%	11.9%	21.2%
	% SAND:	97.7%	78.0%	97.2%	83.0%	81.6%	77.8%
	% MUD:	0.7%	0.0%	0.0%	7.5%	6.5%	1.0%
	% V COARSE GRAVEL:	0.0%	0.0%	0.0%	0.0%	0.0%	0.0%
	% COARSE GRAVEL:	0.0%	0.0%	0.0%	0.0%	0.0%	0.0%
	% MEDIUM GRAVEL:	0.0%	0.0%	0.0%	0.0%	0.0%	0.0%
	% FINE GRAVEL:	0.0%	9.4%	0.7%	2.6%	2.6%	9.4%
	% V FINE GRAVEL:	1.6%	12.6%	2.1%	6.7%	9.3%	11.8%
	% V COARSE SAND:	13.9%	7.3%	3.2%	6.4%	4.6%	0.3%
	% COARSE SAND:	36.7%	33.5%	29.6%	27.8%	21.6%	16.0%
	% MEDIUM SAND:	31.6%	31.0%	46.2%	31.6%	36.2%	43.3%
	% FINE SAND:	13.6%	6.1%	17.8%	13.1%	16.9%	17.9%
	% V FINE SAND:	2.0%	0.0%	0.3%	4.2%	2.3%	0.2%
	% V COARSE SILT:	0.5%	0.0%	0.0%	3.4%	3.0%	0.8%
	% COARSE SILT:	0.2%	0.0%	0.0%	1.9%	1.8%	0.2%
	% MEDIUM SILT:	0.0%	0.0%	0.0%	1.1%	0.9%	0.0%
	% FINE SILT:	0.0%	0.0%	0.0%	0.7%	0.6%	0.0%
	% V FINE SILT:	0.0%	0.0%	0.0%	0.3%	0.2%	0.0%
	% CLAY:	0.0%	0.0%	0.0%	0.0%	0.0%	0.0%

		WS-7	WS-8	WS-9
	ANALYST AND DATE:	Tony, 11/13/2007	Tony, 11/13/2007	Tony, 11/13/2007
	SIEVING ERROR:	0.0%	0.0%	0.0%
	SAMPLE TYPE:	Bimodal, Poorly Sorted	Unimodal, Moderately Sorted	Bimodal, Poorly Sorted
	TEXTURAL GROUP:	Gravelly Sand	Slightly Gravelly Sand	Gravelly Sand
	SEDIMENT NAME:	Very Fine Gravelly Medium Sand	Slightly Very Fine Gravelly Medium Sand	Very Fine Gravelly Medium Sand
METHOD OF MOMENTS Arithmetic (μm)	MEAN ($\bar{x}_a$):	752.8	412.3	706.8
	SORTING (σ_a):	869.2	466.2	1144.3
	SKEWNESS:	2.880	5.971	2.765
	KURTOSIS:	11.55	45.64	9.490
METHOD OF MOMENTS Geometric (μm)	MEAN ($\bar{x}_g$):	514.5	322.8	364.5
	SORTING (σ_g):	2.278	1.904	2.992
	SKEWNESS:	-0.287	-0.253	-0.753
	KURTOSIS:	10.80	11.78	11.29
METHOD OF MOMENTS Logarithmic (φ)	MEAN ($\bar{x}_\phi$):	0.935	1.622	1.353
	SORTING (σ_ϕ):	1.102	0.897	1.329
	SKEWNESS:	-0.903	-0.412	-1.213
	KURTOSIS:	3.638	6.913	4.940
FOLK AND WARD METHOD (μm)	MEAN (M_g):	492.2	321.1	338.7
	SORTING (σ_g):	2.129	1.668	2.153
	SKEWNESS:	0.233	0.013	0.329
	KURTOSIS:	1.277	0.976	1.937
FOLK AND WARD METHOD (φ)	MEAN (M_ϕ):	1.023	1.639	1.562
	SORTING (σ_ϕ):	1.090	0.738	1.106
	SKEWNESS:	-0.233	-0.013	-0.329
	KURTOSIS:	1.277	0.976	1.937
FOLK AND WARD METHOD (Description)	MEAN:	Medium Sand	Medium Sand	Medium Sand
	SORTING:	Poorly Sorted	Moderately Sorted	Poorly Sorted
	SKEWNESS:	Coarse Skewed	Symmetrical	Very Coarse Skewed
	KURTOSIS:	Leptokurtic	Mesokurtic	Very Leptokurtic
	MODE 1 (μm):	423.4	299.7	299.7
	MODE 2 (μm):	3400.0		3400.0
	MODE 3 (μm):			
	MODE 1 (φ):	1.242	1.741	1.741
	MODE 2 (φ):	-1.743		-1.743
	MODE 3 (φ):			
	D_{10} (μm):	222.7	166.7	177.9
	D_{50} (μm):	485.1	319.9	323.7
	D_{90} (μm):	1479.0	622.8	2756.5
	(D_{90} / D_{10}) (μm):	6.640	3.735	15.51
	(D_{90} - D_{10}) (μm):	1256.3	456.1	2580.6
	(D_{75} / D_{25}) (μm):	2.429	2.020	2.002
	(D_{75} - D_{25}) (μm):	441.1	230.3	234.3
	D_{10} (φ):	-0.565	0.683	-1.464
	D_{50} (φ):	1.104	1.644	1.627
	D_{90} (φ):	2.167	2.584	2.491
	(D_{90} / D_{10}) (φ):	-3.837	3.783	-1.702
	(D_{90} - D_{10}) (φ):	2.731	1.901	3.955
	(D_{75} / D_{25}) (φ):	4.081	1.896	1.915
	(D_{75} - D_{25}) (φ):	1.281	1.014	1.002
	% GRAVEL:	9.4%	2.4%	12.4%
	% SAND:	90.6%	96.2%	86.1%
	% MUD:	0.0%	1.4%	1.5%
	% V COARSE GRAVEL:	0.0%	0.0%	0.0%
	% COARSE GRAVEL:	0.0%	0.0%	0.0%
	% MEDIUM GRAVEL:	0.0%	0.0%	0.0%
	% FINE GRAVEL:	1.6%	0.4%	5.0%
	% V FINE GRAVEL:	7.9%	2.0%	7.5%
	% V COARSE SAND:	6.4%	0.0%	0.0%
	% COARSE SAND:	29.8%	17.3%	9.3%
	% MEDIUM SAND:	39.9%	48.5%	48.6%
	% FINE SAND:	14.2%	28.7%	27.4%
	% V FINE SAND:	0.3%	1.7%	0.8%
	% V COARSE SILT:	0.0%	1.0%	1.0%
	% COARSE SILT:	0.0%	0.3%	0.4%
	% MEDIUM SILT:	0.0%	0.0%	0.0%
	% FINE SILT:	0.0%	0.0%	0.0%
	% V FINE SILT:	0.0%	0.0%	0.0%
	% CLAY:	0.0%	0.0%	0.0%

		T1H0	T1H1	T1H2	T1H3	T1H4	T1H5	T2B1
	ANALYST AND DATE:	Tony, 11/15/2007	Tony, 11/15/2007	Tony, 11/15/2007	Tony, 11/15/2007	Tony, 11/15/2007	Tony, 11/15/2007	Tony, 11/15/2007
	SIEVING ERROR:	0.7%	1.1%	1.1%	0.7%	1.1%	1.1%	0.3%
	SAMPLE TYPE:	Bimodal, Poorly Sorted	Unimodal, Moderately Well Sorted	Bimodal, Poorly Sorted	Bimodal, Poorly Sorted	Bimodal, Poorly Sorted	Bimodal, Moderately Sorted	Bimodal, Poorly Sorted
	TEXTURAL GROUP:	Gravelly Sand	Slightly Gravelly Sand	Slightly Gravelly Sand	Gravelly Sand	Gravelly Sand	Gravelly Sand	Slightly Gravelly Sand
	SEDIMENT NAME:	Very Fine Gravelly Fine Sand	Slightly Very Fine Gravelly Fine Sand	Slightly Very Fine Gravelly Medium Sand	Very Fine Gravelly Coarse Sand	Very Fine Gravelly Very Coarse Sand	Very Fine Gravelly Coarse Sand	Slightly Very Fine Gravelly Fine Sand
METHOD OF MOMENTS Arithmetic (μm)	MEAN	681.0	256.0	561.9	1190.7	1029.6	1180.2	446.0
	SORTING	965.2	225.1	524.1	892.7	720.9	772.3	420.5
	SKEWNESS	2.071	6.506	2.829	0.925	0.999	1.163	1.525
	KURTOSIS	5.856	65.20	13.52	2.895	3.580	3.654	5.172
METHOD OF MOMENTS Geometric (μm)	MEAN	281.1	219.4	404.8	813.6	717.7	923.4	311.2
	SORTING	5.308	1.636	2.463	3.114	3.269	2.411	2.224
	SKEWNESS	-1.729	0.110	-2.268	-3.052	-3.496	-4.031	0.533
	KURTOSIS	7.742	20.15	18.76	19.04	20.29	33.29	3.387
METHOD OF MOMENTS Logarithmic (ϕ)	MEAN	1.282	2.179	1.216	0.145	0.268	0.025	1.680
	SORTING	1.428	0.672	1.013	1.108	0.991	0.851	1.140
	SKEWNESS	-0.791	-1.601	-0.557	0.089	0.068	-0.342	-0.714
	KURTOSIS	2.660	8.060	2.856	2.044	2.071	2.095	2.276
FOLK AND WARD METHOD (μm)	MEAN	496.6	213.0	441.3	930.3	839.8	976.9	344.8
	SORTING	3.3	1.5	2.1	2.3	2.1	1.8	2.4
	SKEWNESS	0.471	0.048	0.217	0.042	0.053	0.281	0.434
	KURTOSIS	1.018	1.002	0.927	0.785	0.790	0.784	1.069
FOLK AND WARD METHOD (ϕ)	MEAN	1.010	2.231	1.180	0.104	0.252	0.034	1.536
	SORTING	1.7	0.5	1.0	1.2	1.1	0.9	1.2
	SKEWNESS	-0.471	-0.048	-0.217	-0.042	-0.053	-0.281	-0.434
	KURTOSIS	1.018	1.002	0.927	0.785	0.790	0.784	1.069
FOLK AND WARD METHOD (Description)	MEAN:	Medium Sand	Fine Sand	Medium Sand	Coarse Sand	Coarse Sand	Coarse Sand	Medium Sand
	SORTING:	Poorly Sorted	Moderately Well Sorted	Poorly Sorted	Poorly Sorted	Poorly Sorted	Moderately Sorted	Poorly Sorted
	SKEWNESS:	Very Coarse Skewed	Symmetrical	Coarse Skewed	Symmetrical	Symmetrical	Coarse Skewed	Very Coarse Skewed
	KURTOSIS:	Mesokurtic	Mesokurtic	Mesokurtic	Platykurtic	Platykurtic	Platykurtic	Mesokurtic
	MODE 1 (μm):	212.2	212.2	336.3	2400.0	1700.0	946.7	212.2
	MODE 2 (μm):	3400.0		1200.0	598.1	598.1	1700.0	1200.0
	MODE 3 (μm):							
	MODE 1 (ϕ):	2.239	2.239	1.574	-1.243	-0.743	0.081	2.239
	MODE 2 (ϕ):	-1.743		-0.243	0.744	0.744	-0.743	-0.243
	MODE 3 (ϕ):							
	D_{16} (μm):	141.4	132.7	186.7	324.2	333.0	486.9	134.0
	D_{50} (μm):	314.3	211.7	386.8	893.2	813.2	855.1	248.8
	D_{84} (μm):	3314.0	349.8	1216.7	2622.6	2146.5	2383.2	1199.5
	(D_{84} / D_{16}) (μm):	23.44	2.636	6.518	8.088	6.446	4.895	8.950
	(D_{84} - D_{16}) (μm):	3172.6	217.1	1030.0	2298.4	1813.5	1896.3	1065.4
	(D_{75} / D_{25}) (μm):	3.897	1.672	2.612	3.716	3.256	2.682	2.522
	(D_{75} - D_{25}) (μm):	565.1	110.4	412.9	1345.7	1086.8	1063.7	266.5
	D_{16} (ϕ):	-1.729	1.515	-0.283	-1.391	-1.102	-1.253	-0.262
	D_{50} (ϕ):	1.670	2.240	1.370	0.163	0.298	0.226	2.007
	D_{84} (ϕ):	2.822	2.914	2.421	1.625	1.586	1.038	2.899
	(D_{84} / D_{16}) (ϕ):	-1.633	1.923	-8.558	-1.168	-1.440	-0.829	-11.050
	(D_{84} - D_{16}) (ϕ):	4.551	1.398	2.704	3.016	2.688	2.291	3.162
	(D_{75} / D_{25}) (ϕ):	5.961	1.398	3.389	-1.150	-1.622	-0.868	2.132
	(D_{75} - D_{25}) (ϕ):	1.962	0.741	1.385	1.894	1.703	1.423	1.334
	% GRAVEL:	18.2%	0.3%	3.6%	22.1%	11.6%	15.6%	0.2%
	% SAND:	81.8%	99.7%	96.4%	77.9%	88.4%	84.4%	99.8%
	% MUD:	0.0%	0.0%	0.0%	0.0%	0.0%	0.0%	0.0%
	% V COARSE GRAVEL:	0.0%	0.0%	0.0%	0.0%	0.0%	0.0%	0.0%
	% COARSE GRAVEL:	0.0%	0.0%	0.0%	0.0%	0.0%	0.0%	0.0%
	% MEDIUM GRAVEL:	0.0%	0.0%	0.0%	0.0%	0.0%	0.0%	0.0%
	% FINE GRAVEL:	0.0%	0.0%	0.0%	0.0%	0.0%	0.0%	0.0%
	% V FINE GRAVEL:	18.2%	0.3%	3.6%	22.1%	11.6%	15.6%	0.2%
	% V COARSE SAND:	2.4%	2.9%	13.6%	23.9%	31.6%	20.5%	21.1%
	% COARSE SAND:	13.1%	0.0%	19.0%	28.6%	30.0%	52.8%	1.9%
	% MEDIUM SAND:	27.8%	29.9%	40.2%	21.0%	23.5%	11.1%	26.4%
	% FINE SAND:	32.5%	59.9%	22.6%	4.3%	3.3%	0.0%	43.2%
	% V FINE SAND:	6.0%	7.0%	1.0%	0.0%	0.0%	0.0%	7.1%
	% V COARSE SILT:	0.0%	0.0%	0.0%	0.0%	0.0%	0.0%	0.0%
	% COARSE SILT:	0.0%	0.0%	0.0%	0.0%	0.0%	0.0%	0.0%
	% MEDIUM SILT:	0.0%	0.0%	0.0%	0.0%	0.0%	0.0%	0.0%
	% FINE SILT:	0.0%	0.0%	0.0%	0.0%	0.0%	0.0%	0.0%
	% V FINE SILT:	0.0%	0.0%	0.0%	0.0%	0.0%	0.0%	0.0%
	% CLAY:	0.0%	0.0%	0.0%	0.0%	0.0%	0.0%	0.0%

		T1H5	T2B1	T2B2	T2B3	T2B3	T2B4	T2B5	T2B6
	ANALYST AND DATE:	Tony, 11/15/2007	Tony, 11/15/2007	Tony, 11/15/2007	Tony, 11/15/2007	Tony, 11/15/2007	Tony, 11/15/2007	Tony, 11/15/2007	Tony, 11/15/2007
	SIEVING ERROR:	1.1%	0.3%	0.7%	0.0%	0.0%	0.0%		
	SAMPLE TYPE:	Bimodal, Moderately Sorted	Bimodal, Poorly Sorted	Unimodal, Moderately Well Sorted	Unimodal, Moderately Well Sorted	Unimodal, Moderately Well Sorted	Unimodal, Moderately Well Sorted	Bimodal, Moderately Sorted	Unimodal, Moderately Sorted
	TEXTURAL GROUP:	Gravelly Sand	Slightly Gravelly Sand	Sand	Sand	Sand	Sand	Gravelly Sand	Gravelly Sand
	SEDIMENT NAME:	Very Fine Gravelly Coarse Sand	Slightly Very Fine Gravelly Fine Sand	Moderately Well Sorted Medium Sand	Moderately Well Sorted Fine Sand	Moderately Well Sorted Fine Sand	Moderately Well Sorted Fine Sand	Very Fine Gravelly Coarse Sand	Very Fine Gravelly Coarse Sand
METHOD OF MOMENTS Arithmetic (μm)	MEAN	1180.2	446.0	280.4	248.4	223.8	222.9	1129.3	1017.8
	SORTING	772.3	420.5	112.4	94.59	89.85	88.86	772.4	713.6
	SKEWNESS	1.163	1.525	0.893	0.761	1.044	0.983	1.211	1.417
	KURTOSIS	3.654	5.172	3.554	3.148	4.195	3.910	3.933	4.824
METHOD OF MOMENTS Geometric (μm)	MEAN	923.4	311.2	259.1	231.0	207.2	206.4	869.5	777.3
	SORTING	2.411	2.224	1.483	1.462	1.473	1.473	2.375	2.422
	SKEWNESS	-4.031	0.533	0.013	-0.045	0.089	0.063	-3.295	-3.198
	KURTOSIS	33.29	3.387	2.464	2.437	2.553	2.524	27.59	25.39
METHOD OF MOMENTS Logarithmic (ϕ)	MEAN	0.025	1.680	1.948	2.114	2.271	2.276	0.130	0.288
	SORTING	0.851	1.140	0.569	0.548	0.559	0.559	0.932	0.960
	SKEWNESS	-0.342	-0.714	-0.013	0.045	-0.089	-0.063	-0.104	0.138
	KURTOSIS	2.095	2.276	2.464	2.437	2.553	2.524	2.248	3.149
FOLK AND	MEAN	976.9	344.8	259.0	231.3	206.7	206.1	916.6	835.4
WARD METHOD (μm)	SORTING	1.8	2.4	1.5	1.5	1.5	1.5	2.0	2.0
	SKEWNESS	0.281	0.434	0.004	-0.006	0.020	0.016	0.129	0.085
	KURTOSIS	0.784	1.069	0.941	0.939	0.949	0.948	0.843	0.966
FOLK AND	MEAN	0.034	1.536	1.949	2.112	2.274	2.279	0.126	0.260
WARD METHOD (ϕ)	SORTING	0.9	1.2	0.6	0.6	0.6	0.6	1.0	1.0
	SKEWNESS	-0.281	-0.434	-0.004	0.006	-0.020	-0.016	-0.129	-0.085
	KURTOSIS	0.784	1.069	0.941	0.939	0.949	0.948	0.843	0.966
FOLK AND WARD METHOD (Description)	MEAN:	Coarse Sand	Medium Sand	Medium Sand	Fine Sand	Fine Sand	Fine Sand	Coarse Sand	Coarse Sand
	SORTING:	Moderately Sorted	Poorly Sorted	Moderately Well Sorted	Moderately Well Sorted	Moderately Well Sorted	Moderately Well Sorted	Moderately Sorted	Moderately Sorted
	SKEWNESS:	Coarse Skewed	Very Coarse Skewed	Symmetrical	Symmetrical	Symmetrical	Symmetrical	Coarse Skewed	Symmetrical
	KURTOSIS:	Platykurtic	Mesokurtic	Mesokurtic	Mesokurtic	Mesokurtic	Mesokurtic	Platykurtic	Mesokurtic
	MODE 1 (μm):	946.7	212.2	267.1	238.1	212.2	212.2	752.9	671.0
	MODE 2 (μm):	1700.0	1200.0					1700.0	
	MODE 3 (μm):								
	MODE 1 (ϕ):	0.081	2.239	1.907	2.073	2.239	2.239	0.412	0.578
	MODE 2 (ϕ):	-0.743	-0.243					-0.743	
	MODE 3 (ϕ):								
	D_{16} (μm):	486.9	134.0	153.4	139.1	124.6	123.9	402.9	359.5
	D_{50} (μm):	855.1	248.8	258.7	231.5	205.9	205.4	854.7	799.8
	D_{84} (μm):	2383.2	1199.5	439.1	384.1	347.6	346.5	2311.7	2099.1
	(D_{95} / D_5) (μm):	4.895	8.950	2.863	2.762	2.788	2.795	5.738	5.839
	(D_{84} - D_{16}) (μm):	1896.3	1065.4	285.7	245.0	222.9	222.5	1908.8	1739.6
	(D_{75} / D_{25}) (μm):	2.682	2.522	1.769	1.737	1.741	1.743	2.798	2.548
	(D_{75} - D_{25}) (μm):	1063.7	266.5	149.8	129.4	115.9	115.9	1014.2	802.2
	D_{16} (ϕ):	-1.253	-0.262	1.187	1.380	1.525	1.529	-1.209	-1.070
	D_{50} (ϕ):	0.226	2.007	1.951	2.111	2.280	2.284	0.227	0.322
	D_{84} (ϕ):	1.038	2.899	2.705	2.846	3.004	3.012	1.312	1.476
	(D_{95} / D_5) (ϕ):	-0.829	-11.050	2.278	2.062	1.970	1.970	-1.085	-1.380
	(D_{84} - D_{16}) (ϕ):	2.291	3.162	1.518	1.466	1.479	1.483	2.520	2.546
	(D_{75} / D_{25}) (ϕ):	-0.868	2.132	1.535	1.465	1.426	1.427	-1.254	-2.366
	(D_{75} - D_{25}) (ϕ):	1.423	1.334	0.823	0.796	0.800	0.802	1.484	1.349
	% GRAVEL:	15.6%	0.2%	0.0%	0.0%	0.0%	0.0%	14.0%	11.1%
	% SAND:	84.4%	99.8%	100.0%	100.0%	100.0%	100.0%	86.0%	88.8%
	% MUD:	0.0%	0.0%	0.0%	0.0%	0.0%	0.0%	0.0%	0.1%
	% V COARSE GRAVEL:	0.0%	0.0%	0.0%	0.0%	0.0%	0.0%	0.0%	0.0%
	% COARSE GRAVEL:	0.0%	0.0%	0.0%	0.0%	0.0%	0.0%	0.0%	0.0%
	% MEDIUM GRAVEL:	0.0%	0.0%	0.0%	0.0%	0.0%	0.0%	0.0%	0.0%
	% FINE GRAVEL:	0.0%	0.0%	0.0%	0.0%	0.0%	0.0%	0.0%	0.0%
	% V FINE GRAVEL:	15.6%	0.2%	0.0%	0.0%	0.0%	0.0%	14.0%	11.1%
	% V COARSE SAND:	20.5%	21.1%	0.0%	0.0%	0.0%	0.0%	27.0%	26.7%
	% COARSE SAND:	52.8%	1.9%	4.9%	1.3%	1.0%	0.8%	40.2%	39.1%
	% MEDIUM SAND:	11.1%	26.4%	48.2%	41.3%	31.0%	30.9%	17.6%	20.2%
	% FINE SAND:	0.0%	43.2%	43.9%	51.8%	57.9%	57.9%	1.2%	2.4%
	% V FINE SAND:	0.0%	7.1%	2.9%	5.6%	10.1%	10.4%	0.0%	0.4%
	% V COARSE SILT:	0.0%	0.0%	0.0%	0.0%	0.0%	0.0%	0.0%	0.1%
	% COARSE SILT:	0.0%	0.0%	0.0%	0.0%	0.0%	0.0%	0.0%	0.0%
	% MEDIUM SILT:	0.0%	0.0%	0.0%	0.0%	0.0%	0.0%	0.0%	0.0%
	% FINE SILT:	0.0%	0.0%	0.0%	0.0%	0.0%	0.0%	0.0%	0.0%
	% V FINE SILT:	0.0%	0.0%	0.0%	0.0%	0.0%	0.0%	0.0%	0.0%
	% CLAY:	0.0%	0.0%	0.0%	0.0%	0.0%	0.0%	0.0%	0.0%

		T3H1	T3H2	T3H3	T3H4	T3H5	T3H6	T4H1	T4H2
	ANALYST AND DATE:	Tony, 11/15/2007	Tony, 11/15/2007	Tony, 11/15/2007	Tony, 11/15/2007	Tony, 11/15/2007	Tony, 11/15/2007	Tony, 11/15/2007	Tony, 11/15/2007
	SIEVING ERROR:	0.0%	0.0%	0.4%	0.0%	0.8%	0.1%	0.0%	0.0%
	SAMPLE TYPE:	Unimodal, Well Sorted	Unimodal, Well Sorted	Unimodal, Moderately Well Sorted	Unimodal, Well Sorted	Unimodal, Moderately Well Sorted	Unimodal, Moderately Sorted	Unimodal, Moderately Well Sorted	Unimodal, Moderately Well Sorted
	TEXTURAL GROUP:	Sand	Sand	Sand	Sand	Slightly Gravelly Sand	Gravelly Sand	Sand	Sand
	SEDIMENT NAME:	Well Sorted Fine Sand	Well Sorted Fine Sand	Moderately Well Sorted Medium Sand	Well Sorted Fine Sand	Slightly Very Fine Gravelly Coarse Sand	Very Fine Gravelly Coarse Sand	Moderately Well Sorted Fine Sand	Moderately Well Sorted Fine Sand
METHOD OF MOMENTS Arithmetic (μm)	MEAN	250.1	190.1	275.4	253.5	1048.3	1091.0	229.9	234.1
	SORTING	75.95	60.15	93.66	78.90	478.9	676.2	93.52	93.93
	SKEWNESS	0.675	0.766	0.693	0.701	1.766	1.266	1.076	0.939
	KURTOSIS	3.181	3.399	3.094	3.231	8.436	4.601	4.298	3.714
METHOD OF MOMENTS Geometric (μm)	MEAN	238.7	180.8	259.7	241.4	949.6	875.9	212.5	216.4
	SORTING	1.352	1.366	1.404	1.362	1.520	2.196	1.479	1.480
	SKEWNESS	-0.030	0.018	-0.056	-0.027	0.068	-3.359	0.106	0.044
	KURTOSIS	2.558	2.576	2.493	2.571	3.156	29.22	2.554	2.482
METHOD OF MOMENTS Logarithmic (ϕ)	MEAN	2.067	2.468	1.945	2.051	0.075	0.141	2.235	2.208
	SORTING	0.435	0.450	0.490	0.446	0.604	0.898	0.564	0.566
	SKEWNESS	0.030	-0.018	0.056	0.027	-0.068	0.474	-0.106	-0.044
	KURTOSIS	2.558	2.576	2.493	2.571	3.156	4.159	2.554	2.482
FOLK AND WARD METHOD (μm)	MEAN	238.9	180.6	260.2	241.6	933.5	928.7	212.0	216.3
	SORTING	1.4	1.4	1.4	1.4	1.5	1.8	1.5	1.5
	SKEWNESS	-0.004	0.005	-0.010	-0.003	-0.117	0.075	0.027	0.016
	KURTOSIS	0.949	0.967	0.945	0.950	1.018	0.945	0.953	0.947
FOLK AND WARD METHOD (ϕ)	MEAN	2.065	2.469	1.942	2.049	0.099	0.107	2.238	2.209
	SORTING	0.4	0.5	0.5	0.5	0.6	0.9	0.6	0.6
	SKEWNESS	0.004	-0.005	0.010	0.003	0.117	-0.075	-0.027	-0.016
	KURTOSIS	0.949	0.967	0.945	0.950	1.018	0.945	0.953	0.947
FOLK AND WARD METHOD (Description)	MEAN:	Fine Sand	Fine Sand	Medium Sand	Fine Sand	Coarse Sand	Coarse Sand	Fine Sand	Fine Sand
	SORTING:	Wel Sorted	Well Sorted	Moderately Well Sorted	Well Sorted	Moderately Wel Sorted	Moderately Sorted	Moderately Well Sorted	Moderately Well Sorted
	SKEWNESS:	Symmetrical	Symmetrical	Symmetrical	Symmetrical	Fine Skewed	Symmetrical	Symmetrical	Symmetrical
	KURTOSIS:	Mesokurtic	Mesokurtic	Mesokurtic	Mesokurtic	Mesokurtic	Mesokurtic	Mesokurtic	Mesokurtic
	MODE 1 (μm):	238.1	189.1	267.1	238.1	1200.0	844.8	212.2	212.2
	MODE 2 (μm):								
	MODE 3 (μm):								
	MODE 1 (ϕ):	2.073	2.405	1.907	2.073	-0.243	0.246	2.239	2.239
	MODE 2 (ϕ):								
	MODE 3 (ϕ):								
	D_{16} (μm):	160.3	119.6	164.8	160.6	539.3	435.1	127.4	128.9
	D_{50} (μm):	239.0	180.5	260.4	241.6	979.6	893.7	210.9	215.6
	D_{84} (μm):	354.8	273.8	407.8	363.2	1570.6	2015.7	357.6	365.9
	(D_{95} / D_{16}) (μm):	2.213	2.290	2.475	2.262	2.912	4.633	2.807	2.840
	(D_{95} - D_{16}) (μm):	194.5	154.2	243.0	202.6	1031.3	1580.6	230.2	237.1
	(D_{75} / D_{25}) (μm):	1.542	1.555	1.633	1.556	1.765	2.353	1.746	1.758
	(D_{75} - D_{25}) (μm):	104.3	80.40	128.9	107.7	541.0	823.8	119.5	123.5
	D_{16} (ϕ):	1.495	1.869	1.294	1.461	-0.851	-1.011	1.484	1.450
	D_{50} (ϕ):	2.065	2.470	1.941	2.050	0.030	0.162	2.245	2.213
	D_{84} (ϕ):	2.641	3.064	2.601	2.639	0.891	1.201	2.973	2.956
	(D_{95} / D_{16}) (ϕ):	1.767	1.640	2.010	1.806	-1.368	-1.187	2.004	2.038
	(D_{95} - D_{16}) (ϕ):	1.146	1.195	1.307	1.177	1.542	2.212	1.489	1.506
	(D_{75} / D_{25}) (ϕ):	1.357	1.296	1.445	1.369	-1.562	-1.378	1.437	1.451
	(D_{75} - D_{25}) (ϕ):	0.625	0.637	0.707	0.638	0.820	1.234	0.804	0.814
	% GRAVEL:	0.0%	0.0%	0.0%	0.0%	3.9%	10.2%	0.0%	0.0%
	% SAND:	100.0%	100.0%	100.0%	100.0%	96.1%	89.7%	100.0%	100.0%
	% MUD:	0.0%	0.0%	0.0%	0.0%	0.0%	0.1%	0.0%	0.0%
	% V COARSE GRAVEL:	0.0%	0.0%	0.0%	0.0%	0.0%	0.0%	0.0%	0.0%
	% COARSE GRAVEL:	0.0%	0.0%	0.0%	0.0%	0.0%	0.0%	0.0%	0.0%
	% MEDIUM GRAVEL:	0.0%	0.0%	0.0%	0.0%	0.0%	0.0%	0.0%	0.0%
	% FINE GRAVEL:	0.0%	0.0%	0.0%	0.0%	0.0%	0.0%	0.0%	0.0%
	% V FINE GRAVEL:	0.0%	0.0%	0.0%	0.0%	3.9%	10.2%	0.0%	0.0%
	% V COARSE SAND:	0.0%	0.0%	0.0%	0.0%	44.5%	32.2%	0.0%	0.0%
	% COARSE SAND:	0.2%	0.0%	2.1%	0.4%	44.7%	42.6%	1.3%	1.3%
	% MEDIUM SAND:	44.2%	15.9%	52.4%	45.5%	7.0%	13.1%	32.9%	35.0%
	% FINE SAND:	54.3%	71.6%	44.3%	52.8%	0.0%	1.0%	56.7%	55.2%
	% V FINE SAND:	1.3%	12.5%	1.3%	1.4%	0.0%	0.9%	9.1%	8.5%
	% V COARSE SILT:	0.0%	0.0%	0.0%	0.0%	0.0%	0.1%	0.0%	0.0%
	% COARSE SILT:	0.0%	0.0%	0.0%	0.0%	0.0%	0.0%	0.0%	0.0%
	% MEDIUM SILT:	0.0%	0.0%	0.0%	0.0%	0.0%	0.0%	0.0%	0.0%
	% FINE SILT:	0.0%	0.0%	0.0%	0.0%	0.0%	0.0%	0.0%	0.0%
	% V FINE SILT:	0.0%	0.0%	0.0%	0.0%	0.0%	0.0%	0.0%	0.0%
	% CLAY:	0.0%	0.0%	0.0%	0.0%	0.0%	0.0%	0.0%	0.0%

		T3H1	T3H2	T3H3	T3H4	T3H5	T3H6	T4H1	T4H2
	ANALYST AND DATE:	Tony, 11/15/2007	Tony, 11/15/2007	Tony, 11/15/2007	Tony, 11/15/2007	Tony, 11/15/2007	Tony, 11/15/2007	Tony, 11/15/2007	Tony, 11/15/2007
	SIEVING ERROR:	0.0%	0.0%	0.4%	0.0%	0.8%	0.1%	0.0%	0.0%
	SAMPLE TYPE:	Unimodal, Well Sorted	Unimodal, Well Sorted	Unimodal, Moderately Well Sorted	Unimodal, Well Sorted	Unimodal, Moderately Well Sorted	Unimodal, Moderately Sorted	Unimodal, Moderately Well Sorted	Unimodal, Moderately Well Sorted
	TEXTURAL GROUP:	Sand	Sand	Sand	Sand	Slightly Gravelly Sand	Gravely Sand	Sand	Sand
	SEDIMENT NAME:	Well Sorted Fine Sand	Well Sorted Fine Sand	Moderately Well Sorted Medium Sand	Well Sorted Fine Sand	Slightly Very Fine Gravelly Coarse Sand	Very Fine Gravelly Coarse Sand	Moderately Well Sorted Fine Sand	Moderately Well Sorted Fine Sand
METHOD OF MOMENTS Arithmetic (μm)	MEAN	250.1	190.1	275.4	253.5	1048.3	1091.0	229.9	234.1
	SORTING	75.95	60.15	93.66	78.90	478.9	676.2	93.52	93.93
	SKEWNESS	0.675	0.766	0.693	0.701	1.766	1.266	1.076	0.939
	KURTOSIS	3.181	3.399	3.094	3.231	8.436	4.601	4.298	3.714
METHOD OF MOMENTS Geometric (μm)	MEAN	238.7	180.8	259.7	241.4	949.6	875.9	212.5	216.4
	SORTING	1.352	1.366	1.404	1.362	1.520	2.196	1.479	1.480
	SKEWNESS	-0.030	0.018	-0.056	-0.027	0.068	-3.359	0.106	0.044
	KURTOSIS	2.558	2.576	2.493	2.571	3.156	29.22	2.554	2.482
METHOD OF MOMENTS Logarithmic (ϕ)	MEAN	2.067	2.468	1.945	2.051	0.075	0.141	2.235	2.208
	SORTING	0.435	0.450	0.490	0.446	0.604	0.898	0.564	0.566
	SKEWNESS	0.030	-0.018	0.056	0.027	-0.068	0.474	-0.106	-0.044
	KURTOSIS	2.558	2.576	2.493	2.571	3.156	4.159	2.554	2.482
FOLK AND WARD METHOD (μm)	MEAN	238.9	180.6	260.2	241.6	933.5	928.7	212.0	216.3
	SORTING	1.4	1.4	1.4	1.4	1.5	1.8	1.5	1.5
	SKEWNESS	-0.004	0.005	-0.010	-0.003	-0.117	0.075	0.027	0.016
	KURTOSIS	0.949	0.967	0.945	0.950	1.018	0.945	0.953	0.947
FOLK AND WARD METHOD (ϕ)	MEAN	2.065	2.469	1.942	2.049	0.099	0.107	2.238	2.209
	SORTING	0.4	0.5	0.5	0.5	0.6	0.9	0.6	0.6
	SKEWNESS	0.004	-0.005	0.010	0.003	0.117	-0.075	-0.027	-0.016
	KURTOSIS	0.949	0.967	0.945	0.950	1.018	0.945	0.953	0.947
FOLK AND WARD METHOD (Description)	MEAN:	Fine Sand	Fine Sand	Medium Sand	Fine Sand	Coarse Sand	Coarse Sand	Fine Sand	Fine Sand
	SORTING:	Well Sorted	Wel Sorted	Moderately Well Sorted	Well Sorted	Moderately Well Sorted	Moderately Sorted	Moderately Well Sorted	Moderately Well Sorted
	SKEWNESS:	Symmetrical	Symmetrical	Symmetrical	Symmetrical	Fine Skewed	Symmetrical	Symmetrical	Symmetrical
	KURTOSIS:	Mesokurtic	Mesokurtic	Mesokurtic	Mesokurtic	Mesokurtic	Mesokurtic	Mesokurtic	Mesokurtic
	MODE 1 (μm):	238.1	189.1	267.1	238.1	1200.0	844.8	212.2	212.2
	MODE 2 (μm):								
	MODE 3 (μm):								
	MODE 1 (ϕ):	2.073	2.405	1.907	2.073	-0.243	0.246	2.239	2.239
	MODE 2 (ϕ):								
	MODE 3 (ϕ):								
	D_{16} (μm):	160.3	119.6	164.8	160.6	539.3	435.1	127.4	128.9
	D_{50} (μm):	239.0	180.5	260.4	241.6	979.6	893.7	210.9	215.6
	D_{84} (μm):	354.8	273.8	407.8	363.2	1570.6	2015.7	357.6	365.9
	(D_{95} / D_{16}) (μm):	2.213	2.290	2.475	2.262	2.912	4.633	2.807	2.840
	(D_{95} - D_{16}) (μm):	194.5	154.2	243.0	202.6	1031.3	1580.6	230.2	237.1
	(D_{75} / D_{25}) (μm):	1.542	1.555	1.633	1.556	1.765	2.353	1.746	1.758
	(D_{75} - D_{25}) (μm):	104.3	80.40	128.9	107.7	541.0	823.8	119.5	123.5
	D'_{16} (ϕ):	1.495	1.869	1.294	1.461	-0.651	-1.011	1.484	1.450
	D_{50} (ϕ):	2.065	2.470	1.941	2.050	0.030	0.162	2.245	2.213
	D_{84} (ϕ):	2.841	3.064	2.601	2.639	0.891	1.201	2.973	2.956
	(D_{95} / D_{16}) (ϕ):	1.767	1.640	2.010	1.806	-1.368	-1.187	2.004	2.038
	(D_{95} - D_{16}) (ϕ):	1.146	1.195	1.307	1.177	1.542	2.212	1.489	1.506
	(D_{75} / D_{25}) (ϕ):	1.357	1.298	1.445	1.369	-1.562	-1.378	1.437	1.451
	(D_{75} - D_{25}) (ϕ):	0.625	0.637	0.707	0.638	0.820	1.234	0.804	0.814
	% GRAVEL:	0.0%	0.0%	0.0%	0.0%	3.9%	10.2%	0.0%	0.0%
	% SAND:	100.0%	100.0%	100.0%	100.0%	96.1%	89.7%	100.0%	100.0%
	% MUD:	0.0%	0.0%	0.0%	0.0%	0.0%	0.1%	0.0%	0.0%
	% V COARSE GRAVEL:	0.0%	0.0%	0.0%	0.0%	0.0%	0.0%	0.0%	0.0%
	% COARSE GRAVEL:	0.0%	0.0%	0.0%	0.0%	0.0%	0.0%	0.0%	0.0%
	% MEDIUM GRAVEL:	0.0%	0.0%	0.0%	0.0%	0.0%	0.0%	0.0%	0.0%
	% FINE GRAVEL:	0.0%	0.0%	0.0%	0.0%	0.0%	0.0%	0.0%	0.0%
	% V FINE GRAVEL:	0.0%	0.0%	0.0%	0.0%	3.9%	10.2%	0.0%	0.0%
	% V COARSE SAND:	0.0%	0.0%	0.0%	0.0%	44.5%	32.2%	0.0%	0.0%
	% COARSE SAND:	0.2%	0.0%	2.1%	0.4%	44.7%	42.6%	1.3%	1.3%
	% MEDIUM SAND:	44.2%	15.9%	52.4%	45.5%	7.0%	13.1%	32.9%	35.0%
	% FINE SAND:	54.3%	71.6%	44.3%	52.8%	0.0%	1.0%	56.7%	55.2%
	% V FINE SAND:	1.3%	12.5%	1.3%	1.4%	0.0%	0.9%	9.1%	8.5%
	% V COARSE SILT:	0.0%	0.0%	0.0%	0.0%	0.0%	0.1%	0.0%	0.0%
	% COARSE SILT:	0.0%	0.0%	0.0%	0.0%	0.0%	0.0%	0.0%	0.0%
	% MEDIUM SILT:	0.0%	0.0%	0.0%	0.0%	0.0%	0.0%	0.0%	0.0%
	% FINE SILT:	0.0%	0.0%	0.0%	0.0%	0.0%	0.0%	0.0%	0.0%
	% V FINE SILT:	0.0%	0.0%	0.0%	0.0%	0.0%	0.0%	0.0%	0.0%
	% CLAY:	0.0%	0.0%	0.0%	0.0%	0.0%	0.0%	0.0%	0.0%

		T4H3	T4H4	T4H5	T4H6	T5H0	T5H1	T5H2	T5H3
	ANALYST AND DATE:	Tony, 11/15/2007	Tony, 11/15/2007	Tony, 11/15/2007	Tony, 11/15/2007	Tony, 11/15/2007	Tony, 11/15/2007	Tony, 11/15/2007	Tony, 11/15/2007
	SIEVING ERROR:	0.0%	0.2%	0.0%	0.6%	0.0%	0.0%	0.0%	0.0%
	SAMPLE TYPE:	Unimodal, Moderately Well Sorted	Unimodal, Moderately Well Sorted	Unimodal, Moderately Well Sorted	Bimodal, Moderately Sorted	Unimodal, Moderately Sorted	Bimodal, Moderately Sorted	Unimodal, Moderately Well Sorted	Bimodal, Poorly Sorted
	TEXTURAL GROUP:	Slightly Gravelly Sand	Sand	Sand	Gravelly Sand	Gravelly Sand	Gravelly Sand	Sand	Gravelly Sand
	SEDIMENT NAME:	Slightly Very Fine Gravelly Fine Sand	Moderately Well Sorted Medium Sand	Moderately Well Sorted Fine Sand	Very Fine Gravelly Coarse Sand	Very Fine Gravelly Coarse Sand	Very Fine Gravelly Coarse Sand	Moderately Well Sorted Fine Sand	Very Fine Gravelly Fine Sand
METHOD OF MOMENTS Arithmetic (μm)	MEAN	231.7	274.0	254.4	1140.9	867.8	940.3	263.9	614.5
	SORTING	171.8	95.80	89.79	798.2	596.0	622.1	107.9	847.5
	SKEWNESS	7.389	0.722	0.770	1.365	2.000	1.787	0.924	2.020
	KURTOSIS	78.73	3.159	3.269	4.130	8.024	6.077	3.620	6.207
METHOD OF MOMENTS Geometric (μm)	MEAN	205.3	257.5	239.1	846.6	691.3	784.5	243.2	249.1
	SORTING	1.554	1.417	1.418	2.897	2.229	1.853	1.494	5.110
	SKEWNESS	0.949	-0.053	-0.015	-4.125	-3.573	-1.957	0.018	-1.388
	KURTOSIS	6.423	2.500	2.497	27.60	31.44	27.93	2.488	6.538
METHOD OF MOMENTS Logarithmic (ϕ)	MEAN	2.284	1.957	2.065	0.071	0.464	0.331	2.040	1.583
	SORTING	0.636	0.503	0.504	0.852	0.849	0.784	0.579	1.688
	SKEWNESS	-0.949	0.053	0.015	-0.481	-0.198	-0.605	-0.018	0.014
	KURTOSIS	6.423	2.500	2.497	2.393	2.924	2.894	2.488	3.485
FOLK AND WARD METHOD (μm)	MEAN	202.1	258.2	239.1	981.0	717.3	825.6	243.3	391.8
	SORTING	1.5	1.4	1.4	1.9	1.8	1.8	1.5	3.4
	SKEWNESS	0.034	-0.006	0.001	0.308	0.071	0.261	0.013	0.420
	KURTOSIS	0.968	0.947	0.951	0.901	1.037	1.370	0.947	0.902
FOLK AND WARD METHOD (ϕ)	MEAN	2.307	1.953	2.064	0.028	0.479	0.276	2.039	1.352
	SORTING	0.6	0.5	0.5	0.9	0.9	0.8	0.6	1.8
	SKEWNESS	-0.034	0.006	-0.001	-0.308	-0.071	-0.261	-0.013	-0.420
	KURTOSIS	0.968	0.947	0.951	0.901	1.037	1.370	0.947	0.902
FOLK AND WARD METHOD (Description)	MEAN:	Fine Sand	Medium Sand	Fine Sand	Coarse Sand	Coarse Sand	Coarse Sand	Fine Sand	Medium Sand
	SORTING:	Moderately Well Sorted	Moderately Well Sorted	Moderately Well Sorted	Moderately Sorted	Moderately Sorted	Moderately Sorted	Moderately Well Sorted	Poorly Sorted
	SKEWNESS:	Symmetrical	Symmetrical	Symmetrical	Very Coarse Skewed	Symmetrical	Coarse Skewed	Symmetrical	Very Coarse Skewed
	KURTOSIS:	Mesokurtic	Mesokurtic	Mesokurtic	Mesokurtic	Mesokurtic	Leptokurtic	Mesokurtic	Mesokurtic
	MODE 1 (μm):	189.1	267.1	238.1	844.8	671.0	844.8	238.1	212.2
	MODE 2 (μm):				1700.0		1700.0		1700.0
	MODE 3 (μm):								
	MODE 1 (ϕ):	2.405	1.907	2.073	0.246	0.578	0.246	2.073	2.239
	MODE 2 (ϕ):				-0.743		-0.743		-0.743
	MODE 3 (ϕ):								
	D_{16} (μm):	120.1	161.9	150.0	475.3	344.0	423.6	143.2	108.9
	D_{50} (μm):	200.9	258.3	239.1	848.1	709.5	737.3	242.6	263.0
	D_{84} (μm):	347.3	409.5	381.7	2519.2	1571.9	1869.3	416.3	2513.8
	(D_{95} / D_{16}) (μm):	2.892	2.530	2.545	5.300	4.570	4.413	2.908	23.08
	(D_{84} - D_{16}) (μm):	227.2	247.6	231.7	2043.9	1227.9	1445.8	273.1	2404.9
	(D_{75} / D_{25}) (μm):	1.767	1.651	1.655	2.530	2.258	1.737	1.781	5.787
	(D_{75} - D_{25}) (μm):	116.5	130.9	121.7	949.9	604.6	406.2	142.1	779.4
	D_{16} (ϕ):	1.526	1.288	1.390	-1.333	-0.652	-0.903	1.264	-1.330
	D_{50} (ϕ):	2.315	1.953	2.064	0.238	0.495	0.440	2.044	1.927
	D_{84} (ϕ):	3.058	2.627	2.737	1.073	1.540	1.239	2.804	3.199
	(D_{95} / D_{16}) (ϕ):	2.004	2.040	1.970	-0.805	-2.360	-1.373	2.218	-2.405
	(D_{84} - D_{16}) (ϕ):	1.532	1.339	1.348	2.406	2.192	2.142	1.540	4.528
	(D_{75} / D_{25}) (ϕ):	1.433	1.455	1.427	-1.056	-8.942	13.70	1.512	30.47
	(D_{75} - D_{25}) (ϕ):	0.822	0.724	0.727	1.339	1.175	0.796	0.832	2.533
	% GRAVEL:	0.2%	0.0%	0.0%	17.1%	6.2%	7.5%	0.0%	13.0%
	% SAND:	99.8%	100.0%	100.0%	82.9%	93.8%	92.5%	100.0%	82.9%
	% MUD:	0.0%	0.0%	0.0%	0.0%	0.0%	0.0%	0.0%	4.0%
	% V COARSE GRAVEL:	0.0%	0.0%	0.0%	0.0%	0.0%	0.0%	0.0%	0.0%
	% COARSE GRAVEL:	0.0%	0.0%	0.0%	0.0%	0.0%	0.0%	0.0%	0.0%
	% MEDIUM GRAVEL:	0.0%	0.0%	0.0%	0.0%	0.0%	0.0%	0.0%	0.0%
	% FINE GRAVEL:	0.0%	0.0%	0.0%	0.0%	0.0%	0.0%	0.0%	0.0%
	% V FINE GRAVEL:	0.2%	0.0%	0.0%	17.1%	6.2%	7.5%	0.0%	13.0%
	% V COARSE SAND:	0.6%	0.0%	0.0%	18.9%	23.0%	13.5%	0.0%	11.7%
	% COARSE SAND:	1.1%	2.3%	1.2%	51.9%	43.6%	60.7%	3.6%	4.9%
	% MEDIUM SAND:	28.4%	51.1%	44.1%	12.1%	24.3%	18.1%	43.6%	22.8%
	% FINE SAND:	57.8%	44.9%	51.7%	0.0%	2.9%	0.2%	48.0%	33.6%
	% V FINE SAND:	11.9%	1.7%	3.0%	0.0%	0.0%	0.0%	4.8%	9.9%
	% V COARSE SILT:	0.0%	0.0%	0.0%	0.0%	0.0%	0.0%	0.0%	1.1%
	% COARSE SILT:	0.0%	0.0%	0.0%	0.0%	0.0%	0.0%	0.0%	1.9%
	% MEDIUM SILT:	0.0%	0.0%	0.0%	0.0%	0.0%	0.0%	0.0%	0.6%
	% FINE SILT:	0.0%	0.0%	0.0%	0.0%	0.0%	0.0%	0.0%	0.3%
	% V FINE SILT:	0.0%	0.0%	0.0%	0.0%	0.0%	0.0%	0.0%	0.2%
	% CLAY:	0.0%	0.0%	0.0%	0.0%	0.0%	0.0%	0.0%	0.0%

		T5H4	T5H5	T5H6	T6H0	T6H1	T6H2	T6H3	T6H4
	ANALYST AND DATE:	Tony, 11/15/2007	Tony, 11/15/2007	Tony, 11/15/2007	Tony, 11/15/2007	Tony, 11/15/2007	Tony, 11/15/2007	Tony, 11/15/2007	Tony, 11/15/2007
	SIEVING ERROR:	0.0%	0.0%	0.0%	0.0%	0.0%	0.0%	0.0%	0.0%
	SAMPLE TYPE:	Unimodal, Poorly Sorted	Bimodal, Poorly Sorted	Bimodal, Poorly Sorted	Bimodal, Poorly Sorted	Unimodal, Moderately Wel Sorted	Unimodal, Poorly Sorted	Unimodal, Moderately Sorted	Bimodal, Poorly Sorted
	TEXTURAL GROUP:	Gravelly Sand	Slightly Gravelly Sand	Gravelly Sand	Gravelly Sand	Slightly Gravelly Sand	Gravelly Sand	Slightly Gravelly Sand	Gravelly Sand
	SEDIMENT NAME:	Very Fine Gravelly Coarse Sand	Slightly Very Fine Gravely Coarse Sand	Very Fine Gravely Coarse Sand	Very Fine Gravelly Coarse Sand	Slightly Very Fine Gravelly Coarse Sand	Very Fine Gravelly Coarse Sand	Slightly Very Fine Gravelly Medium Sand	Very Fine Gravelly Coarse Sand
METHOD OF MOMENTS Arithmetic (µm)	MEAN	1047.3	906.2	1134.2	1148.5	602.6	1120.8	586.3	910.6
	SORTING	848.7	579.5	874.3	1006.9	295.9	854.8	543.2	672.2
	SKEWNESS	1.308	1.154	1.109	1.116	2.440	1.346	3.112	1.570
	KURTOSIS	4.060	4.784	3.479	3.011	16.67	3.994	14.37	5.934
METHOD OF MOMENTS Geometric (µm)	MEAN	687.9	700.0	733.6	620.3	542.6	757.1	441.2	664.9
	SORTING	3.360	2.302	3.646	5.310	1.600	3.597	2.266	2.651
	SKEWNESS	-2.902	-1.861	-2.998	-2.716	-1.888	-3.595	-2.413	-2.830
	KURTOSIS	16.48	10.38	15.73	11.28	30.06	19.68	22.86	19.27
METHOD OF MOMENTS Logarithmic (ϕ)	MEAN	0.354	0.503	0.226	0.186	0.873	0.132	1.111	0.498
	SORTING	1.170	1.159	1.197	1.108	0.624	0.931	0.927	1.084
	SKEWNESS	0.403	1.482	0.784	-0.281	-0.203	-0.389	-0.733	0.564
	KURTOSIS	3.630	6.981	4.773	2.000	3.124	2.329	3.633	4.001
FOLK AND	MEAN	819.2	760.0	924.0	945.3	542.6	953.4	446.9	713.1
WARD METHOD (µm)	SORTING	2.3	2.0	2.3	2.4	1.5	2.1	1.9	2.1
	SKEWNESS	0.088	-0.134	0.051	0.282	0.013	0.274	0.170	-0.051
	KURTOSIS	0.934	1.173	0.928	0.732	0.991	0.906	1.167	1.001
FOLK AND	MEAN	0.288	0.396	0.114	0.081	0.882	0.069	1.162	0.488
WARD METHOD (ϕ)	SORTING	1.2	1.0	1.2	1.3	0.6	1.0	0.9	1.1
	SKEWNESS	-0.088	0.134	-0.051	-0.282	-0.013	-0.274	-0.170	0.051
	KURTOSIS	0.934	1.173	0.928	0.732	0.991	0.906	1.167	1.001
FOLK AND WARD METHOD (Description)	MEAN:	Coarse Sand	Coarse Sand	Coarse Sand	Coarse Sand	Coarse Sand	Coarse Sand	Medium Sand	Coarse Sand
	SORTING:	Poorly Sorted	Poorly Sorted	Poorly Sorted	Poorly Sorted	Moderately Well Sorted	Poorly Sorted	Moderately Sorted	Poorly Sorted
	SKEWNESS:	Symmetrical	Fine Skewed	Symmetrical	Coarse Skewed	Symmetrical	Coarse Skewed	Coarse Skewed	Symmetrical
	KURTOSIS:	Mesokurtic	Leptokurtic	Mesokurtic	Platykurtic	Mesokurtic	Mesokurtic	Leptokurtic	Mesokurtic
	MODE 1 (µm):	598.1	671.0	671.0	533.0	533.0	671.0	377.4	1200.0
	MODE 2 (µm):		1200.0	1200.0	2400.0				598.1
	MODE 3 (µm):								
	MODE 1 (ϕ):	0.744	0.578	0.578	0.910	0.910	0.578	1.408	-0.243
	MODE 2 (ϕ):		-0.243	-0.243	-1.243				0.744
	MODE 3 (ϕ):								
	D_{10} (µm):	292.9	317.3	328.8	344.3	311.8	417.7	216.9	277.3
	D_{50} (µm):	772.2	761.2	880.0	773.2	543.2	827.0	431.6	737.6
	D_{90} (µm):	2511.2	1713.9	2647.5	3361.3	940.7	2722.9	1101.2	1822.8
	(D_{90} / D_{10}) (µm):	8.575	5.402	8.051	9.764	3.017	6.518	5.077	6.573
	(D_{90} - D_{10}) (µm):	2218.3	1396.7	2318.6	3017.0	628.9	2305.1	884.3	1545.5
	(D_{75} / D_{25}) (µm):	3.261	2.464	3.231	4.316	1.814	2.815	2.228	2.761
	(D_{75} - D_{25}) (µm):	1035.2	719.7	1147.5	1586.7	327.9	1024.2	362.2	774.4
	D_{10} (ϕ):	-1.328	-0.777	-1.405	-1.749	0.088	-1.445	-0.139	-0.866
	D_{50} (ϕ):	0.373	0.394	0.184	0.371	0.880	0.274	1.212	0.439
	D_{90} (ϕ):	1.772	1.656	1.605	1.538	1.681	1.259	2.205	1.850
	(D_{90} / D_{10}) (ϕ):	-1.334	-2.131	-1.142	-0.880	19.05	-0.871	-15.850	-2.136
	(D_{90} - D_{10}) (ϕ):	3.100	2.434	3.009	3.287	1.593	2.705	2.344	2.717
	(D_{75} / D_{25}) (ϕ):	-1.949	-3.705	-1.309	-1.016	2.900	-1.236	2.908	-4.233
	(D_{75} - D_{25}) (ϕ):	1.705	1.301	1.692	2.110	0.859	1.493	1.155	1.465
	% GRAVEL:	15.4%	4.4%	19.0%	26.0%	0.5%	18.5%	4.3%	7.8%
	% SAND:	83.8%	93.6%	79.9%	74.0%	99.5%	81.5%	95.7%	91.5%
	% MUD:	0.8%	2.0%	1.1%	0.0%	0.0%	0.0%	0.0%	0.8%
	% V COARSE GRAVEL:	0.0%	0.0%	0.0%	0.0%	0.0%	0.0%	0.0%	0.0%
	% COARSE GRAVEL:	0.0%	0.0%	0.0%	0.0%	0.0%	0.0%	0.0%	0.0%
	% MEDIUM GRAVEL:	0.0%	0.0%	0.0%	0.0%	0.0%	0.0%	0.0%	0.0%
	% FINE GRAVEL:	0.0%	0.0%	0.0%	0.0%	0.0%	0.0%	0.0%	0.0%
	% V FINE GRAVEL:	15.4%	4.4%	19.0%	26.0%	0.5%	18.5%	4.3%	7.8%
	% V COARSE SAND:	23.8%	30.7%	25.9%	15.1%	6.8%	20.2%	7.0%	29.0%
	% COARSE SAND:	31.9%	39.1%	31.4%	31.5%	50.1%	43.2%	29.0%	32.5%
	% MEDIUM SAND:	22.1%	19.0%	18.3%	25.1%	39.5%	17.9%	43.7%	22.9%
	% FINE SAND:	5.2%	2.3%	3.1%	2.2%	3.1%	0.2%	15.8%	6.1%
	% V FINE SAND:	0.8%	2.5%	1.3%	0.0%	0.0%	0.0%	0.2%	1.0%
	% V COARSE SILT:	0.5%	1.3%	0.7%	0.0%	0.0%	0.0%	0.0%	0.8%
	% COARSE SILT:	0.2%	0.4%	0.2%	0.0%	0.0%	0.0%	0.0%	0.2%
	% MEDIUM SILT:	0.0%	0.3%	0.1%	0.0%	0.0%	0.0%	0.0%	0.0%
	% FINE SILT:	0.0%	0.0%	0.0%	0.0%	0.0%	0.0%	0.0%	0.0%
	% V FINE SILT:	0.0%	0.0%	0.0%	0.0%	0.0%	0.0%	0.0%	0.0%
	% CLAY:	0.0%	0.0%	0.0%	0.0%	0.0%	0.0%	0.0%	0.0%

		T6H5	T6H6	T6H7
	ANALYST AND DATE:	Tony, 11/15/2007	Tony, 11/15/2007	Tony, 11/15/2007
	SIEVING ERROR:	0.0%	0.0%	0.0%
	SAMPLE TYPE:	Bimodal, Moderately Sorted	Bimodal, Moderately Sorted	Bimodal, Poorly Sorted
	TEXTURAL GROUP:	Gravelly Sand	Gravelly Sand	Gravelly Sand
	SEDIMENT NAME:	Very Fine Gravely Coarse Sand	Very Fine Gravelly Coarse Sand	Very Fine Gravelly Coarse Sand
METHOD OF MOMENTS Arithmetic (μm)	MEAN	1190.4	969.2	1016.1
	SORTING	725.6	615.6	792.1
	SKEWNESS	0.781	1.351	1.343
	KURTOSIS	2.915	5.373	4.389
METHOD OF MOMENTS Geometric (μm)	MEAN	954.1	764.4	676.1
	SORTING	2.088	2.308	3.367
	SKEWNESS	-2.200	-3.347	-2.913
	KURTOSIS	20.72	26.81	15.77
METHOD OF MOMENTS Logarithmic (ϕ)	MEAN	0.042	0.324	0.392
	SORTING	0.936	0.930	1.230
	SKEWNESS	0.279	0.523	1.098
	KURTOSIS	2.457	4.050	6.217
FOLK AND WARD METHOD (μm)	MEAN	975.1	814.3	827.0
	SORTING	1.9	1.9	2.2
	SKEWNESS	-0.010	-0.005	0.097
	KURTOSIS	0.810	0.938	0.990
FOLK AND WARD METHOD (ϕ)	MEAN	0.036	0.296	0.274
	SORTING	1.0	0.9	1.1
	SKEWNESS	0.010	0.005	-0.097
	KURTOSIS	0.810	0.938	0.990
FOLK AND WARD METHOD (Description)	MEAN:	Coarse Sand	Coarse Sand	Coarse Sand
	SORTING:	Moderately Sorted	Moderately Sorted	Poorly Sorted
	SKEWNESS:	Symmetrical	Symmetrical	Symmetrical
	KURTOSIS:	Platykurtic	Mesokurtic	Mesokurtic
	MODE 1 (μm):	1700.0	1200.0	671.0
	MODE 2 (μm):	752.9	671.0	1700.0
	MODE 3 (μm):			
	MODE 1 (ϕ):	-0.743	-0.243	0.578
	MODE 2 (ϕ):	0.412	0.578	-0.743
	MODE 3 (ϕ):			
	D_{90} (μm):	410.8	362.6	322.9
	D_{50} (μm):	966.3	813.5	766.4
	D_{10} (μm):	2274.5	1815.1	2324.7
	(D_{90} / D_{10}) (μm):	5.536	5.006	7.198
	(D_{90} - D_{10}) (μm):	1863.7	1452.6	2001.8
	(D_{75} / D_{25}) (μm):	2.825	2.444	2.958
	(D_{75} - D_{25}) (μm):	1088.0	754.9	957.6
	D_{90} (ϕ):	-1.186	-0.860	-1.217
	D_{50} (ϕ):	0.049	0.298	0.384
	D_{10} (ϕ):	1.283	1.464	1.631
	(D_{90} / D_{10}) (ϕ):	-1.083	-1.702	-1.340
	(D_{90} - D_{10}) (ϕ):	2.469	2.324	2.848
	(D_{75} / D_{25}) (ϕ):	-0.992	-2.647	-1.936
	(D_{75} - D_{25}) (ϕ):	1.498	1.289	1.564
	% GRAVEL:	15.0%	6.4%	13.4%
	% SAND:	85.0%	93.3%	84.8%
	% MUD:	0.0%	0.3%	1.9%
	% V COARSE GRAVEL:	0.0%	0.0%	0.0%
	% COARSE GRAVEL:	0.0%	0.0%	0.0%
	% MEDIUM GRAVEL:	0.0%	0.0%	0.0%
	% FINE GRAVEL:	0.0%	0.0%	0.0%
	% V FINE GRAVEL:	15.0%	6.4%	13.4%
	% V COARSE SAND:	33.4%	33.2%	23.3%
	% COARSE SAND:	34.8%	37.7%	37.3%
	% MEDIUM SAND:	15.3%	19.5%	20.1%
	% FINE SAND:	1.4%	2.1%	2.4%
	% V FINE SAND:	0.2%	0.8%	1.7%
	% V COARSE SILT:	0.0%	0.3%	1.0%
	% COARSE SILT:	0.0%	0.0%	0.5%
	% MEDIUM SILT:	0.0%	0.0%	0.3%
	% FINE SILT:	0.0%	0.0%	0.0%
	% V FINE SILT:	0.0%	0.0%	0.0%
	% CLAY:	0.0%	0.0%	0.0%

Appendix 2. 3 Table of sedimentary statistical analysis results for beach sediment samples form Wonga Beach (samples were collected at the seaward end of transects indicated in Figure 3-1).

		Most northern sample					
		B-1	B-2	B-3	B-4	B-5	B-6
	ANALYST AND DATE:	Tony, 11/15/2007	Tony, 11/15/2007	Tony, 11/15/2007	Tony, 11/15/2007	Tony, 11/15/2007	Tony, 11/15/2007
	SIEVING ERROR:						
	SAMPLE TYPE:	Trimodal, Moderately Well Sorted	Unimodal, Well Sorted	Unimodal, Well Sorted	Unimodal, Very Well Sorted	Polymodal, Moderately Sorted	Unimodal, Poorly Sorted
	TEXTURAL GROUP:	Sand	Sand	Sand	Sand	Sand	Sandy Gravel
	SEDIMENT NAME:	Moderately Well Sorted Fine Sand	Well Sorted Medium Sand	Well Sorted Medium Sand	Very Well Sorted Coarse Sand	Moderately Sorted Coarse Sand	Sandy Very Fine Gravel
METHOD OF	MEAN	250.933	426.632	503.416	639.101	476.681	1408.585
MOMENTS	SORTING	104.192	135.474	137.818	139.643	210.417	1033.726
Arithmetic (μm)	SKEWNESS	0.907	0.776	0.663	0.298	0.016	0.221
	KURTOSIS	3.550	3.489	3.225	2.399	2.520	1.496
METHOD OF	MEAN	230.633	405.599	484.433	622.424	413.575	902.948
MOMENTS	SORTING	1.504	1.367	1.311	1.247	1.824	2.965
Geometric (μm)	SKEWNESS	0.019	0.015	-0.009	-0.175	-1.377	-0.659
	KURTOSIS	2.418	2.561	2.616	2.473	4.611	2.200
METHOD OF	MEAN	2.116	1.302	1.046	0.684	1.274	0.147
MOMENTS	SORTING	0.589	0.451	0.391	0.318	0.867	1.568
Logarithmic (ϕ)	SKEWNESS	-0.019	-0.015	0.009	0.175	1.377	0.659
	KURTOSIS	2.418	2.561	2.616	2.473	4.611	2.200
FOLK AND	MEAN	229.061	405.150	484.267	622.062	446.661	922.555
WARD METHOD	SORTING	1.531	1.378	1.318	1.258	1.741	3.089
(μm)	SKEWNESS	-0.013	-0.001	-0.003	-0.037	-0.325	-0.403
	KURTOSIS	0.929	0.956	0.957	0.993	1.427	0.773
FOLK AND	MEAN	2.126	1.303	1.046	0.685	1.163	0.116
WARD METHOD	SORTING	0.614	0.463	0.399	0.331	0.800	1.627
(ϕ)	SKEWNESS	0.013	0.001	0.003	0.037	0.325	0.403
	KURTOSIS	0.929	0.956	0.957	0.993	1.427	0.773
FOLK AND	MEAN:	Fine Sand	Medium Sand	Medium Sand	Coarse Sand	Medium Sand	Coarse Sand
WARD METHOD	SORTING:	Moderately Well Sorted	Well Sorted	Well Sorted	Very Well Sorted	Moderately Sorted	Poorly Sorted
(Description)	SKEWNESS:	Symmetrical	Symmetrical	Symmetrical	Symmetrical	Very Fine Skewed	Very Fine Skewed
	KURTOSIS:	Mesokurtic	Mesokurtic	Mesokurtic	Mesokurtic	Leptokurtic	Platykurtic
	MODE 1 (μm):	145.795	423.398	475.061	671.041	533.027	2900.000
	MODE 2 (μm):	238.094				103.119	
	MODE 3 (μm):	103.119				72.981	
	MODE 1 (ϕ):	2.779	1.242	1.076	0.578	0.910	-1.535
	MODE 2 (ϕ):	2.073				3.278	
	MODE 3 (ϕ):	3.278				3.777	
	D_{10} (μm):	137.145	267.492	337.951	459.881	154.595	149.168
	D_{50} (μm):	230.881	405.362	484.433	626.812	472.324	1228.860
	D_{90} (μm):	397.769	614.502	692.249	832.333	751.941	2893.353
	(D_{90} / D_{10}) (μm):	2.900	2.297	2.048	1.810	4.864	19.397
	(D_{90} - D_{10}) (μm):	260.625	347.010	354.299	372.451	597.346	2744.184
	(D_{75} / D_{25}) (μm):	1.824	1.563	1.469	1.373	1.838	5.659
	(D_{75} - D_{25}) (μm):	139.763	182.590	187.715	198.655	283.274	2014.669
	D_{10} (ϕ):	1.330	0.703	0.531	0.265	0.411	-1.533
	D_{50} (ϕ):	2.115	1.303	1.046	0.674	1.082	-0.297
	D_{90} (ϕ):	2.866	1.902	1.565	1.121	2.693	2.745
	(D_{90} / D_{10}) (ϕ):	2.155	2.708	2.950	4.233	6.548	-1.791
	(D_{90} - D_{10}) (ϕ):	1.536	1.200	1.034	0.856	2.282	4.278
	(D_{75} / D_{25}) (ϕ):	1.512	1.657	1.724	2.012	2.279	-0.937
	(D_{75} - D_{25}) (ϕ):	0.867	0.645	0.555	0.458	0.878	2.501
	% GRAVEL:	0.000	0.000	0.000	0.000	0.000	0.339
	% SAND:	1.000	1.000	1.000	1.000	0.994	0.661
	% MUD:	0.000	0.000	0.000	0.000	0.006	0.000

"#$%#"&$'()*%#+,-(

		B-7	B-8	B-9	B-10	B-11
	ANALYST AND DATE:	Tony, 11/15/2007	Tony, 11/15/2007	Tony, 11/15/2007	Tony, 11/15/2007	Tony, 11/15/2007
	SIEVING ERROR:					
	SAMPLE TYPE:	Unimodal, Poorly Sorted	Bimodal, Poorly Sorted	Bimodal, Poorly Sorted	Bimodal, Poorly Sorted	Bimodal, Moderately Sorted
	TEXTURAL GROUP:	Gravelly Sand	Sandy Gravel	Gravelly Sand	Sandy Gravel	Gravelly Sand
	SEDIMENT NAME:	Very Fine Gravelly Coarse Sand	Sandy Very Fine Gravel	Very Fine Gravelly Coarse Sand	Sandy Very Fine Gravel	Very Fine Gravelly Coarse Sand
METHOD OF	MEAN	927.837	861.552	748.781	740.904	933.311
MOMENTS	SORTING	677.022	801.881	721.963	773.514	697.692
Arithmetic (μm)	SKEWNESS	0.760	0.806	1.158	1.097	0.734
	KURTOSIS	2.815	2.366	3.366	3.000	2.778
METHOD OF	MEAN	444.817	227.812	214.324	151.344	357.635
MOMENTS	SORTING	7.700	14.679	13.234	17.661	11.037
Geometric (μm)	SKEWNESS	-2.336	-1.348	-1.411	-1.043	-1.893
	KURTOSIS	7.363	3.213	3.423	2.375	4.975
METHOD OF	MEAN	0.257	0.294	0.465	0.379	0.124
MOMENTS	SORTING	0.941	1.074	1.046	1.031	0.800
Logarithmic (ϕ)	SKEWNESS	0.498	0.500	0.359	0.325	0.255
	KURTOSIS	3.026	2.905	2.732	2.574	3.214
FOLK AND	MEAN	958.990	966.723	887.236	872.838	1104.823
WARD METHOD	SORTING	2.014	2.122	2.233	2.023	1.831
(μm)	SKEWNESS	-0.129	-0.402	-0.190	-0.407	-0.078
	KURTOSIS	0.756	0.470	0.509	0.415	0.516
FOLK AND	MEAN	0.060	0.049	0.173	0.196	-0.144
WARD METHOD	SORTING	1.010	1.085	1.159	1.017	0.872
(ϕ)	SKEWNESS	0.129	0.402	0.190	0.407	0.078
	KURTOSIS	0.756	0.470	0.509	0.415	0.516
FOLK AND	MEAN:	Coarse Sand	Coarse Sand	Coarse Sand	Coarse Sand	Very Coarse Sand
WARD METHOD	SORTING:	Poorly Sorted	Poorly Sorted	Poorly Sorted	Poorly Sorted	Moderately Sorted
(Description)	SKEWNESS:	Fine Skewed	Very Fine Skewed	Fine Skewed	Very Fine Skewed	Symmetrical
	KURTOSIS:	Platykurtic	Very Platykurtic	Very Platykurtic	Very Platykurtic	Very Platykurtic
	MODE 1 (μm):	946.684	2400.000	844.791	671.041	946.684
	MODE 2 (μm):		752.921	2400.000	2400.000	2400.000
	MODE 3 (μm):					
	MODE 1 (ϕ):	0.081	-1.243	0.246	0.578	0.081
	MODE 2 (ϕ):		0.412	-1.243	-1.243	-1.243
	MODE 3 (ϕ):					
	D_{10} (μm):	340.719	283.815	255.434	277.007	454.021
	D_{50} (μm):	917.212	1021.446	819.133	941.088	967.266
	D_{90} (μm):	2715.985	3709.550	3642.264	4542.096	3060.589
	(D_{90} / D_{10}) (μm):	7.971	13.070	14.259	16.397	6.741
	(D_{90} - D_{10}) (μm):	2375.265	3425.735	3386.830	4265.089	2606.568
	(D_{75} / D_{25}) (μm):	2.905	4.872	4.841	5.738	3.016
	(D_{75} - D_{25}) (μm):	1079.685	1901.634	1754.847	2219.892	1305.782
	D_{10} (ϕ):	-1.441	-1.891	-1.865	-2.183	-1.614
	D_{50} (ϕ):	0.125	-0.031	0.288	0.088	0.048
	D_{90} (ϕ):	1.553	1.817	1.969	1.852	1.139
	(D_{90} / D_{10}) (ϕ):	-1.078	-0.961	-1.056	-0.848	-0.706
	(D_{90} - D_{10}) (ϕ):	2.995	3.708	3.834	4.035	2.753
	(D_{75} / D_{25}) (ϕ):	-1.138	-0.815	-0.987	-0.767	-0.649
	(D_{75} - D_{25}) (ϕ):	1.538	2.285	2.275	2.521	1.593
	% GRAVEL:	0.186	0.325	0.281	0.356	0.243
	% SAND:	0.814	0.673	0.719	0.644	0.757
	% MUD:	0.000	0.002	0.0%	0.0%	0.0%

Appendix 3 Copyright Declaration for journal articles comprising Chapters 2 to 4.

This administrative form has been removed

Appendix 4 Copyright Declaration for journal article comprising Chapter 5.

Every reasonable effort has been made to gain permission and acknowledge the owners of copyright material. I would be pleased to hear from any copyright owner who has been omitted or incorrectly acknowledged.